An investigation into the structure and activity of monometallic and bimetallic copper and gold catalysts for propene oxidation

Thesis submitted in accordance with the requirements of the University of Cardiff for the degree of Doctor of Philosophy by Charlotte. L. Bracey

Supervisors: Professor G.J.Hutchings and Dr.A.Carley

October 2012

Acknowledgements

I would like to thank my academic supervisors: Professor Graham Hutchings and Dr. Alvert Carley for their help and guidance throughout my PhD project. They have encouraged and motivated me during my three years research and I have learnt a great deal of scientific knowledge from them both.

I would especially like to thank my industrial supervisor, Dr. Peter Ellis for his continued support and involvement with this thesis. His help and guidance have been much appreciated and made my project an interesting and enjoyable challenge. I would like to thank Cardiff University and my sponsors Johnson Matthey for allowing me the chance to carry out this research.

Finally, I would like to thank my friends and family for their constant support and encouragement to achieve my goals.

Abstract

$CuAu/SiO_2$ catalysts were prepared in a number of ways, the main route being incipient wetness impregnation, but other methods, like deposition precipitation and high dispersion, were also used. Bimetallic and monometallic catalysts were prepared for this investigation and most were characterised by various techniques such as XRD, SEM, TPR, BET, UV visible and TEM.

Theoretical and characterisation studies of CuAu catalysts have generated considerable interest. However, little research has been carried out on their catalytic activity. Therefore, propene oxidation was chosen as the principal reaction, as it was previously examined by Chimentao and group.[1]

This study showed that the reduction of the catalysts in H_2/Ar was fundamental to alloy formation. The most active catalyst was made by a sequential procedure that deposited the copper onto the silica support by high dispersion, followed by depositing gold onto the support by deposition precipitation. The catalyst was then treated by a Sinfelt thermal treatment which involved a reduction in H_2/Ar at 315^oC for 2h followed by a high temperature calcination at 676^oC in air for 15h. Propene oxidation was performed in the presence of hydrogen and a propene conversion of 10% was observed at 320^oC, with a selectivity towards acrolein (90%) and some carbon dioxide (10%).

The purpose of this study was to obtain an understanding of the nature of these $CuAu/SiO_2$ catalysts and to determine if there were any relationship towards their activity for propene oxidation.

References

1. J. Llorca, M. Dominguez, C. Ledesma, R. J. Chimentao, F. Medina, J. Sueiras, I. Angurell, M . Seco and O. Rossell, *Journal of Catalysis*, 258 (2005) 187-198.

Aims

- The gain an understanding of bimetallic $CuAu/SiO_2$ samples as oxidation catalysts.
- To understand the structure and properties of the bimetallic catalysts, compared to the monometallic Cu and Au materials.
- To test the catalysts for propene oxidation and try and determine the effect of catalyst preparation on the activity and selectivity.

Objectives

- To prepare several $CuAu/SiO_2$ catalysts by mainly impregnation, as well as other techniques, such as deposition precipitation, precipitation, high dispersion and sol immobilisation.
- These catalysts will be characterised by various instruments, such as XRD, BET, XPS, SEM and TPR to identify their structure and properties.
- Propene oxidation will be the focus of the catalytic study and all the catalysts will be tested for this reaction under different conditions and preparation methods.

Contents Page

Chapter 1: Introduction

1.1 History of catalysis

The first concept of catalysis [1] was introduced by Fulhame in 1794, who found that small amounts of water were needed for carbon monoxide oxidation and that the water used was unchanged after the reaction. Eventually, after some years of studying reactions, it became apparent that the use of catalysis could have great industrial gain and this revolutionized catalytic chemical processes.

In 1884, Le Chatelier discovered a relationship between temperature and pressure on the rate of reaction.[2] This, along with other research at the time helped to further understand chemical reactions and catalysts.

In 1898, industrial catalysis increased worldwide and new catalytic processes were developed. The ammonia process [3] was the biggest reaction at this time and was used to make fertilizer. In 1902, Haber stated that for this reaction to operate at the highest efficiency it had to be carried out under high pressures. The first, small scale, catalytic production of the ammonia reaction was performed in 1905 by Haber, using an iron based catalyst. This initial work by Haber and others led onto large scale industrial reactions and also to theories about adsorption isotherms by Langmuir, which were based on this early reaction.

Manufacturing of synthetic fuels and new innovative processes, such as Fischer-Tropsch, were a significant development when, in 1922, Franz Fischer and Hans Tropsch produced hydrocarbons from hydrogen and carbon monoxide.[4] They continued their research and, by 1925, they could achieve high yields by using high pressures. Catalysis took an important turn when, in 1927, Hinshelwood introduced a kinetic theory based on earlier work by Langmuir and devised the Langmuir-Hinshelwood theory.

Due to the high demand for automobiles, the petroleum industry continued to thrive. In 1950, the first conference dedicated to heterogeneous catalysis was organized by the Faraday Society. After this, further catalytic discoveries were made by Ziegler and Natta, associated with polymerization. More studies produced many new catalyst systems with some being introduced to the commercial market. In 1965, Wilkinson developed a rhodium metal complex which could catalyze alkene hydrogenation reactions.[5] Today, the main focus of research is environmental catalysis and, with new scientific technologies and equipment, new branches of catalysis have been created, such as catalytic modeling. Over the last 30 years developments in exhaust gas catalysts have resulted in major reductions in their emissions, which have had a positive environmental effect. Other processes like the Selective Catalytic Reduction (SCR) are significant in recent times, controlling the NO_x emissions from nitric acid and power plants.

Catalysis is now used in almost every process, from the production of fine chemicals for pharmaceutical applications to the production of bulk chemicals and exhaust gas catalysts. The future of catalysis is very exciting and will continue to be a vital part in the scientific field.

1.2 Defining catalysis

A catalyst is a substance which can affect the rate of a chemical reaction without itself being changed in the process. The catalyst participates in the reaction but is unchanged at the end of the reaction. Usually the catalytic pathway will have lower activation energy (Ea) than the uncatalysed mechanism.

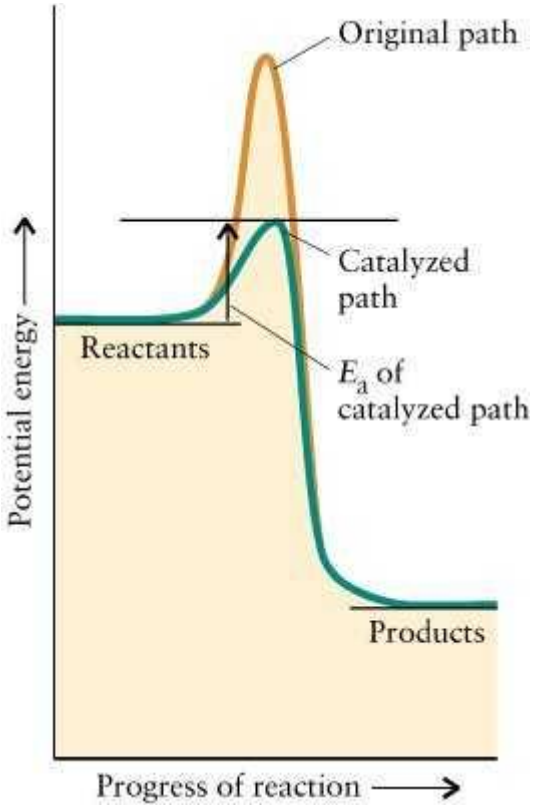

Figure 1.1 Catalytic reaction pathways

In homogeneous catalysis, the reaction takes place in one phase whereas in heterogeneous catalysis, the catalysed reaction arises at the interface between two phases. The presence of a catalyst in a reaction will alter the kinetics and may allow the reaction to occur under lower temperature conditions. However, the use of a catalyst will not alter the equilibrium constant of a reaction. The equilibrium constant is determined by ΔG^o and as a result, is independent of the reaction mechanism. An efficient catalyst must possess certain properties:

- High activity for a particular reaction.
- Good selectivity towards a desired product.
- Stable activity with no substantial deactivation over a long period of time (have a long catalyst lifetime).

1.3. Properties and characteristics of catalysts

Catalytic oxidation is a useful reaction which is quite efficient because it can occur at low temperature. However, there are certain properties and characteristics which the catalyst must possess in order for it to be considered an effective catalyst on the industrial scale.

1.3.1 Activity and selectivity

It is essential for a catalyst to exhibit a good activity, which is either established in the high productivity from a small quantity of sample or by using mild operating conditions (especially low temperature) which display a superior selectivity and stability for a desired reaction.

High selectivity is also an important requirement for determining a good catalyst. A catalyst that achieves high selectivity towards a product that is wanted from a certain reaction, whilst suppressing any other products caused by unwanted side reactions, is very desirable to industry.

1.3.2 Stability

A good stability is needed for an effective catalyst, which remains unchanged as the reaction proceeds over a period of time and after re-use, so that the catalyst shows resistance and durability. Below are a few factors that contribute to a reduced stability:

- Poisons, reactants or products may interfere with active components or the support to reduce activity or selectivity.

- Coking can form on some catalysts from reactions like polymerisation and hydrogenenolysis.
- Sintering of the catalyst.

1.3.3 Regeneration and Reproducibility

All catalysts go through some form of ageing after a certain time and it is vital for a process to be put into effect that can regenerate the catalyst through an action that will return some or all of the catalytic properties of the original sample. The regeneration must try to recover as much of the catalyst activity and selectivity, but also maintain its mechanical strength after each treatment.

Reproducing catalyst activity is also important, especially for industrial purposes since a catalyst that changes its performance, when a new batch of catalyst is prepared is unreliable and economically unacceptable.

1.3.4 Morphology and particle size

The shape and grain size of a catalyst can affect the performance of a catalyst in a reaction, and different processes will require different morphologies to achieve the best activity. Different reactors require different morphologies, e.g. fixed bed reactors use mostly beads and pellets. The particle size of a catalyst is also key to its performance as some reactions will only proceed when a metal particle size is between a certain range. Haruta and co-workers [6] found that for propene oxidation their Au particles had to be less than 4 nm in size to produce

propene oxide with 90% selectivity and a conversion of 1-2% at a temperature between 30 ^{o}C to 120 ^{o}C.

1.3.5 Porosity

Porous materials are widely found in nature and are mainly used in the industrial field and research. Chemical industries use porous materials as catalysts and adsorbents, such as activated carbon, silica and alumina. These and many other materials require careful consideration of their porous structure and physical properties. It is also important to take into account their application and performance, as all of these are strongly influenced by their pore size, volume and shape.

1.4 Propene oxidation: A heterogeneous catalytic oxidation reaction

Heterogeneous oxidation of alkenes, such as propene, have a particular interest because two of the major products, propene oxide and acrolein which are formed from the partial oxidation, are valuable intermediates for industry. Many catalysts that have been tested for this reaction only generate a low selectivity towards the epoxide over a variety of conditions and, as an consequence, propene oxide is currently made either from the chlorohydrin [7] process, which is a old method and environmentally undesirable as it uses chlorine, or the hydroperoxide process. Propene oxide is one of the most important feedstocks for the production of many useful chemicals, such as polyurethane, polyester resins and surfactants. Acrolein is also formed from propene oxidation and requires a C-H cleavage. In industry,

acrolein is beneficial as it is used in the preparation of polyester resin, polyurethane, propene glycol, acrylic acid, acrylonitrile and glycerol.

Silver catalysts have been commonly used for the ethene epoxidation process and studies found that atomic oxygen was the active species for the reaction. If oxygen is unable to dissociate, then epoxidation will not occur. Due to the success of silver catalysts for ethene epoxidation, these catalysts have been tried for propene epoxidation. Silver on calcium carbonate, which also consists of promoters, such as, molybdenum, potassium and chloride, has been tested for propene epoxidation. There have been a number of reports showing the performance of silver catalysts, supported on alkali carbonates. A selective silver catalyst (60%), supported on an alkali metal carbonate, formed propene oxide at a conversion of 3% when chloroethane, nitrous oxide and carbon dioxide were used.[7] The effect of a chloride promoter was studied and it was reported that preparing a silver catalyst, with chloride from AgCl, gave a propene oxide selectivity of 30% and a propene conversion of 11%. However, when the catalyst was made without the chloride promoter, a lower activity was observed (3.6% propene oxide selectivity and 4.8% conversion).[8] Lambert and co-workers studied the effect of metal particle size for propene epoxidation with K-promoted $Ag/CaCO_3$ catalysts.[9] They found that unpromoted $Ag/CaCO_3$ catalysts had a 3.7% selectivity towards propene oxide, which was lower than the catalyst promoted with 1.7% potassium (15.2% selectivity towards propene oxide and a conversion of 6%). This promoted catalyst had the best performance and they found that it had silver particle sizes between 20-40 nm. From their work, they concluded that the silver particle size was important in achieving the best selectivity, and particles had to be between 20-40 nm and not larger or smaller to obtain the highest propene oxide selectivity. Silica supported molybdenum oxide has also been used for propene epoxidation.[10] A propene conversion of 17.6% and a propene oxide selectivity of 43.6% were achieved from a MoO_x/SiO_2 catalyst with a loading of 0.255 mmol/g at 300^{o}C

and with the flow rates: 10/5/10 cm^3 min^{-1} for propene/oxygen/helium. From their characterisation of the catalyst, they concluded that crystalline MoO_3 nano-particle species was more active than molybdenum oxide species for propene oxide formation. Different molybdenum oxide precursors were studied and it was determined that H_2MoO_4 had the highest activity. The active MoO_3 species' role was to remove hydrogen from propene, and the formed radicals could desorb into the gas phase and react with oxygen to form propene oxide.

Silver supported on titania has also been used. However, this catalyst requires both hydrogen and oxygen in the reactor feed. Wang *et al.* studied the effects of calcination on Ag/Ti catalysts for propene epoxidation.[11] It was reported that when the catalysts were calcined in air, the optimum activity of 0.43% conversion and a 92.8% selectivity towards propene oxide was achieved. Calcination in other gases was not as effective and the use of hydrogen and nitrogen calcinations decreased the activity. The XRD analysis showed that a catalyst only calcined in air had a weak metal silver reflection. Upon comparison with gold on titania, the silver catalyst was not as active as the gold catalyst for propene epoxidation.[6]

Hydrogen peroxide has been applied instead of oxygen only systems. A money saving benefit of this process is that no separation of hydrogen peroxide is required and it can therefore be used directly to form propene oxide. Degussa-Headwaters effectively made propene oxide with hydrogen peroxide by using hydrogen and oxygen to generate hydrogen peroxide.[12] An alternative oxidising agent that has had considerable research carried out on it is nitrous oxide. Conversions of up to 5% were formed with selectivities of 80% for a catalyst consisting of potassium-promoted iron oxide on SBA-15.[13] The FeO_x/SBA-15 catalyst was prepared by impregnation and after calcination of 600 ^oC, the sample was modified with KCl by impregnation, followed by a calcination at 600 ^oC for 6 hours. They suggested that the iron was the active site for the reaction since SBA-15, with or without KCl, was inactive. For

the FeO_x/SBA-15 catalyst without the alkali salt, acrolein was the major product. When KCl was added, propene oxide became the major product, with a selectivity of 72% and a conversion of 4.51% at 325 ^oC. Their work also showed that an increase in the amount of modifier used increased the selectivity towards propene oxide. Further studies into the shift of allylic oxidation to epoxidation, were carried out with other potassium modifiers, such as KBr and KNO_3. These modifiers also showed similar shifts and it was deduced that the potassium, not the chlorine, played a significant role in this reaction. They concluded that the potassium prevented allylic oxidation by reducing the reactivity of the lattice oxygen.

Propene epoxidation using molten salts (a mixture of $NaNO_3$ and KNO_3) has been studied by Olin and co-workers and these achieved a propene conversion of 15% with a propene oxide selectivity at 65%. The reactor conditions consisted of a temperature of 200 ^oC and a propene- air mixture that flowed through a molten alkali- nitrate salt solution.[14] Nijhuis and group used a number of different molten salt mixtures and additives, like potassium hydroxide, to improve selectivity. This paper suggested that the role of the salt was to act as a catalyst to generate free radicals necessary for the homogeneous gas-phase reaction, occurring in the gas bubbles in the molten salt medium. Other work described the use of sodium hydroxide addition to the molten salts, and palladium catalysts increased the selectivity.[15,16] Propene oxide was also found to be produced in a homogeneous gas-phase reaction by Olin and co-workers, reaching a propene conversion of 7% with a propene oxide selectivity of 65%.[17] However, it is known that homogeneous gas-phase reactions are extremely sensitive to the reactor conditions. Homogeneous catalysts have also been tested in propene oxidation, using hydroperoxides, and a propene conversion of 10% with high selectivity can be obtained. The use of oxygen as an oxidant has also been studied but the selectivity is greatly reduced (<15%). It appears that homogeneous catalysts are more active than the heterogeneous catalysts mentioned so far. However, there are disadvantages for

homogeneous catalysts. The two main problems are pressure and separation, since extra separation is required to remove the catalyst from the liquid stream. Propene has a high vapour pressure and, as a result, a solvent is needed for the reaction. Both these problems can be costly and have to be seriously considered when using homogeneous catalysts, compared with heterogeneous ones.

Gold on titania catalysts have been extensively covered by many papers and have shown promise for propene epoxidation.[6] Haruta and co-workers were the first to use gold on titania catalysts for this reaction and they discovered that the size and shape of the gold particles was significant on the catalytic activity. The highest performance for propene epoxidation was observed in catalysts with a particle size between 2-5 nm. An improved propene oxide yield could be achieved by using a Ti-Si support. A higher temperature was required (about 50-100 K more) when compared with gold-titania catalysts but the stability was improved and the propene oxide yield increased. A catalyst, consisting of gold supported on titanium and dispersed on silica, has been tested for propene epoxidation in the presence of oxygen and hydrogen, and showed a good selectivity to propene oxide (greater than 90% selectivity at a conversion of 0.2%).[18] Promoters, such as sodium, lithium and magnesium, have been utilized to improve the catalyst and it has been suggested that their role is to block acidic sites on the catalyst, which can decompose propene oxide.[19,20] Platinum and palladium have also been reported to improve the activity of gold-titania catalysts. [1]

Propene oxidation has recently been studied, using ceria catalysts supported on titania.[22] The ceria loadings (0.004, 0.3, 0.5 and 0.9 wt%) did not appear to affect the reaction temperature of propene oxidation and all of the catalysts had propene oxidation ignition at around 195^{o}C. Baylet and co-workers stated that the lowest light-off temperature was obtained for the 0.5 wt% Ce sample with a T_{50} of 284 ^{o}C. A trend for the T_{50} order from lowest to highest was as follows: 0.5 wt% Ce > 0.9 wt% Ce > 0.4 wt% Ce> 0.3 wt% Ce. For all the catalysts, only

carbon dioxide and carbon monoxide were detected as products. The catalyst with a ceria loading of 0.5 wt% was the most active for propene oxidation to carbon dioxide.

1.5 Reactions using Cu catalysts

Copper is a frequently used metal for industrial catalysis, as it is cheap and readily available. The common reactions it is used for are the Water Gas Shift reaction, NO reduction, methanol synthesis and propene epoxidation which are discussed below.

1.5.1 Water gas shift reaction

The water-gas shift reaction (WGS) can be expressed as:

$CO + H_2O \longrightarrow CO_2 + H_2$ $\Delta H° = -41.2$ kJ/mol $\Delta G° = -28.8$ kJ/mol at T= 300 ^oC

This reaction has had much interest because of fuel cell technology, which can convert chemical energy into electrical or heat energy, without the need for combustion. The WGS process is essential for providing clean hydrogen and is used to remove large amounts of carbon monoxide in the automotive industry. Ceria oxide based catalysts are very good WGS catalysts and Li [23] and co-workers have reported their use for low temperature WGS reaction. The presence of Cu (2 wt %) on the Ce (La) Oxide increased the activity greatly with a 90% CO conversion at 400 ^oC. At a lower temperature range, the copper modified catalyst had similar activity to the commercial Cu-ZnO-Al_2O_3 catalyst. Cu based mixed oxides for the WGS reaction have also been studied by Tanaka [24] who discovered that $CuMn_2O_4$ had a high activity over 225 ^oC, similar to that of Cu/ZnO/Al_2O_3. $CuAl_2O_4$ showed a high activity at

lower temperature with an 80% CO conversion at 150 ^{o}C. Both $CuAl_2O_4$ and $CuMn_2O_4$ had higher rates of CO conversion than the commercial catalyst. Different metal dopants have been added to CuM_2O_4 and the order of activity was found to be Mn>Al>La>Cr>Fe>Y.

The type of support has a significant effect on the performance of Cu catalysts, and Yahiro *et al.*[25] studied the influence of such supports. They showed that Al_2O_3, MgO and CeO_2 were all highly active for WGS reaction, whereas others like SiO_2-Al_2O_3 and SiO_2-MgO and β-zeolite showed a lower activity in the temperature range 150-250 ^{o}C. Other factors that have an effect on the activity are calcination temperature and metal oxide additives. The influence of calcination temperature on the WGS reaction has been investigated by Yahiro and co-workers[26] for Cu/Al_2O_3 catalysts prepared by an impregnation method. Their studies showed that CO conversion increased as the calcination temperature increased, reaching an optimum conversion at 800 ^{o}C and then rapidly decreasing at 900 ^{o}C. This occurrence is different to the commercially available $Cu/ZnO/Al_2O_3$ catalyst where the activity decreases with increasing calcination temperature.[27,28] The authors concluded that the main factor controlling the catalytic activity for the WGS reaction was the Cu (0) surface area. The catalyst that was calcined at 800 ^{o}C had the highest surface area of Cu (0) and there was a high dispersion of CuO on this sample. The group found that spinel $CuAl_2O_4$ was formed from the CuO reacting with the support. The presence of highly dispersed Cu (0) is very important to the catalytic activity of the WGS reaction and as well as calcination temperature, the promotional effect of FeO_x on Cu/Al_2O_3[29] has been reported to form highly dispersed Cu (0) and increase its performance.

Copper oxide catalysts demonstrate a good activity for the WGS reaction, with either Cu or Cu^{+} being the active species for the reaction. The preparation conditions, i.e. calcination temperature and the type of support used, can have a significant effect on the reactions success.

1.5.2 NO reduction

Air pollution caused by industrial emissions has generated a lot of concern, as pollutants like nitrogen oxides (NO_x), are the main contributors to the formation of acid rain and smog. Therefore, a method to remove these harmful gases is important and catalytic NO reduction is a worthwhile reaction to follow. At present, most use precious metals but these are very expensive to utilize, and so a replacement by other metals, like copper, has regenerated new interest.

Bera *et al.*[30] studied Cu/CeO_2 (5 wt%) catalysts for NO reduction and discovered that they could achieve nearly 100% conversion of NO by NH_3 below 300 ^oC. NO reduction by CO was also carried out and also showed similar conversions below 300 ^oC. Their work also showed hydrocarbon oxidation by NO to CO_2 N_2 and H_2O in the low temperature range of 150-350 ^oC.

1.5.3 Methanol reforming and methanol synthesis

There have been a number of studies carried out on copper catalysts, used for steam reforming of methanol. Matsumura *et al.*[31] studied $Cu/ZnO/ZrO_2$ catalysts that were prepared by a co-precipitation method and used for methanol reforming at high temperatures. Recently, monometallic Cu/ZrO_2 and bimetallic $Cu\text{-}Ni/ZrO_2$ have been prepared by deposition precipitation and used to produce hydrogen by steam reforming in the temperature range 250-360 ^oC.[32] The bimetallic catalysts had a better activity than the monometallic samples and a selectivity of 60% towards hydrogen was observed at the highest temperature.

Carbon dioxide is the most well known greenhouse gas and therefore its transformation into other chemicals, such as methanol, is favourable. The most popular way to form methanol is from $CO/CO_2/H_2$ by using $Cu/ZnO/Al_2O_3$ catalysts at 250-300 ^oC and 10 MPa.[33] Other groups have also used $Cu/ZnO/Al_2O_3$ catalysts but employed a novel low temperature route to perform very high methanol activity.[34] They studied the effect of the preparation method and composition on the structure and activity for methanol synthesis. They found that a high activity of methanol production from CO_2 hydrogenation was achieved at 170 ^oC and 5 MPa in a slurry-phase reactor over the copper catalysts prepared by an oxalate-gel co-precipitation (OC) method.

1.5.4 Propene oxidation

Copper, as a catalyst for propene oxidation, has been studied by numerous groups on different supports and under various conditions. A single crystal study of Cu_2O was carried out by Schultz *et al.* [35] under UHV conditions and at 27 ^oC and 0.01 MPa. Propene, acrolein, allyl alcohol, propane and the combustion products CO_2 and H_2O were detected. Reitz and co-workers[36] have also examined Cu_2O catalysts for propene oxidation and have, like Schultz, used XPS and TPD to understand this reaction further. They studied cupric and cuprous oxide and found that cupric oxide was more reactive for propene oxidation. They also deduced that the rate of propene oxidation on the copper oxide surfaces was proportional to the rate of the H atom abstraction step and an increased CuO reduction favoured H atom abstraction.

The role of low basicity oxygen atoms in propene epoxidation has been investigated by Torres and co-workers.[37] A density functional theory (DFT) study was carried out on (111)

silver and copper surfaces to deduce the thermochemistry and activation energy barrier for combustion and selective oxidation reactions for propene epoxidation. They showed that, from the theoretical data, there was a big difference between silver and copper for the formation of the intermediates for this reaction. Copper favoured metallacycle formation, whereas silver favoured allylic hydrogen abstraction.

Copper has been introduced to zirconium catalysts by Labaki[38] *et al.* and the catalyst was used for propene oxidation. Their study mainly focused on the effect that the preparation method had on the catalytic performance. The three methods used were: co-precipitation with copper nitrate and zirconium oxychloride ($Cu/ZrO(OH)_2$); wet impregnation with copper nitrate and zirconium oxyhydroxide (Cu/Zr); and alternatively, impregnation with Cu on zirconium oxyhydroxide previously calcined at 600^oC (Cu/Zr600). The study revealed that the catalysts made via impregnation were more active than the co-precipitation. The catalyst activity was enhanced when there was more copper in it. The group also suggested the presence of new active sites due to the addition of copper to the zirconium, as the light off curve shifted to lower temperature. For the same copper content, the order of activity is: Cu/Zr> Cu/Zr600> $Cu/ZrO(OH)_2$. Therefore, the investigation concluded that the best catalyst for activity and stability was the impregnated catalyst, previously calcined at 600 ^oC.

Another study that compared preparation techniques, but solely used Cu for propene epoxidation without any additional metal, was carried out by Vaughan and co-workers.[39] They made a Cu/silica catalyst in the presence of oxygen without hydrogen addition. A 1 wt% catalyst was made *via* a microemulsion route and a 5 wt% catalyst by wet impregnation. For the catalyst prepared by the microemulsion method, propene oxide and acrolein were the major products and the best selectivity of 53% was achieved at a temperature of 225 ^oC with 0.25% conversion. The activity for the other catalyst was similar, although it only reached a selectivity of 15% at 225 ^oC and a conversion of 0.24%. Below a temperature of 250 ^oC, they

deduced that dispersed metallic Cu (Cu (0)) was the active species for propene epoxidation and that their activity was close to what Haruta had obtained with his Au/TiO_2 catalysts. Recently, copper phalocyanine has been used as an copper precursor for an active catalyst for propene oxidation.[40] The catalyst was made by wet impregnation on a silica support and the best selectivity and activity was observed in the temperature range 475-500 ^{o}C. The group discovered that the key parameters for high acrolein selectivities were copper loading and oxygen partial pressure in the gas mixture. As copper content increased, acrolein selectivity dramatically dropped from 42% to 11%, when the loadings were increased from 0.06 to 0.9wt% respectively. As the oxygen partial pressure decreased, the acrolein selectivity increased. The group could only hypothesize the state of the copper species, which they suggested were copper (II) oxide, although the copper levels during their experiments were too low to actually determine.

A recent investigation of propene epoxidation on a Cu/SiO_2 catalyst, using O_2 as an oxidant,[41] showed that propene oxide was produced below 227 ^{o}C. However, at higher temperatures, acrolein and CO_x were the major products. From IR studies, they concluded that Cu (0) and Cu (1+) were the active species for the formation of propene oxide, and Cu (2+) was an active species for forming acrolein and CO_x. Li *et al.* [23] studied the performance of Cu/SiO_2 catalysts, with the addition of several promoters, for propene epoxidation by oxygen. Out of all the promoters used, they found that samples modified with KAc and NaAc showed the highest propene oxide selectivity (100%) at the start of the propene reaction. Their work suggested that the addition of these modifiers switched the formation form acrolein to propene oxide. As the temperature was increased, the conversion increased and the propene oxide selectivity decreased. At 1% conversion, the KAc promoted Cu/SiO_2 catalyst had a propene oxide selectivity of 40%. The group's work revealed that there was a trend associated with the effect of the promoter on the propene oxide selectivity and conversion.

An increase in the propene oxide selectivity and conversion was observed in the order: KCl < NaCl < NaAc < KAc. The study also showed that KAc was the best promoter for propene oxide formation, which was not dependent on pretreatment in N_2 or H_2. The size of the copper (II) oxide particles was also investigated and the smaller particles were more favourable for propene oxide formation, particularly when the catalyst was modified with KAc.

Cu/SiO_2 catalysts have recently been prepared by a sol-gel method and tested for propene epoxidation by a high throughput screening process.[42] SiO_2 was the support of choice and many metals were used to synthesise catalysts for this reaction. The most promising was the Cu/SiO_2 catalyst. Their work also revealed that multimetallic systems could have a positive effect on the reactivity for propene oxidation. The propene oxide yield was increased by several fold when copper was promoted with silver, and this suggested a synergy between the two metals. Copper and manganese supported on Al_2O_3 also showed an improvement in the catalytic performance. Senkan and team have highlighted the importance of mutimetallic systems for this reaction, which needs to be explored in more detail to generate a catalyst that fulfils the potential of these metal systems for propene epoxidation. Recently, a new high throughput pulsed laser ablation (PLA) study was carried out by Senkan and co-workers, which emphasized the capability of Cu-on-Mn/SiO_2 for propene epoxidation by oxygen at the temperature of 375^{o}C.[43] For the Mn-on Cu/SiO_2 catalyst, propene oxide selectivity was maintained around 8% and carbon dioxide was the main product. Cu/SiO_2 and Mn/SiO_2 propene oxide selectivities of 17% and 8% were observed, at a propene conversion of between 0.2 and 0.4% respectively. However, for the $Cu/Mn/SiO_2$ catalyst, propene oxide yields were increased by a factor of five, compared to the mono-metallic catalysts. A propene oxide selectivity of 22% was observed at a propene conversion of 1%. These investigations showed that the sequence of deposition of each metal onto the silica support was vital

because it had a major impact on the outcome of the catalyst performance for propene epoxidation. Combinational methodologies have been used to identify new formulations for propene selective oxidation catalysts.[44] Senken *et al.* prepared catalysts by impregnation of various metals on standard pellets of γ-Al_2O_3. At different loadings, many different catalysts were prepared, processed and tested for propene oxidation in oxygen. Initial results showed that Rh was an active metal for propene oxide formation and showed good performance, when combined with V, Cr, Mo and Sn. Copper was tested and a much lower activity was detected which favoured selectivity towards acrolein.

Copper promoted by vanadium has shown a significant effectiveness for propene epoxidation, using oxygen, from work carried out by Yang *et al.*[45] This study suggested a synergistic effect between the vanadium and the copper, especially with a V/Cu ratio of 0.11-0.20 which showed the highest activity towards propene epoxidation. One reason for the enhanced performance of the copper, when promoted by vanadium, was that the addition of the promoter increased the copper dispersion of the catalyst. As previously seen in other work,[46] a pre-reduction of the catalyst, rather than an oxidative pre-treatment, also increased the catalytic activity. An in situ XRD study revealed that Cu (0) in the reduced catalyst was transformed to Cu (+1), which (they suggested) accounted for propene epoxidation, and the presence of VO_x encouraged this change. A conversion of 2.7% was observed when using the vanadium promoted copper catalyst with a selectivity of 16% towards propene oxide, whereas the unsupported copper catalyst, without vanadium addition, gave a conversion of 0.045% and a selectivity of 9.2% towards propene oxide.

For copper catalysts to be effective, it is important to consider the type of support used. It was previously reported that, for the water gas shift reaction,[25] an alumina support was more active than silica. Other factors that should be considered when using copper catalysts are the preparation method, calcination temperature, dispersion and, in the case of propene oxidation,

the type of oxidant used. The oxidation state of the copper also seems to be significant, as different copper species can give different product selectivities.

1.6 Reactions using Au catalysts

1.6.1 CO oxidation

CO oxidation has been extensively researched since Au nanoparticles were shown to be active for this reaction.[47,48] The size (2-5 nm) and shape of the Au particles, as well as the type of support used, have been reported by many to be crucial for CO oxidation.[49-51] The typical preparation method is deposition precipitation.[52] Work carried out on the activity of supported Au catalysts for this reaction has revealed that smaller Au nanoparticles are much more active than larger particles at $0^{o}C$, and this activity is not altered by the nature of the oxide support (reducible or irreducible).

Silica was, in the past, believed to be an unsuccessful support to disperse Au for many reactions. However, it has been used by Zhu *et al.* [53] to form an active and stable catalyst for CO oxidation. The process uses a $[Au(en)_2]^{3+}$ (en= ethylenediamine) salt as a precursor in a unique deposition precipitation method.

Recently, CO oxidation has been investigated for oleyamine coated AuAg alloy nanoparticles.[54] A one pot synthesis was devised which involved the simultaneous reduction of gold and silver in octadecane. TEM analysis showed that the nanoparticles were monodispersed with a size of 8 nm. UV-visible spectroscopy proved that an AuAg alloy was formed and not a core shell structure. The $Au_{0.52}$ $Ag_{0.48}$ alloy catalyst was the most active for

CO oxidation and had a 100% conversion at 150 ^{o}C. This indicated that the gold performance was enhanced by the presence of silver in the catalyst.

An investigation into the effect of different Au species on a Au/SiO_2 catalyst for CO oxidation has been carried out by Wu and co-workers.[55] Diffuse reflectance infrared spectroscopy (DRIFTS) and quadrupole mass spectroscopy (QMS) were used to analyse the catalysts. They discovered that the choice of pre-treatment, had an effect on the Au species and, as a consequence, on the performance for CO oxidation. High temperature calcination (500 ^{o}C) formed cationic Au species which were inactive for CO oxidation. However, a reduction in either H_2 or CO produced a metallic Au species which was active towards CO oxidation. The role of water was also studied and the group concluded that it had a positive influence on the activity, facilitating the reduction of the Au cationic species, and on the activation of oxygen.

1.6.2 Propene oxidation

Gold catalysts have been extensively studied for propene oxidation over past 10 to 20 years. Haruta and co-workers [6] discovered that Au could be an effective catalyst for propene epoxidation and the activity was dependent on the size of the Au particles. They used Au/TiO_2 catalysts, prepared by deposition precipitation (DP) and for comparison, Au catalysts were also made by impregnation and on a TiO_2/SiO_2 support. Hydrogen and oxygen were included in the propene reactor feed in the temperature range 30 to 120 ^{o}C. Conversions of 1-2%, with selectivity of 90% towards propene oxide were observed for the Au/TiO_2 catalyst made by DP and the addition of H_2 improved the catalyst performance. Au/TiO_2 was also tested for propene oxidation by Delgass and co-workers [56] with H_2/O_2 and in a temperature range of 100 to 200 ^{o}C. The most promising catalysts were those made by a

deposition precipitation route on a titania modified silica support which had an Au particle size above 2 nm. Other work by Delgass [57] and co-workers, on propene epoxidation for Au/TS-1, agreed with earlier work carried out by Haruta and co-workers, based on the size of the Au particle for propene epoxidation, and their work stated that an Au size of 2-5 nm was critical. Haruta [58] also experimented with Au on a Ti-MCM-41 support and TiO_2-SiO_2 with different ratios. The Au nanoparticles were put on the support by deposition precipitation as this appeared to be the most successful method of preparation for this reaction. The Au/ Ti-MCM-41 catalyst showed increased conversion with an increase in the Ti/Si ratio of 3/100. It reached the highest propene oxide yield with a selectivity of 93.5% towards propene oxide and 3.2% conversion at 100 ^{o}C. Their findings showed that the temperature had an effect on the propene oxide selectivity because, at temperatures greater than 120 ^{o}C, the selectivity decreased. Haruta and co-workers have written many papers [6,48,49,52,59] about Au supported on either TiO_2, TiO_2/SiO_2 or titanosilicates for propene epoxidation, which has led to improvements on the types of support used for this reaction. Part of these studies [60,61] showed that 3D mesoporous titanosilicates could be prepared by a sol-gel technique and used as effective supports for Au to improve propene oxidation yields, with a conversion of 7% and a propene oxide selectivity of more than 90%. The effect of calcination temperature on Au/Ti-SiO_2 support was also investigated [62] at 300, 400, 600, 800 and 1000 ^{o}C, and showed that an increase in the heat treatment temperature of the catalyst increased propene oxide selectivity and yield.

The effect of catalyst preparation on propene oxidation performance [63] was also tested by Sacaliuc and group, who made Au/Ti-SBA-15 catalysts by either grafting or by a hydrothermal route. The grafting technique gave an array of products: mainly propene oxide, acetaldehyde, acrolein, propane, CO_2 and H_2O, whereas the hydrothermal method showed lower activity, with propane and propene oxide as the main products.

Recently, a study by Molina and co-workers [64] has shown that Au clusters (Au_6-Au_{10}) can be selective for propene epoxidation. This work had three major differences, which were as follows: alumina film was used instead of TiO_2, water vapour was incorporated into the reactor feed instead of H_2 and sub-nanometer Au clusters were used instead of larger Au nanoparticles. They demonstrated that this alternative gold catalyst was effective, even when the support was changed from the typical TiO_2, which had previously been thought to be a key feature of the catalyst activity for propene epoxidation.

There are certain factors that have to be considered when trying to develop gold catalysts with good catalytic performance. Gold particles were most active when they were between 2-5 nm in size for CO oxidation and above 2 nm for propene oxidation. The type of support, preparation method and calcination temperature have also all been investigated to optimise catalyst performance. The temperature range of experiments can affect the selectivity towards particular products and therefore has to be taken into account.

The influence of different parameters, such as flow rate, nature of metal and type of support, have been studied for propene epoxidation.[65] TEM analysis revealed a particle size between 6 and 12 nm for the Au catalyst. The effect of flow rate on the propene epoxidation activity was investigated with a reactant mixture of 1000 ppm propene and 9% volume of oxygen in helium carrier gas. Baylet and group used the flow rates: 40, 60, 100, 120 and 145 ml min^{-1} which corresponded to 11,700, 17,500, 29,200, 35,000 and 40,800 h^{-1}. For all the catalysts, only carbon dioxide was the product detected. Their study showed that the higher the contact time, the lower the temperature ignition of the reaction. There was a 35-40 ^oC temperature difference between the T_{50} (temperature at 50% of propene conversion) at the lowest and highest flow rates. They found that for all the catalysts, at low temperatures equivalent to a conversion lower than 20%, the trend between reaction rate and the flow rate had a linear

relationship (between 40 and 145 mL min^{-1}). They also suggested that the presence of large gold particles affected the propene epoxidation activity.

Gold catalysts have been tested for propene oxidation and several parameters have been studied, such as the type of support and the gold metal loading.[66] Ceria, titania and alumina were the supports analysed and only ceria showed activity for propene oxidation and the most active catalyst was an Au/CeO_2 system. The group also found that, for the Au/CeO_2 catalyst, the activity was enhanced when the catalyst was activated under H_2 at 300 ^oC, compared to activation in He/O_2 at 500 ^oC. Au/CeO_2 (1 wt%) had a $T_{50\%}$ (conversion at 50% temperature) for propene oxidation at 165 ^oC, compared to Au/Al_2O_3 (1 wt%) and Au/TiO_2 (1 wt%) at 410 ^oC and 320 ^oC respectively. At a gold loading of 4 wt% on the ceria support, a $T_{50\%}$ was observed at 140 ^oC. 100% conversion towards carbon dioxide could be achieved at temperatures as low as 200^oC for Au/CeO_2 catalysts.

Gold catalysts loaded on a ceria-alumina support ($Au/_xCeO_2$-Al_2O_3) have been tested for propene oxidation and the CeO_2 loadings and activation treatment investigated.[67] Loadings of 1.5, 3, 5 and 10 wt% CeO_2 were studied. The Au/CeO_2 catalysts were more active than the Au/Al_2O_3 or $Au/CeO_2/Al_2O_3$ catalysts. This work showed that all the calcined catalysts were less active for propene oxidation than the reduced catalysts. They suggested that this could have been due to the size of the gold particles because the calcined catalysts had larger particles. The activity of the reduced catalysts increased with the ceria loading, whereas the activity decreased for the calcined catalysts. The group stated that this was because the metallic gold was more active than oxidised Au, and that Au (0) on ceria was more active than Au (0) on alumina.

A density functional theory study on the effectiveness of partial oxidation of propene by gold has been reported by Roldan and co-workers.[68] They deduced that the formation of propene epoxide on Au(111) was greatly hindered, with the pathway to allyl radical being more likely

than the formation of the oxametallacycle intermediates. Their investigation involved carrying out periodic density functional calculations for a modelled Au(111) surface. Roldan and co-workers concluded that the Au surface was inefficient for the selective oxidation of propene, even when covered by atomic oxygen. Their results showed that the required formation of oxametallacycle reaction intermediates was thermodynamically favourable but not kinetically favoured. The pathway leading to an adsorbed allyl radical and adsorbed OH from hydrogen stripping was more kinetically favourable.

Transient kinetic experiments have been performed by Nijhuis *et al.* on gold-titania catalysts for the epoxidation of propene, using hydrogen and oxygen.[69] Their results showed that oxygen was playing a role in the reaction mechanism. The side product water also indicated that the oxygen was from the support. Oxygen-18 was used to substitute non-labelled oxygen and, by analysing the time and rate at which the labeled oxygen appeared in the products, information could be deduced on the reaction mechanism. Au/TiO_2 and Au/Ti-SBA-15 catalysts have a large oxygen pool of species which include intermediates and products (propene oxide, water and carbon dioxide). Their investigations revealed that carbon dioxide was formed by at least two different pathways. They also found that the support oxygen was present in the water produced and they suggested this was either due to the role of the support oxygen in its formation, or by an exchange with the support afterwards.

Bimetallic gold catalysts have been prepared and tested for propene epoxidation in the presence of hydrogen and oxygen.[70] Moulijn and group prepared the catalysts three different ways: deposition precipitation (DP), ion exchange (IE) and size-controlled gold colloids (SGC). It was discovered that the modification of the $Au/TiO_2/SiO_2$ catalyst with platinum enhanced the selectivity and activity for this reaction. For the catalyst prepared by DP, the highest yield of propene oxide was obtained (1.2%). A homogeneous distribution of gold particles was observed for both the DP and IE methods. Tetrakis (hydroxymethyl)

phosphonium chloride (THPC) was the stabiliser used for the SGC route and the presence of this stabilising agent appeared to reduce the propene epoxidation activity (yield < 0.01%). When platinum was added to the gold catalyst, a propene oxide yield of a propene oxide yield of 1% was detected and it was reported that the water-propene oxide ratio was reduced, whilst the epoxidation activity was kept constant. They also did another study, using gold/titania catalysts, that explored ways of increasing the product yield to propene oxide, which they deduced was low due to product inhibition.[71] Moulijn *et al.* explained the low yield of propene oxide (less than 2%) by using a non-Langmuir adsorption model and concluded that an increase in the catalyst loading did not lead to higher propene oxide yield, which they suggested was due to two possible reasons. The first was due to the consecutive reaction over Ti-O-Ti and the second was because of the presence of propene oxide adsorption-desorption equilibrium over active epoxidation centres. Therefore, it was reported that catalyst development was needed for this reaction and a possible change in the temperature and pressure parameters could help improve the propene oxide yield.

Trimethylamine (TMA) has been used to produce highly efficient epoxidation of propene over supported gold catalysts.[72] TMA is a strong Lewis acid and at very low concentrations (10-20 ppm) they have shown an improved activity in terms of catalyst regeneration, lifetime and propene oxide selectivity. The results showed lower deactiviation for the trimethylsilylated $Ba(NO_3)_2$ promoted Au/titanosilicate catalyst in the presence of 13-15 ppm TMA in the gas feed. After 5 hours, propene oxide selectivity remained as high as 80%. At around 200 ^{o}C, with trace amounts of the TMA promoter, it was shown that propene conversions of 8.5% and propene oxide selectivity of 91% could be achieved in a gas feed of propene, oxygen, hydrogen and argon (1:1:1:7).

The effect of reaction and preparation conditions for propene epoxidation using Ag/ TS-1 has been discussed by Wang *et al.*[73] Their work revealed that the presence of hydrogen was key

in the effective performance of the catalyst. The best activity and selectivity were obtained with a 2 wt% Ag loading, a ratio of Si/Ti in TS-1 of 64, a calcination temperature of 450 ^{o}C and the gas feed composition of propene: oxygen: hydrogen: nitrogen of 1:2:3:12, with a space velocity of 4000 h^{-1}. With these conditions, a propene conversion of 1.37% and selectivity towards propene oxide of 93.5% was achieved.

The reaction of propene epoxidation over Au/Ti-MCM-41 catalysts was studied with and without the promoter CsCl.[74] It was reported that the presence of the promoter increased the propene oxide selectivity. Without the promoter, a propene conversion of 3.1% and a propene oxide selectivity of 92% were observed, compared to a 1.7% conversion and a selectivity if 97% with the addition of CsCl. This work suggested that the promoter reduced the reaction of hydrogen with oxygen with little effect on the reaction of propene with oxygen. The presence of CsCl also caused the gold to agglomerate due to the chloride anions.

Propene epoxidation with H_2 and O_2 has been carried out for Au/titanium silicalite (TS-1) catalysts and the effect of composition and promoters studied.[75] The catalysts were prepared by deposition precipitation (DP) and the group found that the gold loading and catalytic activity were dependent on the pH of the solution used for the DP preparation. Gold catalysts, prepared at a low pH close to 7 gave high activity and stability due to formation of the surface with an isoelectric point, which improved the capture of anionic gold species. The work revealed that group two metal promoters, such as Mg, Sr, Ba and Ca, increased both the gold loading and the activity for propene oxidation. The best promoter was Mg, and the Au/Mg/TS-1 catalyst gave a propene oxide formation rate of 88 g PO h^{-1} kg_{cat}^{-1}, whereas the unpromoted Au/TS-1 catalyst had a propene oxide formation rate of 57 g PO h^{-1} kg_{cat}^{-1}.

1.7 Review of AuCu catalysts

The use of nanoalloys in catalysis is a rapidly expanding field. There has been immense interest in the use of supported gold nanoparticles as catalysts and bimetallic catalysts, containing gold in combination with other metals, represent an emerging field of research. While bulk copper–gold alloys are well-known and, indeed, are much studied systems, bimetallic copper–gold nanoalloys have received relatively little attention.

1.7.1 Introduction

Copper and gold are metals that have for a long time had many uses in catalysis. Superficially, they have similar chemistries - they are coinage metals found in the same group of the periodic table. However, their catalytic behaviour is quite different. Heterogeneous copper catalysts are well-known hydrogenation and oxidation catalysts, e.g. in the production of methanol.[76,77]

Bimetallic catalysts have attracted considerable attention recently,[78] in particular, since they offer a way to fine-tune the catalytic properties of metals. The structures of bimetallic catalyst particles have been analysed by microscopy, and studied using theoretical methods, as well as being used as catalysts for many reactions. Understanding the structure–activity relationships of these complex systems is a difficult task, but some progress has been made.

1.7.2. Preparation of CuAu bimetallic catalysts

A broad range of preparation methods have been discussed in the literature for AuCu catalysts, and the papers that have been highlighted indicate that the method chosen can have a significant effect on the structure and behaviour of the AuCu catalyst. Of the methods studied, impregnation using suitable soluble Au and Cu precursors is possibly the most straightforward. With this method, there is also the possibility of modification of the calcination and reduction procedures, following impregnation to fine-tune the structure. Catalysts, prepared by co-impregnation of silica with copper nitrate and tetrachloroauric acid, gave catalysts which were active for acrolein synthesis from propene.[79] They were activated by reduction for 2 h in flowing hydrogen at 315 ^{o}C, followed by calcination for 15 h at 676 ^{o}C. The copper–gold catalysts were more selective to acrolein than their monometallic counterparts. In addition, these materials could also be used for the selective oxidation of other alkenes. The structure of the co-impregnated catalyst after reduction was investigated using electron X-ray absorption fine structure spectroscopy (EXAFS),[80] and a degree of mixing was observed between copper and gold. In a reducing hydrogen environment, the gold segregated to the surface, whilst, in an oxidising atmosphere, the gold migrated towards the core. Such core–shell structures are commonly encountered in bimetallic alloy nanoparticles and these structures can be used to control catalyst performance. Similarly, co-impregnation of zeolites NaY (SiO_2/Al_2O_3 molar ratio = 5) and ammonium mordenite (SiO_2/Al_2O_3 molar ratio = 20) was also used to prepare bimetallic CuAu catalysts.[81] Here, the nature of the zeolite influenced the gold particle size markedly. For ammonium mordenite, particle sizes of about 8 nm were observed, whereas it was reported that sizes of 80 nm were recorded for the NaY zeolite. Transmission electron microscopy (TEM) showed that sintering of the nanoparticles did not occur on calcination at 500 ^{o}C. The nature of the zeolite also

affected the catalyst activity for CO oxidation. When supported on NaY, the Cu-only and CuAu catalysts exhibit similar activities, whilst the Au-only catalyst is much less active. On ammonium mordenite, however, the Cu-only catalyst is more active than the CuAu and Au-only materials. There was a significant hysteresis for the AuCu/zeolite catalysts, which suggests that the structure changes with temperature or time on-stream. Analysis of the catalyst after use would be interesting to determine if the catalyst nanoparticles remained bimetallic in nature. Co-impregnation of TiO_2 with tetrachloroauric acid and copper (II) chloride gave catalysts which were active after hydrogen reduction for propene epoxidation, with N_2O as oxidant.[82] The presence of copper–gold alloys was confirmed by XRD, the lattice parameter changing linearly with the Cu:Au ratio. Temperature programmed reduction showed two reduction peaks which were assigned to CuO and isolated Cu (+2) ions. These two reductions occur at the same temperatures for $AuCu_3/TiO_2$, $AuCu/TiO_2$ and Au_3Cu/TiO_2. Use of pre-formed CuAu core–shell nanoparticles supported on titania, instead of co-impregnated materials, was found to give an order of magnitude increase in activity.[83] The pre-formed nanoparticles were prepared, using copper nitrate and tetrachloroauric acid transferred into toluene and using tetraoctylammonium bromide as phase transfer agent. Cu (+2) and Au (+3) were reduced, using sodium borohydride and stabilised with dodecanethiol. The particles were impregnated onto titania and calcined at 300–600 ^{o}C. Thermogravimetric analysis (TGA), infrared (IR) spectroscopy and X-ray photoelectron spectroscopy (XPS) showed that the stabiliser was not present after calcination. The as-prepared particles were confirmed as being bimetallic by electron energy-loss spectroscopy (EELS) and high resolution transmission electron microscopy (HRTEM). A detailed HRTEM study of the catalysts was performed. The particle size of uncalcined samples was in the range 1.6–2.3 nm and this increased on calcination to 6–10 nm. The catalyst with the highest copper content, $AuCu_3/TiO_2$, sintered the least. Analysis of the lattice fringes confirmed the presence of

CuAu alloy particles. EELS showed a signal at 24 eV which is indicative of a CuAu alloy.[82] Figure 1.2 shows the TPR profiles for the $AuCu_3/TiO_2$ catalyst calcined at different temperatures. Calcination at 300 ^oC or 400 ^oC gave similar TPR profiles.

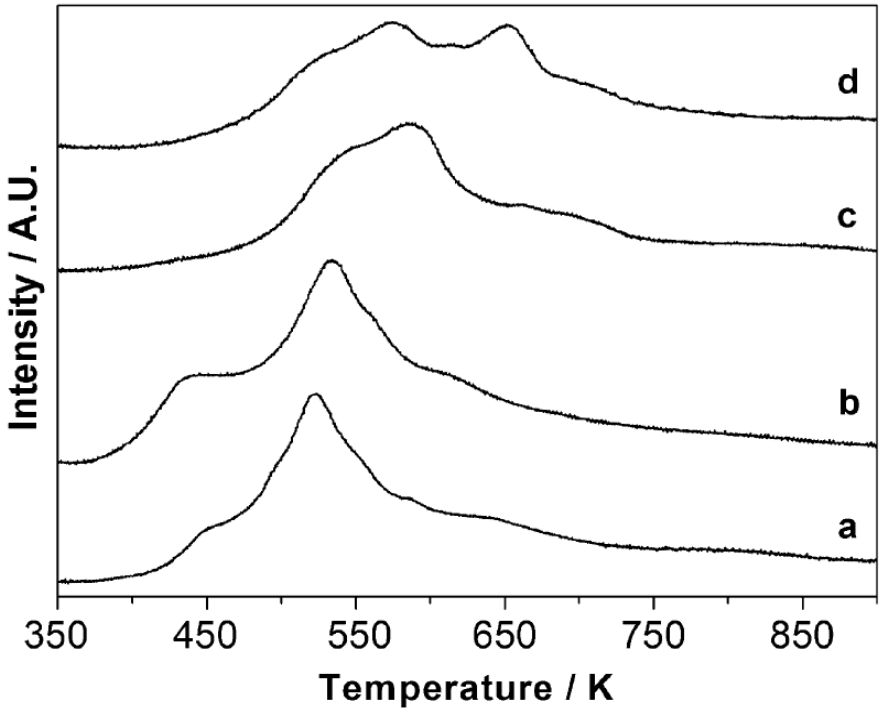

Figure 1.2 TPR profiles of $AuCu_3/TiO_2$ catalysts calcined at (a) 300 ^oC, (b) 400 ^oC, (c) 500 ^oC and (d) 600 ^oC.[83]

The low temperature peak was tentatively ascribed to small copper-rich clusters, whilst the main peak was due to the reduction of copper in AuCu nanoparticles. The increase in the low temperature peak, when the calcination temperature is raised from 300 ^oC to 400 ^oC, was thought to be due to better reduction of the TiO_2 support, due to an increased alloy–support interaction. The hydrogen uptake is greater than expected from reduction of the metal, and so

could be explained by surface adsorption of hydrogen, removal of residual ligands or reduction of the support. A further increase of the calcination temperature resulted in a loss of the low temperature peak and the appearance of intensity at higher temperature 377 ^{o}C to 477 ^{o}C. This was thought to be a consequence of increased particle size, as observed by TEM. The $AuCu_3/TiO_2$ composition with a loading of 1.2 wt% total metal displayed the best catalytic performance, both in terms of propene conversion and propene oxide selectivity. The composition of the catalysts, which were calcined at 400 ^{o}C, affected the propene conversion in the following order: $AuCu_3/TiO_2$ > $AuCu/TiO_2$ > Au_3Cu/TiO_2 > Au/TiO_2. Therefore, it was confirmed that AuCu alloy catalysts were more active than Au/TiO_2 monometallic catalysts after calcination at 400 ^{o}C. However, when the catalysts were calcined at higher temperatures, e.g. 500 ^{o}C and 600 ^{o}C, the catalytic performance declined. The same trend was observed for the selectivity towards propene oxide. Increasing the copper content increased the catalytic activity, which leads to the possibility that well-dispersed copper is responsible for the activity observed. Interestingly, this reason for activity can be linked to work carried out previously by Smolentseva *et al*.[81] which showed that the addition of copper stabilised the gold nanoparticles for CO oxidation, whereas, in this paper, the addition of gold enabled the formation of finely dispersed copper that enhanced activity. Preparation of a monometallic Cu/TiO_2 catalyst by this route was not possible. However, earlier work[82] showed that bimetallic $AuCu/TiO_2$ catalysts were more active than Cu/TiO_2 for propene oxidation.

CuAu catalysts have also been prepared by a modified impregnation–precipitation route, using titania nanotubes as a support.[84] Copper was first added to the nanotubes by impregnation using copper nitrate, followed by deposition of gold using ammonia to hydrolyse the tetrachloroaurate. The product was annealed under hydrogen at 150 ^{o}C. The effect of gold doping on the activity of 8% Cu/TiO_2 is shown in Figure 1.3.

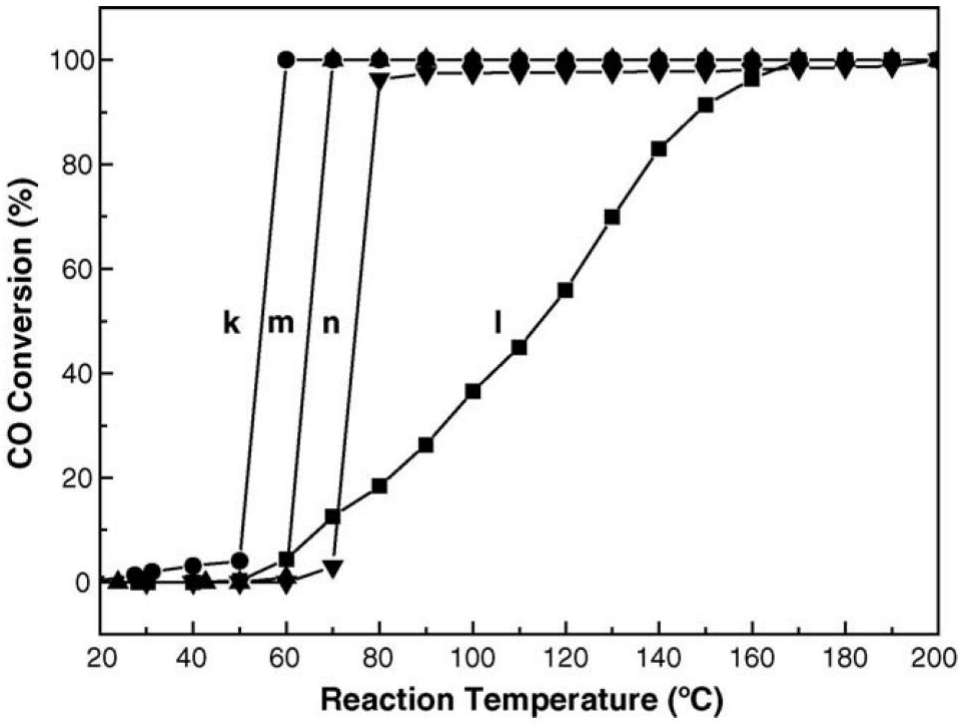

Figure 1.3 CO oxidation activity of (k) 0.5% Au/TiO_2, (l) 0.1% Au/TiO_2 (m) 0.1% Au-8% Cu/TiO_2 and (n) 8% Cu/TiO_2 [84]

The result of this doping is to slightly lower the temperature at which 100% conversion of CO oxidation is obtained. The addition of copper was suggested as a method of thrifting gold. It is possible that the redox chemistry of copper would lead to hysteresis in the observed catalysis with increasing and decreasing temperature under reaction conditions.

1.7.2.1. Preparation methodology for CuAu nanoparticles

The preparation of nanoalloy particles is a rapidly expanding field, which has recently been reviewed.[85] Materials scientists commonly approach this task in a very different manner to catalytic scientists but, typically, the materials produced by the materials science community

are not tested as catalysts. Nanoparticles can be prepared by many different methods, from those where only a few particles are synthesised through to those used in larger scale material preparations. Many of these methods are potentially suited to catalyst preparation but have not been exploited, thereby highlighting an interesting possibility where the fields of catalysis and materials synthesis can be united to mutual benefit. An illustration of relevant processes is given below. Ligands have been used in many reactions to help control the reactivity of metals. Suitable ligands (e.g. 1,2-dimyristoyl-snglycero-3-[phospho-rac-(1-glycerol)](sodium salt) (DMPG) or hexamethylene-1,6-bis (dodecyldimethylammonium bromide) (12-6-12) are often used to control particle growth in liquid phase syntheses of nanoparticles. Schaak *et al.* studied the reduction of copper acetate and tetrachloroauric acid, either by thermolysis in tetraethylene glycol[86] or by borohydride reduction[87,88] in the presence of polyvinylpyrrolidone (PVP) stabiliser, to produce gold–copper colloids of various compositions. XRD was again used to demonstrate alloy formation; it also showed that Cu_2O was also observed in some cases due to re-oxidation. Selected area electron diffraction (SAED) showed that the particles were bimetallic, in agreement with bulk XRD data. The particles synthesised by thermolysis at 310 ^{o}C were ordered alloys, whilst those prepared at lower temperatures were disordered. CuAu particles with an unusual structure have been prepared by seed growth[88] using DMPG as stabiliser. Gold seed particles were prepared by borohydride reduction of a tetrachloroauric acid–sodium citrate solution, and these were used to grow particles from a tetrachloroauric acid–copper sulfate–DMPG solution. The amount of copper added to the CuAu growth solution affected the structure of the gold particles and, at higher copper concentrations, decoration of the gold particles with smaller copper particles was observed. These are similar to the species which are believed to form, following reduction and high temperature calcination,[79,80] and so could possess similar catalytic properties. TEM showed that in the presence of DMPG, there was a pseudo-core–shell arrangement. Interestingly, when the

stabiliser was changed to hexamethylene-1,6-bis (dodecyldimethylammonium bromide), the effect of the copper on the structure of the gold particles was small, although some elongated particles were observed. In this system, higher copper content led to sintering of the gold particles, in contrast to the particles produced by borohydride reduction and dodecanethiol capping (described above), where the particles with the highest copper content sintered least on calcination. The stabiliser, sodium bis (2-ethylhexyl) sulfosuccinate (AOT), was used to prepare bimetallic CuAu particles using anionic microemulsion.[90] $Cu(AOT)_2$ was added to AOT in isooctane–water to form oil-in-water microemulsions. The copper was reduced by the addition of hydrazine and then, after 2 h, $HAuCl_4$ was added. The resulting particles were stabilised by the addition of 1-dodecanethiol to prevent further agglomeration. Characterisation of the nanoparticle solution by TEM and UV/visible spectroscopy demonstrated the formation of bimetallic particles. The nanoparticles produced were dispersed in polymers for sensor applications. However, a gold-containing polymer composite, without copper added, was a more sensitive detector for both ammonium hydroxide and hydrogen peroxide. Copper–gold particles in a silica matrix have been prepared by a sol–gel reaction of copper nitrate and tetrachloroauric acid with tetraethyl orthosilicate.[91] A high-temperature hydrogen reduction (500–900 ^{o}C for 5 h) was used to produce the alloys after calcination at 250 ^{o}C. The alloy structure was confirmed by electron diffraction, TEM and XRD. Electrodeposition from suitable copper–gold solutions has also been used to synthesise AuCu alloy particles.[92] A cyanoalkaline solution (made up of 6.4–8.0 g KCN, 6.4–8.8 g $KCu(CN)_2$, and 1.0–3.0 g $KAu(CN)_2$) in de-ionized water was used to electroplate a 10–20 mm thick AuCu foil onto a titanium substrate. The as-deposited material required a vacuum annealing treatment to form a crystalline CuAu alloy, as demonstrated by XRD. The stability of the nanocrystalline grain size of the alloy coating was of interest, as it is strongly linked to mechanical properties such as hardness and strength. Physical methods

have also been used to prepare CuAu particles. Implantation of Cu^+ and Au^+ ions onto a silica slide, followed by annealing in hydrogen at 900 ^oC [93-95] and sputtering of atoms from gold and copper metals onto a suitable support, both gave bimetallic particles.[96-98] A high temperature reduction step was found to be crucial to the alloy formation in systems where the particles are produced directly from ions or atoms. Mattei *et al.* [99] showed, using visible spectroscopy, that a reduction treatment for their sputtered CuAu/SiO_2 materials was required to give alloying. For the as-prepared samples, only a gold plasmon band was observed, whilst, for the reduced bimetallic systems, the plasmon band position changed monotonically with the copper content, showing that the Cu was alloyed with the gold particles. There are many synthetic methods which can be applied to the synthesis of bimetallic copper–gold particles, from straightforward procedures, such as co-impregnation, through to methods which need highly complex and expensive instrumentation. One common theme is that a high-temperature reduction step is necessary for the formation of alloyed particles.

1.7.3 Characterisation of AuCu alloys

A number of techniques are typically used to characterise CuAu alloys; in particular, XRD, UV/visible spectroscopy and TEM.

1.7.3.1 UV-visible spectroscopy

The key question when analysing copper–gold particles is whether the metals are alloyed, or present as separate monometallic species. One way to determine this is to carry out a surface plasmon resonance (SPR) study using UV-visible spectroscopy. A number of studies have used this characterisation technique.[90,91,99] Mattei *et al.*[99] evaluated the effect of annealing in a

reducing atmosphere on AuCu alloys and found that, before annealing, no surface plasmon resonance band was observed, except for pure Au which had a minimal plasmon band. They suggested that this indicated that the copper was present in an oxidised form. After annealing, there were more noticeable plasmon bands for the CuAu materials, confirming alloy formation. Del Castillo-Castro *et al.* [90] used UV/visible spectroscopy to examine CuAu systems, prepared using a microemulsion technique. Prior to gold addition, no plasmon resonance was observed, despite the presence of small copper nanoparticles. The plasmon band was thought to be too weak to be observed, due to the low concentration of copper used and the small nanoparticle size. However, ten minutes after the addition of $HAuCl_4$, a plasmon band was observed at 530 nm intermediate to that for Au (520 nm) and copper (570 nm). Analysis of the plasmon band position was also used to understand the annealing of AuCu particles in a silica thin film,[91] after high temperature treatment in hydrogen. For the AuCu system, the band position moved to shorter wavelength with temperatures from 500 to 700 ^{o}C. However, above 700 ^{o}C, there was no further change, which indicates that AuCu nanocrystal formation was complete after annealing at 700 ^{o}C. Optical spectroscopy has been carried out on CuAu nanoparticles in silica glass to assess the effect of thermal annealing.[97] Figure 1.4 shows the optical absorption spectra for both pure Cu and Au on silica, as well as three compositions of AuCu samples. The study revealed that during the annealing process a SPR band was observed.

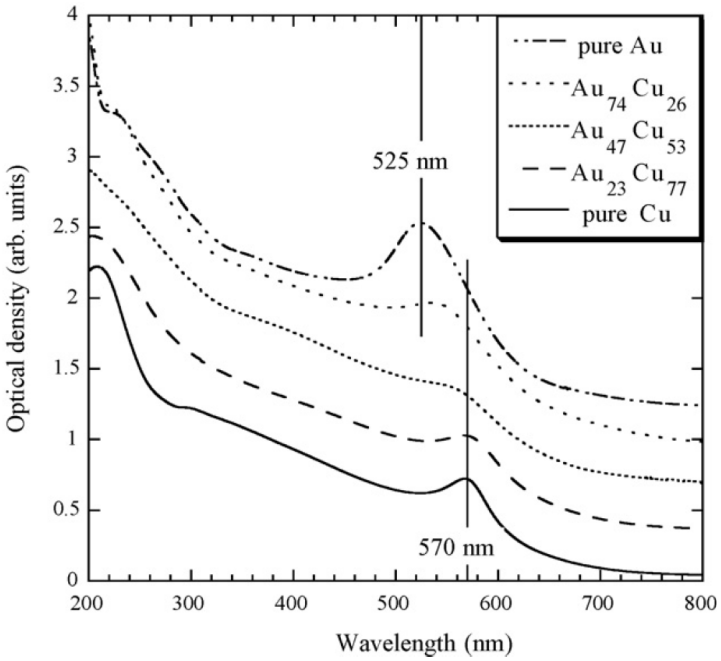

Figure 1.4 UV-visible spectra of annealed (Au + Cu)–silica samples prepared by sputtering.[97]

The spectra obtained of the different Au–Cu ratios showed that the band shifted from the standard wavelength at 570–580 nm, associated with spherical Cu nanoparticles,[100] to the typical wavelength for spherical Au nanoparticles at 525 nm. The plasmon band position increased with increasing copper content.

1.7.3.2 Transmission electron microscopy

Del Castillo-Castro and co-workers [90] characterised CuAu nanoparticles, formed from a microemulsion technique, using TEM. The study showed CuAu nanoparticles which had an average diameter of 8 nm with a particle size range of 4–12 nm. Bakshi and group [89] similarly used TEM to characterise AuCu nanoparticles, produced using a $Cu(SO_4)_2/HAuCl_4$ sample with a 0.8 ratio that also consisted of the capping agent DMPG. The study revealed that the Au nanoparticles were arranged in a necklace-like structure, with copper present in a pseudo-core–shell arrangement and the shell made up of small Cu nanoparticles. The Cu

nanoparticles are not spherical but are observed to be more polyhedral and of size, around 5 nm. The investigation showed that a higher Cu–Au ratio formed larger Au particles, which is interesting, and also that the Cu initiated destabilisation of the Au system. TEM together with selected area electron diffraction (SAED) is a powerful tool for understanding the structure of AuCu bimetallic particles. An investigation by Sra et al. showed AuCu particles prepared by a modified polyol process.[86] Disordered alloys are formed from reactions performed at 150 and 250 ^{o}C in tetraethyleneglycol, and this is supported by their SAED patterns, whereas atomic ordering is observed in particles synthesised at 310 ^{o}C. SAED shows clearly the reflections of a face centred tetragonal AuCu structure, as would be observed for a bulk AuCu alloy. For the sample formed at 150 ^{o}C, the nanoparticles appear small and spherical, although closer inspection determines that some are elongated. Particle length and width were determined as 5 nm and 4 nm respectively, for AuCu at 150 ^{o}C. The AuCu alloy, formed at 250 ^{o}C, exhibited ellipsoidal distortion (6 x 7 nm). The AuCu nanoparticles, formed at 310 ^{o}C, were more ellipsoidal (8 x 10 nm) than those prepared at lower temperatures. This study highlights the ability to control the size, shape and structure of AuCu alloys by using the synthesis temperature as a key parameter, which is important for the application of AuCu alloys in catalysis. TEM was also used by Gwak *et al.*[91] to determine the morphology of an AuCu silica thin film, made *via* a sol–gel method, followed by thermal treatment in air for 10 h at 250 ^{o}C and H_2 at 500–900 ^{o}C for 5 h. The study showed the TEM micrograph of an AuCu alloy, heat treated to 900 ^{o}C. The data they obtained from this characterisation method showed that the nanoparticles were spherical in shape and had an average diameter of 45 nm, and the silica support had a thickness of 165 nm. They concluded that the AuCu nanoparticles exhibited a face centred cubic structure, which was supported by XRD. High-resolution TEM has been used to analyse CuAu/TiO_2 catalysts produced from thiol-capped CuAu particles.[83] Individual nanoparticles were observed, and the effects of calcination and composition on

particle size were determined. EELS showed a signal which was assigned to the presence of a CuAu alloy.[82]

1.7.3.3 Atomic force microscopy

Atomic force microscopy (AFM) has been used by Twardowski and Nuzzo [98] to study an AuCu thin film. The film was produced by co-sputtering onto a Ti-modified glass slide, using gold and copper sputtering targets. When the resulting material is cleaned with "piranha solution" (3:1 concentrated H_2SO_4–30% H_2O_2), followed by treatment with 3:1:16 HCl–HNO_3–H_2O, the metal grains increase in size to larger, irregular shaped nanoparticles. Copper was shown to be more reactive to the oxidising piranha solution/aqua regia treatment than gold; a copper-only sample had all its copper removed after 5 s treatment. However, the CuAu samples exhibited some stability to the treatment due to alloy formation. AFM was used to probe the surface roughness of the thin films produced. All the CuAu samples showed significant crystal growth after the piranha solution–aqua regia treatment, and this increased with increasing copper loading. The surface roughness of the films was calculated by analysis of the AFM images and found to decrease with increasing Cu loading for the treated thin film samples. Maldonado and co-workers [101] prepared AuCu alloys by thermal evaporation and then annealed the AuCu systems in argon between 100 ^{o}C and 400 ^{o}C. The AuCu film morphology was analysed using AFM. The AFM images show that after the annealing treatment the grain size increased. For an AuCu film thickness below 33 nm, Au coverage was not complete and instead islands were formed. The use of AFM allows structural features such as grain size to be investigated. This would be less easy to understand using other techniques, for example TEM or XRD.

1.7.3.4 X-Ray diffraction

XRD characterisation can be readily applied to AuCu alloys and, as long as the nanoparticles are sufficiently large, the XRD pattern can be used to determine if alloy formation has occurred during synthesis. XRD characterisation has been used to determine the crystalline structure of AuCu films (Figure 1.4).[101]

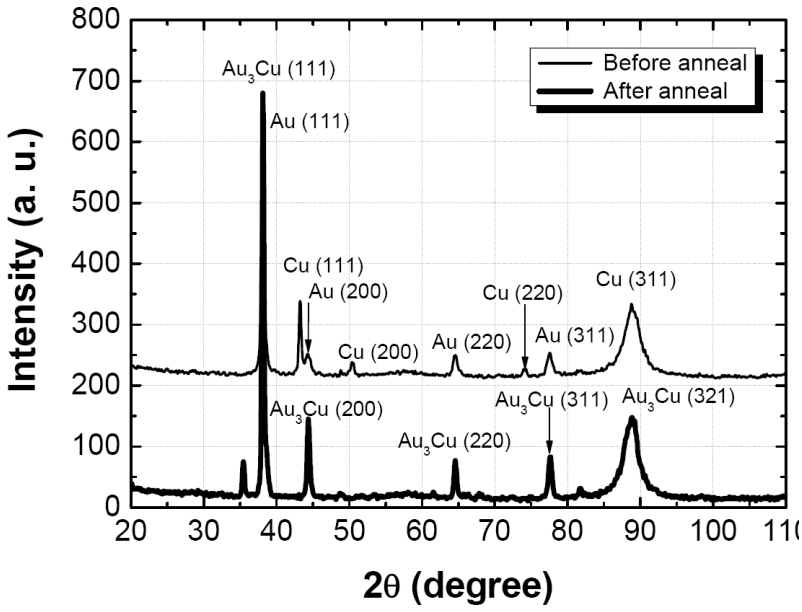

Figure 1.4 XRD patterns for AuCu films before and after annealing [101]

Annealing was required to form a CuAu alloy; monometallic Cu and Au were identified in non-annealed samples. For calcined samples, CuO (tenorite) can be present, but this is often obscured by more highly crystalline gold species. Bogdanovite (Au_3Cu) also overlaps with all the gold reflections.[102] XRD analysis of CuAu nanoclusters in a silica matrix [91] gave a single sharp reflection at 40.28^o 2θ superimposed on a broad background arising from the silica. The sharp reflection was assigned to AuCu with lattice parameter 3.872 Å. Some asymmetry of this reflection was observed, especially following a lower temperature annealing treatment

(500–700 ^{o}C), due to the presence of residual amounts of gold. $CuAu_4$ nanoclusters in the same system gave three reflections which were assigned to the (111), (200) and (220) reflections, with a lattice parameter of 3.995 Å. Kameoka and Tsai [103] obtained an active Au/TiO_2 catalyst for CO oxidation by selective leaching of Cu from ordered $AuCu_3$. Two precursors were used for this study: an ordered $AuCu_3$ which is an intermetallic compound and a disordered $AuCu_3$ which is a solid solution. The precursors were prepared from the pure metals in an arc furnace, and thermally treated in different ways to create or minimise structural disorder. By using ordered and disordered forms of $AuCu_3$, the microstructure and catalytic activity could be investigated after leaching, without considering the composition. The intermetallic $AuCu_3$ was characterised using XRD, before and after the compound was leached in 50% HNO_3 aqueous solution. The study showed that, after leaching, the ordered $AuCu_3$ diffraction peaks disappeared, whereas the initial disordered phase was still present. Only Au peaks were observed after leaching; no copper or copper oxide were observed for the ordered $AuCu_3$. As with much characterisation, different techniques give information on different aspects of CuAu materials. Some are good for determining whether an alloy has been formed (e.g. visible spectroscopy or XRD) whilst others give information on particle size distribution. Yet each has limitations or drawbacks. Therefore, it is important to consider results together, rather than rely on one technique.

1.7.4 Theoretical studies of CuAu alloys

Theoretical investigation of copper–gold particles has given considerable insight into their structures and properties. Ferrando *et al.* [85] have recently reviewed the area. Theoretical work aims to establish the structure of copper–gold alloy particles and the distribution of gold and copper throughout the nanoparticles. Most studies conclude that the particles are not

homogeneous alloys, but that there is some degree of segregation of copper into the core and gold towards the mantle (outer part of the particle). Bimetallic particles can often be significantly different to monometallic ones. For example, the effect of exchanging a copper atom into a gold cluster has been investigated.[104] Pure copper clusters were found to adopt an icosahedral geometry, whilst pure gold clusters were significantly less symmetrical and in fact, amorphous in some cases. However, substitution of one gold atom by copper was enough to change the structure back to an icosahedral fragment. Clusters with compositions CuAu and $CuAu_3$ were comprised of layered Cu and Au; whereas those with composition Cu_3Au had Cu and Au atoms in a more mixed arrangement. For the icosohedral structures, Cu was the central atom in the cluster due to its smaller size.

When layered structures are formed, the surfaces of the clusters comprise mainly gold atoms, whereas the copper atoms are located preferentially in the bulk. A trend was observed for the bulk cohesive energies that decreased in the order: Au ~3.81 eV > $CuAu_3$ ~3.75 eV > CuAu ~3.74 eV > Cu_3Au ~3.64 eV > Cu ~3.49 eV. Therefore, it was concluded that the atomic mixing and segregation was determined by a number of factors e.g. minimisation of surface energy, reducing internal strain, atomic packing efficiency and structures that can take advantage of strong Au–Au or Au–Cu interactions. Johnston and co-workers [105] discovered that copper-rich CuAu clusters had more disordered structures. Many geometries were found to be possible for the different 34-atom CuAu clusters. An Au_{34} cluster was disordered, whilst perfect core–shell structures are observed for $Au_{28}Cu_6$and $Au_{27}Cu_7$. Joshi and co-workers [106] studied hydrogen peroxide formation from H_2 and O_2 and investigated the effect of gold–silver, gold–copper and gold–palladium dimers and trimers. Using DFT methodology, they determined the ground state geometries of the clusters and based the reaction pathway on these to determine the thermodynamics and kinetics of the reaction. They investigated a total of fifteen clusters to observe the thermodynamic and kinetic constraints on H_2O_2 formation.

The first H_2 addition to form an OOH species was thermodynamically unfavourable for all the Cu-containing dimers and trimers, except $CuAu_2$, and H_2O_2 formation was unfavourable for $CuAu_2$. However, the formation of the OOH and H_2O_2 species for PdAu and Pd_3 kinetically and thermodynamically favourable and was therefore active for H_2O_2 production, in line with experimental results for PdAu catalysts. The structure of copper–gold clusters with three different compositions—Cu_3Au, CuAu and $CuAu_3$—has been investigated by simulation of their growth, starting from three different seeds.[107] Atoms of copper and gold were added, one-by-one, to the seeds, using molecular dynamics. Interestingly, the structure of the CuAu particles was found to depend on the particle size. For clusters of size 160 atoms or 200 atoms, the CuAu clusters were all icosahedral; whilst for 100 atoms, the CuAu particle was icosohedral, $CuAu_3$ was a double icosohedron and Cu_3Au was decahedral. Some segregation of copper and gold was also observed in the particles. In a separate experiment, copper atoms deposited onto an Au_{147} core did not migrate into the core. This information is very applicable to catalysts; for example, core–shell has been reported for both Au_{core}–Cu_{shell} and Cu_{core}–Au_{shell} compositions, depending on the atmosphere.[80] A molecular dynamic study of the bimetallic nanoparticles Au_xCu_y [108] found the structures to be octahedral, decahedral or icosahedral. At low cluster sizes, with composition between $AuCu_3$ and Au_9Cu_1, the AuCu clusters were stable icosahedra. However, for compositions between $AuCu_3$ and Au_3Cu, a (pseudo) cuboctahedral phase was present. It was determined that the main factors that affected the structural behaviour of the clusters were the cluster size, alloy composition and temperature. It showed the thermal behaviour for different alloy concentrations in a cluster of 561 atoms. The melting temperature was determined as 277 ^oC and this lowered as the particle size decreased. The density and specific heat, for the undercooled liquid AuCu alloys in a wide composition range (Au, Au_3Cu, AuCu, $AuCu_3$ and Cu), have been studied by a molecular dynamic method, [109] above and below the melting point. The magnitude and

temperature dependence of the alloy density increased with an increase in the Au concentration, and the specific heat of the alloys increase exponentially with an increase in the copper concentration. The theoretical studies highlighted in this review have concentrated on clusters derived from the three well-known stable, bulk AuCu compositions, i.e. AuCu, Au_3Cu and $AuCu_3$. They also focus on the differences between these AuCu clusters and pure Au and Cu clusters. Only one copper atom doped into a gold cluster is required to cause the structure of the cluster to rearrange. Clearly, the purpose of these studies has been to try to understand the structure, properties and compositional relationships in bimetallic clusters. It is anticipated that these theoretical studies will be informative in catalysis with nanoalloys of AuCu.

1.7.5. Use of CuAu alloys as catalysts

1.7.5.1 CO oxidation

CO oxidation is an exceptionally well studied reaction, due to its importance in many applications, e.g. removal of CO from fuel cell feedstocks and CO_2 lasers and the water gas shift reaction. There has also been intense academic interest in the active species in gold catalysts for the reaction and, despite significant effort, this remains a controversial area. In a series of Au/TiO_2 nanotube catalysts [84] with gold added by deposition–precipitation, modification of the nanotube with copper nitrate, followed by calcination before the addition of gold, gave a more active catalyst than one without copper present. The temperature at which there was 100% CO conversion was 70 ^oC for $AuCu/TiO_2$ but was much higher (170 ^oC) for Au/TiO_2. The monometallic copper catalyst was also active for CO oxidation but less so than the CuAu catalyst. The paper showed that the CuAu catalyst containing 0.1% Au was

significantly more active than the 0.1% Au/TiO_2 catalyst, and more active than the corresponding Cu/TiO_2 catalyst. This was ascribed to a synergistic interaction between copper and gold, which enhanced the catalytic activity. It was not clear whether both copper and gold are active in this catalyst (i.e. the increase in activity was due to one metal aiding the dispersion of the second metal), or whether one metal was acting as a promoter for the other. The $AuCu/TiO_2$ catalyst was shown to be stable for at least 10 h under reaction conditions. Iwasawa and co-workers studied CO oxidation [110] for a number of catalysts, containing Au precipitated on metal hydroxides, including $Cu(OH)_2$. The catalytic activities were compared and $Au(PPh_3)(NO_3)/Mn(OH)_2$ had a 50% conversion at a temperature less than -70 ^oC and 100% conversion at 0 ^oC, whereas the $Au(PPh_3)(NO_3)/Cu(OH)_2$ catalyst did not perform as well, achieving 50% conversion at 61 ^oC and 100% conversion at 170 ^oC. However, the $Au(PPh_3)(NO_3)/Cu(OH)_2$ catalyst was more active than similar catalysts based on hydroxides of V, Al or Cr. Cu/zeolite materials were found to be more active for CO oxidation than either Au/zeolite or Au/Cu/zeolite [81] for zeolites NaY and ammonium mordenite. When the activity of the Au/Cu/zeolite catalysts was compared at increasing and decreasing reaction temperatures, a distinct hysteresis was observed. The decreasing reaction temperature part of the experiment showed higher activity than the increasing temperature section for Au/Cu/NaY, whereas Au/Cu/ammonium mordenite had a higher activity for the increasing temperature section than the decreasing temperature section. The hysteresis showed that the structure of the nanoparticles is changing during the experiment. As the monometallic Cu/zeolite was the most active catalyst observed in the study, this could relate to Cu segregation for Au/Cu/NaY and Au segregation for Au/Cu/ammonium mordenite. AuCu catalysts have also been used in a study to generate gold catalysts for CO oxidation, by the dissolution of copper from an intermetallic $AuCu_3$ compound.[103] The performance of the Au catalyst, after the Cu was leached from $AuCu_3$, was comparable to the activity of a standard

Au/TiO_2 catalyst for CO oxidation. It is possible that the activity was due to a residual Cu oxide phase which was not detected by XRD. Gold catalysts derived from ordered $AuCu_3$ were more catalytically active than those generated from disordered $AuCu_3$. This could be due to a higher number of low-coordinate kink and step sites in the former sample.

Recently, Au-Cu alloy nanoparticles supported on silica gel have been studied for carbon monoxide oxidation by Liu *et al*.[111] Their main aim was to show the effect of different Au/Cu ratios between 3:1 and 20:1 on the activity for CO oxidation. The monometallic gold catalysts had a larger particle size of 5.7 nm, compared to between 3-3.6 nm for the Au-Cu bimetallic catalysts. The Au-Cu catalysts exhibited an enhanced activity, compared to the monometallic gold catalysts which, they suggested, indicated a synergy between copper and gold. They showed that the silica supported gold catalyst reached a full conversion of CO at 200 ^oC, whereas, the copper silica catalyst showed a poor activity. Irrespective of the Au/Cu ratio, all the bimetallic catalysts reached 100% conversion at a temperature of 30 ^oC. The $Au_{20}Cu_1/SiO_2$ catalyst had superior activity at room temperature out of all the catalysts tested. AuCu silica supported nanoparticle catalysts have, in recent times,[112] been studied for CO oxidation and the effects of their pre-treatments investigated. Dai and group confirmed alloy formation by XRD analysis. These catalysts were initially inactive towards CO oxidation. However, upon certain pre-treatments, they became highly active with 100% CO conversion below room temperature. If the $AuCu/SiO_2$ catalysts were calcined in O_2 at 200, 300 and 300 in 10% O_2/He, followed by annealing 10% H_2/Ar at 300 ^oC T_{50}, conversions were observed at 220^oC, 176^oC and 167^oC respectively. They suggested that the suppressed CO oxidation activity was due to the low calcination temperatures not removing all of the organic surfactants and, therefore, not allowing access to the catalytically active sites. But, if the catalysts were calcined at higher temperatures between 400-500 ^oC, the T_{50} conversions were observed at much lower temperatures of 25 ^oC and 6 ^oC. They concluded that the high

temperature calcination pre-treatments produced Au and amorphous CuO heterostructures, with a high degree of interfacial contact and strong thermal stability. Their work showed the importance of experimenting with catalyst pre-treatments to achieve the most effective catalytic composition for a chosen reaction.

1.7.5.2 Propene epoxidation

A number of different catalyst systems show activity for propene oxidation. Selectivity to acrolein or propene oxide can be observed, depending on whether the reaction proceeds via oxidation of the double bond, or via C–H activation.

Epoxidation of propene with N_2O was studied using $AuCu/TiO_2$ catalysts [82] at temperatures between 250 and 380 ^oC. The most active catalyst was 4% $AuCu_3/TiO_2$, giving a propene conversion of 40% at 380 ^oC. The major product was propanal with greater than 70% selectivity. The formation of propanal may be by isomerisation of propene oxide. The Au/TiO_2 catalyst was the least active and, at 300^oC, had a propanal selectivity of 6.4%; at the same temperature, 4% $AuCu_3/TiO_2$ had 12.7% selectivity to propanal. As the copper content increased in the bimetallic catalyst, the propene conversion and selectivity to propene oxide increased. As previously mentioned, Cu catalysts are used for propene epoxidation,[62] but this study showed that they were less selective than the AuCu catalysts with the same total metal loading. At 300 ^oC, the 4% $AuCu_3/TiO_2$ had a propene oxide selectivity of 26.3%, compared with 12.6% for the 4% Cu/TiO_2 catalyst. The propene conversions were also higher for the bimetallic catalysts with 4% $AuCu_3/TiO_2$ giving 4.3% conversion at 300 ^oC, compared with 2.4% conversion for 4% Cu/TiO_2 at the same temperature. The use of $AuCu/TiO_2$ catalysts prepared from thiol capped nanoparticles [83] gave a range of products. Propene oxide was observed as the major product, with smaller amounts of propanal, acetone, acrolein and

carbon oxides. As expected, the conversion increased as the reaction temperature increased. The catalysts deactivated after 10 h, although they could be reactivated if calcined at 300 ^{o}C in oxygen. Propene conversion increased with increasing copper content. The selectivity towards propene oxide also increased with increasing copper content. A maximum of 50% selectivity to propene oxide at 2.5% propene conversion was observed for $AuCu_3/TiO_2$ at 200 ^{o}C. The catalysts had the following order with respect to the propene oxide selectivity: $AuCu_3/TiO_2$ > $AuCu/TiO_2$ > Au_3Cu/TiO_2 > Au/TiO_2. The catalysts made from thiol-stabilised, pre-formed AuCu alloy particles were ten times more active than those prepared by impregnation. This effect was explained by the broad size distributions of the particles prepared by impregnation, compared to the pre-formed thiol capped method, which had nanoparticles of 4–7 nm. The selectivity towards propene oxide was higher for the catalysts made *via* the pre-formed method than impregnation. $AuCu_3/TiO_2$ was observed to give the highest yields of propene oxide. There was a clear improvement in both the conversion and the selectivity towards propene oxide, when the calcination temperature increased from 300 ^{o}C to 400 ^{o}C with a $AuCu_3/TiO_2$ catalyst. However, once the calcination temperature was increased to 500 ^{o}C above, there was a decrease in activity due to the nanoparticles being progressively decorated with oxidised Cu species.

Recently, a seed-based diffusion method of preparing monodisperse intermetallic CuAu and $CuAu_3$ nanocrystals has been designed.[113] XRD characterisation showed that $AuCu_3$ was formed at 300 ^{o}C when the Cu/Au ratio was set at 3:1. TEM images revealed spherical shaped particles for Cu_3Au with a particle size of 11±0.3 nm and CuAu with a size of 11±0.6 nm. They discovered that the size of the Au seeds was important for controlling the size of the nanoparticles. Another study has utilized the seed growth method, and rod-shaped copper and gold single crystal nanoparticles have been formed by Henkel *et al.*,[114] using this technique. The process involved the growth of small seeds of gold, which were pre-formed,

and a solution containing copper and gold ions was added, with the addition of a surfactant and mild reducing agent. Copper-gold alloy formation was confirmed from characterisation by TEM, UV-Visible and Dark Field Spectroscopy. They deduced that the particles had unique spectral properties and the copper content could control two central plasmon properties - the resonance position and line width.

The preparation and characterisation of an $AuCu_3$ alloy electrode for electrocatalytic applications has been designed by Zen and co-workers.[115] The alloy film was formed by a thermal annealing process onto a barrel-plated gold electrode plate (AuBPE). An electrochemical activation in alkaline solution formed a nanostructured $AuCu_3$ alloy film. They discovered that, after the annealing process, new reflections in their XRD pattern appeared which represented an $AuCu_3$ phase. The alloy film was tested for glucose oxidation, in pH neutral solution, to study its ability for use in electrochemical sensing applications. They showed that the nanostructured $AuCu_3$ alloy film had excellent performance because of its high electrocatalytic ability.

Nieuwenhuys *et al.* [116] investigated the total oxidation of propene and propane over gold-copper oxide on alumina catalysts and compared the results with Pt/Al_2O_3 and $Au/Co_3O_4/Al_2O_3$. The amount of gold present in the catalysts appeared to be more important on the catalytic performance than the copper oxide loading. They determined that the 7.4 wt% $Au/CuO/Al_2O_3$ sample was almost as active as the Pt/Al_2O_3. For propane oxidation, the most active catalysts were the 4 wt% $Au/CuO/Al_2O_3$ and 4 wt% $Au/Co_3O_4/Al_2O_3$ samples. The propene oxidation study revealed that the activation of O_2 was more effective with the Au-CuO system than the Au-Co_3O_4 system because of the ability of CuO to supply active oxygen during the catalytic reaction.

1.7.5.3 Benzyl alcohol oxidation

The selective oxidation of benzyl alcohol to benzaldehyde, catalysed by bimetallic AuCu catalysts, has been reported recently.[102] One of the most efficient catalysts for this reaction was a $AuCu/SiO_2$ sample with AuCu ratio of 4:1 by weight (approximately 4:3 molar ratio) and a total metal loading of 1 wt%, which gave a benzaldehyde yield of 98%. The catalysts were made by incipient wetness impregnation of SiO_2 with $HAuCl_4$ and $CuCl_2$ and reduced with $NaBH_4$. The oxidation of benzyl alcohol was performed between 250 and 350 ^oC. The monometallic Au catalyst gave 98% selectivity to benzaldehyde at 75% conversion at 326 ^oC, whereas the Cu-only catalyst showed the lowest activity with 78% selectivity at 326 ^oC. Careful optimisation of the bimetallic catalysts gave 100% selectivity at almost total conversion (98%). This was obtained by catalyst with weight ratio of AuCu = 0.25 at 313 ^oC. As the Au content of the catalyst increased, the selectivity to benzaldehyde increased.

1.7.6 Future prospects for the use of AuCu alloys in Catalysis

To date, there have only been a few reports on catalysis using supported AuCu nanoparticles and these have been limited to the oxidation of CO, benzyl alcohol and propene. A much larger proportion of studies have been associated with AuCu nanoparticle synthesis and characterisation, as well as fundamental work aimed at understanding the nature of the nanoalloy particles. However, in the absence of catalytic data to support these interesting studies, AuCu alloys will not be chosen over other catalysts for industrial reactions. Therefore, it can be concluded that, whilst the future of AuCu alloy catalysis is promising, there is still a considerable effort needed to find the most efficient synthesis strategy for AuCu nanoparticles that is effective in producing AuCu catalysts. The parameters that are

considered to be important include the particle size, shape and distribution, the type of support, preparation method and pre-treatment. In this respect, the requirements for active catalysts are similar to many reactions that are catalysed by supported metal nanoparticles. Given that gold catalysts display remarkable activity for a broad range of reactions, it can be anticipated that CuAu alloy nanoparticles could be of value in fine-tuning some of the observed activities.

1.8 References

1. K.J. Laider and A. Cornish-Bowden, New beer in an old bottle: Edward Buchner and the Growth of Biochemical Knowledge (1997) 123.

2. J.A. Campbell, *Journal of Chemical Education*, 62 (1985) 231.

3. C.H. Jones, *Chemical and Metallurgical Engineering*, 22 (1920) 1071.

4. E.F.G. Herington and L.A. Woodward, *Transactions of the Faraday Society*, 35 (1939) 985.

5. D.J. Nelson, R. Li and C. Brammer, *Journal of Organic Chemistry*, 70 (2005) 761.

6.T. Hayashi, K. Tanaka and M. Haruta, *Journal of Catalysis*, 178 (1998) 566 .

7. R. Pitchai, A.P. Kahn and A.M. Gaffney, US Patent No. 5,625,084, (1997).

8. B. Cooker, A.M. Gaffney, J.D. Jewson and W.H. Onimus, US Patent No. 5,780,657, (1998).

9. F.W. Zemichael, A. Palermo, M.S. Tikhov and R.M. Lambert, *Catalysis Letters*, 80 (2002) 93.

10. Z. Song, N. Mimura, J.J. Bravo-Suárez, T. Akita, S. Tsubota and S.T. Oyama, *Applied Catalysis A: General*, 316 (2007) 142.

11. R.P. Wang, X.W. Guo, X.S. Wang and J.Q. Hao, *Catalysis Today*, (2004) 217.

12. Venture claims H_2O_2 advance, *Chemical Engineering News*, 83 (2005) 14.

13. X. Wang, Q. Zhang, Q. Guo, Y. Lou, L. Yang and Y. Wang, *Chemical Communications*, (2004) 1396.

14. J.L. Meyer and B.T. Pennington, US Patent No. 4,992,567, (1991).

15. B.T. Pennington (Olin Coporation), US Patent No. 4,883,889, (1989).

16. B.T. Pennington (Olin Coporation), European Patent No. EP 0268870, (1988).

17. M.C. Fullington and B.T. Pennington, Patent Application No. WO 92/09588, (1992).

18. R.G. Bowman, A. Kuperman, H.W. Clark, G.E. Hartwell and G.R. Meima, US Patent No. 6,323,351, (2001).

19. M. Weisbeck, C. Schild. G. Wegener and G. Wiessmeier (BASF Corporation) US Patent No. 6,734,133, (2004).

20. A. Kupermen, R.G. Bowman. G.E. Hartwell, B.J. Schoeman. H.E. Tuinstra and G.R. Meima, US Patent No. 6,255,499, (2001).

21. M. Makkee, A. Zwijnenburg and J.A. Moulijn, Patent Application No. WO 03/062196, (2003).

22. A. Baylet, C. Capdeillayre, L. Retailleau, P. Vernoux, F. Figueras and A. Giroir-Fendler, *Applied Catalysis B: Environmental*, 96 (2010) 434.

23. Y. Li, Q. Fu and M. Flytzani-Stephanopoulos, *Applied Catalysis B: Environmental*, 27 (2000) 179.

24. Y. Tanaka, T. Utaka, R. Kikuchi, K. Sasaki and K. Eguchi, *Applied Catalysis A: General*, 242 (2003) 287.

25. H. Yahiro, K. Murawaki, K. Saiki, T. Yamamoto and H. Yamaura, *Catalysis Today*, 126 (2007) 436.

26. H. Yahiro, K. Nakaya, T. Yamamoto, K. Saiki and H. Yamaura *Catalysis Communications*,7 (2006) 228.

27. M.J.L Gines, N. Amadeo and M.C.R. Apesteguıa, *Applied Catalysis A: General*, 131 (1995) 283 .

28. M. Saito, K. Tomoda, I. Takahara, K. Murata and M. Inaba, *Catalysis Letters*, 89 (2003) 11 .

29. H. Yahiro, K. Sagata, T. Yamamoto, K. Saiki, M. Asamoto and H. Yamaura, *Catalysis Letters*, 124 (2008) 233.

30. P. Bera, S.T. Aruna, K.C. Patil and M.S. Hegde, *Journal of Catalysis*, 186 (1999) 36.

31. Y. Matsumura and H. Ishibe, *Applied Catalysis B: Environmental*, 91(2009) 524.

32. R. Perez-Hernandez, G. Mondragon Galicia, D. Mendoza Anaya, J. Palacios, C. Angeles-Chavez and J. Arenas-Alatorre, *International Journal of Hydrogen Energy*, 33 (2008) 4569 .

33. G.C. Chinchen, P.J. Denny, J.R. Jennings, M.S. Spencer and K.C. Waugh, *Applied Catalysis*, 36 (1988) 1.

34. Y. Liu, Y. Zhang, T. Wang, and N. Tsubaki, *Chemistry Letters*, 36 (2007) 1182.

35. K.H. Schulz and D.F. Cox, *Journal of Catalysis*, 143(1993) 464.

36. J.B. Reitz and E.I. Solomon, *Journal of American Chemical Society*, 120 (1998) 11467.

37. D. Torres, N. Lopez, F. Illas and R.M. Lambert, *Angewande Chem*ie *International Edition*, 119 (2007) 2101.

38. M. Labaki, J.F. Lamonier, S. Siffert, E.A. Zhilinskaya and A. Aboukaıs, *Colloids and Surfaces A: Physiochemical Engineering Aspects*, 227 (2003) 63.

39. O.P.H. Vaughan, G. Kyriakou, N. Macleod, M. Tikhov and R.M. Lambert, *Journal of Catalysis*, 236 (2005) 401.

40. H. Tüysüz, J.L. Galilea and F. Schüth, *Catalysis Letters*, 131 (2009) 49.

41. W. Su, S. Wang, P. Ying, Z. Feng and C. Li, *Journal of Catalysis*, 268 (2009) 165.

42. I. Onal, D. Düzenli, A. Seubsai, M. Kahn, E. Seker and S. Senkan, *Topics in Catalysis*, 53 (2010) 92.

43. M. Kahn, A. Seubsai, I. Onal and S. Senken, *Combinatorial Chemistry and High Throughput Screening,* 13 (2010) 67.

44. T. Miyazaki, S. Ozturk, I. Onal and S. Senken, *Catalysis Today,* 81 (2003) 473.

45. L. Yang, J. He, Q. Zhang and Y. Wang, *Journal of Catalysis*, 276 (2010) 76.

46. P. Lakshamanan, L. Delannoy, V. Richard, C. Méthivier, C. Potvin and C. Louis, *Applied Catalysis B: Environmental*, 96 (2010) 117.

47. M. Haruta, T. Kobayashi, H. Sano and N. Yamada, *Chemistry Letters*, (1987) 405 .

48. M. Haruta, N. Yamada, T. Kobayashi and S. Iijima, *Journal of Catalysis,* 115 (1989) 301.

49. G.C. Bond and D.T. Thompson, *Catalysis Reviews - Science and Engineering,* 41 (1999) 319 .

50. H.H. Kung, M.C. Kung and C.K. Costello, *Journal of Catalysis,* 216 (2003) 425 .

51. G.J.Hutchings, *Gold Bulletin*, 37 (2004) 3 .

52. M. Haruta, *Catalysis Today,* 36 (1997) 153 .

53. H. Zhu, C. Liang, W. Yan, S.H. Overbury and S. Dai, *Journal of Physical Chemistry B*, 110 (2006) 10842 .

54. C. Wang, H. Yin, R. Chan, S. Peng, S. Dai and S. Sun, *Chemistry of Materials*, 21 (2009) 433.

55. Z. Wu, S. Zhou, H. Zhu, S. Dai and S.H. Overbury, *Journal of Physical Chemistry C,* 113 (2009) 3726.

56. E.E. Stangland, K.B. Stavens, R.P. Andres and W.S. Delgass, *Journal of Catalysis*, 191 (2000) 332.

57. N. Yap, R.P. Andres and W.N. Delgass, *Journal of Catalysis*, 226 (2004) 156.

58. B.S. Uphade, Y. Yamada, T. Akita, T. Nakamura and M. Haruta, *Applied Catalysis A: General*, 215 (2001) 137.

59. A.K. Sinha, S. Seelana, S. Tsubotaa and M. Haruta, *Topics in Catalysis*, 29 (2004) 95.

60. A.K. Sinha, S. Seelan, M. Okumura, T. Akita, S. Tsubota and M. Haruta, *Journal of Physical Chemistry B*, 109 (2005) 3956.

61. A.K. Sinha, S. Seelan, S. Tsubota and M. Haruta, *Angewande Chemie International Edition*, 43 (2004) 1546.

62. C. Qi, T. Akita, M. Okumura and M. Haruta, *Applied Catalysis A: General*, 218 (2001) 81.

63. E. Sacaliuc, A.M. Beale, B.M. Weckhuysen and T.A. Nijhuis, *Journal of Catalysis*, 248 (2007) 235.

64. S. Lee, L.M. Molina, M. Lopez, J.A. Alonso, B. Hammer, B. Lee, S. Seifert, R.E. Winans, J.W. Elam and M.J. Pellin, *Angewande Chemie Interntional Edition*, 48 (2009) 1467.

65. A. Baylet, C. Capdeillayre, L. Retailleau, J.L. Valverde, P. Vernoux and A. Giroir-Fendler, *Applied Catalysis B: Environmental*, 102 (2011) 180.

66. L. Delannoy, K. Fajerwerg, P. Lakshmanan, C. Potvin, C. Méthivier and C. Louis, *Applied Catalysis B: Environmental*, 94 (2010) 117.

67. P. Lakshamanan, L. Delannoy, V. Richard, C. Méthivier, C. Potvin and C. Louis, *Applied Catalysis B: Environmental*, 96 (2010) 117.

68. A. Roldan, D. Torres, J. M. Ricart and F. Illas, *Journal of Molecular Catalysis A: Chemical*, 306 (2009) 6.

69. T.A. Nijhuis, E. Sacaliuc-Parvulescu, N.S. Govender, J.C. Schouten and B.M. Weckhuysen, *Journal of Catalysis*, 265 (2009) 161.

70. A. Zwijnenburg, M. Saleh, M. Makkee and J. A. Moulijn, *Catalysis Today*, (2002) 59.

71. A. Zwijnenburg, M. Saleh, M. Makkee and J.A. Moulijn, *Applied Catalysis A: General*, 270 (2004) 49.

72. B. Chowdhury, J.J. Bravo-Suárez, M. Daté, S. Tsubota and M. Haruta, *Angewande Chemie International Edition*, 45 (2006) 412.

73. R. Wang, X. Guo, X. Wang, J. Hao, G. Li and J. Xu, *Applied Catalysis A: General*, 261 (2004) 7.

74. B.S. Uphade, M. Okumura, S. Tsubota and M. Haruta, *Applied Catalysis A: General*, 190 (2000) 43.

75. J. Lu, X. Zhang, J.J. Bravo- Suárez, T. Fujitani and S.T. Oyama, *Catalysis Today*, 147 (2009) 186.

76. H. Iwai, T. Umeki, M. Yokomatsu and C. Egawa, *Surface Science*, 602 (2008) 2541.

77. R. Pérez-Hernández, G. Mondragon Galicia, D. Mendoza Anaya, J. Palacios, C. Angeles-Chavez and J. Arenas-Alatorre, *International Journal of Hydrogen Energy*, 33 (2008) 4569.

78. R. Ferrando, J. Jellinek and R.L. Johnson, *Chemical Society Reviews*, 108 (2008) 846.

79. H. Sinfelt and R.J Baron,*US Pat* 3989674, (1976).

80. G. Meitzner, G.H. Via, F.W. Lytle and J.H. Sinfelt, *Journal of Chemical Physics*, 83 (1985) 4793.

81. E. Smolentseva, N. Bogdanchikova, A. Simakov, A. Pestryakov, I. Tusovskaya, M. Avalos, M. H. Farias, J. A. Diaz and V. Gurin, *Surface Science*, 600 (2006) 4256.

82. R.J. Chimentao, F. Medina, J.L.G. Fierro, J. Llorca, J.E. Sueiras, Y. Cesteros and P. Salagre, *Journal of Molecular Catalysis A: Chemcal*, 274 (2007) 159.

83. J. Llorca, M. Dominguez, C. Ledesma, R.J. Chimentao, F. Medina, J. Sueiras, I. Angurell, M. Seco and O. Rossell, *Journal of Catalysis*, 258 (2008) 187.

84. B. Zhu, Q. Guo, X. Huang, S. Wang, S. Zhang, S. Wu and W. Huang, *Journal of Molecular Catalysis A: Chemical*, 249 (2006) 211.

85. R. Ferrando, J. Jellinek and R.L. Johnston, *Chemical Society Reviews*, 108 (2008) 845.

86. A.K. Sra, T.D. Ewers and R.E. Schaak, *Chemistry of Materials*, 17 (2005) 759 .

87. A.K. Sra, T.D. Ewers and R.E. Schaak, *Journal of American Chemical Society*, 126 (2004) 6667.

88. R.E. Schaak, A.K. Sra, B. M. Leonard, R.E. Cable, J.C. Bauer, Y-F. Han, J. Means, W. Teizer, Y. Vasquez, and E.S. Funck, *Journal of American Chemical Society*, 127 (2005) 3506.

89. M.S. Bakshi, F. Possmayer and N.O. Petersen, *Chemistry Materials*, 19 (2007) 1257.

90. T. Del Castillo-Castro, E. Larios-Rodriguez, Z. Molina-Arenas, M.M. Castillo-Ortega and J. Tanori, *Composites, Part A*, 38 (2006) 107.

91. J.H. Gwak, S.J. Kim and M. Lee, *Journal of Physical Chemistry: B*, 102 (1998) 7699.

92. A.F. Jankowski, C.K. Saw, J.P. Hayes, *Thin Solid Films*, 515 (2006) 1152.

93. K. Fukumi, A. Chayahara, K. Kadono, T. Sakaguchi, Y. Horino, M. Miya, K. Fujii, J. Hayakawa and M. Satou, *Journal of Applied Physics*, 75 (1994) 3075.

94. C. Maurizio, G. Mattei, P. Mazzoldi, S. Padovani, E. Cattaruzza, F. Gonella, F. D'Acapito and F. Zontone, *Nuclear Instruments and Methods in Physics Research Section B*, 200 (2003) 178.

95. F. Gonnella, G. Mattei, P. Mazzoldi, C. Sada, G. Battaglin and E. Cattaruzza, *Applied Physics Letters*, 75 (1999) 55.

96. S. Maupai, A.S. Dakkouri and P. Schmuki, *Surface Science*, 97 (2005) 20.

97. E. Cattaruzza,G. Battaglin, P. Canton T. Finotto and C. Sada, *Applied Surface Science*, 254 (2007) 1017.

98. M. Twardowski and R.G. Nuzzo, *Langmuir* , 18 (2002) 5529.

99. G. Mattei, G. Battaglin, E. Cattaruzza, C. Maurizio, P. Mazzoldi, C. Sada and B.F. Scremin, *Journal of Non-Crystalline Solids*, 353 (2007) 697.

100. G.C. Papavassiliout and T. Kokkinakist, *Journal of Physics F:Metal Physics*, 4 (1974) L67-L68 .

101. R.D. Maldonado, J.E. Corona and A.I. Olivia, *International Conference of Electrical Electronic Engineering, 3rd, Veracruz, Mexico,* (2006), *Sepetember 6-8* .

102. C. Della Pina, E. Falletta and M. Rossi, *Journal of Catalysis*, 260 (2008) 384.

103. S. Kameoka and A.P. Tsai, *Catalysis Letters*, 121 (2008) 337.

104. S. Darby, T.V. Mortimer-Jones, R.L. Johnston and C. Roberts, *Journal of Chemical Physics*, 116 (2002) 1536.

105. A. Rapallo, G. Rossi, R. Ferrando, R.L. Johnston, *Journal of Chemical Physics*, 122 (2005) 194308 .

106. A.M. Joshi, W.N. Delgass and K.T. Thomson, *Journal of Physical Chemistry C*, 111 (2007) 7384.

107. T.J. Toai, G. Rossi and R. Ferrando, *Faraday Discussions*, 138 (2008) 49.

108. J.L. Rodríguez-Lopez, J.M. Montejano-Carrizalesc, *Applied Surface Science,* 219 (2003) 56.

109. X.J. Han, M. Chen and Z.Y. Guo, *Journal of Physics:Condensed Matter*, 16 (2004) 705.

110. Y. Yuan, A. P. Kozlova, K. Asakura, H .Wan, K. Tsai, and Y. Iwasawa, *Journal of Catalysis*, 170 (1997) 191.

111. X. Liu, A. Wang, T. Zhang, D. S. Su and C. Y. Mou, *Catalysis Today*, 160 (2011) 103.

112. C. Bauer, D. Mullins, M. Li, Z. Wu, E. A. Payzant, S. H. Overbury and S. Dai, *Physical Chemistry Chemical Physics*, 13 (2011) 2571.

113. W. Chen, R. Yu, L. Li, A. Wang, Q. Peng and Y. Li, *Angewande Chemie International Edition,* 49 (2010) 2917.

114. A. Henkel, A. Jakab, G. Brunklaus and C. Sönnichsen, *Journal of Physical Chemistry C,* 113 (2009) 2200.

115. C-Y. Tai, J- L. Chang, J- F. Lee, T- S. Chan and J-M. Zen, *Electrochimica Acta*, 56 (2011) 3115.

116. A.C. Gluhoi, N. Bogdanchikova and B.E. Nieuwenhuys, *Catalysis Today*, 113 (2006) 178.

Chapter 2: Experimental

2.1 Introduction to techniques

A wide range of techniques have been used to characterise the $CuAu/SiO_2$ bimetallic samples, which will help to provide a better understanding of the nature and morphology of the catalyst. These techniques will be crucial to understanding the activity of the catalysts in the reactions discussed subsequently in this thesis.

2.1.1 X-ray Diffraction (XRD)

2.1.1.1 Introduction to XRD

X-ray diffraction is a bulk technique that can provide information about solid materials that can be used to determine:

- Crystal structure of an unknown material
- Crystallite size and shape
- Orientation of a crystal or grain

2.1.1.2 Theoretical principles

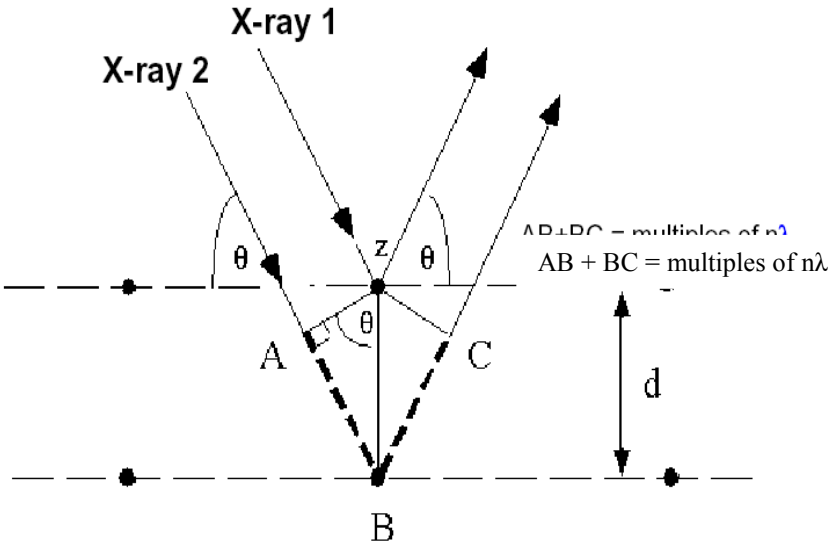

Figure 1 Derivation of the Bragg equation.

Bragg's Law

n λ =2dsinϴ

d - the distance between lattice planes in the crystal

λ - the wavelength of the incident X-ray beam

ϴ - the angle of diffraction

n - an integer

William Lawrence and William Henry Bragg discovered that crystalline solids generated patterns of X-rays. They found that these crystals, at certain specific wavelengths and incident angles, produced intense peaks of diffracted radiation called Bragg peaks. Bragg's law explains the condition for constructive interference from crystallographic planes. For a crystalline solid, the X-rays are diffracted from lattice planes separated by the interplanar distance *d*. Where the diffracted waves interfere constructively, they remain in phase since the path length of each wave is equal to an integer multiple of the wavelength. $2d\sin\theta$ is the

path difference between two waves undergoing constructive interference and θ is the diffracted angle. Bragg's law is a powerful tool for studying crystals in the form of X-ray diffraction and can help determine crystal structures.

2.1.1.3 Instrumentation

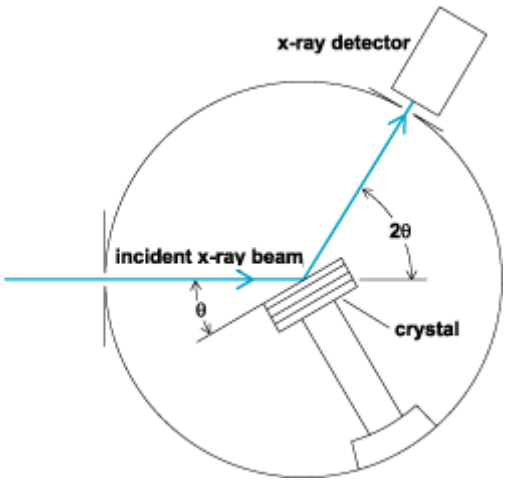

Figure 2 Diagram of a Powder X-ray diffractometer

Powder XRD was performed on a PANalytical X'pert Pro diffractometer using a Cu source operating with 40 mA and 40 kV. A Ge (111) monochromator was used to select Cu Kα X-rays. The powdered samples were compressed into an aluminium sample holder, which was rotated during data collection to compensate for any ordering of crystallite orientation which might have occurred during sample packing.

Data were calibrated against a silicon standard. Qualitative phase analysis can be used to match up the line positions and intensities to determine certain phases of the sample using the International Centre for Diffraction Data (ICDD) database. Crystallite sizes can be calculated using FWHM (full width half maximum) *via* the Scherrer equation:

FWHM = kλ x 57.3/ D cos θ

FWHM is in θ, k is the crystallite shape form factor, λ is the x-ray wavelength, D is the crystallite size and θ is the Bragg angle related to the maximum of the diffraction peak.

In situ X-ray diffraction was also carried out with the sample placed in a cell and exposed to different atmospheres and temperatures. This method allowed the different phase transitions to be monitored depending on the temperature and reduction/oxidation environment introduced to catalyst.

2.1.2 Surface area determination (BET)

2.1.2.1 Introduction to BET

The most widely used method of determining surface areas of solid catalysts is by using the B.E.T method which was derived by Brunauer, Emmett and Teller in 1938.

In this method the sample was first degassed to remove adsorbed contaminated molecules. The sample was placed into the vacuum chamber of the machine and Nitrogen flowed over the sample at 77 K (-196 ^{o}C) at different pressures to obtain an adsorption isotherm.

2.1.2.2 Principles of the BET method

The concept of the BET theory is an extension of the Langmuir theory, which is a theory for monolayer molecular adsorption, to multilayer adsorption with the following hypotheses: (a) gas molecules physically adsorb on a solid in layers infinitely; (b) there is no interaction between each adsorption layer; and (c) the Langmuir theory can be applied to each layer.

The BET equation is expressed below:

$$1/ X ((P_0/P) -1) = 1/X_mC + C-1/X_mC (P/P_0)$$

P and P_0 are the equilibrium and the saturation pressure of adsorbates at the temperature of adsorption.

X = quantity of gas adsorbed

P/P_0 = relative pressure

X_m = quantity of adsorbate as monolayer

C = BET constant

A straight line graph can be plotted of $1/[X(P_0/P)- 1]$ against (P/P_0). The intercept (I) and slope (S) can then be used to solve for X_m and C.

$S = C-1/X_mC$ $I = 1/X_mC$ $X_m = 1/ S + I$

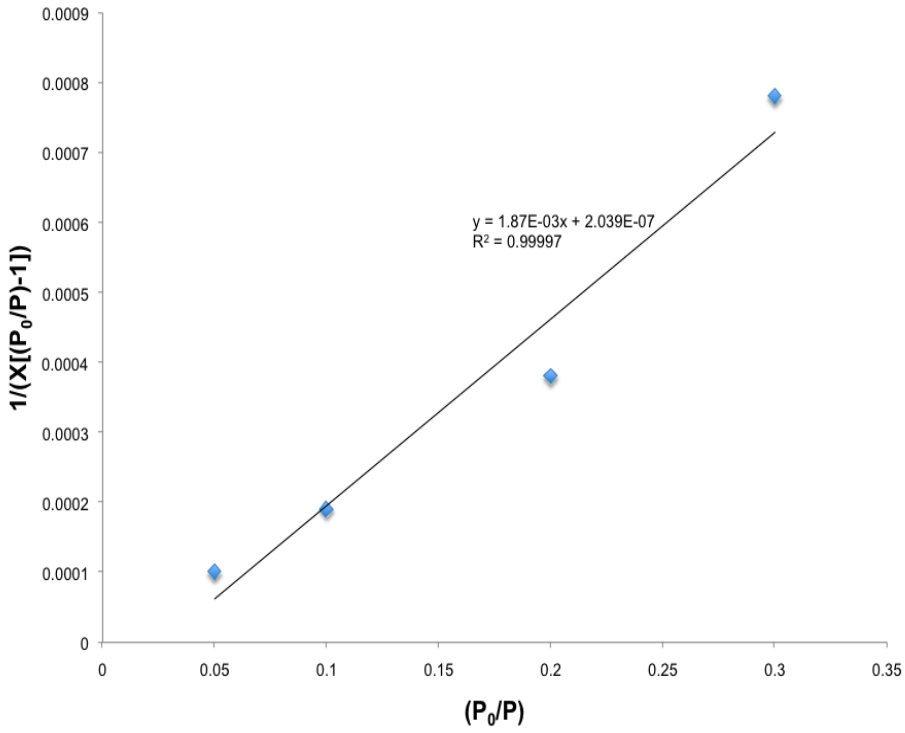

Figure 3 An example of a BET plot to derive X and C.

The BET method is widely used for the calculation of surface areas of solids by physical adsorption of gas molecules.

BET is a multilayer process and has five assumptions:

1. Adsorptions occur only on well-defined sites of the sample surface (one per molecule)

2. The only considered molecular interaction is the following one: a molecule can act as a single adsorption site for a molecule of the upper layer.

3. The uppermost molecule layer is in equilibrium with the gas phase, i.e. similar molecule adsorption and desorption rates.

4. Desorption is a kinetically-limited process.

5. At the saturation pressure, the molecule layer number tends to infinity (i.e. equivalent to the sample being surrounded by a liquid phase)

2.1.2.3 B.E.T Instrumentation

The Micromeritics Gemini 2360 Analyzer was used to determine the surface areas for all the catalysts. It is a fully automatic, single- or multi-point surface area analyzer. It uses a flowing-gas technique in which the analysis gas flows into a tube containing the sample and into a balance tube at the same time, and provides rapid and accurate sample analysis for solid material.

2.1.3 Temperature programmed reduction (TPR)

2.1.3.1 Introduction to TPR

TPR is used to identify properties and the reactivity of solid material under reducing or oxidising atmospheres when the temperature is changed. This technique is used to provide useful information on the reduction kinetics of oxidation catalysts.

TPR involves a catalyst being heated up at a constant rate in a flow of hydrogen diluted in argon. The amount of reducible species can be determined from the integration of the

hydrogen consumption peaks at specific temperatures. The rate of reduction is constantly followed by measuring the consumption of H_2 of the reducing gas mixture at the outlet of the reactor.

2.1.3.2 Principles of TPR

Different experimental operating variables used in temperature-programmed reduction (TPR) can influence measurements on the reduction profiles. The temperature range and the shape of the resulting TPR profiles can be markedly affected by the experimental conditions. A characteristic number, *K*, is defined to aid in selecting the values for the operating variables which should be chosen in order to obtain optimum reduction profiles. The number relates the heating rate, hydrogen concentration, total flow rate, and the amount of reducible sample in such a way that the operating variables can easily be adjusted. Upper and lower limits have been determined for this characteristic number, and this can be influenced by variation on the sensitivity of the TPR experiment. A peak shape analysis leads to narrower confidence limits for the kinetic parameters than an estimation based on the shift of the temperature of the maximum reduction rate measured for different heating rates.

2.1.3.3 TPR instrumentation

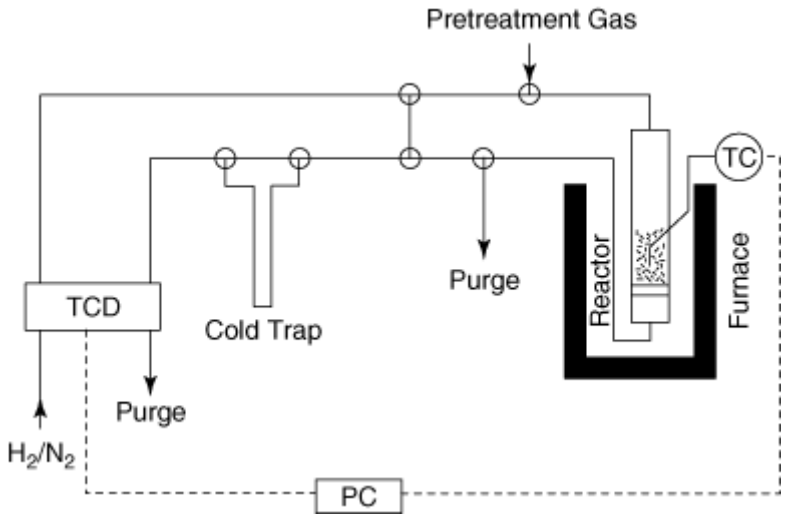

Figure 4 Schematic diagram of a TPR instrument

All samples were run on a TPDRO 1100 series machine. The reducing gas used in all experiments was 10% H_2 in Ar, with a flow rate of 50 ml min^{-1}. The temperature range explored was from room temperature to 600 °C. The heating rate was maintained at 10 °C min^{-1} for all samples while the sample mass employed was 20 mg.

2.1.3.4 TPR/TPO/TPR analysis

Temperature programmed reduction followed by temperature programmed oxidation has been carried out for the $AuCu_3/SiO_2$ catalyst prepared by co-impregnation. For the TPR technique, the oxidised catalyst precursor is submitted to a programmed temperature rise, while a reducing gas mixture is flowed over it (hydrogen in argon). In the TPO technique, the catalysts is in its reduced form and is submitted to a programmed temperature increase, with an oxidising mixture of gas (oxygen in helium) flowing over the sample. This technique is

useful as the analysis of TPR/TPO can obtain evidence for the interactions between atoms of two metallic components.

2.1.4 Scanning electron microscopy (SEM)

2.1.4.1 Introduction to SEM

Scanning electron microscopy (SEM), accompanied by X-ray analysis, is considered a relatively rapid, inexpensive, and basically non-destructive approach to surface analysis. It is often used to survey surface analytical problems before proceeding to techniques that are more surface-sensitive and more specialised. High resolution images of surface topography, with excellent depth of field, are produced using a highly-focused, scanning (primary) electron beam. The primary electrons enter a surface with an energy of 0.5 - 30 keV, and generate many low energy secondary electrons. The intensity of these secondary electrons is largely governed by the surface topography of the sample. An image of the sample surface can thus be constructed by measuring secondary electron intensity as a function of the position of the scanning primary electron beam. High spatial resolution is possible because the primary electron beam can be focused to a very small spot (< 10 nm). High sensitivity to topographic features on the outermost surface (< 5 nm) is achieved when using a primary electron beam with an energy of < 1 keV. In addition to low energy secondary electrons, backscattered electrons and X-rays are also generated by primary electron bombardment. The intensity of backscattered electrons can be correlated to the atomic number of the element within the sampling volume. Hence, some qualitative elemental information can be obtained. The analysis of characteristic X-rays emitted from the sample gives more quantitative elemental information. Such X-ray analysis can be confined to analytical volumes as small as 1 cubic micron.

2.1.4.2 SEM Instrumentation

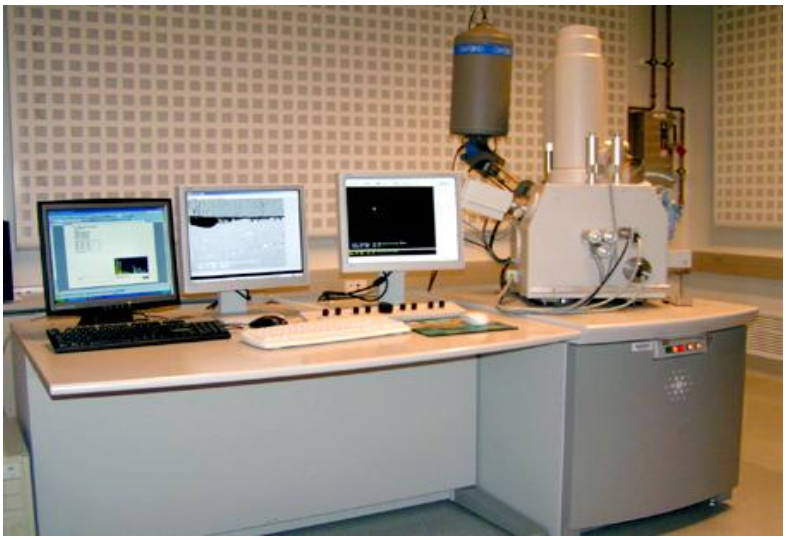

Figure 5 Photograph of a SEM machine in laboratory

The SEM machine used for analysis was a Carl Zeiss EVO 40 SEM. The conditions used were: Detector: Backscattering (BSD), Gun: Electron high tension (EHT) voltage = 10-25 kV Iprobe = 250pA

Essential components of all SEMs include the following:

- Electron Source ("Gun")
- Electron Lenses
- Sample Stage
- Detectors for all signals of interest
- Display / Data output devices
- Infrastructure Requirements:
- Power Supply
- Vacuum System
- Cooling system
- Vibration-free floor

- Room free of ambient magnetic and electric fields

SEMs always have at least one detector (usually a secondary electron detector), and most have additional detectors. The specific capabilities of a particular instrument are critically dependent on which detectors it accommodates.

2.1.4.3 SEM Analysis

For each of the catalysts, a small amount of sample was mounted on a carbon stub and positioned into the machine. The vacuum pump and the electron gun were switched on. An electron backscatter detector (ESBD) was used to obtain an image that could be used to determine the crystallographic structure of the specimen and identify the elements in sample.

2.1.4.4 EDX Analysis

The generation of X-rays from decelerating electrons can be ultilised for elemental analysis of the catalyst sample, known as EDX. This analysis involves the detection of X-rays from the sample area exposed to the electron incident beam. As this incident beam interacts with the sample atom, an inner core electron is removed, followed by relaxation of the electron and the production of an X-ray. This will have a specific energy unique to the element and be used to quantify the elemental composition of the catalyst. EDX analysis was carried out on a Carl Zeiss EVO- 40 and EDX mapping was performed on certain catalysts, using variable operating conditions depending on the sample.

2.1.5 Inductively coupled plasma analysis (ICP)

2.1.5.1 Preparation of samples and analysis

This technique was carried out at Johnson Matthey to determine the weight percentage of copper and gold in the catalysts. The instrument used was a Perkin Elmer Optima 3300RL and the microwave assisted digestion method involved aqua regia leaching of the copper and gold.

Dissolution of the sample was carried out and then the sample solution transported to the plasma. Once nebulised and inside the plasma the sample was vaporised, atomised and ionised. The radiation resulting from emission was transferred directly to a spectrometer where the various wavelengths were sorted optically, electronically detected and analysed.

2.1.6 X-ray photoelectron spectroscopy (XPS)

2.1.6.1 Introduction to XPS

X-ray photoelectron spectroscopy was developed in the mid 1960s by Siegbahn and his research group. The technique was centred on the photoelectric effect where the concept of the photon was used to describe the ejection of electrons from a surface when photons were imposed upon it. This technique is highly surface specific, due to the short range of the photoelectrons that are excited from the solid, and it can provide chemical bonding information.

2.1.6.2 Principles of XPS

The energy of a photon can be represented as: $E = h\upsilon$

h - Planck constant (6.62×10^{-34} Js)

υ - frequency (Hz) of the radiation

In XPS a photon is absorbed by an atom and this causes ionisation which leads to the emission of a core electron.

Every element has a unique binding energy associated with each core atomic orbital which gives a characteristic photoelectron spectrum with distinct peaks at certain kinetic energies determined by the binding and photon energy.

2.1.6.3 Instrumentation

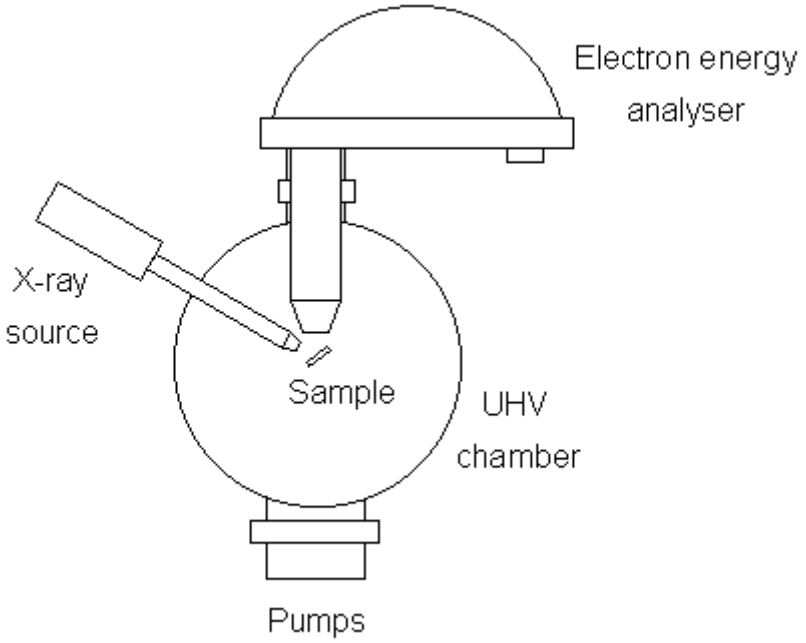

Figure 6 Schematic diagram of an XPS instrument

X-Ray photoelectron spectroscopy (XPS) was performed using a VG EscaLab 220i spectrometer, using a standard Al-Kα X-ray source (300 W) and an analyser pass energy of 20 eV. Samples were mounted using double-sided adhesive tape, and

binding energies were referenced to the C 1s binding energy of adventitious carbon contamination, which was taken to be 284.7 eV.

2.1.7 Transmission electron microscopy (TEM)

2.1.7.1 Introduction

TEM was first used by Knoll and Ruska in 1931 as an alternative to light microscopes. TEM uses electrons instead of light to image and measure materials at high resolution. This technique has many applications in the scientific fields, particularly in surface science.

2.1.7.2 Principles

In theory the maximum resolution (*d*) that can be achieved from a light microscope is limited by the wavelength (λ) of the photons involved and the numerical gap of the system, NA.

$$d = \frac{\lambda}{2\,n\,\sin\alpha} \approx \frac{\lambda}{2\,\mathrm{NA}}$$

It was then realised that electrons could be used instead and their wavelength can be derived from the de Broglie equation:

$$\lambda_e \approx \frac{h}{\sqrt{2m_0E(1+\frac{E}{2m_0c^2})}}$$

h = Planck's constant

m_0 = rest mass

E = energy of the accelerated electron

c = speed of light

TEM requires a "light source" at the top of the microscope to emit electrons that travel through vacuum in the column of the microscope. This technique uses electromagnetic lenses

to focus the electrons into a very thin beam and the electron beam travels through the sample. The image can be studied directly by the operator or photographed with a camera.

2.1.7.3 Instrumentation

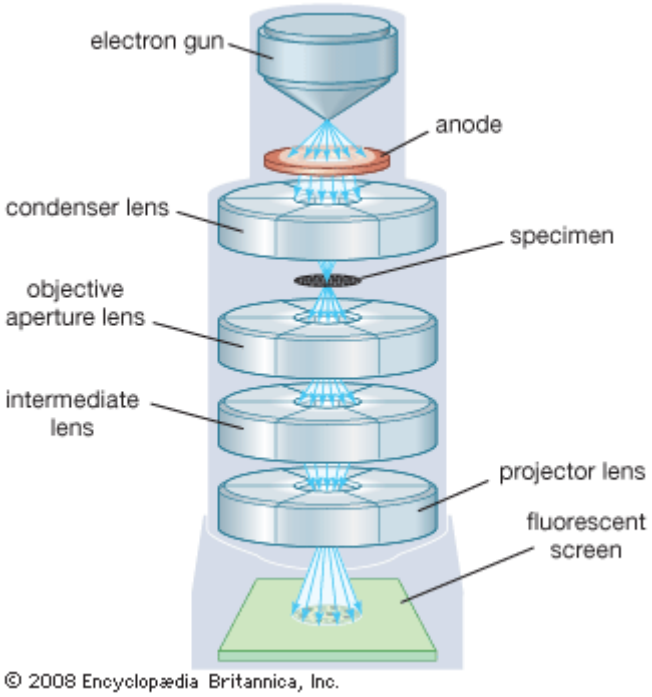

Figure 7 Diagram of a TEM instrument

Johnson Matthey Plc carried out the TEM analysis and line scan on powder samples. A tiny amount of each sample was crushed with glass slides and dusted onto a holey carbon supported Ni TEM grid. Ni rather than ordinary Cu grid was used because the samples themselves contain copper. The Tecnai F20 Transmission Electron Microscope was operated at:

200kV with a C2 aperture = 30 µm in bright field (BF) and high angle annular dark field (HAADF) modes.

Energy dispersive X-ray spectroscopy (EDX) was also used to determine the sample elemental composition.

2.1.8. UV-visible spectroscopy

2.1.8.1 Introduction

UV-visible spectroscopy involves the absorption of light in the ultraviolet-visible region. This technique can be used for identifying functional groups. UV spectroscopy is widely used in laboratories and its assaying ability enables it to be very useful in determining strengths of substances in samples and metal content in alloys.

2.1.8.2 Principles

The method is frequently used in a quantitative way to determine concentrations of an absorbing species in solution and uses the Beer-Lambert law:

$$A = -\log_{10}(I/I_0) = \varepsilon\, c\, L$$

A = Absorbance

I_0 = intensity of incident light at given wavelength

I = transmitted intensity

L = Path length through sample

c =concentration of absorbing species

ε = extinction coefficient

2.1.8.3 Instrumentation

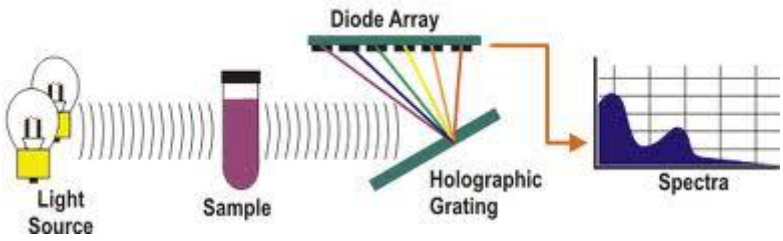

Figure 8 Diagram of how a UV-Visible spectrometer works

The basic parts of a spectrophotometer are a light source, a holder for the sample, a diffraction grating or monochromator to separate the different wavelengths of light, and a detector. The radiation source is often a tungsten filament (300-2500 nm), a deuterium arc lamp, which is continuous over the ultraviolet region (190-400 nm) or more recently, light emitting diodes (LED) and xenon arc lamps for the visible wavelengths. The detector is typically a photodiode or a CCD.

2.1.9 Evolved gas analysis (EGA)

Evolved gas analysis was carried out using a Netszch instrument. A sample of catalyst was placed into a sample pan and loaded into the furnace. The system was flushed for 2 hours with 50 ml/min of 5% H_2/He or air, and then heated under the same gas at 10 °C/min to the desired temperature. The mass changes were measured by thermal gravimetric analysis (TGA). The gases produced were measured by mass spectrometry.

2.2 Catalyst preparation

2.2.1 Impregnation method

Copper (II) nitrate trihydrate (0.93 g) was weighed into a beaker. $HAuCl_4$ (1.84 g) was dissolved in distilled water (28 ml) and added to the beaker containing copper (II) nitrate trihydrate. The solution was stirred until the copper salt dissolved into the Au solution. Silica (19 g) was added to the AuCu solution and stirred until an even mixture was formed. The sample was placed in an oven for 2 h at 120 ^{o}C and calcined in air for 3 h at 400 ^{o}C unless otherwise stated.

2.2.2 Precipitation method

Copper (II) nitrate trihydrate (3.79 g) was weighed into a conical flask and 150 ml distilled water added. NaOH pellets (1.38 g) were weighed into a beaker and 100 ml distilled water added. The NaOH solution was transferred to a dropping funnel and attached to a clamp stand. The copper (II) nitrate trihydrate solution was placed on a stirrer and a stirrer bar added to flask. The dropping funnel was placed above the flask and the NaOH solution added dropwise, slowly to the copper salt solution. As the hydrolysis took place, the solution became more turbid. The pH of the solution was maintained at 11.97. Silica (19 g) was added to the stirred mixture and the solution was allowed to stir for 1 h. The slurry was filtered through a Buchner funnel and the filtrate was placed back into the conical flask and hot water (250 ml) was added. The solution was stirred for 10 minutes and transferred back to the Buchner funnel. The sample was washed several times and the pH monitored until a stable

pH was obtained (8.5). The sample was placed in a beaker and dried in an oven for 2 h at 120 ^{o}C.

2.2.3 Deposition precipitation

A slurry of was prepared by adding 19 g of silica to 800 ml water. A solution of $HAuCl_4$ (2.35 g) in 150 ml water was made up in a beaker. A solution of 0.1 M K_2CO_3 (3.45 g K_2CO_3 in 250 ml of water) was made. The silica slurry was heated to 60 ^{o}C and stirred continuously while K_2CO_3 was added dropwise until a pH of 8 was obtained. Then $HAuCl_4$ was added slowly dropwise from the dropping funnel into the beaker and simultaneously K_2CO_3 was pipetted into the beaker with the support to maintain a pH of 8. When the addition was completed the solution was stirred for a further 1 h, before the solution containing precipitate was decanted and washed with water several times. The sample was placed in a smaller beaker and dried in an oven at 90 ^{o}C. The catalyst was calcined at 500 ^{o}C for 2 h.

2.2.4 Sinfelt method[1]

The copper-gold catalyst system was prepared by impregnating silica gel (Grace Davison) with a solution containing copper (II) nitrate trihydrate and chloro auric acid. The catalyst was dried at 110 ^{o}C and reduced for 2 h in flowing H_2/Ar at 315 ^{o}C, then finally calcined in air for 15 h at 676 ^{o}C.

2.2.5 High dispersion route for the preparation of copper catalysts

Ammonium carbonate (1.88 g) was weighed in a 3-necked round bottomed flask and the water and ammonia solution added to give a clear solution. Copper hydroxycarbonate was added to give an intense blue coloured solution and silica (19 g) was then added. The flask was fitted with a condenser for distillation and heated just below boiling (90-95 ^{o}C). After 3h

of heating the reaction was allowed to cool to room temperature and the resultant blue suspension was filtered and washed with three 200 ml portions of water. The product was transferred to a beaker and dried at 110 ^{o}C overnight.

2.2.6 Sol immobilisation method

$HAuCl_4$ and PVA solution (1.8 ml PVA for Pd, 3.3 ml PVA for Pt) were added to a large beaker. After 3 minutes $NaBH_4$ solution (1 M, 2.9 ml) was added under vigorous stirring. The red Au(0) sol immediately formed. After another 3 minutes, 0.099 mmol of stock MCl_2 (M= Pt or Pd) solution and $NaBH_4$ solution (2 ml) was added forming a brown sol, which could possibly represent the presence of boron species in the catalyst.[2,3] After waiting a few minutes for the sol generation the solution was acidifife to pH 1 with concentrated sulfuric acid and then the colloid was immobilised by adding SiO_2 under vigorous stirring. The amount of support was calculated as having a total final metal loading of 2.5 wt%. After 2 h the slurry was filtered, the catalyst washed thoroughly with distilled water and dried at 120 ^{o}C for 4 h.

2.3 Propene oxidation experimental

2.3.1 Gas Phase reactor

For each propene oxidation experiment, 0.2 g of catalyst was weighed and placed into the quartz reactor tube, which was plugged with glass wool. The tube was screwed into place in the reactor and tested for leaks. The gas feed ratio of C_3H_6:O_2:H_2:He was 1:1:1:7, which Haruta had successfully used those reaction conditions (1.1% conversion with propene oxide selectivity of > 99% using Au/TiO_2 catalyst).[4] Similar experiments were conducted in the

absence of H_2 with the reactant gases C_3H_6:O_2:He = 22:9:69. This particular gas feed ratio was used to compare initial results with previous work in Cardiff.[5]

For the propene oxidation experiments, a continuous flow reactor was used (Figure 9). Product analysis was carried out by injecting a small amount of reaction products, using a 6-port sample valve. He, O_2, H_2 and C_3H_6 gases flowed and the temperature thermostat was switched on. The top and bottom of the reactor were covered with foil to retain heat. A run for an experiment was 25 minutes and four runs for each experiment were carried out at room temperature. The temperature was then increased to 200 ^oC and 3 runs taken. After that, the temperature was increased at 20 ^oC intervals and 3 runs taken at each new temperature up to 320 ^oC and then back down to 200 ^oC for hysteresis experiments. At each temperature an average of the 3 runs were taken with an error value calculated as ± 3%. The gas hourly space velocity (GSHV) was 22,500 h^{-1}, unless otherwise stated, with a total flow rate of 75 ml/min.

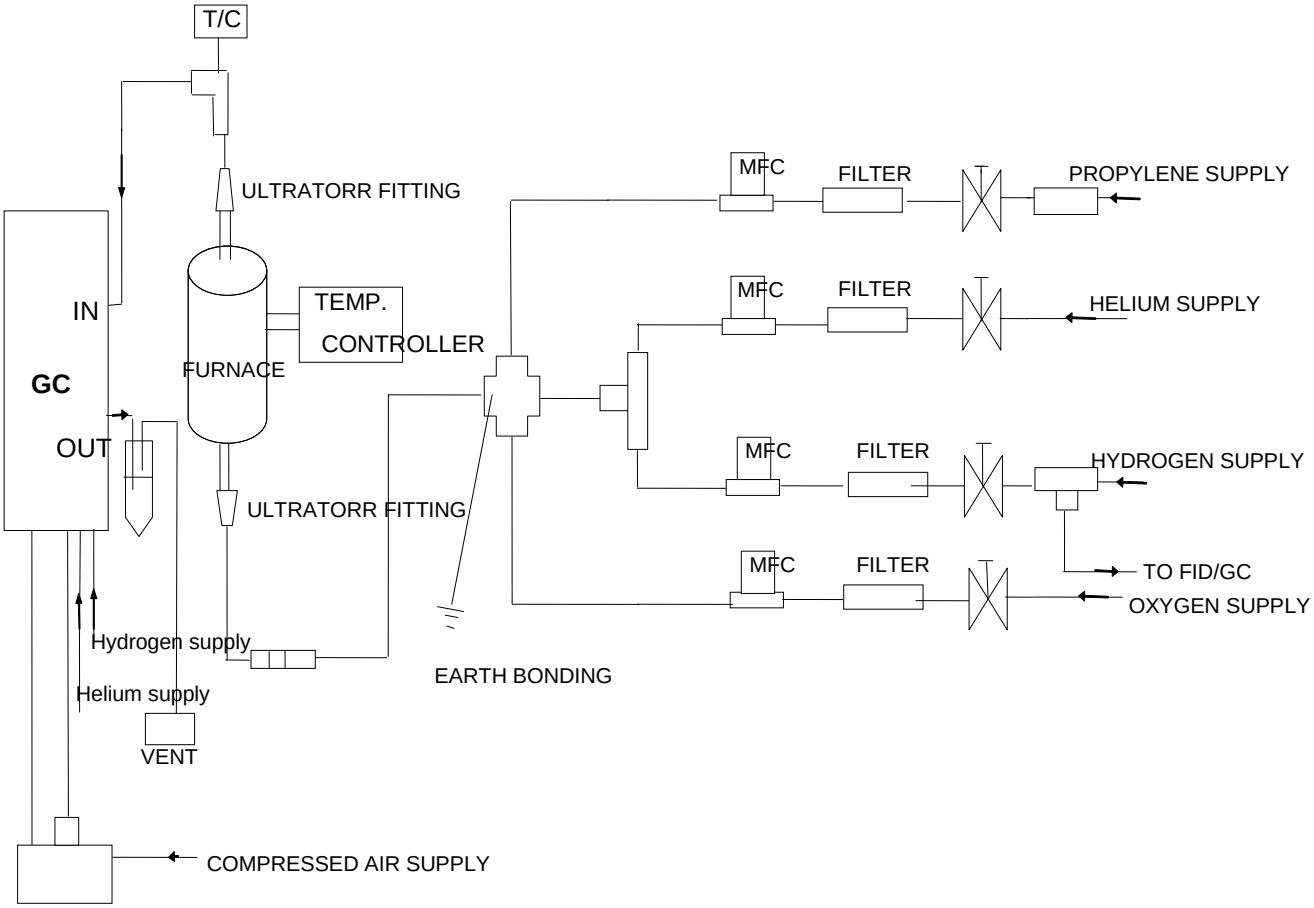

Figure 9 Schematic diagram of reactor for propene oxidation
MFC- Mass flow controller; T/C - Temperature controller

2.3.2 Calculations

2.3.2.1 Calibration:

The calibration and analysis for propene oxide (PO) was performed with an FID detector, while the carbon dioxide (CO_2) was carried out with a TCD detector. The concentrations, vol% of propene oxide and carbon dioxide at time t, $[PO]_t$ and $[CO_2]_t$, can be calculated using equations (1 and 2) where ${}^{PO}A_t$, and ${}^{CO2}A_t$ are the counts of the peak at time t. ${}^{PO}A_c$ and ${}^{CO2}A_c$ are the counts of peak area at standard concentrations [PO]c and $[CO_2]c$, separately.

$$[PO]_t = [PO]_c \frac{^{PO}A_t}{^{PO}A_c} \qquad (1)$$

$$[CO_2]_t = [CO_2]_c \frac{^{CO2}A_t}{^{CO2}A_c} \qquad (2)$$

2.3.2.2 Carbon balance

The carbon mass balance was calculated as follows:

Mass balance (%) = $\sum$[products] / ([propene]$_{out}$) x 100

For the carbon mass balance the number of carbon atoms in the products and reactants was corrected.

Below is an example of a carbon balance taken for the propene oxidation experiment. All the carbon balances taken during this study were in the range 96-100%.

Temperature (^oC)	Carbon balance %
200	100.1
220	98.9
240	100.3
260	98.3
280	98.9
300	99.4

Table 1 Typical carbon mass balance for propene oxidation experiment

Selectivity for each reactant product was calculated as follows:

Selectivity of Carbon dioxide (%) = [Carbon dioxide] / ([Carbon dioxide] + [Ethanal] + [propene] + [propene oxide] + [acrolein] + [acetone]) x 100

This calculation is on a carbon basis and is therefore corrected for the number of carbons present e.g. if CO_2 formed from propene there would be 3 moles of carbon per mole of propene made so you need to correct for this (multiply by 1/3).

Conversion of propene was calculated as follows:

Conversion (%) = ($[propene]_{in}$ – $[propene]_{out}$) / $[propene]_{in}$ x 100

$[propene]_{in}$ = Initial propene counts

$[propene]_{out}$ = Final propene counts

2.4 Glycerol alcohol experimental

2.4.1 Glass reactor

A glass reactor was set up for the glycerol oxidation experiments which are illustrated below. The set up comprised of a three neck round bottom flask, a condenser, stirrer/hot plate and oil bath. Oxygen was supplied to the system from an oxygen cylinder.

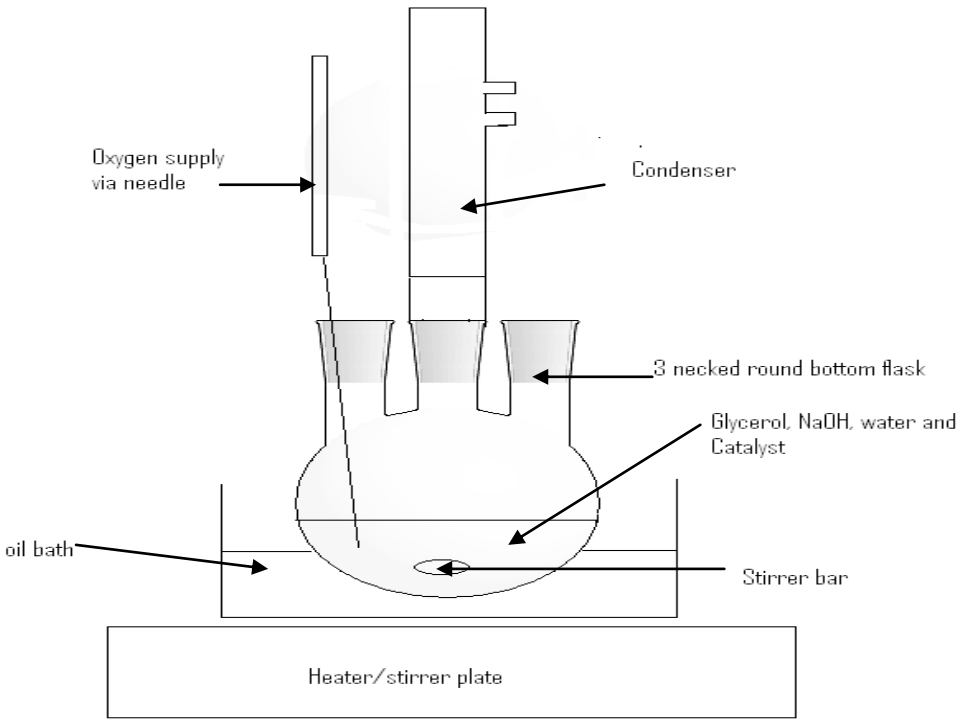

Figure 10 Schematic diagram of Glycerol experiment

2.4.2 Glycerol experimental procedure

Glycerol (0.3 M), 0.42 g, NaOH (0.32 g), water (15 ml), oxygen pressure of 3 bar and an Au/SiO_2 catalyst (0.08 g) were placed into a 50 ml 3 necked round bottomed flask. A stirrer bar was added and the flask was connected to a condenser. The apparatus was refluxed for 4 h at 60 ^oC or 100 ^oC where specified and a sample taken after 30 minutes and then after each hour for 4 hours. The samples were diluted with water and analysed by HPLC to determine the products of the reaction.

2.5 Autoclave experimental

2.5.1 Hydrogen peroxide synthesis

0.05 g of catalyst was weighed and added to a solution of 2.9 g water and 5.6 g methanol. This mixture was placed in an autoclave and screwed shut. 5% H_2 in CO_2 was passed through autoclave to 100 psi three times to purge the system. The pressure was then increased to 420 psi and vented. The pressure was allowed to drop to 390 psi and then 25% O_2 in CO_2 was added so that the pressure increased to 520 psi. The hydrogen to oxygen ratio was 1:2. An ice bath was used to cool the reactor to 2 ^oC and then the stirrer was activated to start the reaction, which ran for 30 minutes. Once the reaction was complete the solution was filtered to remove the catalyst and obtain a filtrate that was titrated against Ce^{IV} to calculate the H_2O_2 productivity.

2.5.2 Hydrogenation reaction

A standard solution containing H_2O_2 (0.68g)(50%), 8.5g solvent (MeOH 5.6g and H_2O 2.22g) was made and titrated against Ce^{IV} solution using a ferroin indicator.

Each hydrogenation reaction required 8.5 ml of the standard solution with a small amount of catalyst (0.012 g), which was placed in a container that was put in the autoclave. The

autoclave was purged 3 times to 100 psi pressure 5% H_2/CO_2. The pressure was then increased to 420 psi with 5% H_2/CO_2 and cooled in an ice bath to 2 ^oC. When the desired temperature was reached, the stirrer was turned on to start the reaction for 30 minutes. After the reaction was complete the catalyst was filtered off and the solution that remained was titrated against the Ce^{IV} solution 3 times to get an average titre. From these results the H_2O_2 concentration was calculated and the decomposition of H_2O_2 worked out.

2.5.3 Benzyl Alcohol Oxidation

50 mg of catalyst was weighed and added to benzyl alcohol (40 ml). This mixture was placed in an autoclave and screwed shut. Oxygen was introduced into the autoclave (10 bar) and the temperature of the autoclave was set to 140 ^oC with a stirrer speed of 1500 rpm. The experiment was run for 3 hours and at 30 minutes and then every hour a sample was to taken to be analysed by HPLC.

2.6 References

1. J.H. Sinfelt, R.J. Baron, *US Pat* 3989674 (1976).

2. R.E. Schaak, A.K. Sra, B.M. Leonard, R.E. Cable, J.C. Bauer, Y.F. Han, J. Means, W. Teizer, Y. Vasquez and E.S. Funck, *Journal of American Chemical Society*, 127 (2005) 3506.

3. G.N. Glavee, K.J. Klabunde, C.M. Sorensen and G.C. Hadjipanayis, *Langmuir*, 10 (1994) 4726.

4. T. Hayashi, K. Tanaka and M. Haruta, *Journal of Catalysis*, 178 (1998) 566-75.

5. Gas-phase selective oxidation of C3- C4 hydrocarbons using only molecular oxygen, Zheng-Qian Xuan, PhD 2009.

Chapter 3: Characterisation

3.0 Introduction

Monometallic and bimetallic Au, Cu and $AuCu/SiO_2$ catalysts have been prepared by impregnation, sol immobilisation, precipitation and deposition precipitation. To attempt to understand the nature and structure of the catalysts made for this study, this section of the thesis will cover the techniques used to characterise the samples. Characterisation techniques used included surface area analysis (BET), inductively coupled plasma (ICP), temperature programmed reduction (TPR), X-ray diffraction (XRD), scanning electron microscopy (SEM), transmission electron microscopy (TEM), X-ray photoelectron spectroscopy (XPS), evolved gas analysis (EGA) and UV-visible spectroscopy.

3.1 BET surface areas measurements

Most of the catalysts used in this study have been characterised by BET and their surface areas are summarised in Table 2. The silica support (Grace Davison) had a high surface area of 299 m^2g^{-1}. All of the catalysts tested have high surface areas and the Au/SiO_2 catalysts prepared by deposition precipitation had the highest at 440 m^2/g^{-1}.

Catalyst Composition	**Uncalcined/ Calcined**	**Preparation method**	**BET Surface Area (m^2/g^{-1})**
Au/SiO_2	Calcined	Deposition precipitation	440
$CuAu/SiO_2$ (1:1)	Calcined	Impregnation	328
$CuAu/SiO_2$ (1:3)	Calcined	Impregnation	333
$CuAu/SiO_2$ (3:1)	Calcined	Impregnation	311
Au/SiO_2	Calcined	Impregnation	327
Cu/SiO_2	Uncalcined	Impregnation (nitrate)	247
Cu/SiO_2	Calcined	Impregnation (nitrate)	281
Cu/SiO_2	Uncalcined	Impregnation (chloride)	275
Cu/SiO_2	Uncalcined	Precipitation	297
Cu/SiO_2	Calcined in H_2	Impregnation	302
Cu/SiO_2	Calcined in N_2	Impregnation	310
Cu/SiO_2	Calcined in air	Impregnation	294
1:1 $CuAu/SiO_2$	Calcined	Co-impregnation (chloride)	302
1:3 $CuAu/SiO_2$	Calcined	Co-impregnation (chloride)	299
3:1 $CuAu/SiO_2$	Calcined	Co-impregnation (chloride)	283
1:1 $CuAu/SiO_2$	Calcined	Co -impregnation (nitrate)	269
1:3 $CuAu/SiO_2$	Calcined	Co-impregnation (nitrate)	296

3:1 $CuAu/SiO_2$	Calcined	Co-impregnation (nitrate)	294
1:1 $CuAu/SiO_2$	Sinfelt (reduced and calcined)	Co-impregnation (chloride)	255
1:3 $CuAu/SiO_2$	Sinfelt (reduced and calcined)	Co-impregnation (chloride)	277
3:1 $CuAu/SiO_2$	Sinfelt (reduced and calcined)	Co-impregnation (chloride)	277
1:1 $CuAu/SiO_2$	Sinfelt (reduced only)	Co-impregnation (nitrate precursor)	265
1:1 $CuAu/SiO_2$	Sinfelt (reduced and calcined)	Co-impregnation (nitrate precursor)	300
1:3 $CuAu/SiO_2$	Sinfelt (reduced only)	Co-impregnation (nitrate precursor)	268
1:3 $CuAu/SiO_2$	Sinfelt (reduced and calcined)	Co-impregnation (nitrate precursor)	306
3:1 $CuAu/SiO_2$	Sinfelt (reduced only)	Co-impregnation (nitrate precursor)	294
3:1 $CuAu/SiO_2$	Sinfelt (reduced and calcined)	Co-impregnation (nitrate precursor)	283
Cu/SiO_2	uncalcined	High dispersion	173

Table 2 BET surface areas of catalysts

All these calcined samples have high surface areas. For the six catalysts made *via* the Sinfelt method[1] (reduced 315 ^{o}C for 2 h in H_2/Ar and then calcined at 676 ^{o}C for 15 h in air) the

samples prepared using the copper nitrate precursors have a slightly higher surface area than the chloride precursors, whereas, for the catalyst made using the standard methodology (calcined 400 ^{o}C in air 2 h) there was no obvious difference using different copper precursors.

3.2 Inductively coupled plasma (ICP) analysis

To determine the wt% of gold and copper in each catalyst prepared by different methods and compositions, ICP analysis was used and the results are shown in Table 3 (appendix). Most of the catalysts have a wt% quite close to that expected ± 1%. The bimetallic $CuAu/SiO_2$ (C97819A-C) catalysts, prepared by impregnation with copper nitrate and $HAuCl_4$ directly calcined, as well as the monometallic gold (C97809) and copper (C97802D) samples by the same procedure, have a weight percentage very close to their expected values. The $CuAu/SiO_2$ and gold and Cu/SiO_2 only catalysts made by co-impregnation with copper nitrate, but instead of being calcined, are reduced in H_2 (C97893A-E), also show extremely good agreement to 5 wt%. However, the gold only catalyst made *via* deposition precipitation (C97836) has an extremely low loading of 0.05%. This could be a consequence of the deposition precipitation method not efficiently depositing particles onto the silica support.

3.3 X-ray diffraction

XRD measurements of catalysts prepared by different methods have been carried out for chemical analysis such as phase identification, which have been matched from the International Centre Diffraction Data (ICDD) database.

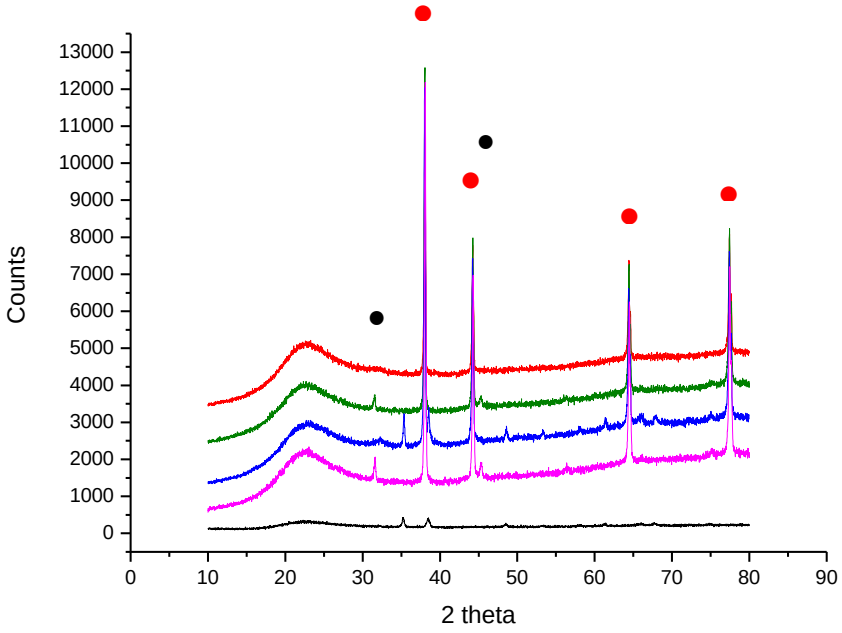

Figure 3.1 XRD of monometallic and bimetallic catalysts prepared by impregnation with copper nitrate and chloroauric acid and calcined at 400 ^{o}C for 2 h in air. (C97819A-C and C97809, C97802D) __1:1 CuAu/SiO_2 __ 1:3 CuAu/SiO_2 __3:1 CuAu/SiO_2 ___Au/SiO_2only ___ Cu/SiO_2 only ● Au metal reflection ● Copper chloride hydroxide

An overlay of three bimetallic CuAu/SiO_2 and a monometallic Cu and Au/SiO_2 catalyst, (prepared by impregnation, with $HAuCl_4$ and copper nitrate, calcined at 400 ^{o}C in air for 2 h) is shown in Figure 3.1. XRD characterization for the silica support was carried out to exclude the peaks due to the support. All the AuCu/SiO_2 catalysts have sharp crystalline reflections. For the 1:1 CuAu/SiO_2 sample the reflections at 38, 44.5, 64.4, 77.3 and 81.6 ^{o} have been assigned to Au metal (ICDD PDF No 00-004-0784), and those at 31.5, 32.6, 45 ^{o} and many smaller peaks are assigned to copper chloride hydroxide (Cu(OH)Cl, ICDD PDF No 00-023-1063). The Au crystallite size was found to be 42 nm. For the 1:3 CuAu/SiO_2 catalyst the diffraction pattern mainly composed of Au metal, a minor amount of poorly crystalline

(broad not sharp well defined reflections) sodium chloride (NaCl, ICDD PDF No 00-005-0628) and a significant amount of amorphous material. There is no evidence of any other crystalline phases. A gold crystallite size of 42 nm was calculated. The 3:1 $CuAu/SiO_2$ sample indicated that the sample was mainly composed of gold, a trace amount of poorly crystalline sodium chloride, a trace amount of poorly crystalline copper oxide – *Tenorite* (CuO, ICDD PDF No 00-048-1548), a trace amount of poorly crystalline copper chloride hydroxide and a significant amount of amorphous material. The gold crystallite size of 45 nm and the copper oxide crystallite size of 55 nm were calculated.

The Au/SiO_2 only catalyst (C97809) had a diffraction pattern which indicated that the sample was mainly composed of poorly crystalline gold, a minor amount of poorly crystalline sodium chloride and a significant amount of amorphous material. A gold crystallite size of 43 nm was calculated. Another method, deposition precipitation, was also used to form Au/SiO_2 (C978/36); however, the XRD pattern (see appendix Figure 1) was amorphous but had a possible trace amount of poorly crystalline gold.

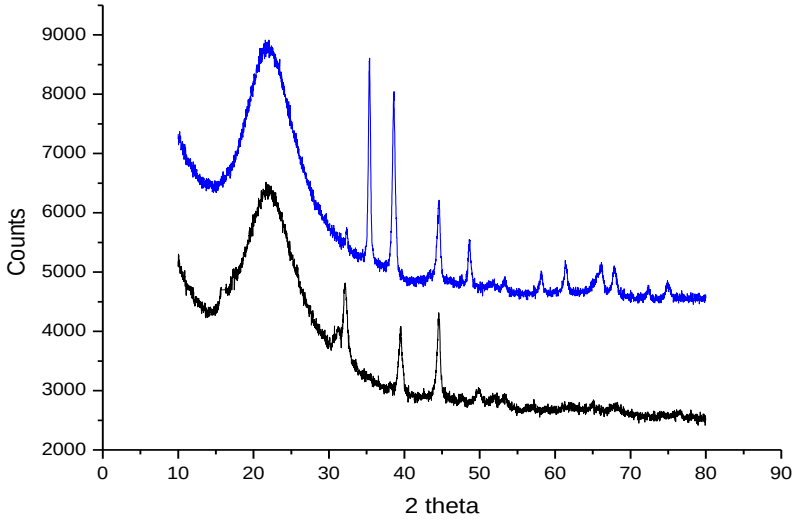

Figure 3.2 XRD of monometallic Cu/SiO_2 catalysts prepared by impregnation with different copper precursors and calcined in air at 400 ^{o}C for 2 h.

__ Copper nitrate (C97802D) __Copper chloride (C97802B)

Since two different copper precursors have been used in this study, the XRD of both copper chloride and copper nitrate was compared in Figure 3.2. Both catalysts have some crystalline reflections but the copper nitrate sample appeared more crystalline with the presence of some copper oxide- *Tenorite*. From this figure there could be sample packing effects as the intensities of the two copper precursors differ quite a bit. XRD relies on the principle that all possible crystallographic orientations are presented to the beam. This concept is known a random orientation. If there is a bias of orientations of one or more particular crystallographic plane, then this is known a preferred orientation. Preferred orientation is likely the most common cause of intensity variations in XRD powder experiments. In future to minimise this possibility samples should be packed and mounted consistently.

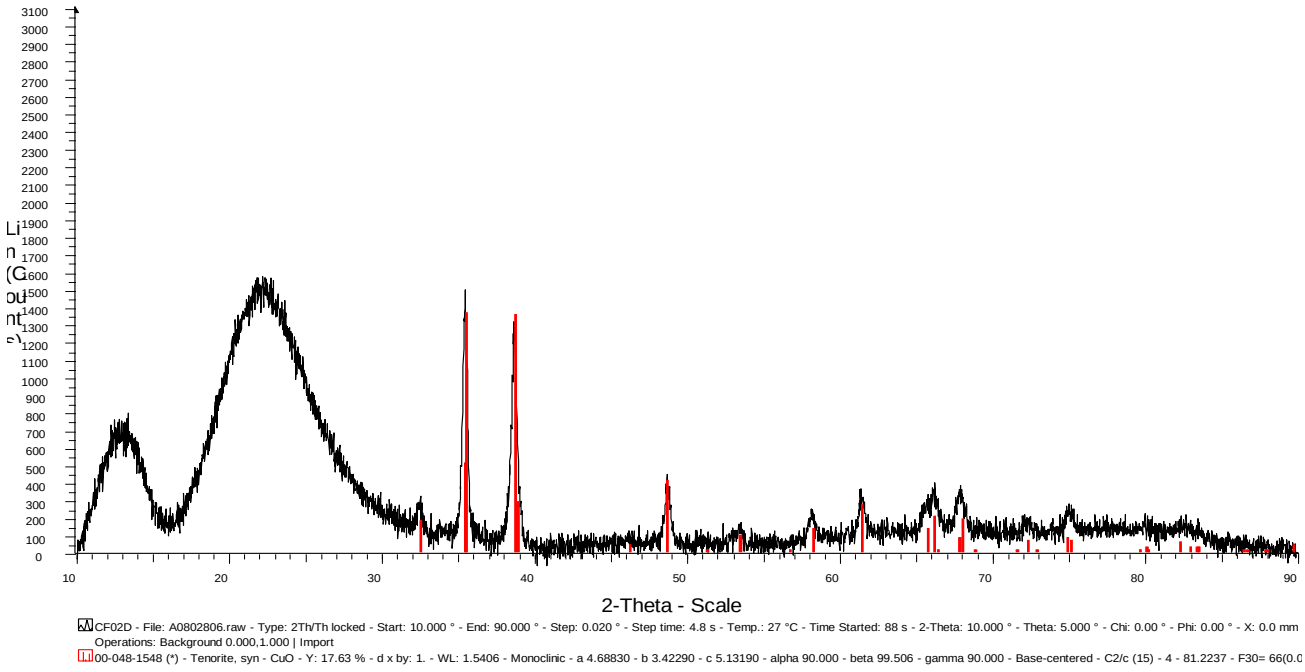

Figure 3.3 XRD of Cu/SiO_2 catalyst prepared by impregnation with copper nitrate and calcined at 400 ^oC for 2 h in air. (C97802D)

As seen from Figure 3.3, the Cu/SiO_2 catalyst made with a copper nitrate precursor had a diffraction pattern which indicated that the sample was mainly composed of amorphous material and a minor amount of poorly crystalline copper oxide – *Tenorite*. A copper oxide crystallite size of 20 nm was calculated.

The effect of different atmospheric conditions to pre-treat catalysts has also been briefly studied. Cu/SiO_2 catalysts have been prepared by impregnation using copper chloride followed by one of three options:

- Heated at 400 ^oC in H_2 (C97815B1) (XRD in appendix Figure 2)
- Heated at 400 ^oC in N_2 (C97815B2) (XRD in appendix Figure 3)

- Heated at 400 ^{o}C in air (C97815B3) (XRD in appendix Figure 4)

The XRD pattern for the treatment in H_2 suggested that the sample was mainly composed of poorly crystalline copper (Cu, PDF No 00-004-0836), a minor amount of poorly crystalline copper oxide – *Cuprite* (Cu_2O, PDF No 00-005-0667) and a significant amount of amorphous material. The copper oxide crystallite size of 6.2 nm and the copper crystallite size of 37 nm were calculated.

The diffraction pattern for the N_2 treatment indicated that the sample was mainly composed of amorphous material and a possible trace amount of poorly crystalline copper chloride hydroxide. This alternative heat treatment appeared to change the copper phase from copper oxide – *Cuprite*.

Treatment in air (appendix Figure 4) showed that the sample was mainly composed of amorphous material and a possible trace amount of poorly crystalline copper chloride hydroxide.

A copper chloride precursor was also used to form another Cu/SiO_2 catalyst by a precipitation (C97828) route (appendix Figure 5). The diffraction pattern indicated that the sample was mainly composed of a major amount of amorphous material and a trace amount of poorly crystalline copper oxide – *Tenorite*. A copper oxide crystallite size of 3.8 nm was calculated.

A novel approach by Sinfelt and group[1] involved the preparation of $CuAu/SiO_2$ catalysts by co-impregnation followed by a reduction in hydrogen at 315 ^{o}C for 2 h and then a high temperature calcination at 675 ^{o}C for 15 h to achieve alloy formation (C978101A-C).

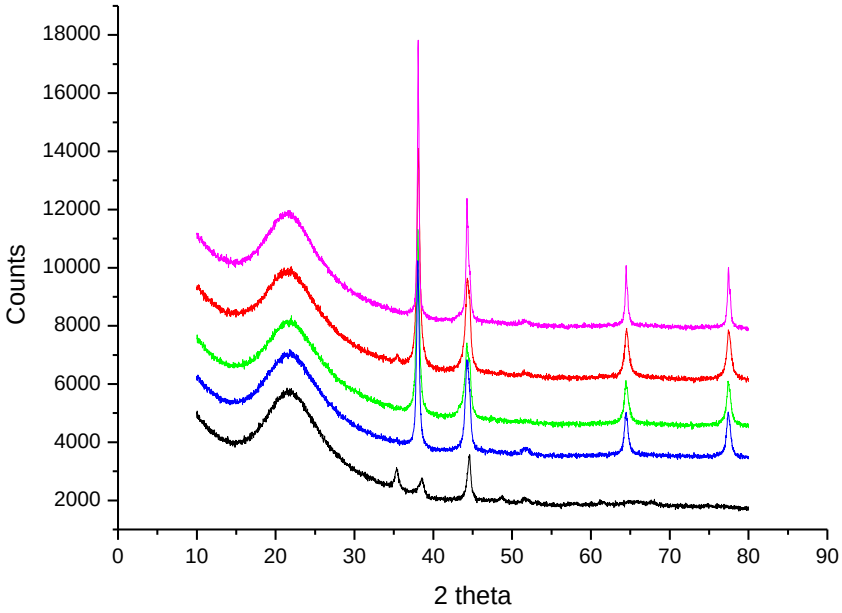

Figure 3.4 XRD overlay of catalysts with a Sinfelt thermal treatment (reduction at 315 ^{o}C in H_2/Ar followed by a calcination in air at 676 ^{o}C for 15 h). All of the catalysts were prepared by impregnation with copper nitrate and chloroauric acid.(C978101A-E) ___ 1:1 $CuAu/SiO_2$ ___ 1:3 $CuAu/SiO_2$ ____ 3:1 $CuAu/SiO_2$ ___ Au only ___Cu Only

An overlay of the XRD pattern for $CuAu/SiO_2$ catalyst, prepared by a Sinflet [1] calcination (reduced 2 h in H_2/Ar and calcined at 676 ^{o}C for 15 h in air), together with the monometallic Au and Cu only comparisons are shown in Figure 3.4. For the 1:1 $CuAu/SiO_2$ sample, the diffraction pattern showed that the sample was mainly composed of a major amount of poorly crystalline gold, a minor amount of poorly crystalline copper oxide – *Tenorite* and a significant amount of amorphous material. A gold crystallite size of 37 nm and a copper oxide crystallite size of 35 nm were calculated. For 1:3 $CuAu/SiO_2$, the diffraction pattern indicated that the sample was mainly composed of a major amount of poorly crystalline gold, a minor amount of poorly crystalline copper oxide – *Tenorite* and a significant amount of amorphous material. A gold crystallite size of 32 nm and a copper oxide crystallite size of

27.2 nm were calculated. For 3:1 $CuAu/SiO_2$, the diffraction pattern indicated that the sample was mainly composed of a major amount of poorly crystalline gold, a minor amount of poorly crystalline copper oxide – *Tenorite* and a significant amount of amorphous material. A gold crystallite size of 27 nm and a copper oxide crystallite size of 23.5 nm were calculated.

Catalyst	Preparation Conditions	Crystallite size nm	Au/ Cu/AuCu phases
1:1 $CuAu/SiO_2$	Direct calcination(C97819A)	7	Au, copper chloride hydroxide
1:3 $CuAu/SiO_2$	Direct calcination(C97819B)	6	Au , no other major phases seen
3:1 $CuAu/SiO_2$	Direct calcination(C97819C)	11	Au, copper oxide *Tenorite*, copper chloride hydroxide
1:1 $CuAu/SiO_2$	Sinfelt (C978101A)	70	Au, copper oxide *Tenorite*
1:3 $CuAu/SiO_2$	Sinfelt(C978101B)	33	Au, copper oxide *Tenorite*
3:1 $CuAu/SiO_2$	Sinfelt(C978101C)	26	Au, copper oxide *Tenorite*

Table 3.1 the crystallite sizes obtained from the Scherrer equation for $CuAu/SiO_2$ catalyst with different molar ratios and different preparation conditions.

Table 3.1 shows the crystallite sizes for the $CuAu/SiO_2$ samples. A larger crystallite size was observed for catalysts made by the Sinfelt method, compared to direct calcination. The only difference in preparation is that the Sinfelt materials were reduced before calcination and were calcined at higher temperatures, at 676 ^oC rather than 400 ^oC, and for 15 h, compared to only 2h for the standard procedure. These factors, therefore, must play a role in affecting the size of the metal particles.

The Sinfelt copper only catalyst was reduced at 315 ^{o}C for 2 h in H_2/Ar and calcined at 676 ^{o}C for 15 h in air. The sample was quite amorphous but did have clear crystalline peaks at 35 and 38 ° which represent CuO (Cu^{2+}). The gold only Sinfelt catalyst was made under the same conditions as the copper only sample and had the four main reflections at 38, 44, 65 and 79 ^{o} that represent metallic gold.

The XRD of a different catalyst preparation, where the copper was deposited by high dispersion first, followed by gold *via* impregnation, showed reflections for metallic gold and copper oxide –Tenorite (appendix Figure 14).

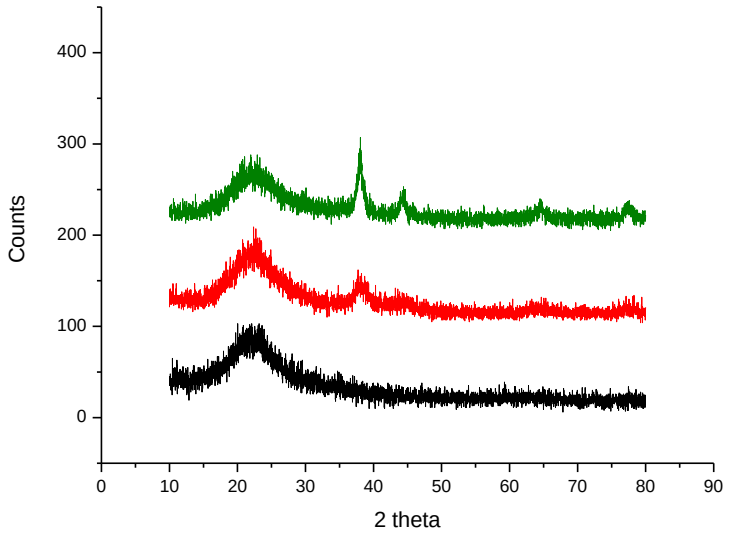

Figure 3.5 XRD of CuAu/SiO_2 catalysts prepared by two different sequential methods overlayed with an Au/SiO_2 catalyst made by a sol immobilisation route.

__ HDC Cu +Au DP uncalcined (C97887) __ HDC Cu + Au DP calcined (C97890)

__ Au/SiO_2 sol dried (C978102)

Another catalyst preparation, used to form CuAu/SiO_2 catalysts, was to combine two methods consecutively. Firstly, copper was deposited onto the silica support by a high dispersion route and then gold was deposited by deposition precipitation (C97887). The uncalcined sample was amorphous but did have peaks for metallic gold. However, upon calcination at 400 ^{o}C for

2 h in air, the sample became more crystalline and the metallic gold reflections became more apparent in the XRD pattern (Figure 3.5). Another preparation method, known as sol immobilisation, was also employed to make an Au/SiO_2 catalyst (C978102). Usually, TiO_2 and carbon are the supports commonly chosen for this technique but, as all the previous catalysts in this study were deposited on SiO_2, the support was kept the same for consistency.

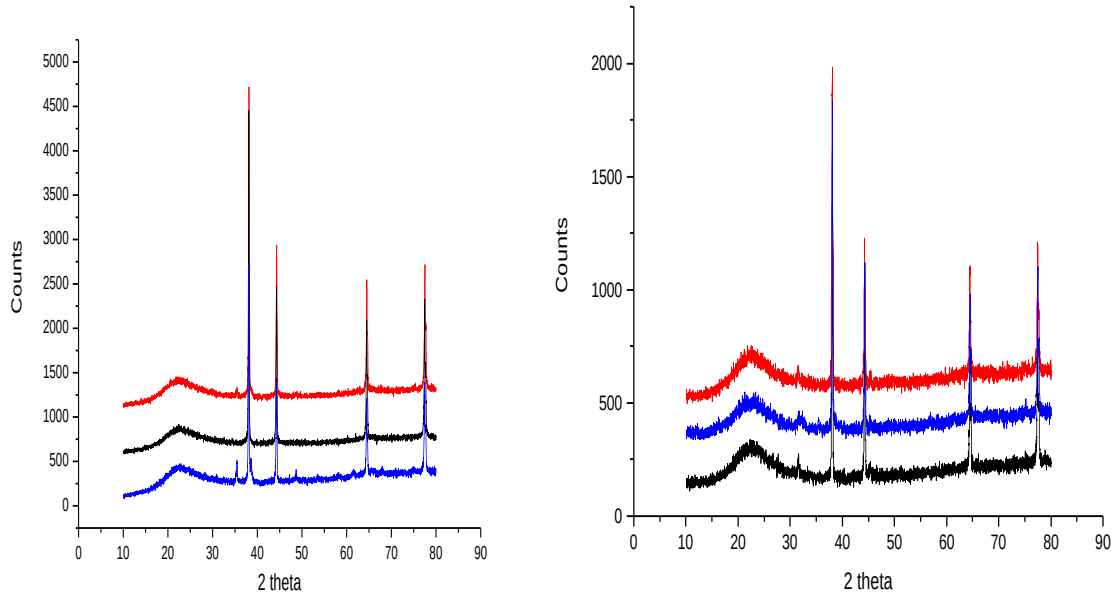

(a) **(b)**

Figure 3.6 (a) - $CuAu/SiO_2$ catalyst made with copper chloride and chloroauric acid *via* co-impregnation calcined at 400 ^oC for 2 h in air (C97863A-C) (b) XRD of $CuAu/SiO_2$ catalysts made by co-impregnation with copper nitrate and chloroauric acid calcined at 400^oC for 2h in air. (C97819A-C)

__ 1:1 $CuAu/SiO_2$ __ 1:3 $CuAu/SiO_2$ __ 3:1 $CuAu/SiO_2$

All three catalysts shown in Figure 3.6a have the distinct crystalline peaks of metallic gold and the 3:1 $CuAu/SiO_2$ catalyst have reflections for copper chloride hydroxide, probably due to the higher copper content. By changing the copper precursor from copper chloride to

copper nitrate (Figure 3.6), the presence of the four metallic gold peaks still remained but the copper reflections could now be assigned to CuO (Cu^{2+}) copper oxide – *Tenorite*, which had more intense reflections as the copper content increased.

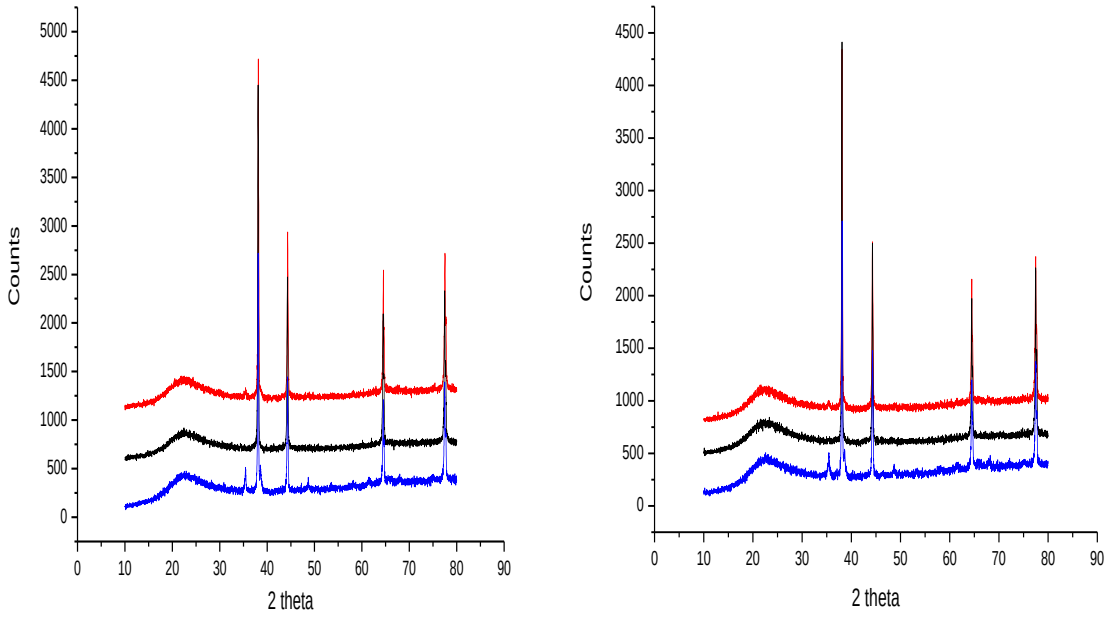

(a) (b)

Figure 3.7(a) XRD of $CuAu/SiO_2$ catalyst made *via* co-impregantion with copper chloride and chloroauric acid followed by a Sinfelt calcination (C97865A-C) (b) XRD of $CuAu/SiO_2$ made *via* co-impregnation with copper nitrate and chloroauric acid followed by a Sinfelt calcination (C978101A-C).

__ 1:1 $CuAu/SiO_2$ __ 1:3 $CuAu/SiO_2$ __ 3:1 $CuAu/SiO_2$

By choosing to reduce the catalyst in H_2/Ar before calcination at a higher temperature (676 ^oC), this appeared to make the samples more crystalline (Figure 3.7). The different copper precursor with a Sinfelt calcination did not show any significant changes to the XRD patterns.

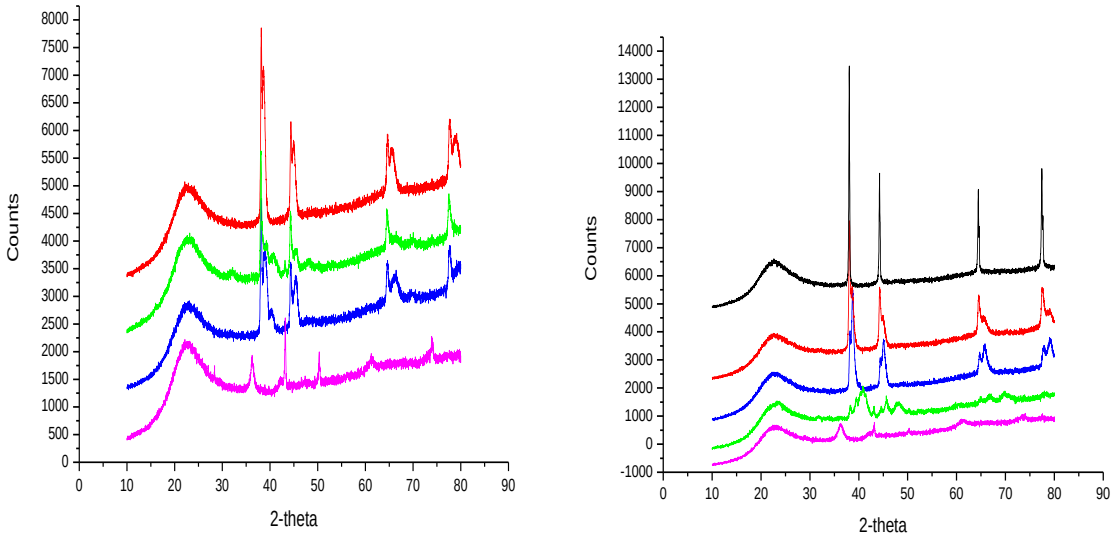

(a) **(b)**

Figure 3.8(a) $CuAu/SiO_2$ made *via* co-impregnation with copper chloride and chloroauric acid reduced in H_2 (C978/99A-E)(b) $CuAu/SiO_2$ made *via* co-impregnation with copper nitrate reduced in H_2 (C978/93A-E).

__ 1:1 CuAu/SiO __ 1:3 $CuAu/SiO_2$ __ 3:1 $CuAu/SiO_2$ __ Au/SiO_2 __Cu/SiO_2

From XRD analysis, reducing the catalyst with H_2, had an interesting effect on the crystalline phases of the $CuAu/SiO_2$ catalysts (Figure 3.8). For the $CuAu/SiO_2$ sample, there was a shift in the reflections, which was due to an AuCu phase (PDF 03-065-2798). The Cu_3Au/SiO_2 catalyst had an AuCu phase (PDF 03-065-2798) (reflections at 31.8, 40.4 45.7, 49.6, 52.4, 60.2, 66.6, 72.0 and 80.9^o), as well as an additional phase that can be assigned to cuproauride, syn Au_3Cu (PDF 01-071-5023) (reflections at 39.2, 45.5, 66.3 and 79.8^o). The $CuAu_3/SiO_2$ sample also had the two AuCu phases, as stated for the Cu_3Au/SiO_2 catalyst. The Cu/SiO_2 catalyst had the reflections that are representative of copper oxide (PDF 01-078-0428). Therefore, these findings suggested possible alloy formation after a reduction in H_2.

When the copper precursor was changed from copper chloride (Figure 3.8a) to copper nitrate (Figure 3.8b), there appeared to be a difference in the XRD patterns, especially for the 3:1 $CuAu/SiO_2$ catalysts. The Au/SiO_2 catalyst, reduced in H_2 (Figure 3.8b), had metallic gold reflections and the Cu/SiO_2 had been assigned to copper oxide – *Tenorite.* Figure 3.8b illustrates that, for the three different molar ratios of CuAu, both the 1:1 and 1:3 $CuAu/SiO_2$, had the AuCu phases (ICDD, PDF 03-065-2798) and cuproauride, syn Au_3Cu (ICDD, PDF 01-071-5023). However, the 3:1 $CuAu/SiO_2$ pattern appeared completely different to the other two CuAu catalysts and had characteristic lines that were broad and also revealed an $AuCu_3$ phase (ICCD, PDF 00-035-1357) (reflections at 33.7, 41.7, 48.5, 54.6, 60.4, 71.0, 76.0, 81.0 and 85.8^o), as well as possible AuCu and Au_3Cu phases. Kameoka *et al* have characterized the $AuCu_3$ phase by XRD and observed three distinct lines (40.4, 45.5 and 51.3).[2] Their study consisted of forming a fine porous Au catalyst by selectively leaching Cu from an ordered $AuCu_3$ intermediate.

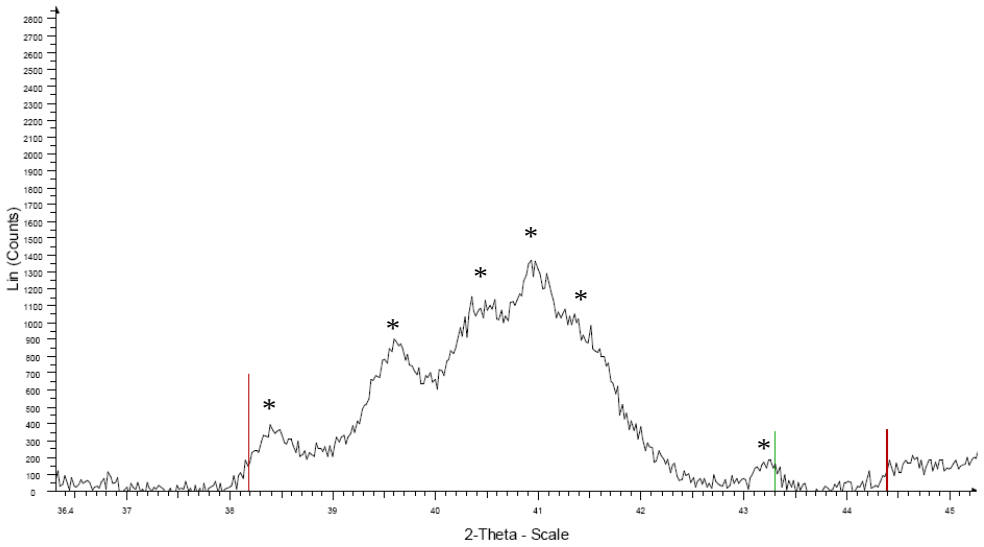

Figure 3.9 Expansion of the 37-48° 2θ region of the reduced Cu_3Au/SiO_2 sample with distinct alloy compositions marked with an asterisk. The red bars represent the positions of reflections due to gold metal, and the green bar represents the position of a reflection due to copper metal.

Figure 3.9 shows an expansion of the CuAu alloy region of the XRD for the Cu_3Au/SiO_2 prepared by reduction in H_2 only (C97893C). For the $CuAu/SiO_2$ and $CuAu_3/SiO_2$ catalysts, the broad reflection did not have any structure. However, for the Cu_3Au/SiO_2 composition, the broad reflection did have maxima which favoured the presence of alloy formation (represented by *).

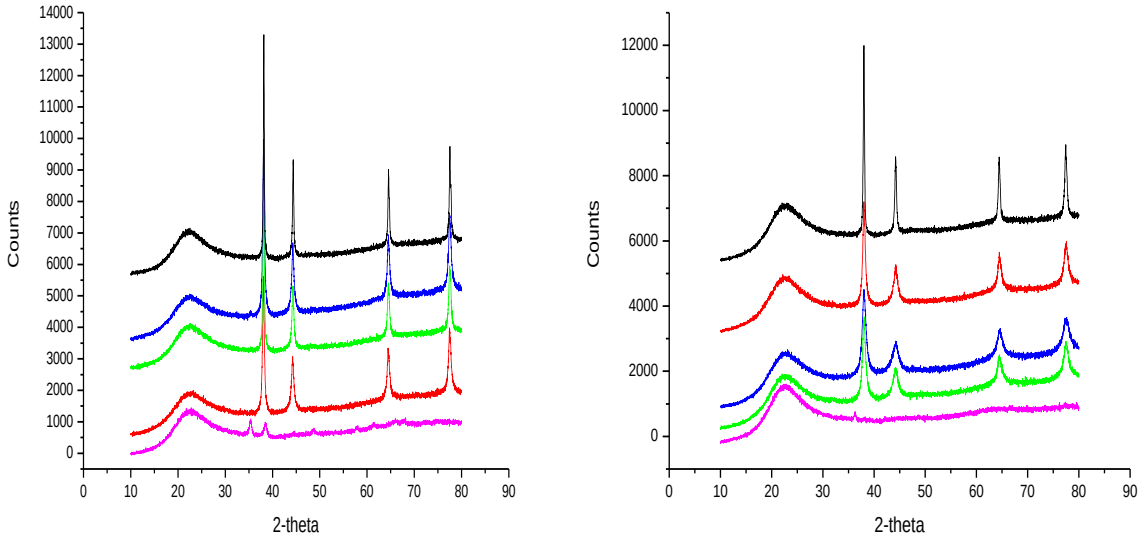

(a) **(b)**

Figure 3.10(a) $CuAu/SiO_2$ made *via* co-impregnation with copper nitrate and chloroauric acid followed by a Sinfelt calcinations (C978101A-E) (b) $CuAu/SiO_2$ catalyst made *via* co-impregnation with copper nitrate and chloroauric acid followed by a reduction by $NaBH_4$.(C97880A-E).

__ 1:1 $CuAu/SiO_2$ __ 1:3 $CuAu/SiO_2$ _ 3:1 $CuAu/SiO_2$ __ Au/SiO_2 __Cu/SiO_2

The preparation technique of using co-impregnation with a copper nitrate precursor and then reducing the catalyst for 2 h in H_2/Ar, followed by a high temperature firing at 676 ^oC, revealed only the metallic gold phases for the $CuAu/SiO_2$ catalyst made in this way (Figure 3.10a). The Cu/SiO_2 sample has phases that can be assigned to copper oxide – *Tenorite.* An alternative reduction with $NaBH_4$ was also incorporated into another preparation method (Figure 3.10b) to assess whether using this reagent made any difference, when compared to hydrogen reduction. The XRD revealed that the material does give a different XRD pattern to the catalyst reduced in H_2/Ar. The catalysts reduced in $NaBH_4$ had a similar pattern to the directly calcined samples, with phases only assigned to metallic gold. The Cu/SiO_2 catalyst

made via this method had a weak pattern that is amorphous but did have weak reflections for copper oxide –*Tenorite.*

3.3.1 In situ XRD

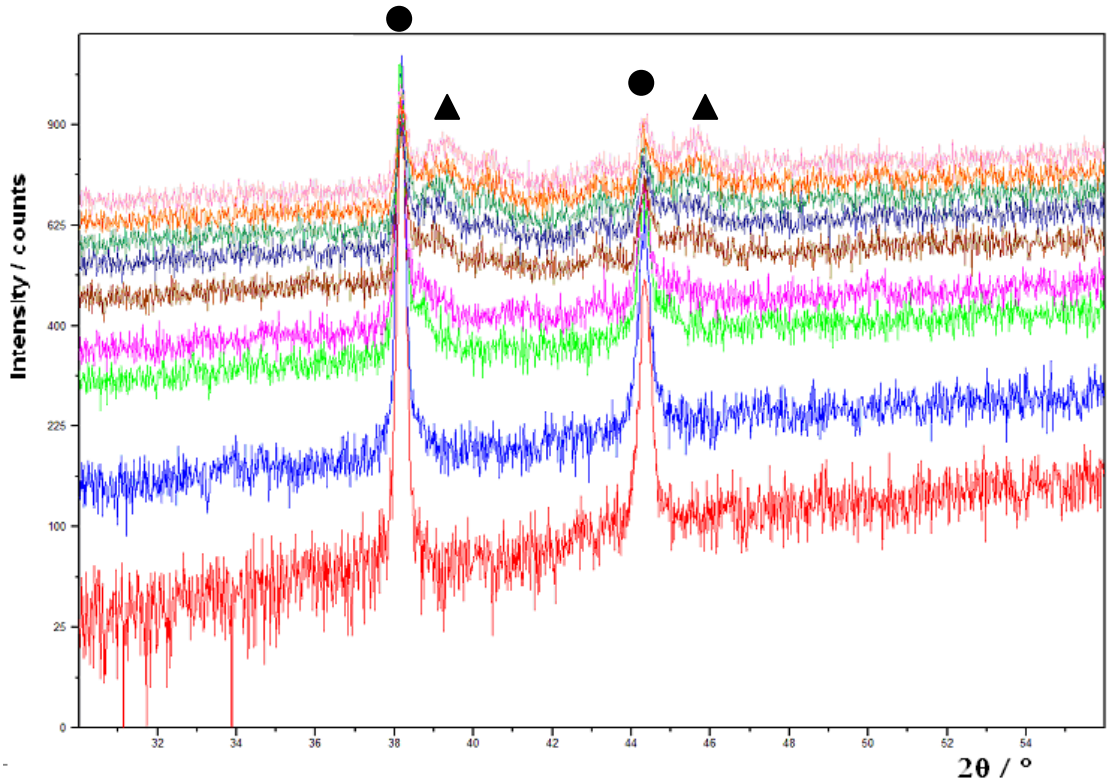

Figure 3.11 *In-situ* XRD analysis of the decomposition of the dried precursor under flowing 5% H_2/N_2. The plots show temperatures of 200 °C (red), 275°C (blue), 300°C (green) and then during the hold at 315°C (pink, brown, dark blue, green, orange and pale pink). The peaks for Au and CuAu are represented by ● and▲ respectively.

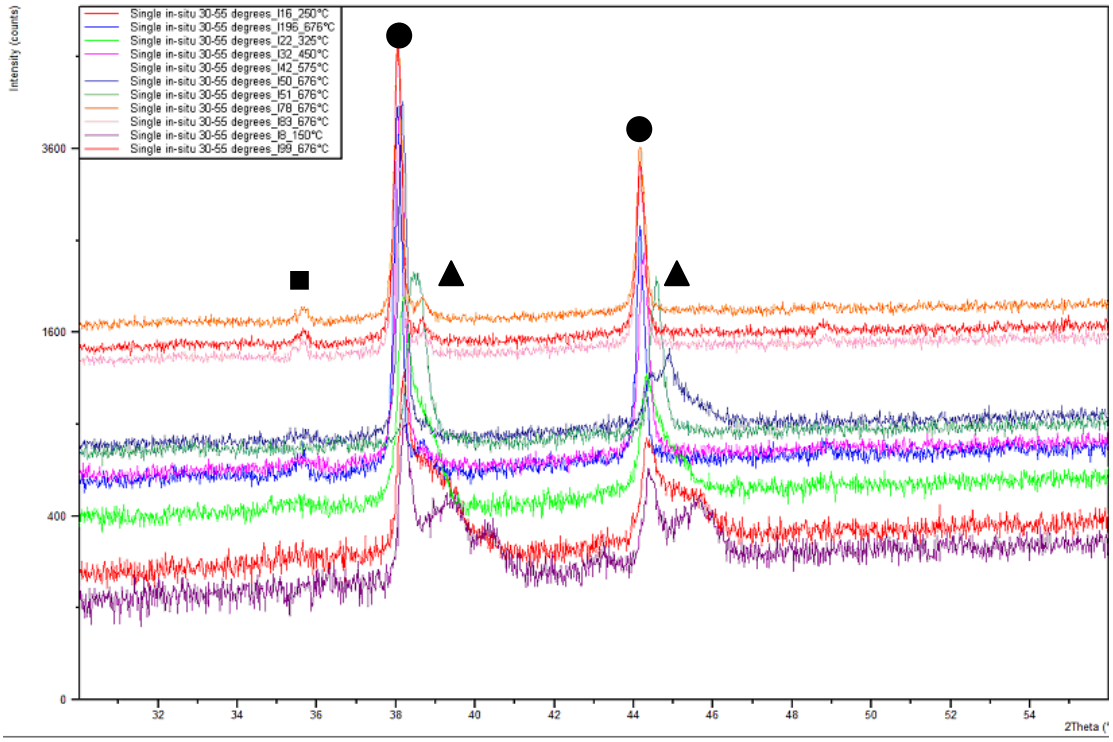

Figure 3.12 *In situ* XRD analysis of the decomposition of the reduced catalyst during high temperature oxidation using air. The plots show temperatures of 150 °C (purple), 250 °C (red), 325 °C (green), 450 °C (purple) and then during the hold at 675 °C. The peaks for Au, CuAu and CuO are represented by ●, ▲ and ■ respectively.

In situ XRD was utilised to study the formation of the $CuAu/SiO_2$ catalysts with a Sinfelt thermal treatment together with a reduction in 5% H_2/N_2 (Figure 3.11) and a high temperature calcination in air (Figure 3.12) (C978101A). During the reduction process, the *in situ* XRD revealed that the main reflections of gold are present throughout the reduction step. At low temperatures (<200 ^{o}C), metallic Au is already present which could have been generated from the decomposition step, and this Au species could be the source of the unalloyed gold. These in situ XRD patterns suggested that the catalyst could be reduced at lower temperatures to attempt to form more alloyed particles and less unalloyed Au particles. The presence of CuAu alloy species could also be confirmed by broader reflections at higher angle than the

gold reflections at >275 ^{o}C. As the temperature increased during the reduction step, the intensity of the alloy reflection increased. The longer the reaction continued, the more alloy species were observed. Therefore, it might be possible to modify the CuAu alloy species by adjusting the temperature and length of time of the reduction step. Once the catalyst underwent oxidation (Figure 3.12), the alloy phase disappeared as the temperature increased and, at the end of the high temperature calcinations, only metallic Au reflections were seen, as well as a copper oxide – *Tenorite* reflection.

3.4 Temperature programmed reduction TPR

Temperature programmed reduction has been used as a technique to help understand the most appropriate reduction temperature for heterogeneous catalysts in many studies.

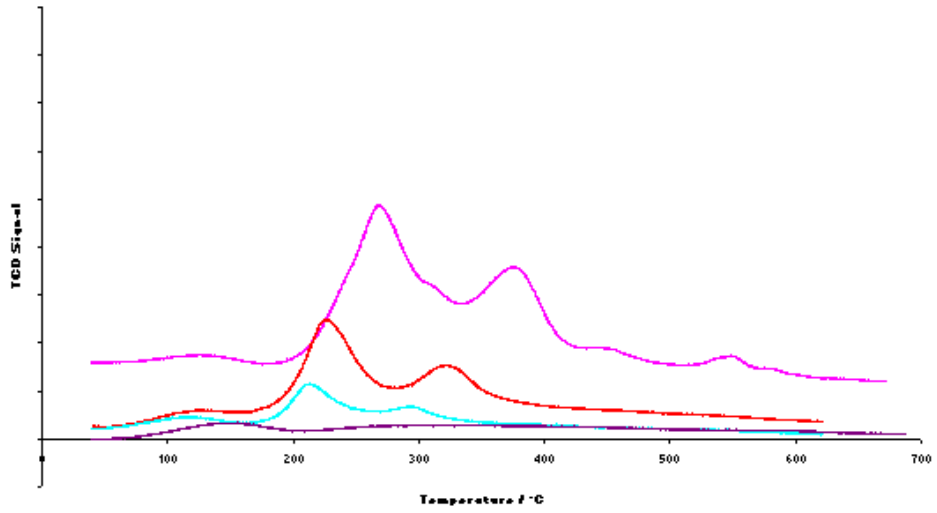

Figure 3.13 Overlay of TPR profiles for $AuCu/SiO_2$ and Au only catalysts prepared by impregnation calcined at 400 ^oC for 2 h in air (C978/19A-C, C97809, C97802D).

___ Au/SiO_2 ___ $CuAu/SiO_2$ ___Cu_3Au/SiO_2 ___$CuAu_3/SiO_2$

A few $CuAu/SiO_2$ catalysts have been chosen for this analysis and Cu and Au only samples have been tested as well for comparison. A trend has been reported by Chimentao *et al*,[3] who studied $CuAu/TiO_2$ catalysts for propene epoxidation. The TPR analysis showed peaks around 167-197 and 356-376 ^oC and, as the Cu content increased, there was a shift to lower temperature reduction. They also thought that this suggested that the copper might affect the electronic structure of the gold by near neighbour interactions. However, Figure 3.13 shows that the $AuCu/SiO_2$ catalyst in this study, with a 3:1 Cu:Au molar ratio (pink line), had a

maximum that was shifted to higher temperatures; whereas, increasing the gold content (light blue line), shifted the maxima to lower temperature values. This trend was different to what Chimentao *et al* observed. However, there were certain factors that were different in both studies, e.g. the support, wt% etc.

Yang *et al* [4] observed a major peak at 227 ^{o}C for CuO/ZnO along with two shoulder peaks at 187 and 252 ^{o}C. The major peak corresponded to the reduction of CuO to metallic copper. The low temperature shoulder peak at 187 ^{o}C was assigned to the reduction of CuO to Cu^{+} and the high temperature shoulder peak at 252 ^{o}C was assigned to the reduction of Cu^{+} to metallic copper. The Cu/SiO_2 catalyst (Figure 9 appendix) had two distinct reduction peaks, at 240 and 380^{o}C, with the higher temperature peak having a shoulder at 450^{o}C. The lower temperature peak could be due to CuO reduction to Cu^{+}, whereas the major higher temperature peak could be due to CuO reduction to metallic Cu, with the shoulder peak representing Cu^{+} to metallic Cu. For the reduction of CuO and Cu_2O different amounts of H_2 are required and are quantified by the TCD which was calibrated. For their Au/CuO/ZnO sample, a broad peak with two unresolved signals at 213 and 227 ^{o}C was identified. The two TPR signals are related to the two step reduction (Cu (II) →Cu (I) →Cu (0)) as suggested by Fang *et al.*[5]

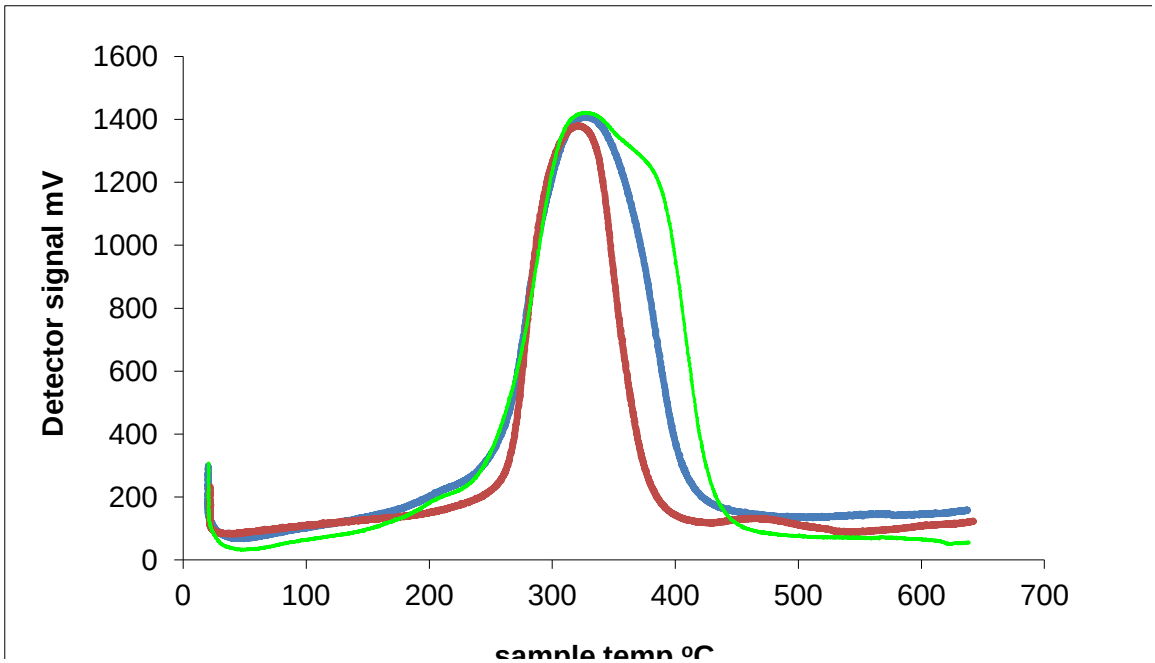

Figure 3.14 TPR profiles of $CuAu/SiO_2$ catalysts with different molar ratios reduced in H_2/Ar at 315 ^oC for 2 h and calcined at 676 ^oC for 15 h in air (C978101A-C).

$CuAu_3/SiO_2$ Cu_3Au/SiO_2 $CuAu/SiO_2$

For the samples prepared by the Sinfelt methology CuAu 1:1, 1:3 and 3:1 (Figure 3.14), the single reduction peak could be assigned to a one step reduction (CuO to Cu metal) as stated by Lian *et al.*[6]

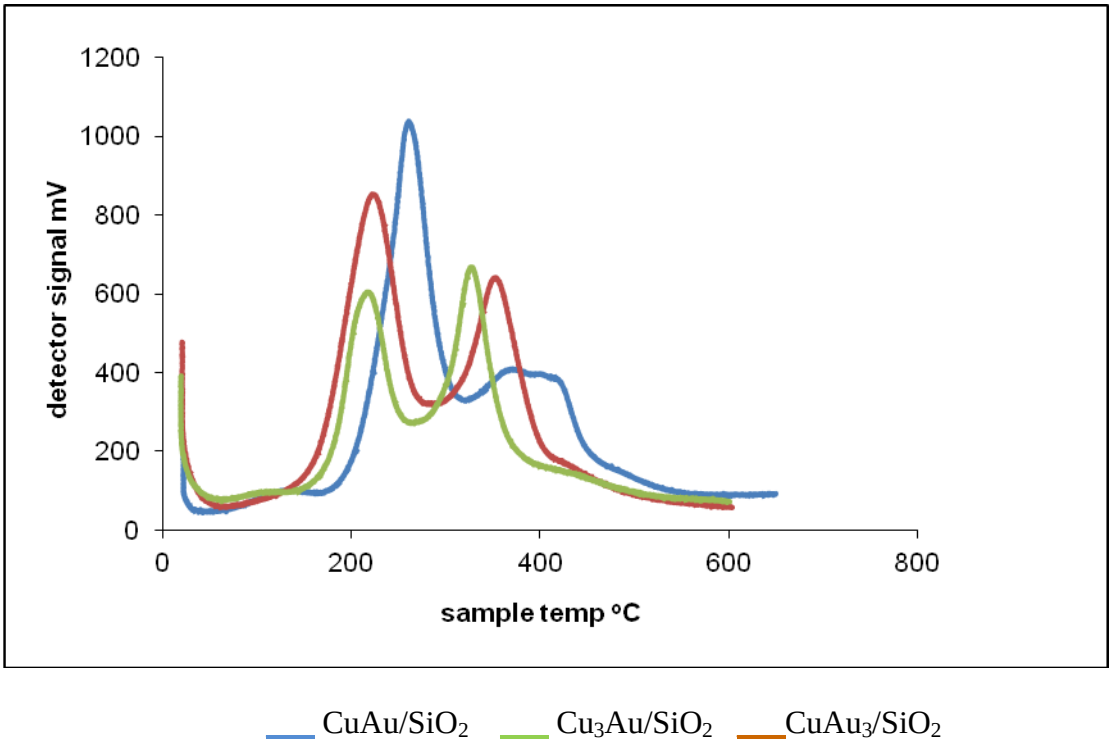

Figure 3.15 TPR profiles for $CuAu/SiO_2$ catalysts prepared by impregnation with copper chloride and chloroauric acid followed by a calcination in air at 400 ^{o}C for 2 h (C97863A-C).

However, for the co- impregnated catalyst (Figure 3.15), the major peak could be assigned to the reduction of CuO to Cu and the smaller peak Cu^{+} reduction to Cu metal. Lian *et al* [6] have also measured the TPR profiles of AuCu catalysts. The profile showed a single peak (190-290 ^{o}C) which they explained was due to a one step reduction of CuO to Cu metal. A reason why their catalysts differed from the ones in this study could be because they used a different preparation route, since Lian used a precipitation method with a calcination at 300 ^{o}C in 20% O_2/Ar for 4 h. The absence of any other peak at lower temperatures suggested that the Au species must have been already reduced to the metallic form. The reduction peak of CuO in the Au/CuO/ZnO sample shifted to a lower temperature, compared with the CuO/ZnO sample. This showed that Au promoted CuO reduction, which occurred at lower temperatures. It agreed with this study because the copper only sample had a slightly higher reduction profile than our AuCu catalysts. Yang *et al* [4] concluded that there was an

interaction between Au and CuO in the Au/CuO/ZnO catalysts, which could enhance the reducibility of CuO. Figure 3.13 showed that there is a shift towards higher reduction temperatures that went in the order 1:3 Au:Cu > 3:1 Au:Cu > 1:1 Au:Cu. This suggested that when there was more copper in the sample, lower reduction temperatures were observed by Chimentao *et al*.[3]

A TPR-TPO-TPR experiment has been undertaken for the $AuCu_3/SiO_2$ catalyst (C97819C) to observe the effect of re-reduction on catalysts that have been oxidised. Figure 11 (appendix) illustrates the initial TPR profile and shows a major reduction peak at 200-250 ^oC and a shoulder peak at 270-380 ^oC, which is probably due to CuO reduction to Cu metal and Cu^+ reduced to metallic Cu. Upon oxidation (Figure 12 appendix), there seemed to be a broad peak. Kameoka *et al* [2] have performed TPO on an AuCu catalyst up to temperatures of 1000 ^oC and noticed an oxidation peak after 400 ^oC. Once the sample was reduced again, two reduction peaks appeared and the second peak had shifted to a slightly lower temperature (Figure 13 appendix).

The TPR results showed that for the Cu/SiO_2 catalysts made by impregnation (IMP) and high dispersion (HD)(appendix Figure 10), two noticeable reduction peaks were seen. For the IMP sample, the peaks were from 210-280, 310-450 ^oC and 450-500 ^oC. For the HD catalyst, there were reductions at 200-300 and 300-400 ^oC. After the impregnated Cu/SiO_2 catalyst was used for propene oxidation, only one reduction peak was observed between 200-400 ^oC (appendix Figure 9). For the Au/SiO_2 catalysts, prepared by impregnation (appendix Figure 8) and deposition precipitation (appendix 7), the peaks were less intense and broader. A peak was seen between 200-500 ^oC for the impregnated Au/SiO_2 catalyst and between 200-450 ^oC for the deposition precipitation sample. A silica only TPR (appendix Figure 6) was carried out to determine if any peaks appeared and there was a small peak showing reduction at 100-200 ^oC that was apparent in most of the catalysts. For the $AuCu/SiO_2$ catalysts, there were two

reductions peak around 190-300 and 300–400 ^{o}C but as the Cu loading increased, the maximum of the peaks shifted to higher temperatures. For example, the 1:1 catalyst (Figure 3.13) had peaks at 190-290 and 300-400 ^{o}C whereas, the 3:1 CuAu catalyst (Figure 3.13) had peaks at 220-350 and 350-420 ^{o}C. A trend was also been seen by Chimentao *et al*,[3] who studied CuAu/TiO_2 catalysts for PO epoxidation. The TPR analysis showed peaks around 167-197 and 356-376 ^{o}C and, as the Cu content increased the shift went to lower values. They also thought that this suggested that the copper might affect the electronic structure of the gold by near neighbour interactions. However, when looking at our samples the higher copper loadings shifted the maxima to higher temperatures, whereas increasing the gold shifted the maxima to lower values.

Comparisons between 1:1 CuAu catalysts with either copper chloride or copper nitrate precursors and direct or Sinfelt calcinations are shown in Figure 3.16. Both the chloride preparations had reduction peaks at slightly lower temperatures than with the nitrate precursors. For the chloride precursor, the calcination technique seemed to have an effect on the position of the two reduction peaks. When the catalyst is directly calcined, two reduction peaks were around 200 and 500 ^{o}C. Whereas, if the Sinfelt route is chosen, the reduction peaks were around 200 and 350 ^{o}C.

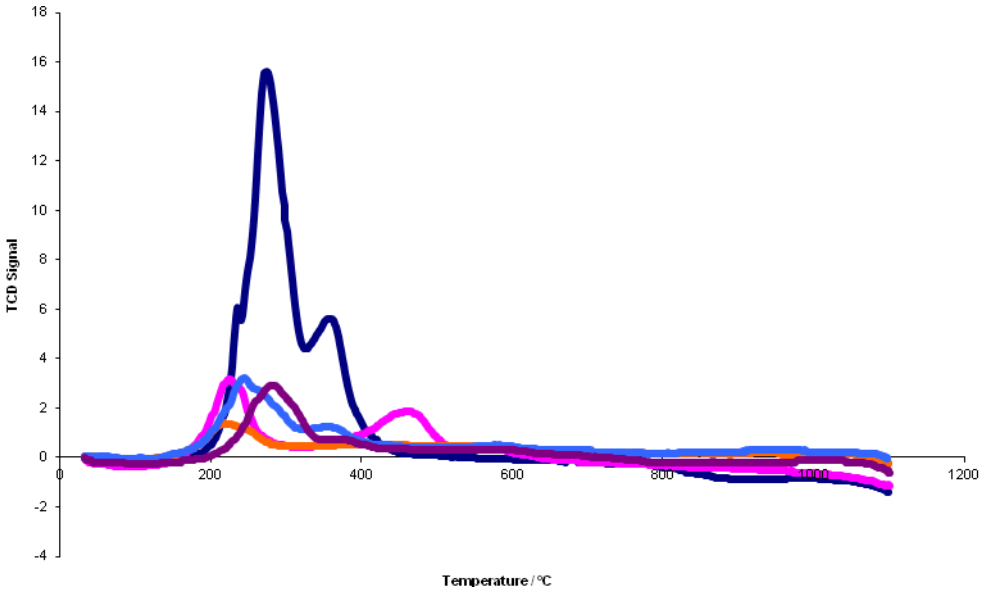

Figure 3.16 Overlay of TPR profiles for catalysts made by co-impregnation with different copper precusors and calcination conditions. ___ Cu/SiO_2 with copper nitrate and directly calcined at 400 ^oC for 2 h in air. (C97802D) ___ 1:1 Cu(chloride)Au/SiO_2 and directly calcined (C97863A)) ___ 1:1 Cu(nitrate)Au/SiO_2 and directly calcined (C97819A) ___ 1:1 Cu(chloride)Au/SiO_2 and Sinfelt treated (reduction in H_2/Ar followed by high temperature calcination)(C97865A) ___ 1:1 Cu(nitrate)Au/SiO_2 and Sinfelt treated (C978101A).

Catalyst	Preparation	Hydrogen uptake μ mol/g
Cu/SiO_2(C97802D)	Impregnation, Cu nitrate, direct calcination	1403
C97802D after propene	Impregnation, Cu nitrate, direct calcination	884
Cu/SiO_2(C97802B)	Impregnation, Cu chloride, direct calcinations	1488
$CuAu/SiO_2$(C97819A)	Impregnation, Cu nitrate, direct calcination	191
$CuAu_3/SiO_2$(C97819B)	Impregnation, Cu nitrate, direct calcination	738
Cu_3Au/SiO_2(C97819C)	Impregnation, Cu nitrate, direct calcination	658
Cu/SiO_2 (C97828)	Precipitation	615
Au/SiO_2(C97836)	Deposition precipitation	277
Cu/SiO_2(CF128)	High dispersion	414
$CuAu/SiO_2$(C978101A)	Sinfelt, Cu nitrate	1754
$CuAu_3/SiO_2$(C978101B)	Sinfelt, Cu nitrate	2186
Cu_3Au/SiO_2(C978101C)	Sinfelt, Cu nitrate	1535
$CuAu/SiO_2$(C97887)	HDC Cu+ AuDP direct calcinations	231
$CuAu/SiO_2$(C97890)	HDC Cu+ AuDP calcination and reduction	111

Table 3.2 Hydrogen consumption data

Hydrogen consumption for catalysts prepared in different ways and with different CuAu molar ratios are presented in Table 3.2. In a calibration experiment, TPR data were collected and used to quantify the H_2 consumption during the reduction, and thus to calibrate the response of the TCD. Large consumptions of hydrogen were measured for the Cu/SiO_2 samples, as expected, since these catalysts were reducing copper (II) oxide to Cu (0) metal and had a weight percentage close to 5 wt%. However, Sinfelt prepared catalysts also had very large consumptions. The lowest consumptions of hydrogen were observed for the Au/SiO_2 (C97836) catalyst prepared by deposition, and the $CuAu/SiO_2$ sample (HDC Cu and Au by DP (C97890)). This was probably due to the technique not dispersing the metal

particles on the support as effectively as other methods. Surprisingly, out of the different molar ratios, the composition with $CuAu_3$ had the highest consumption. The high consumption in the TPR spectrum of the catalyst is due to the high amount of hydrogen needed for the reduction of the copper metal. It appeared that the presence of more gold in the bimetallic samples enhanced the copper reduction, which may have been because the gold helped the hydrogen atoms to dissociate and then reduce the metal oxides.

3.5 SEM images

3.5.1 Direct calcined catalysts:

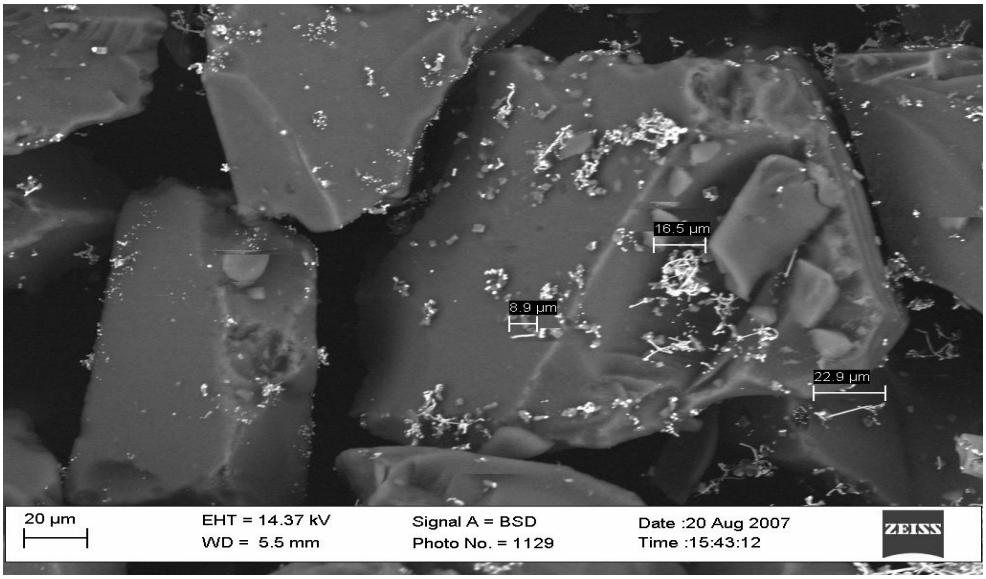

(a)

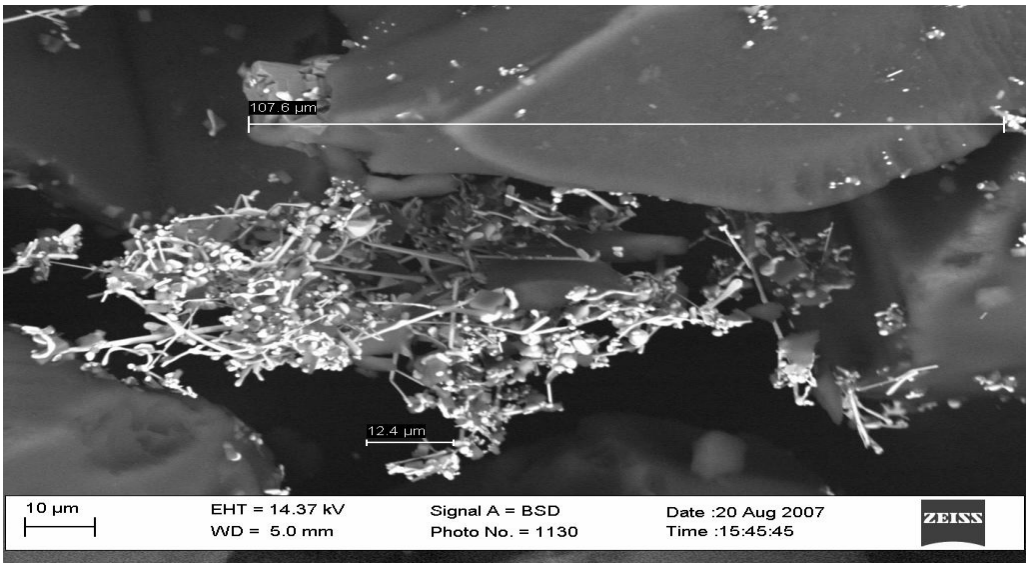

(b)

Figure 3.17 SEM images of $CuAu/SiO_2$ catalyst with direct calcination (C97819A) (a) at low magnification (b) at higher magnification

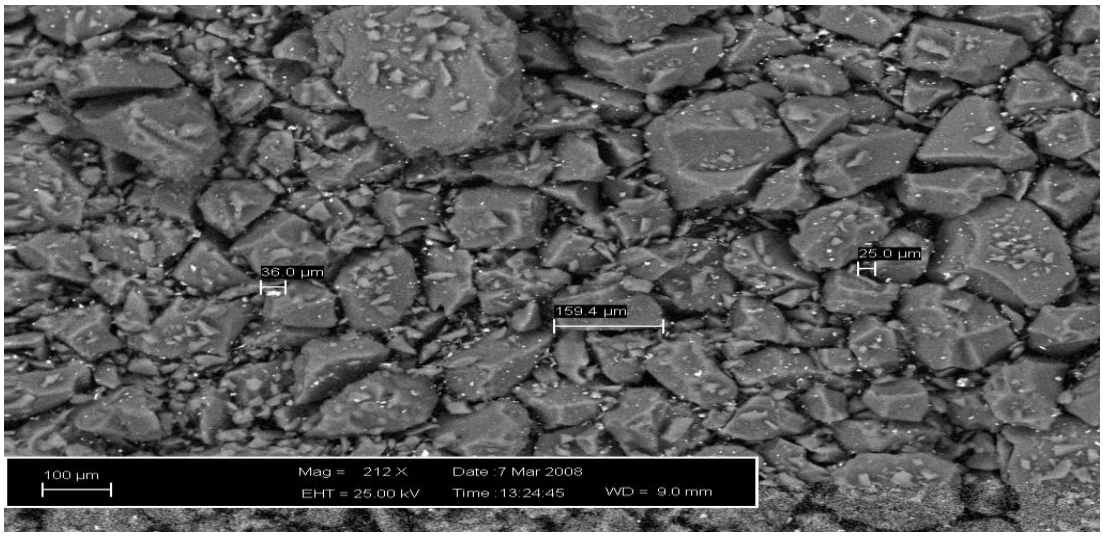

(a)

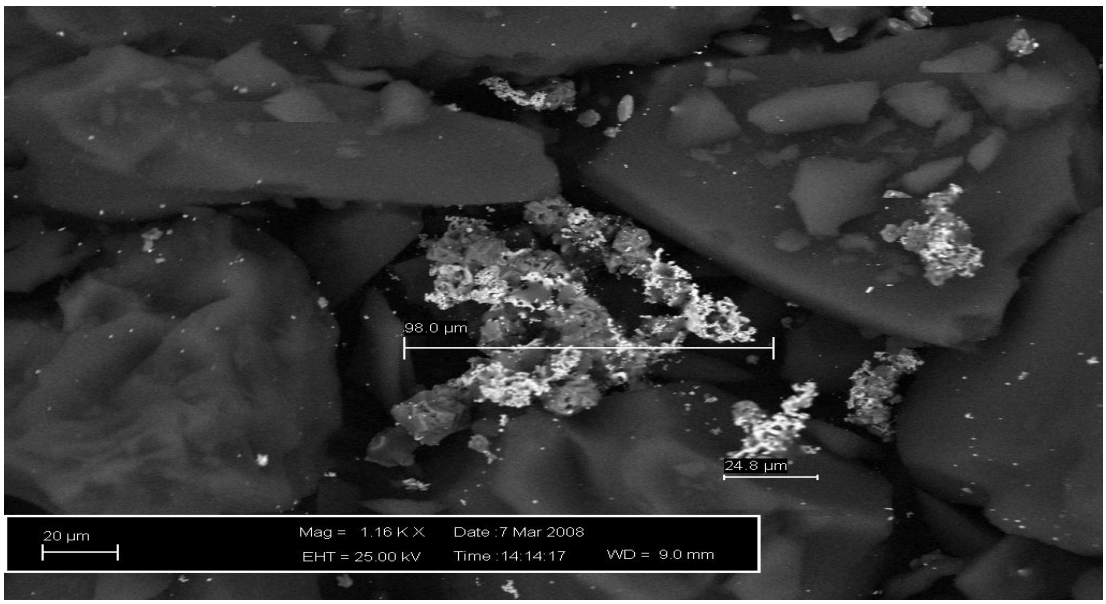

(b)

Figure 3.18 SEM images of $CuAu_3/SiO_2$ directly calcined (C97819B) at (a) low magnification (b) higher magnification

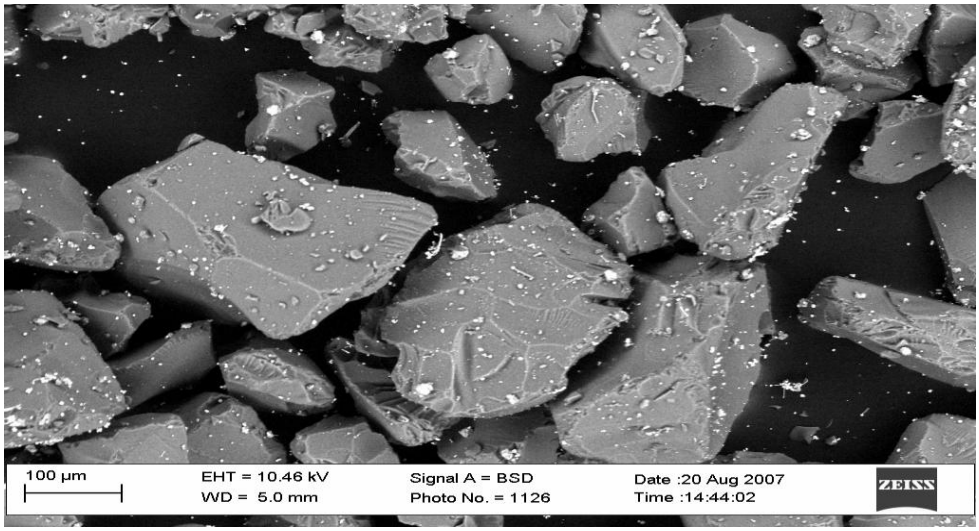

(a)

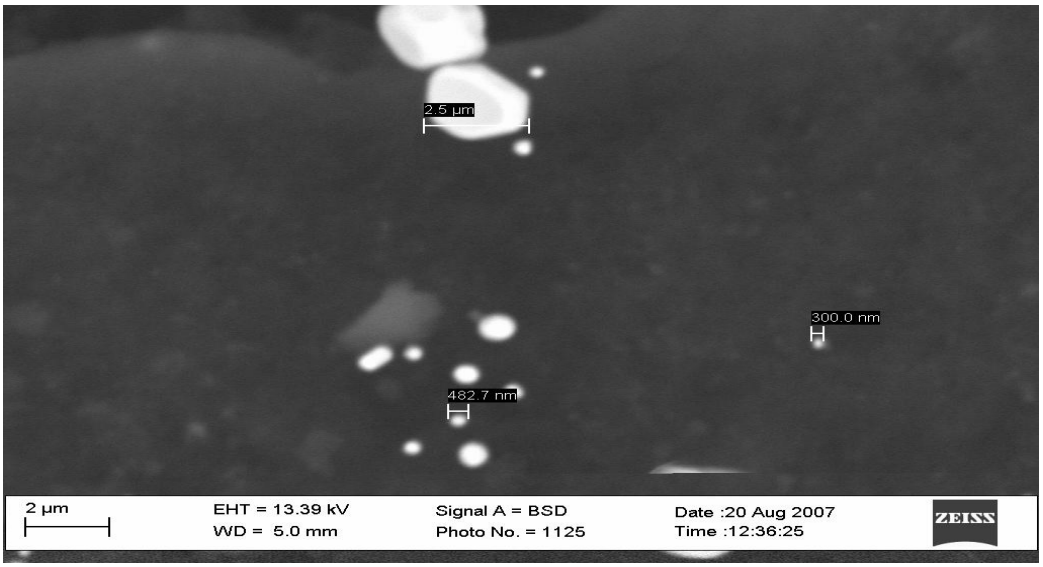

(b)

Figure 3.19 (a) SEM image of Cu_3Au/SiO_2 directly calcined (C978/19C) at low magnification (b) at higher magnification

SEM images were obtained for catalysts made by direct calcination (400 ^oC for 2 h in air). Large needle like ensembles of gold were observed for the $CuAu/SiO_2$ sample (Figure 3.17 a) which was many microns in size. On closer inspection, it appeared that they were made up of smaller particles of Au. The $CuAu_3/SiO_2$ (Figure 3.18a and b) also shows large ensembles, as

well as highly dispersed Cu particles on the SiO_2 support. In addition to the large clusters, the Cu_3Au/SiO_2 SEM analysis also shows small spherical particles of Cu and Au (Figure 3.19b) which were confirmed by EDX analysis (appendix). The Au/SiO_2 comparison shows large Au clusters and therefore are a result of a weak metal support interaction (Figure 3.20a and b). The Cu/SiO_2 catalyst equivalent shows highly dispersed Cu particles on the support (Figure 3.21 a and b). For this catalyst it does not look the same throughout the sample and it appears to show a non homogeneous distribution of the copper.

However, SEM only detects larger big particles whereas TEM analysis will reveal if there are any smaller particles on the catalysts which is in the next section of this chapter.

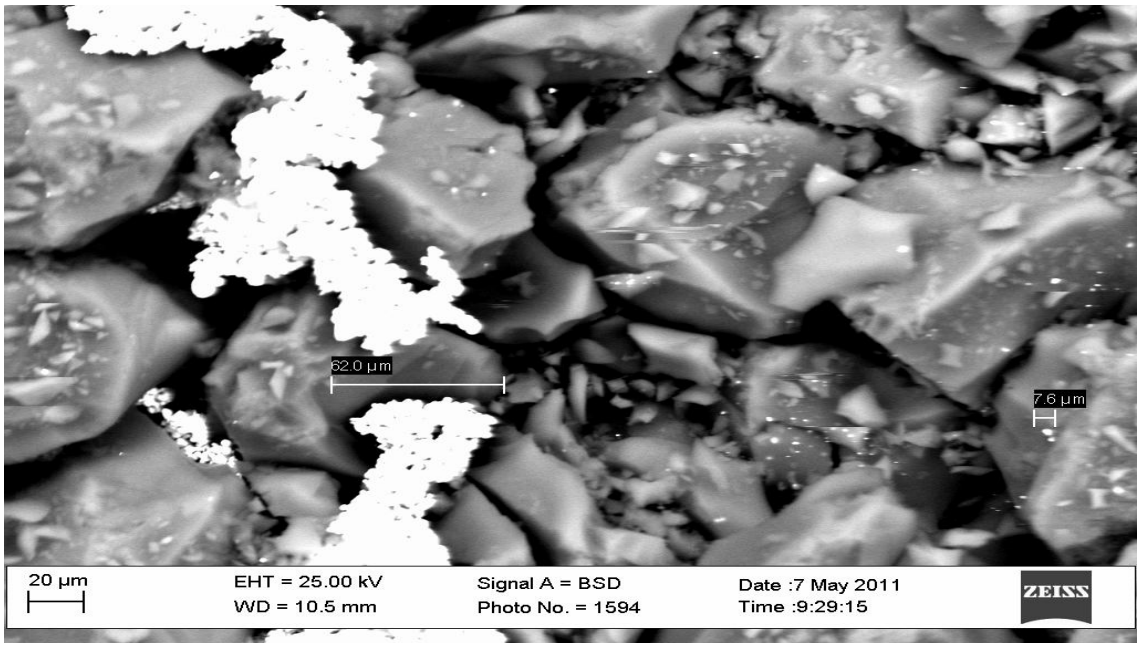

(a)

Figure 3.20 SEM images for Au/SiO_2 impregnated directly calcined (C97809) (a) at low magnification 20 µm

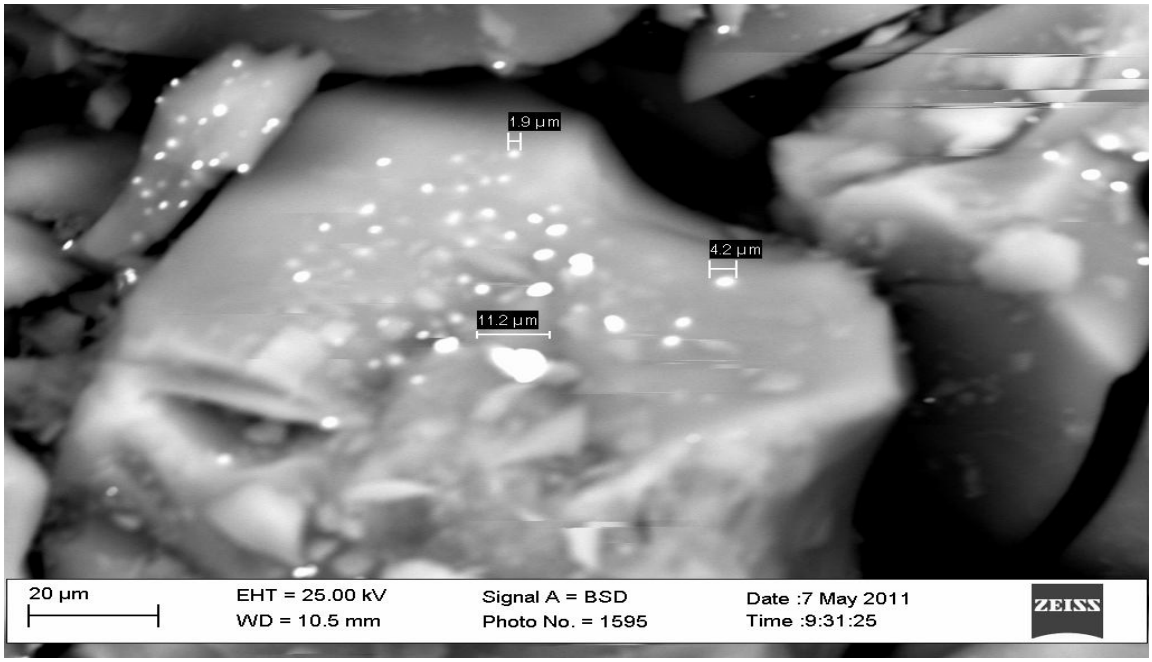

(b)

Figure 3.20 SEM images for Au/SiO_2 impregnated directly calcined (C97809) (b) Gold particles of about 1.9 µm.

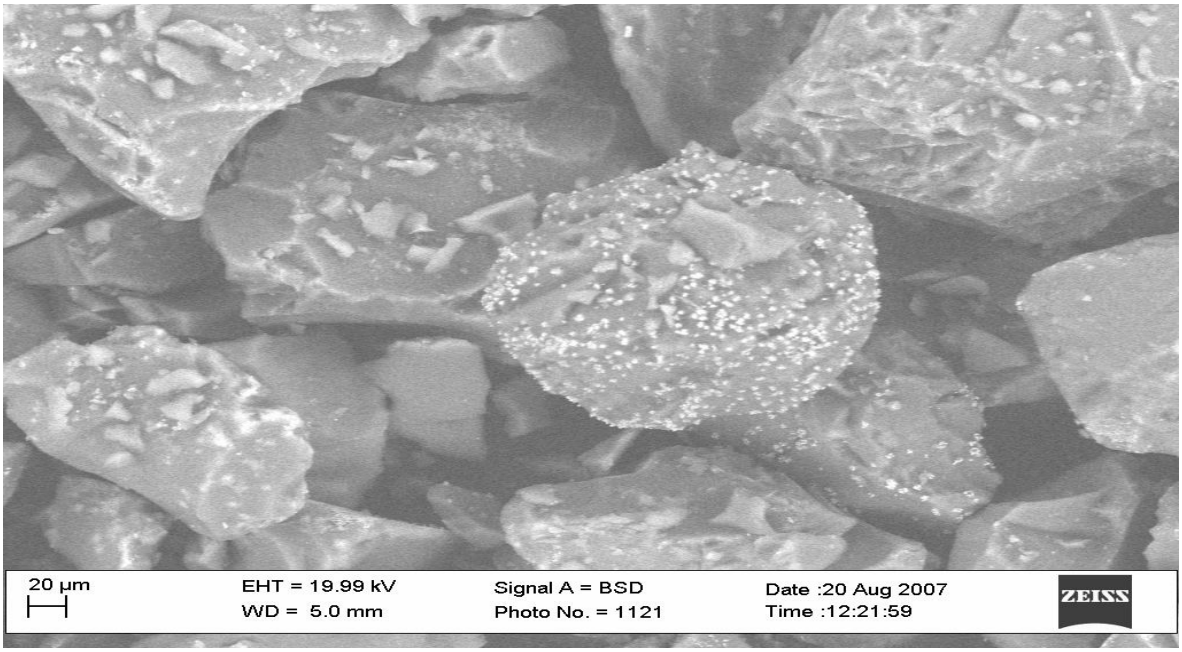

(a)

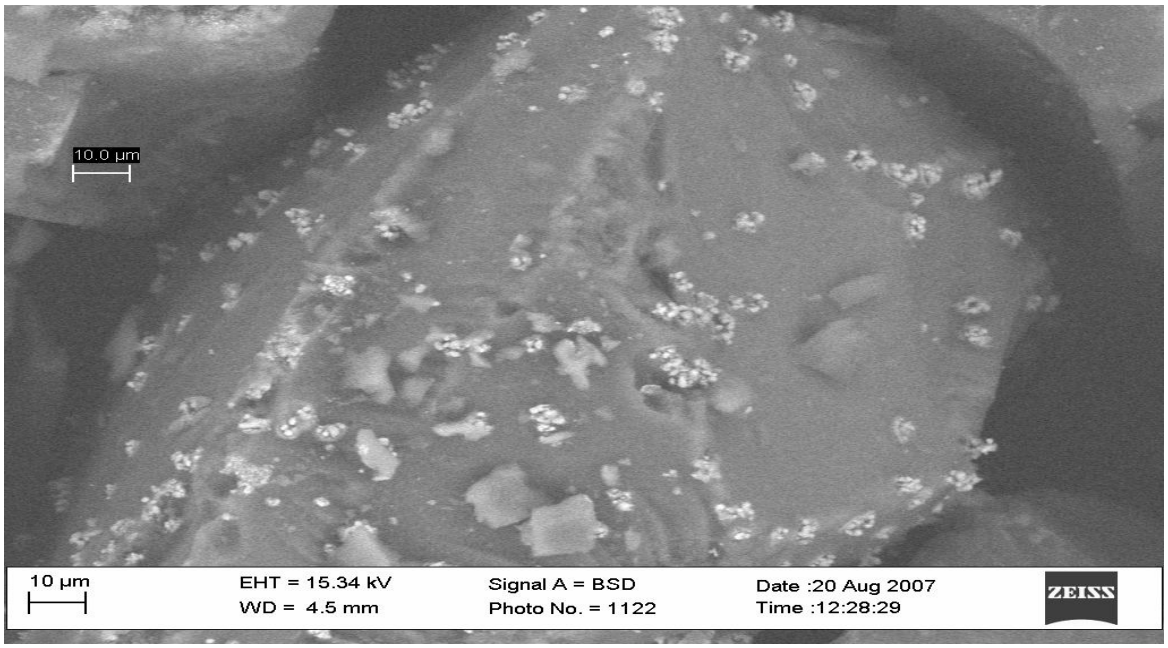

(b)

Figure 3.21 SEM images of Cu/SiO_2 by impregnation directly calcined (C97802D)

(a) at low magnification (b) at higher magnification

3.5.2 Sinfelt catalysts

3.5.2.1 Copper nitrate precursor

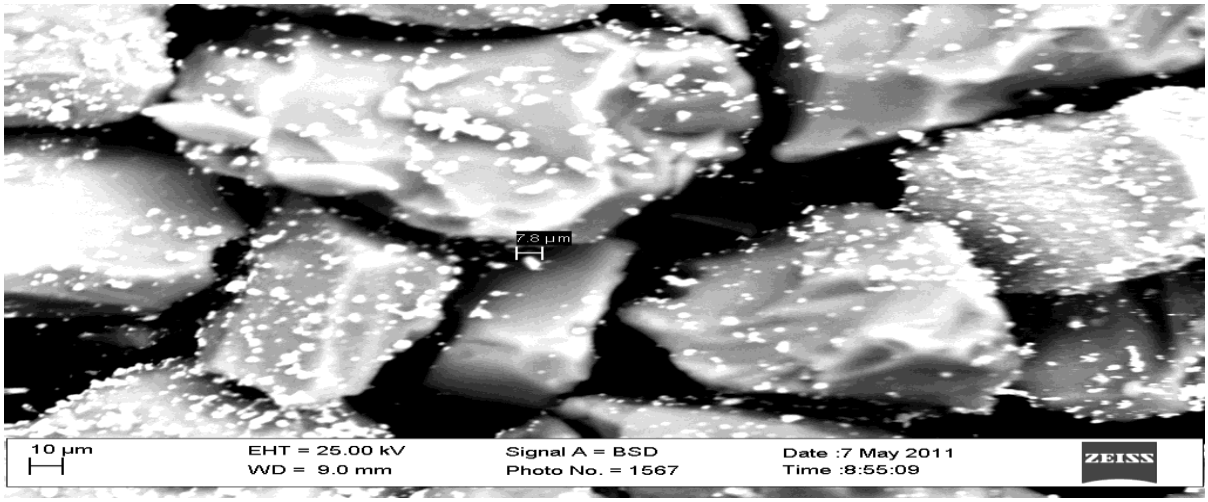

(a)

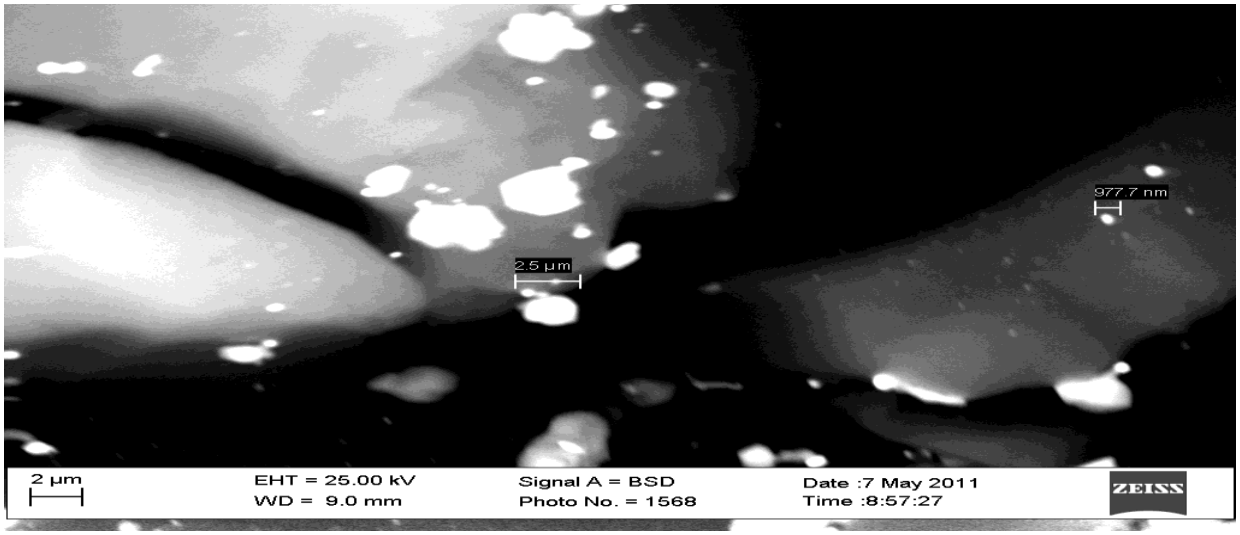

(b)

Figure 3.22 (a) and (b) SEM image of $CuAu/SiO_2$ by Sinfelt procedure (C978101A) reduced at 315 ^{o}C in H_2 only

Figure 3.22(a) and (b) shows the SEM image of CuAu catalyst reduced at 315 ^{o}C for 3 h in H_2 and dispersed particles can be seen on the support. Upon high temperature calcination, the particles appear to be more highly dispersed (Figure 3.23 (a) and (b)).

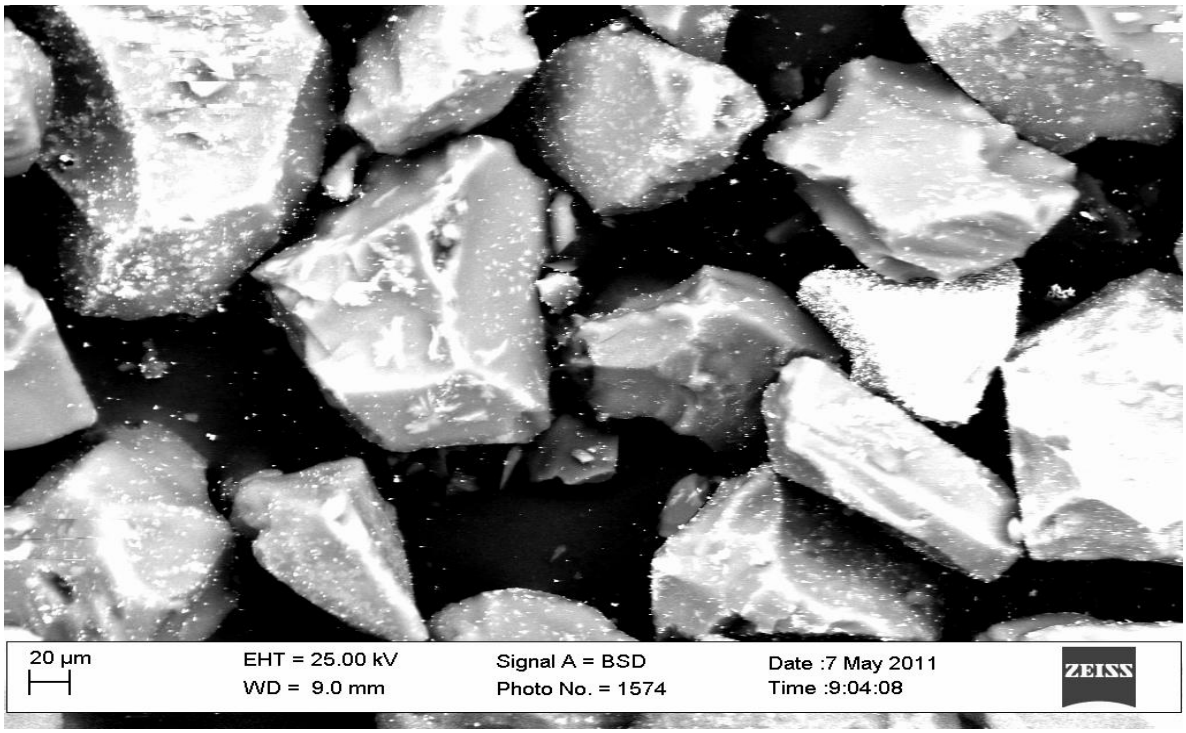

(a)

Figure 3.23 (a) SEM image of CuAu/SiO_2 by Sinfelt procedure (C978101A) reduced at 315 ^{o}C in H_2 followed by calcined at 676 ^{o}C for 15 h in air.

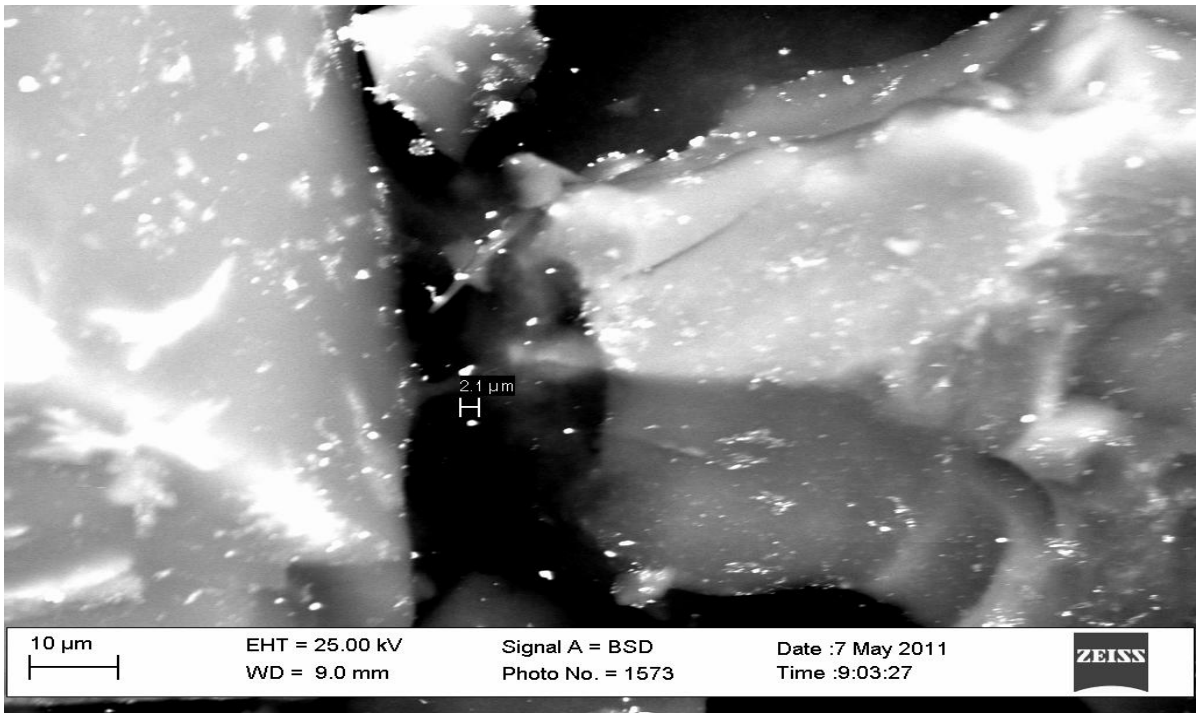

(b)

Figure 3.23 (b) SEM image of $CuAu/SiO_2$ by Sinfelt procedure (C978101A) reduced at 315 ^{o}C in H_2 followed by calcined at 676 ^{o}C for 15 h in air.

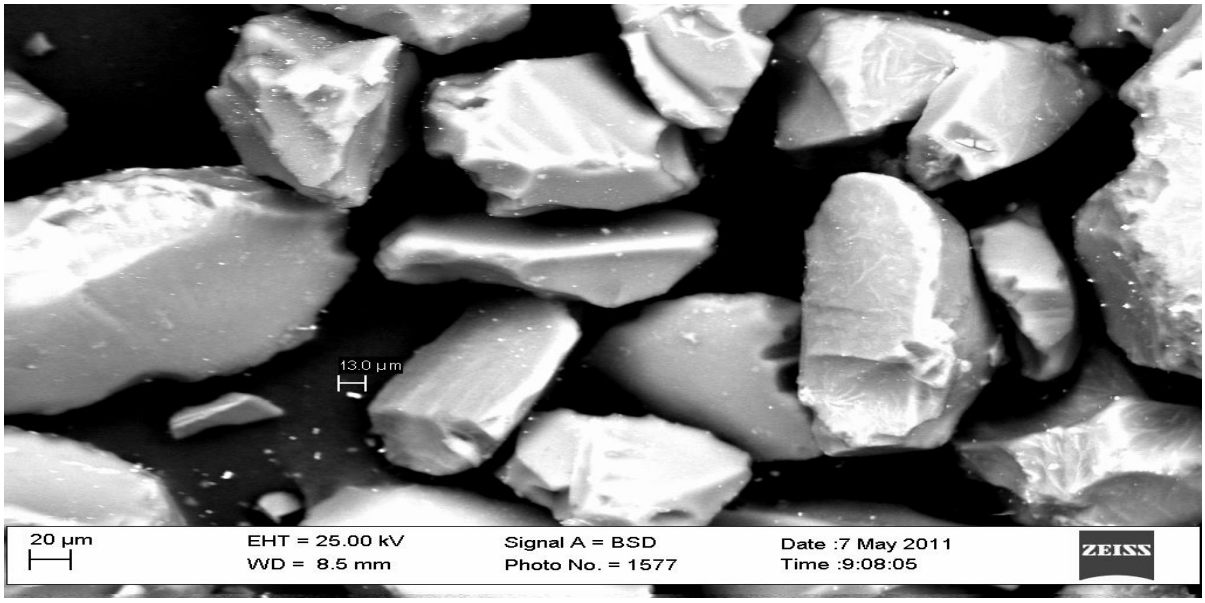

(a)

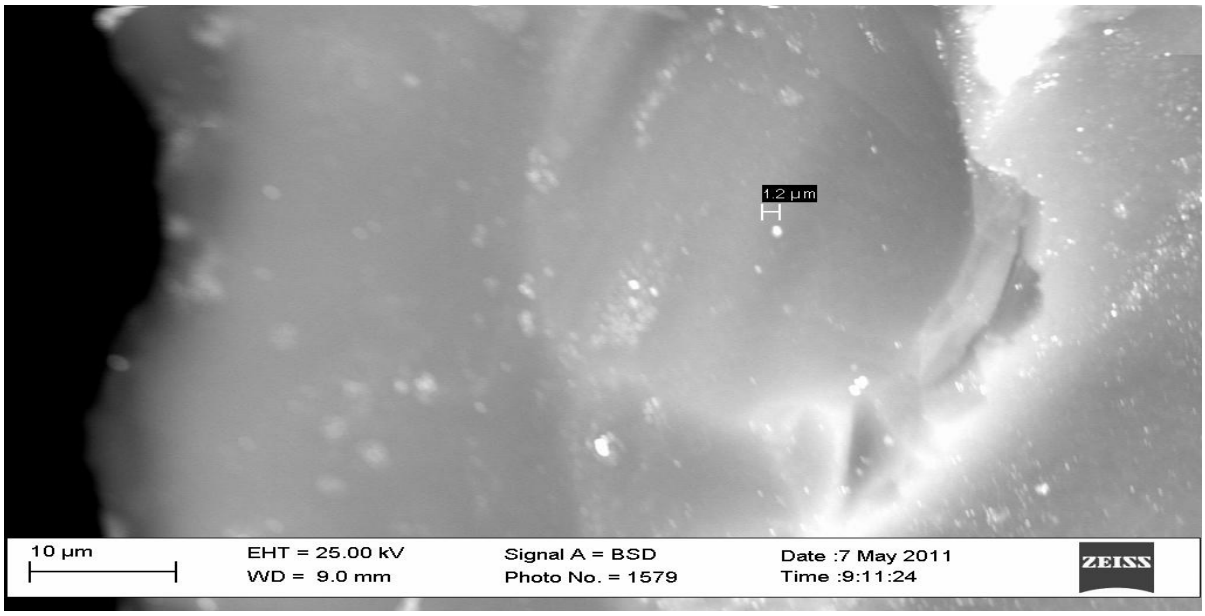

(b)

Figure 3.24 (a) and (b) SEM image of $CuAu/SiO_2$ by Sinfelt procedure (C978101B) reduced at 315 ^oC in H_2 only.

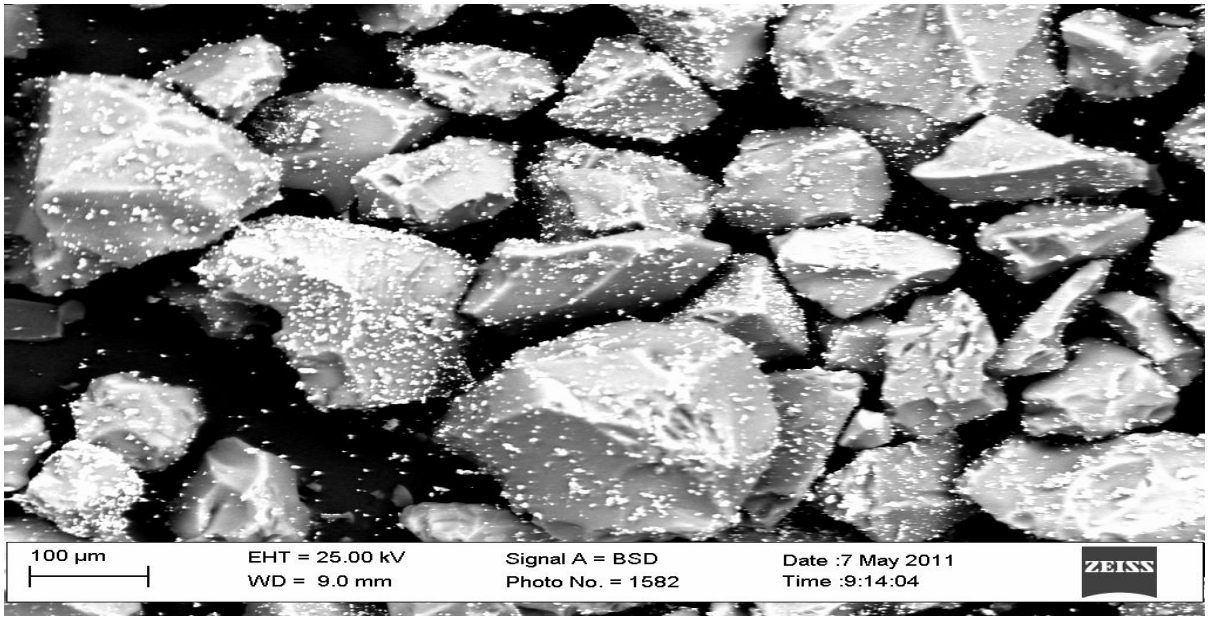

(a)

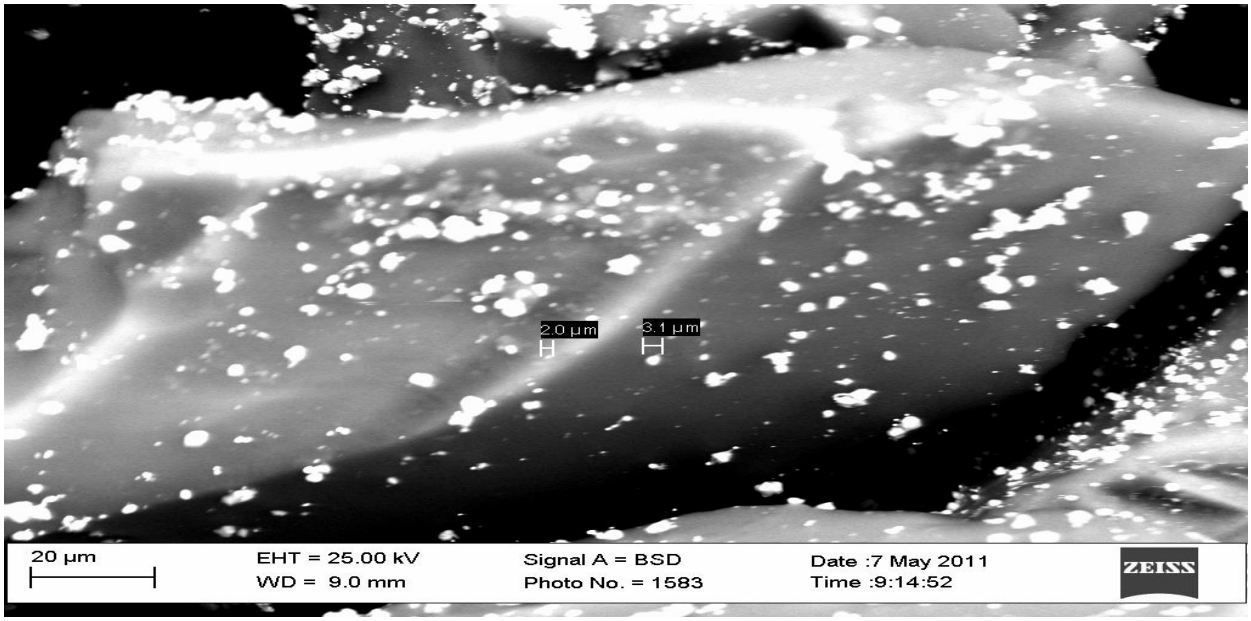

(b)

Figure 3.25 (a) and (b) SEM image of $CuAu/SiO_2$ by Sinfelt procedure (C978/101B) reduced at 315 ^oC in H_2 followed by calcined at 676 ^oC for 15 h in air.

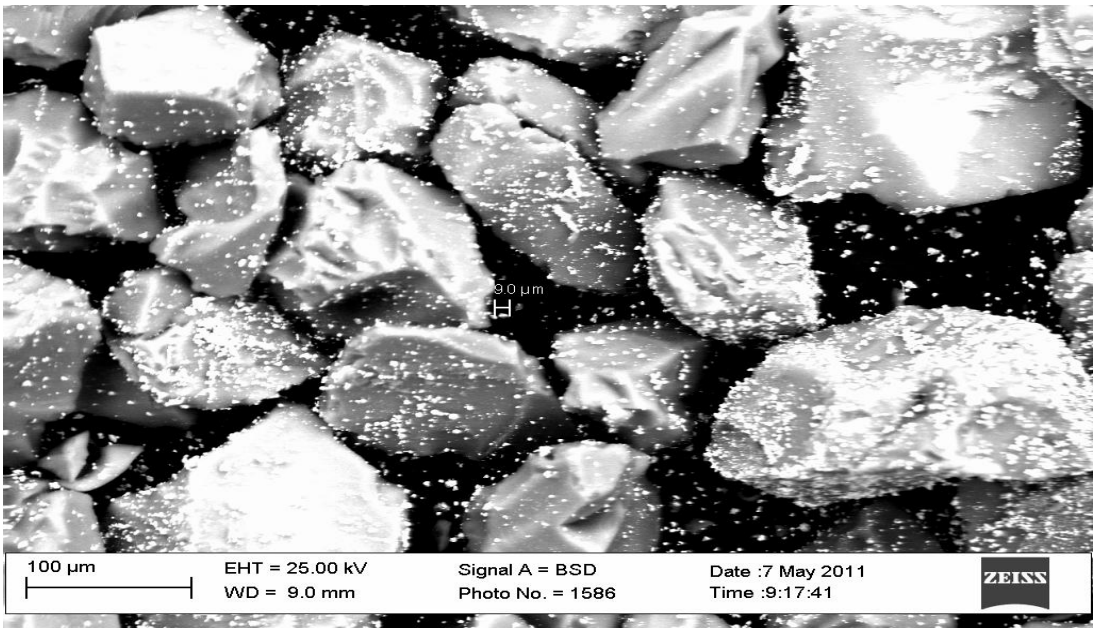

(a)

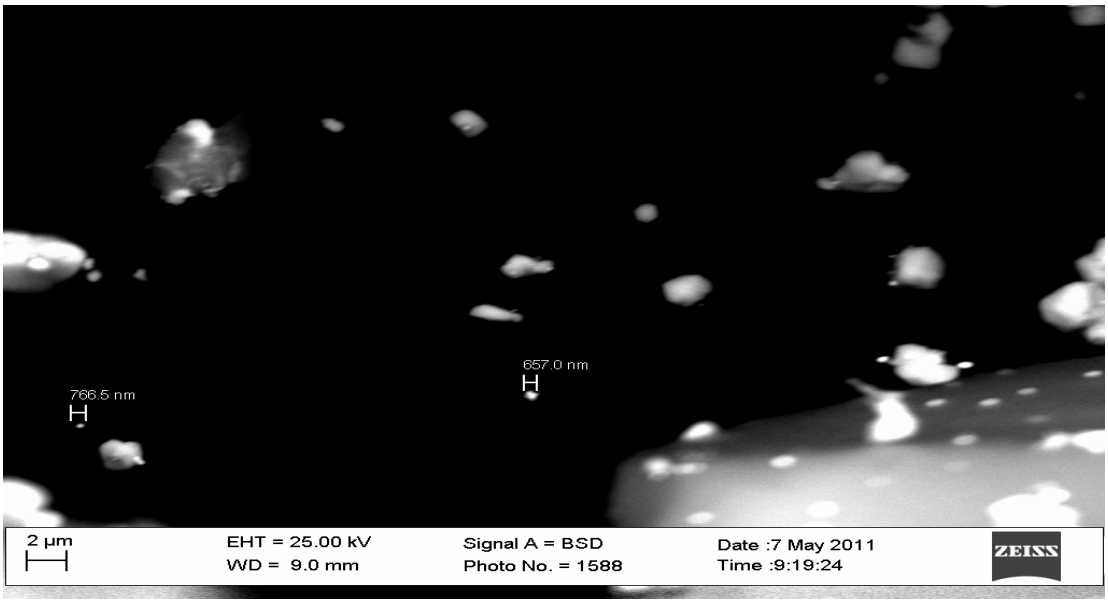

(b)

Figure 3.26 (a) and (b) SEM image of $CuAu/SiO_2$ by Sinfelt procedure (C978101C) reduced at 315 ^{o}C in H_2 only

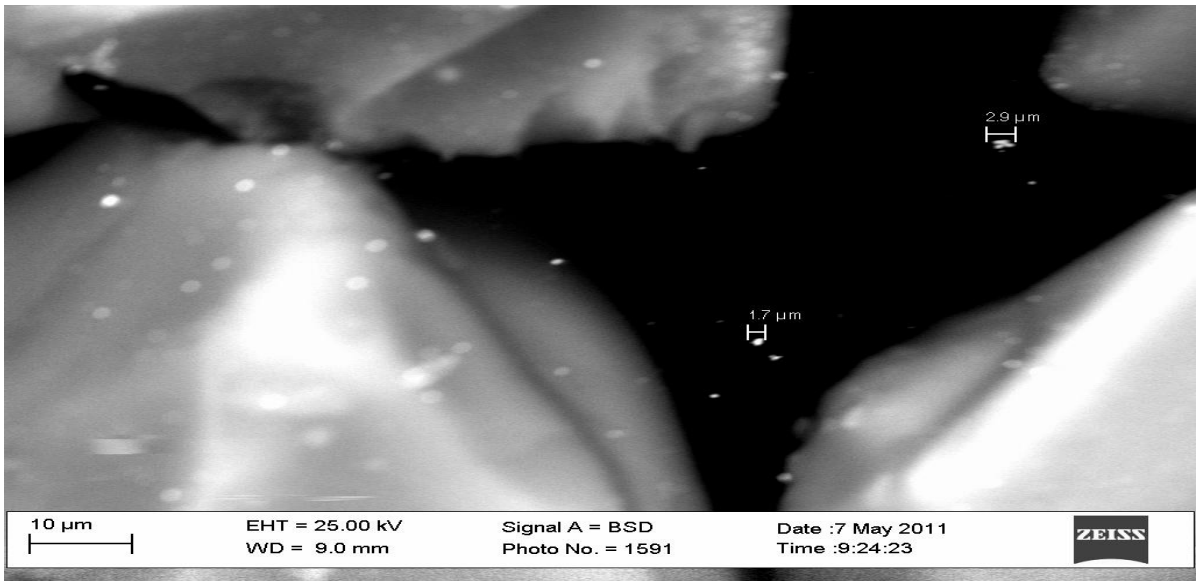

(a)

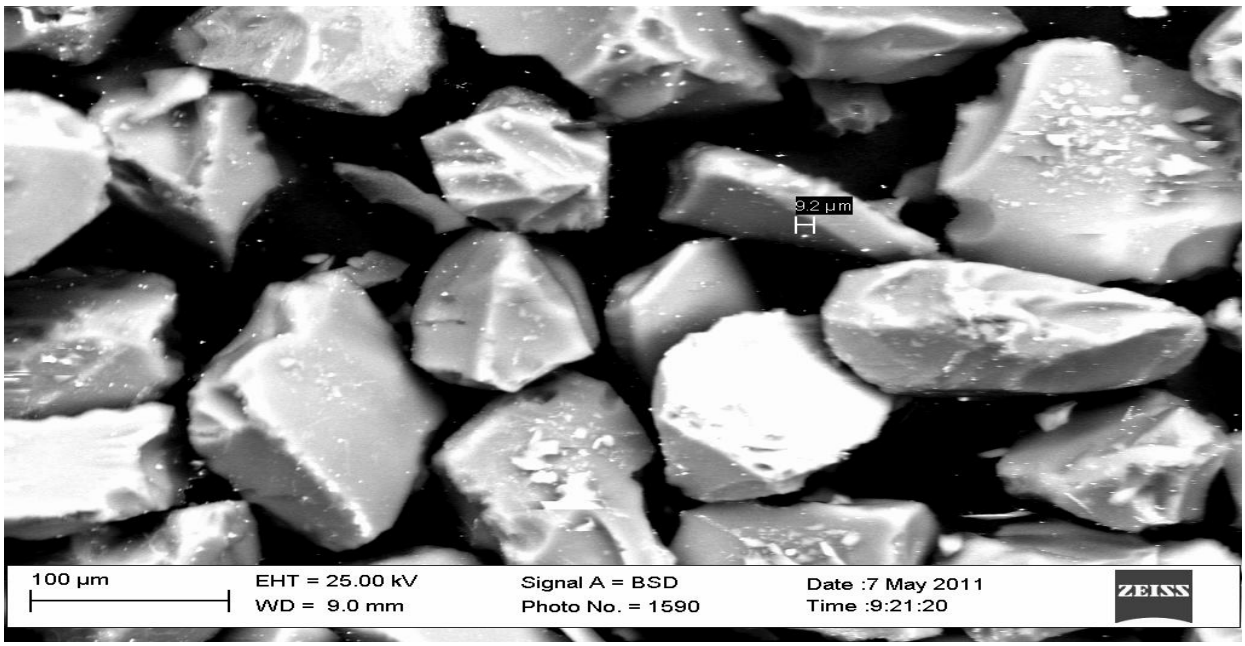

(b)

Figure 3.27 (a) and (b)SEM images of Cu_3Au/SiO_2 by a Sinfelt procedure (C978101C) reduced at 315 ^oC in H_2 followed by calcined at 676 ^oC for 15 h in air.

The $CuAu_3/SiO_2$ catalyst (Figure 3.24 (a) and (b)) is similar to the $CuAu/SiO_2$ catalyst (Figure 3.22 (a) and (b)) because, when reduced, the metal particles are not as dispersed on the support until there has been a high temperature calcination, when the particles are highly dispersed over support (Figure 3.25 (a) and (b)). For the Cu_3Au/SiO_2 catalyst (Figure 3.27 a and b), copper and gold particles are present but are more highly dispersed after the high temperature calcination.

3.5.2.2 Copper chloride precursor

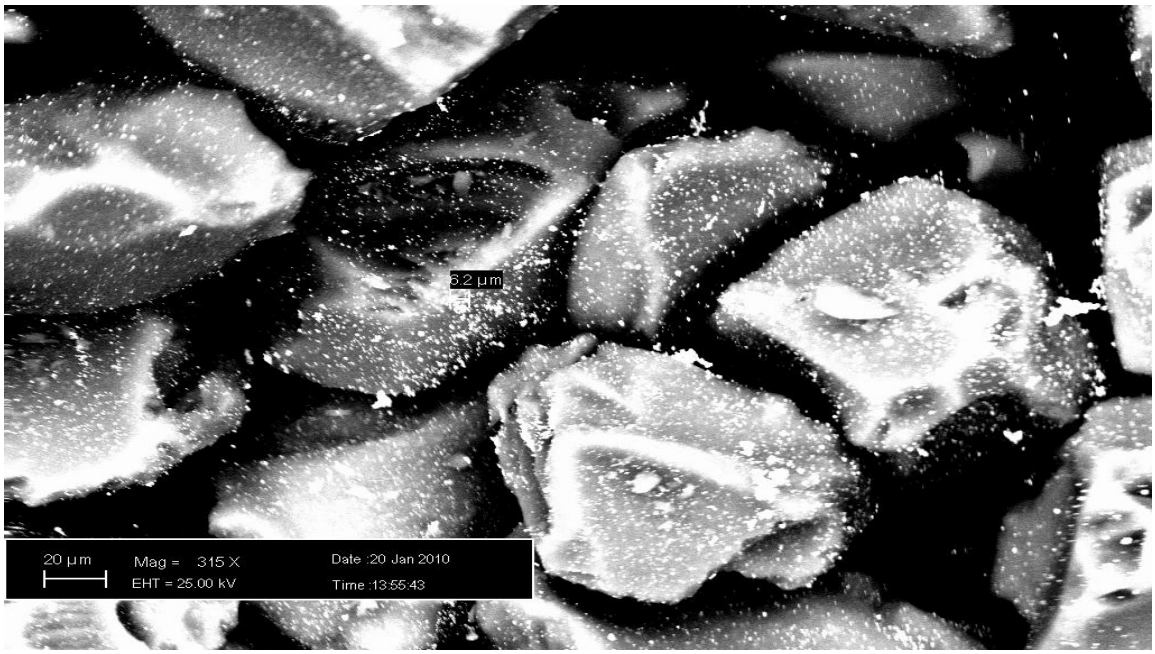

(a)

Figure 3.28 (a) SEM images of $CuAu/SiO_2$ by Sinfelt method (C97865A) reduced at 315 ^oC in H_2 followed by calcined at 676 ^oC for 15 h in air.

(b)

Figure 3.28 (b) SEM images of $CuAu/SiO_2$ by Sinfelt method (C97865A) reduced at 315 ^oC in H_2 followed by calcined at 676 ^oC for 15 h in air.

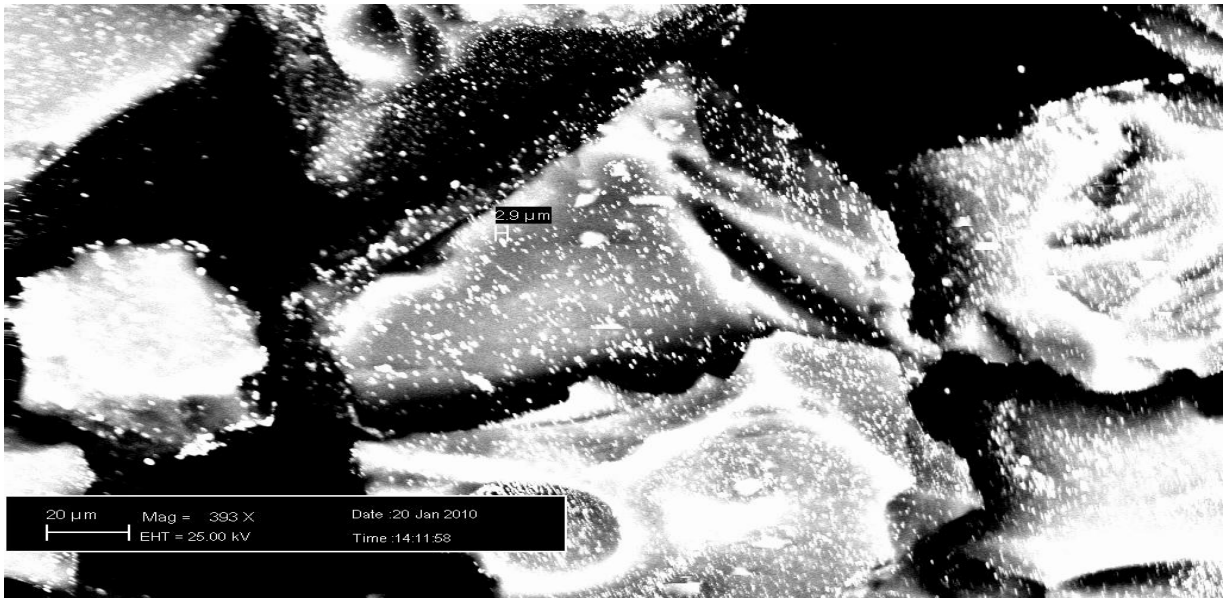

(a)

Figure 3.29 (a) SEM images of $CuAu_3/SiO_2$ by Sinfelt method(C978/65B) reduced at 315 ^oC in H_2 followed by calcined at 676 ^oC for 15 h in air.

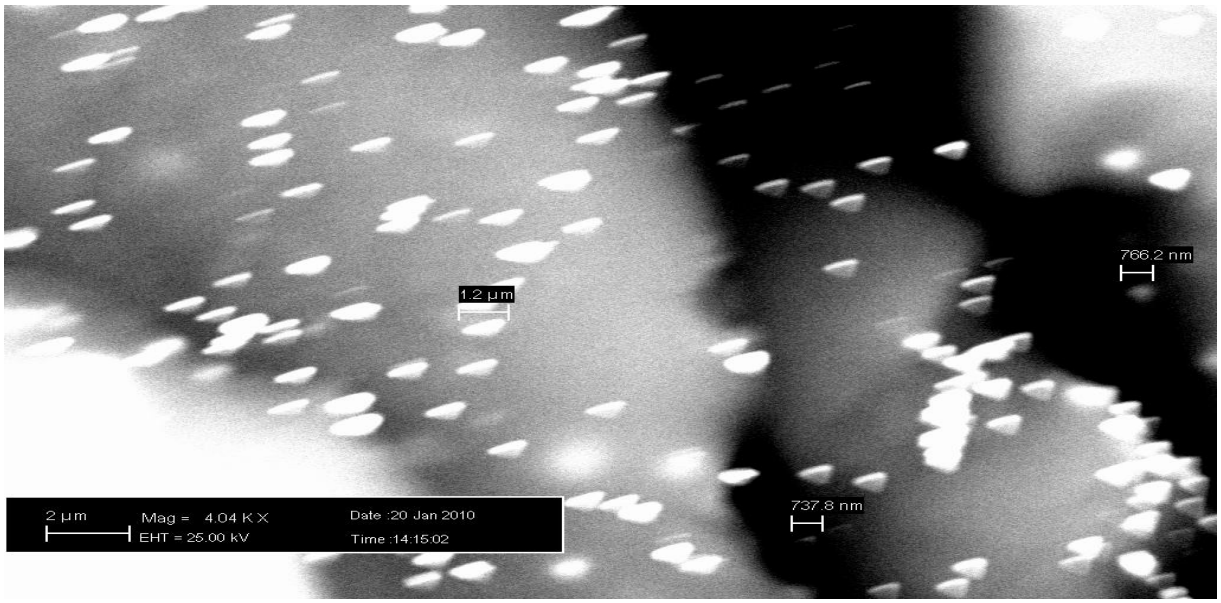

(b)

Figure 3.29 (b) SEM images of $CuAu_3/SiO_2$ by Sinfelt method(C978/65B) reduced at 315 ^oC in H_2 followed by calcined at 676 ^oC for 15 h in air.

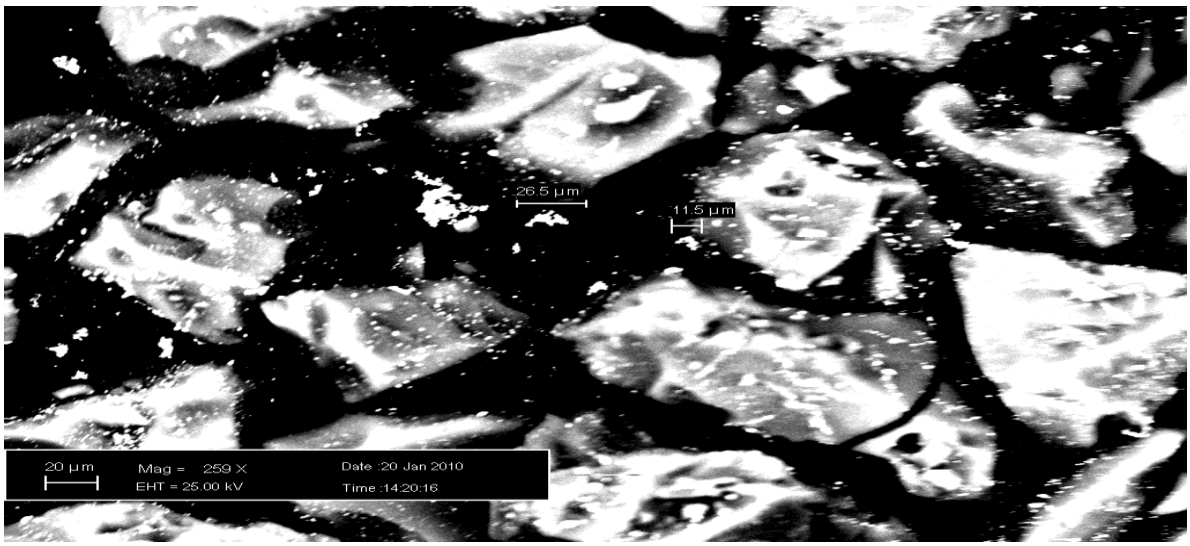

(a)

Figure 3.30 (a) SEM images of Cu_3Au/SiO_2 by Sinfelt method (C97865C) reduced at 315 ^oC in H_2 followed by calcined at 676 ^oC for 15 h in air.

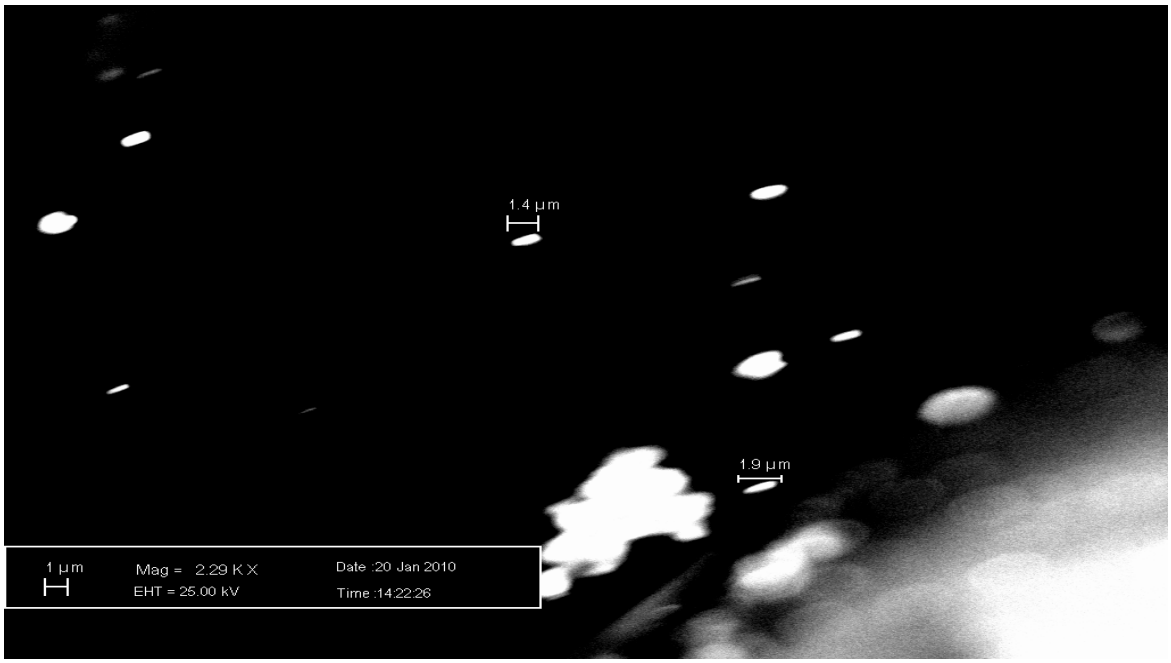

(b)

Figure 3.30 (b) SEM images of Cu_3Au/SiO_2 by Sinfelt method (C97865C) reduced at 315 ^oC in H_2 followed by calcined at 676 ^oC for 15 h in air.

The copper nitrate precursor was replaced with copper chloride and a Sinfelt style method was used to make CuAu, $CuAu_3$ and Cu_3Au catalysts (Figures 3.28 - 3.30). There does not appear to be any significant difference in the SEM images as a result of altering the precursor for this preparation. All the samples after high temperature calcination in air had highly dispersed metal particles ranging in sizes. Spherical metal particles were observed for the catalyst made with the copper chloride precursor.

3.5.3 Other preparation methods

3.5.3.1 HDC Cu + Au DP or Au IW

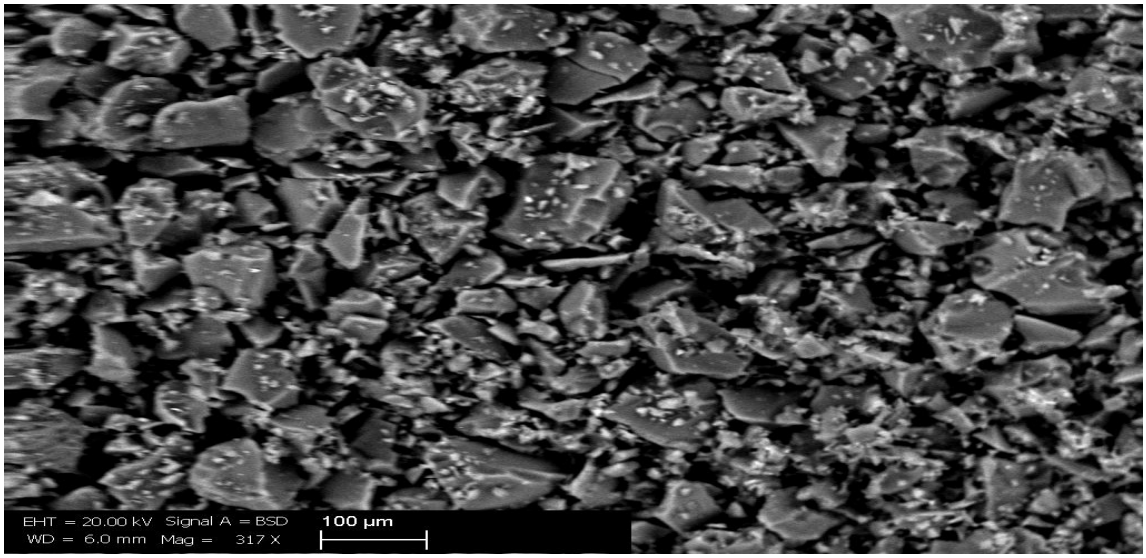

(a)

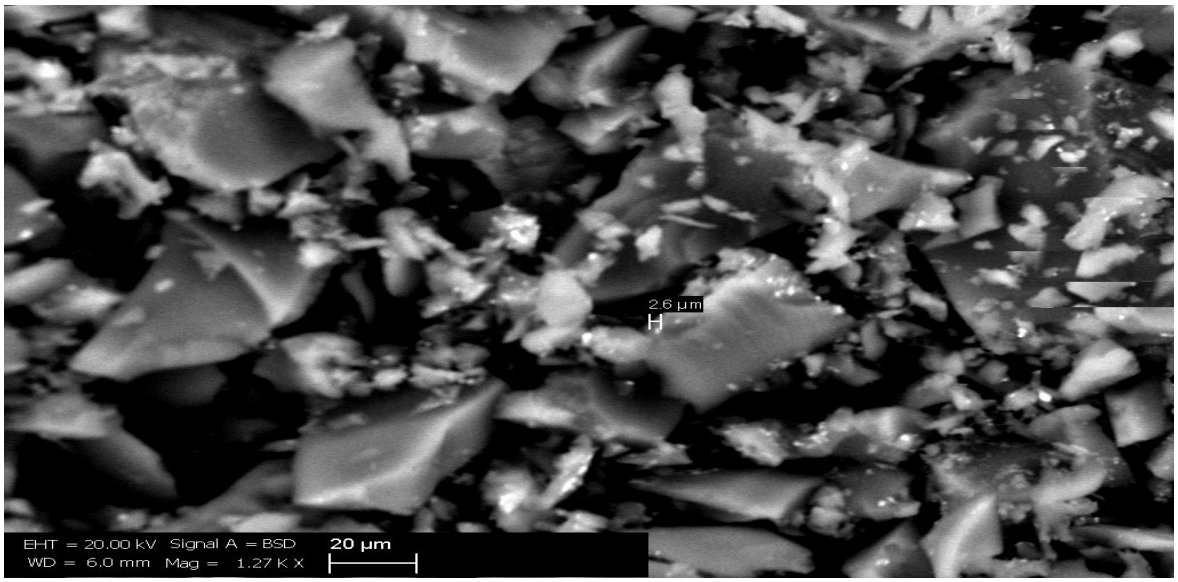

(b)

Figure 3.31 (a) and (b) SEM images of $CuAu/SiO_2$ high dispersion (HDC) Cu + Au Deposition precipitation (DP) (C978/87)

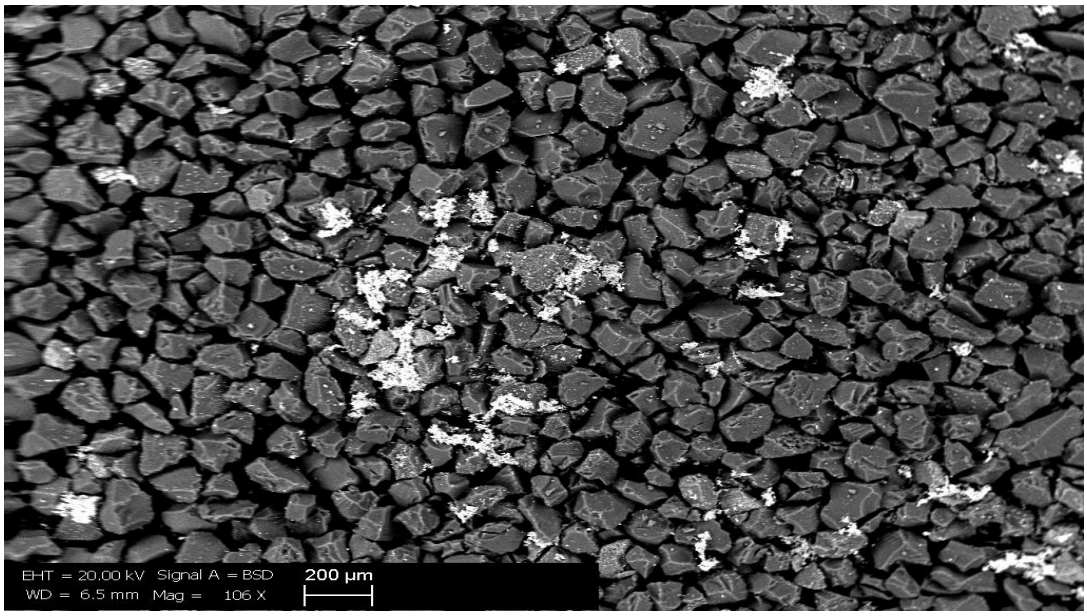

(a)

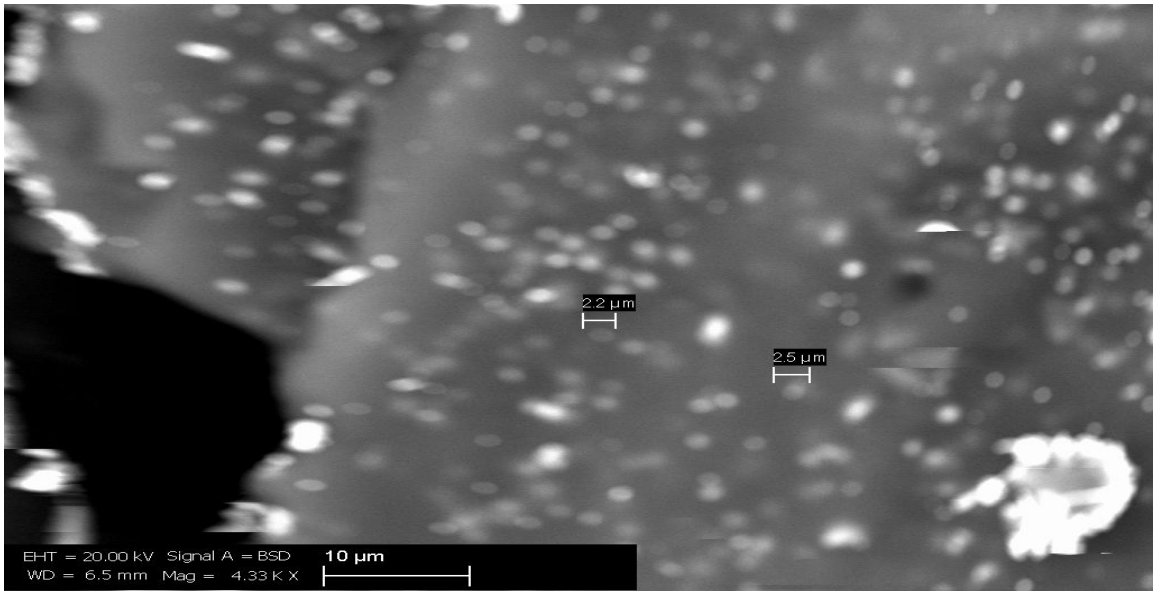

(b)

Figure 3.32 (a) and (b) SEM images of $CuAu/SiO_2$ by high dispersion (HDC) Cu + Au incipient wetness impregnation (IW) (C978/90)

A sequential preparation method (Figure 3.31 and 3.32) was attempted by loading the Cu onto the support and using a high dispersion route, followed by loading the Au onto the

support by either incipient wetness impregnation or deposition precipitation. The SEM images show that when the latter of the two routes is chosen, the metal particles are dispersed on the support, although some of the particles may have been too small to be seen by SEM. However, when the Au is prepared by impregnation, large ensembles can be observed, as well as highly dispersed particles.

3.5.3.2 Reduced in $NaBH_4$

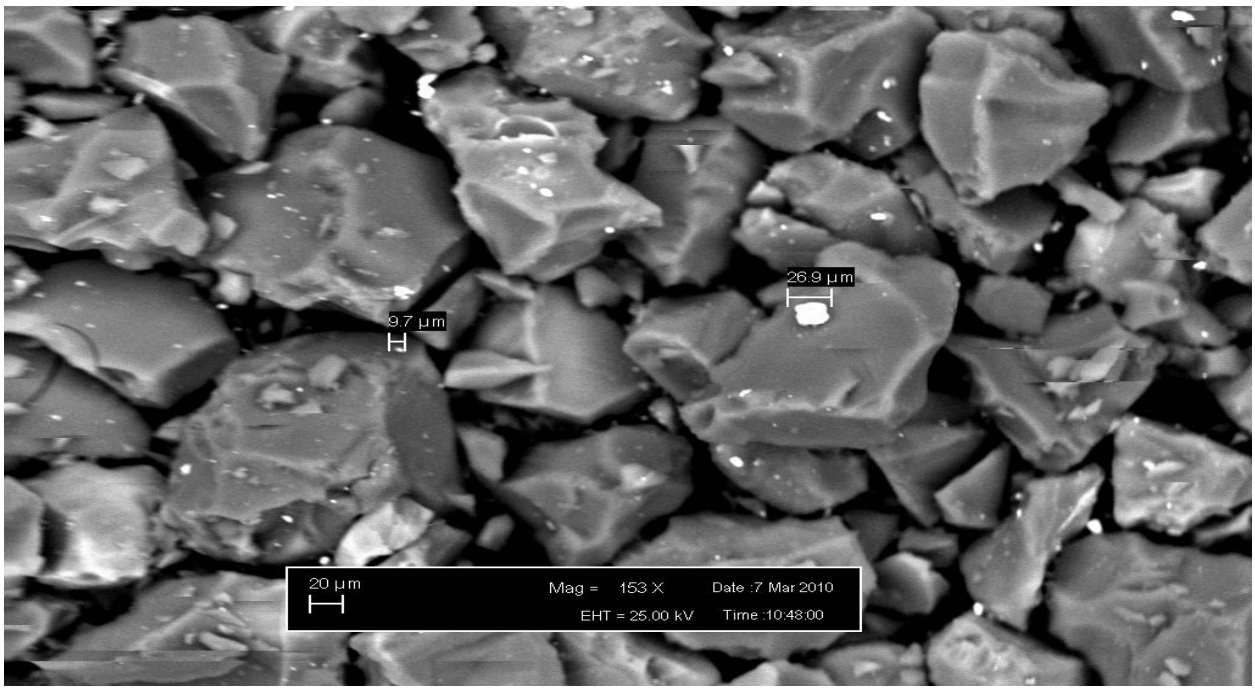

(a)

Figure 3.33 (a) SEM images of $CuAu/SiO_2$ reduced by $NaBH_4$ (C97880A)

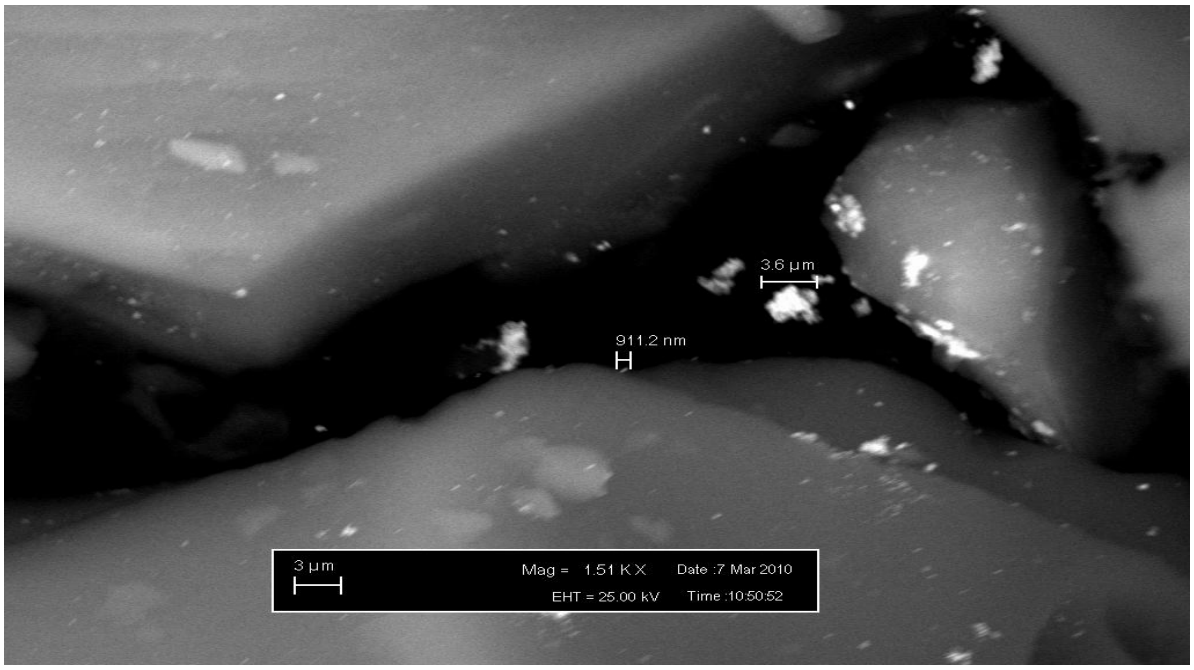

(b)

Figure 3.33 (b) SEM images of $CuAu/SiO_2$ reduced by $NaBH_4$ (C97880A)

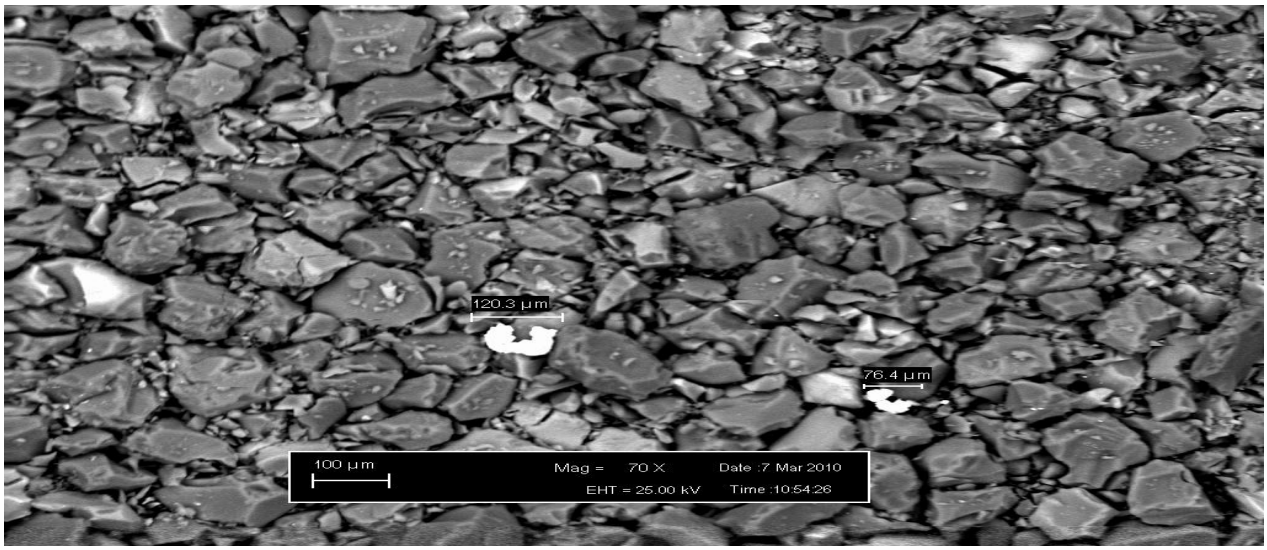

(a)

Figure 3.34 (a) SEM images of $CuAu_3/SiO_2$ reduced in $NaBH_4$ (C97880B)

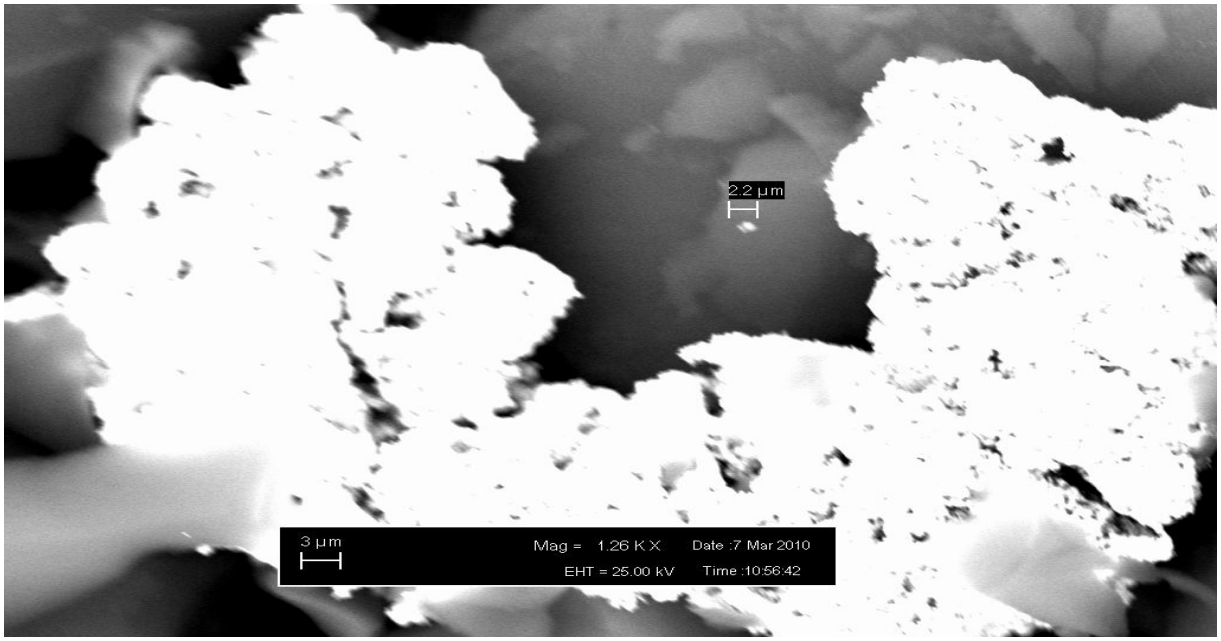

(b)

Figure 3.34 (b) SEM images of $CuAu_3/SiO_2$ reduced in $NaBH_4$ (C97880B)

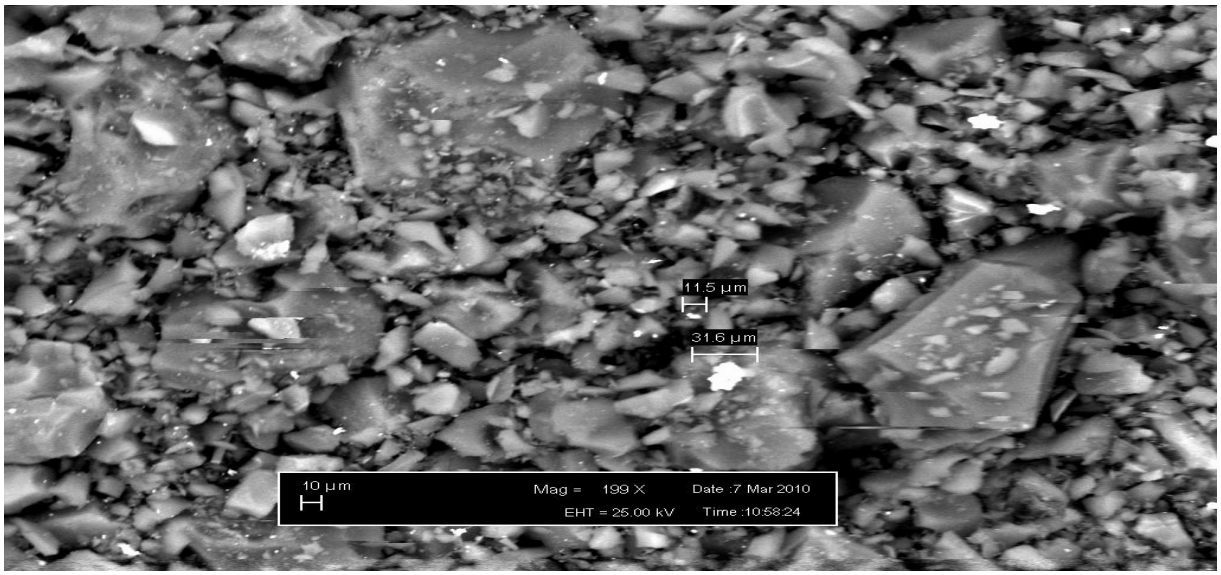

(a)

Figure 3.35 (a) SEM images of Cu_3Au/SiO_2 reduced by $NaBH_4$ (C97880C)

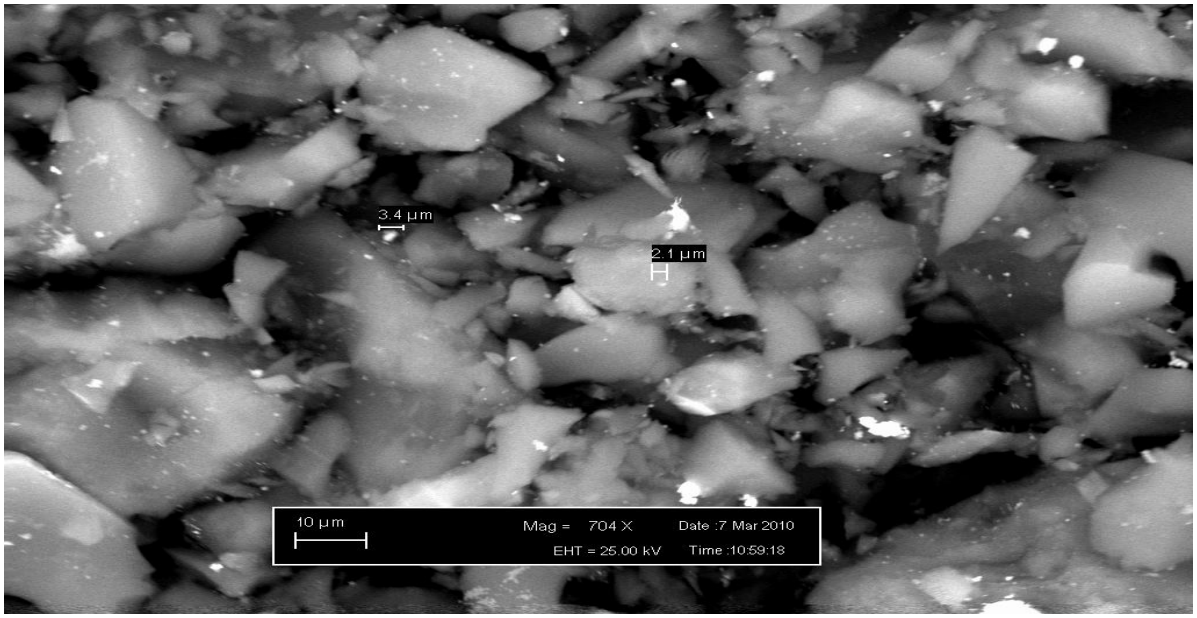

(b)

Figure 3.35 (b) SEM images of Cu_3Au/SiO_2 reduced by $NaBH_4$ (C97880C)

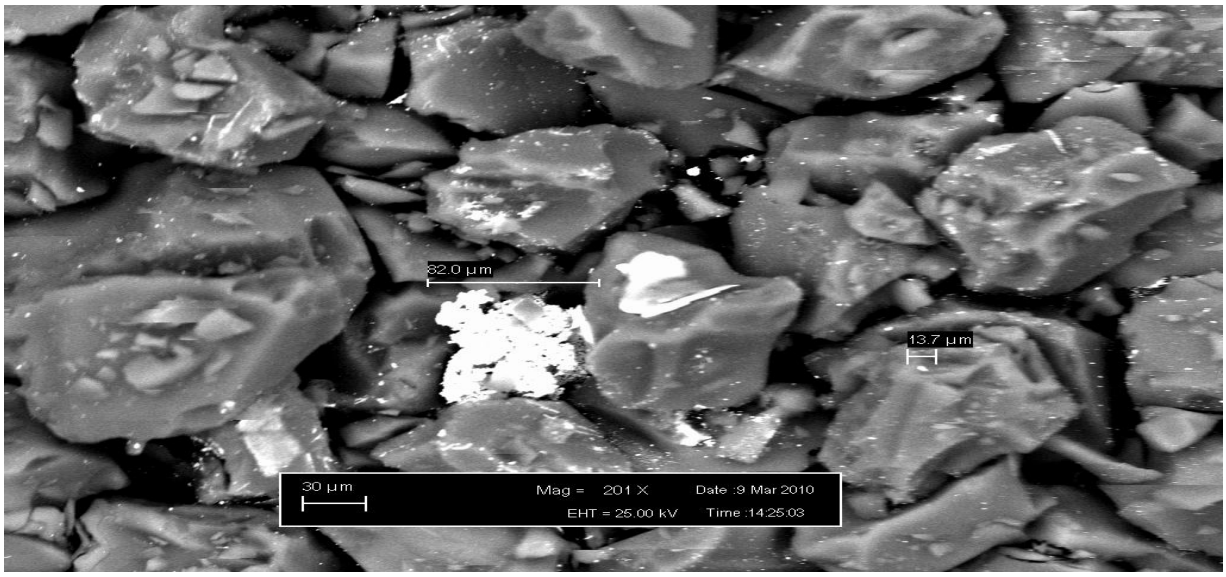

(a)

Figure 3.36 (a) SEM images of Au/SiO_2 reduced by $NaBH_4$ (C97880D)

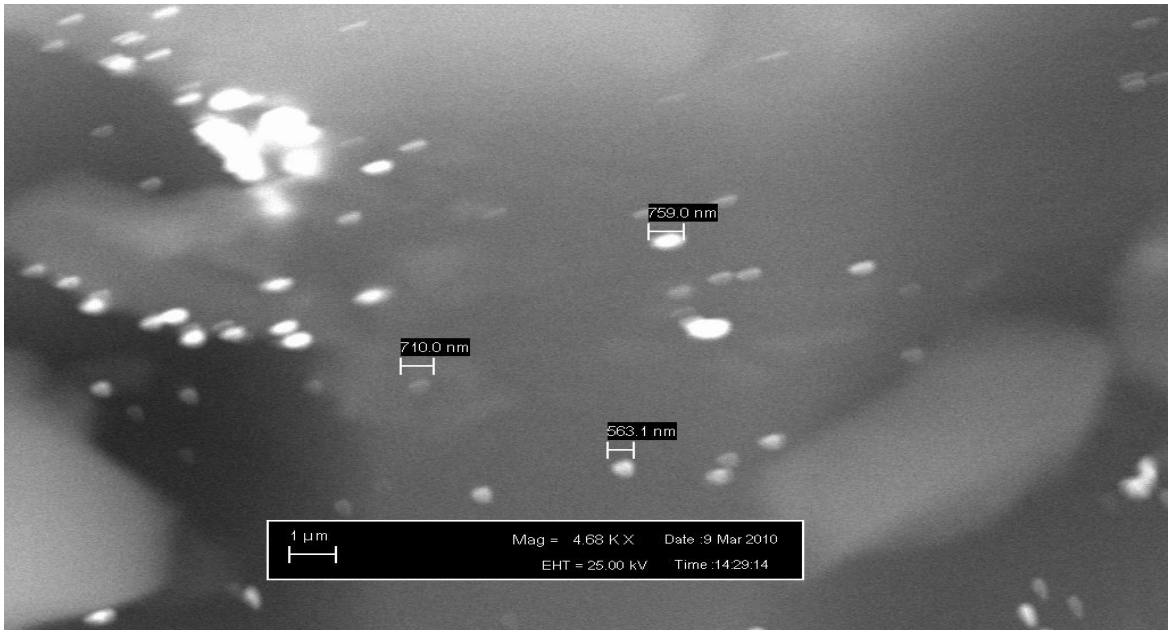

(b)

Figure 3.36 (b) SEM images of Au/SiO_2 reduced by $NaBH_4$ (C97880D)

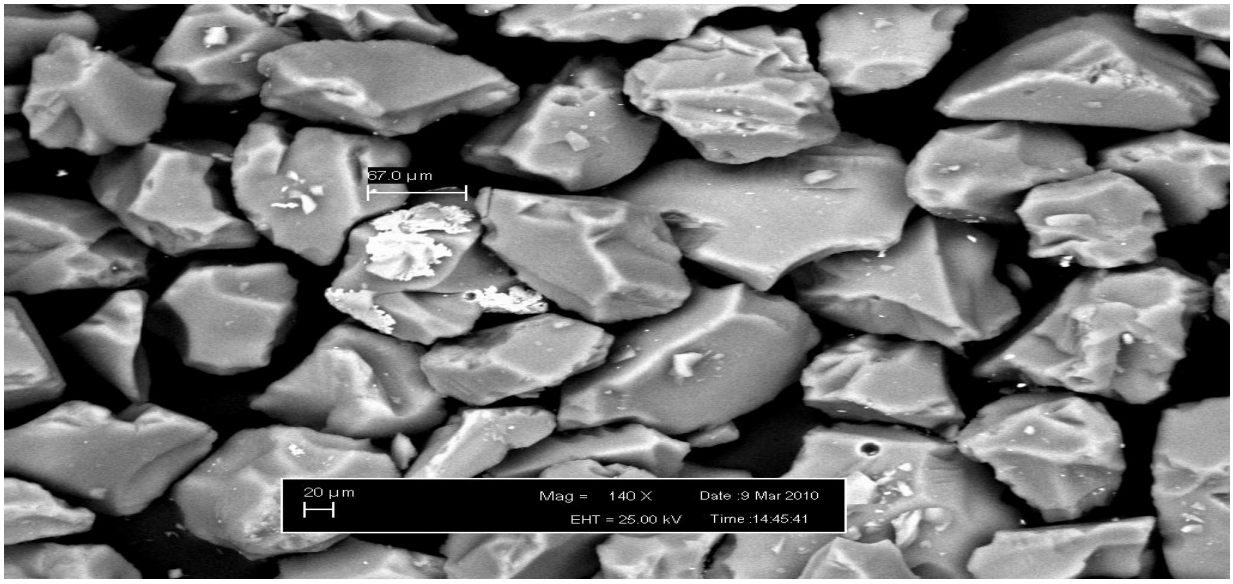

(a)

Figure 3.37 (a) SEM images of Cu/SiO_2 reduced by $NaBH_4$ (C97880E)

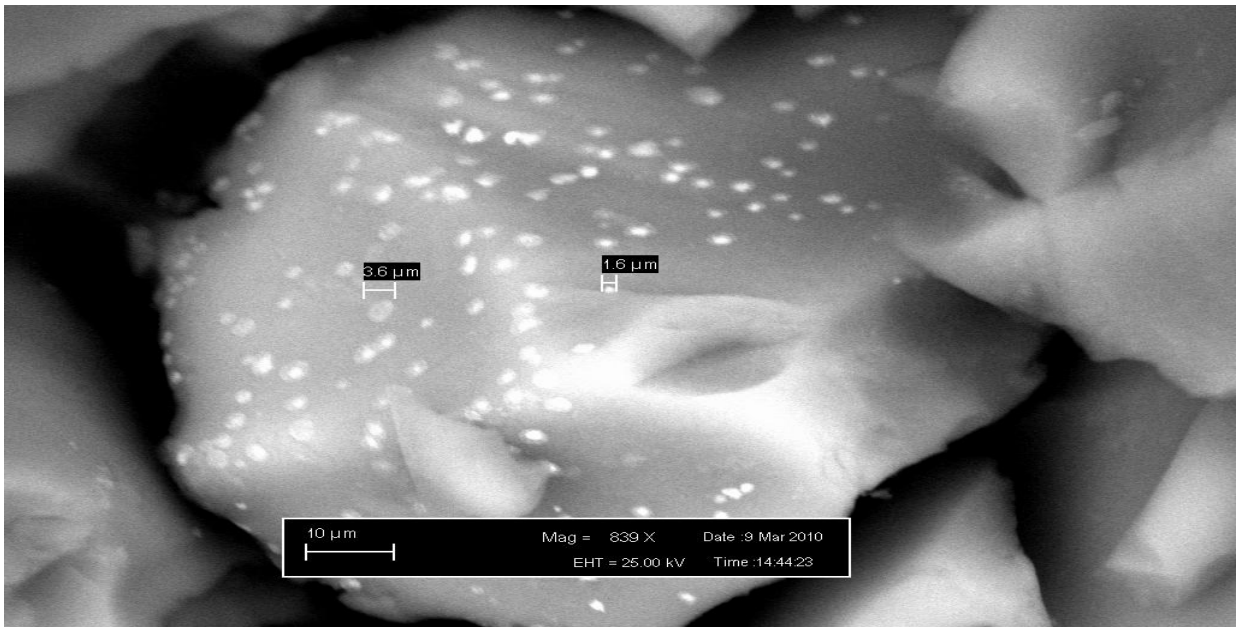

(b)

Figure 3.37 (b) SEM images of Cu/SiO_2 reduced by $NaBH_4$ (C97880E)

As well as using hydrogen to reduce the catalysts, sodium borohydride was also used as a reducing agent. From the SEM images (Figure 3.33-3.37), large micron sized clusters were apparent as well as some smaller dispersed particles. The Au/SiO_2 catalyst showed the presence of large Au ensembles of 82 µm across and smaller Au particles 500-700 nm. The Cu/SiO_2 SEM images showed a mixture of large Cu ensembles and small dispersed particles.

3.5.3.3 Reduced by H_2

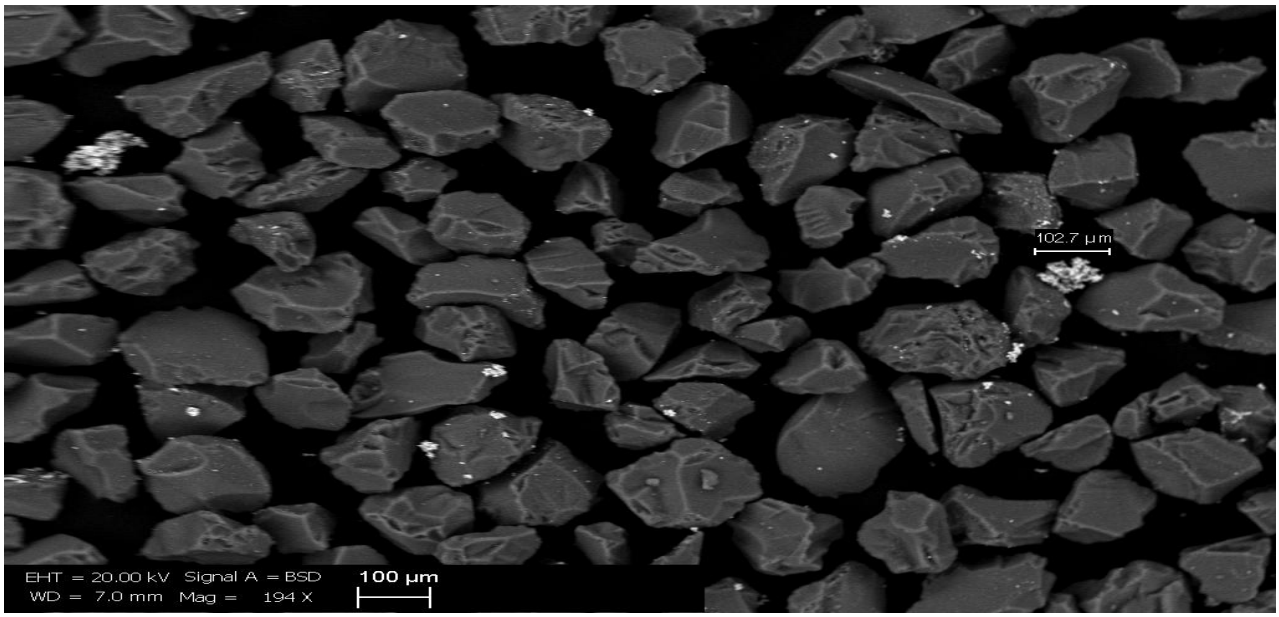

(a)

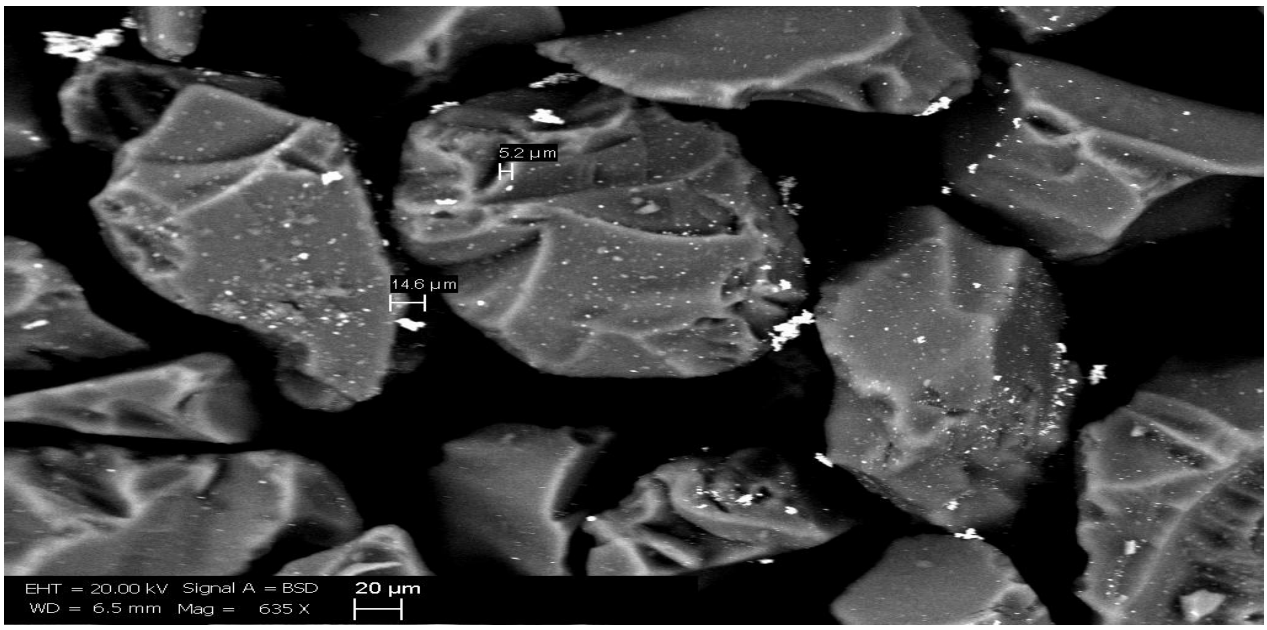

(b)

Figures 3.38 (a) and (b) SEM images of $CuAu/SiO_2$ reduced in H_2 (C97893A)

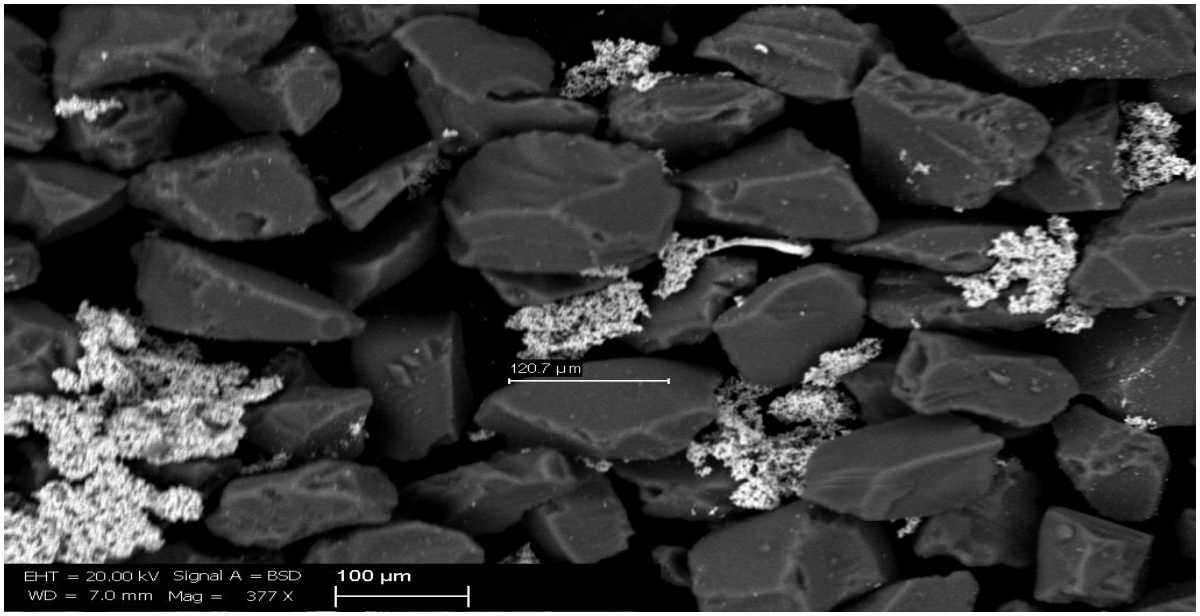

(a)

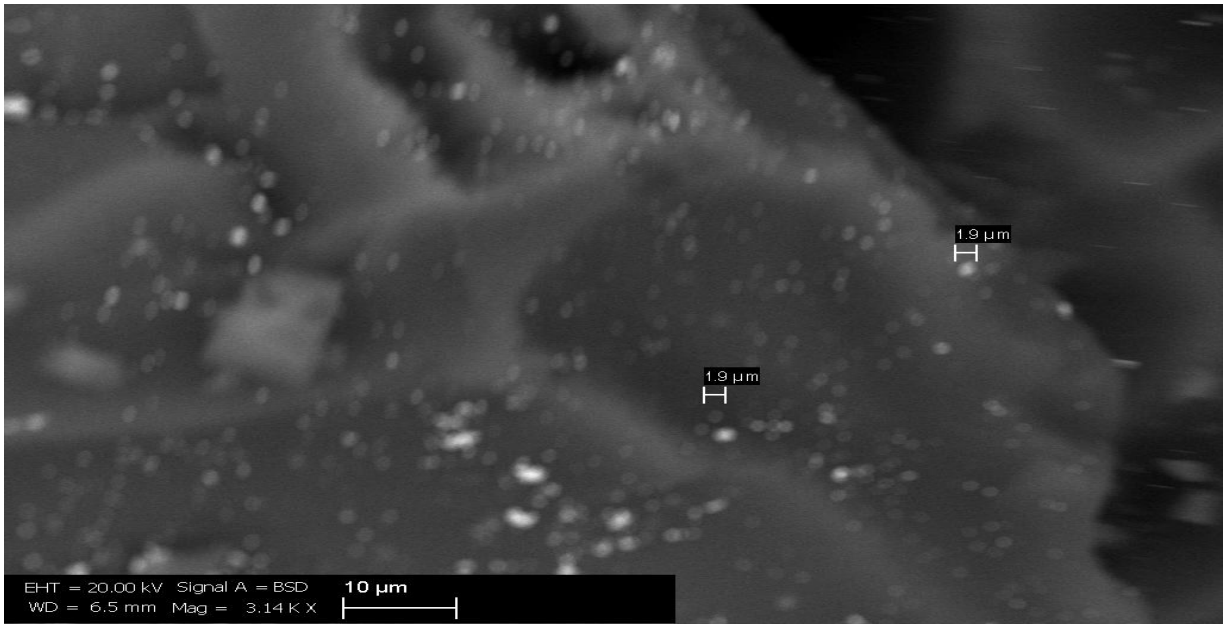

(b)

Figure 3.39 (a) and (b) SEM images of $CuAu_3/SiO_2$ reduced in H_2 (C97893B)

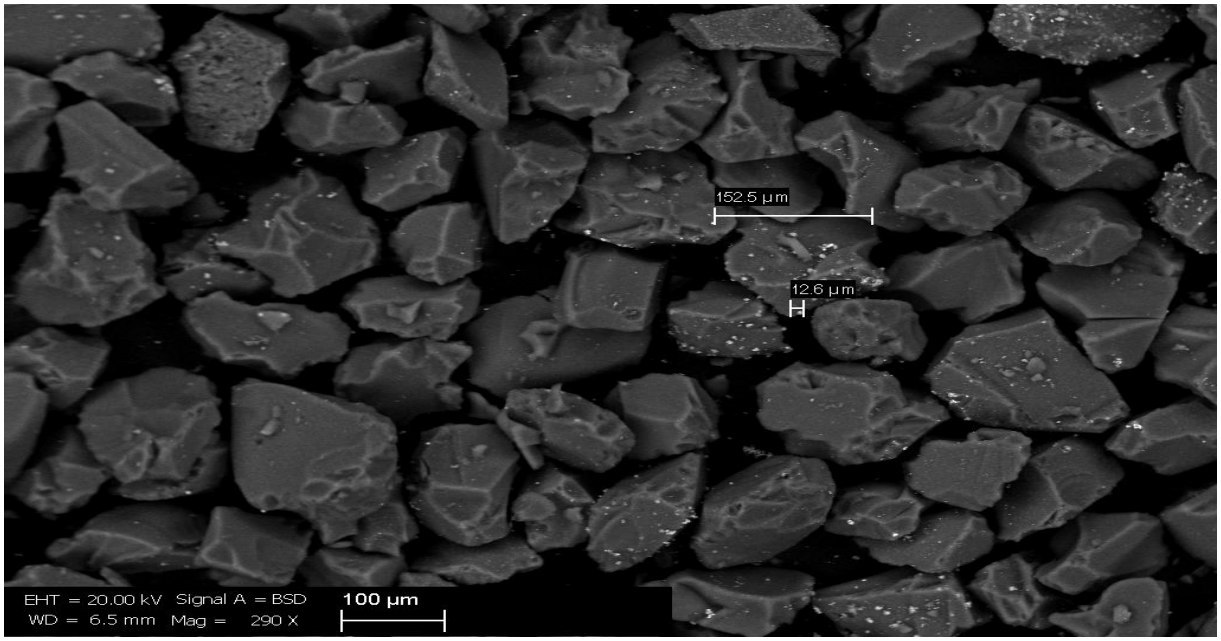

(a)

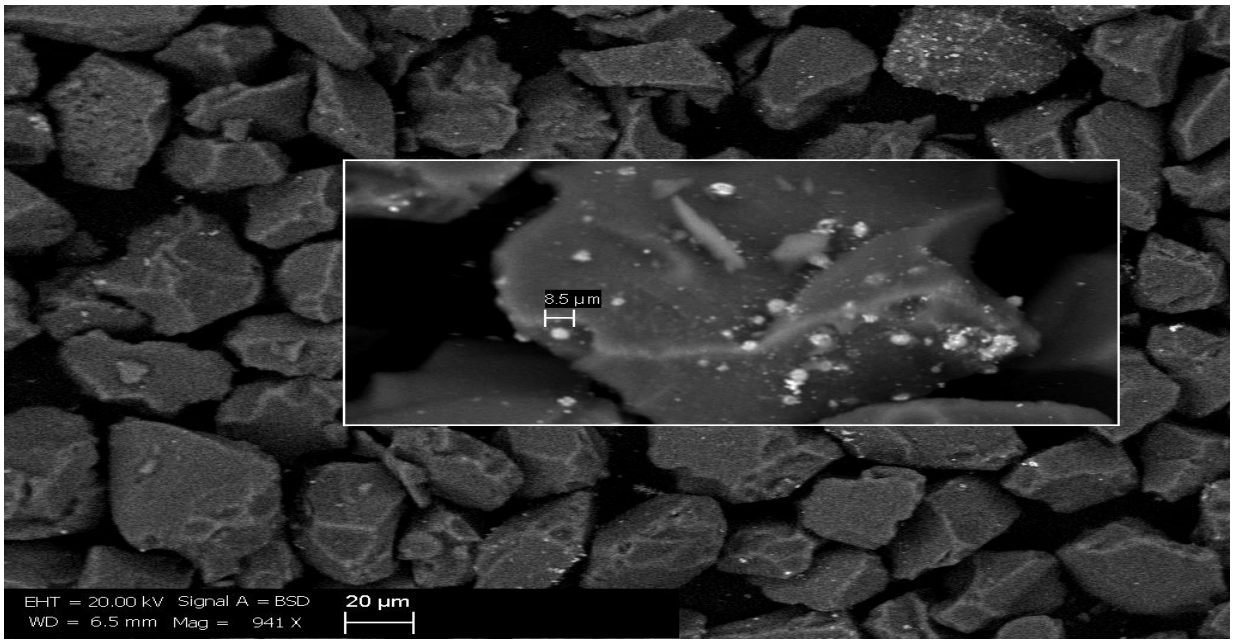

(b)

Figure 3.40 (a) and (b) SEM images of Cu_3Au/SiO_2 reduced in H_2 (C978/93C)

SEM images for AuCu, Au_3Cu and Cu_3Au have been reduced in H_2 at 400 ^oC for 2 h (Figure 3.38 - 3.40). The reduction leads to the formation of highly dispersed particles over the support which TEM analysis will be able to show. The gold rich catalyst consists of large ensembles around 120 µm. However, the Cu rich composition does not have large ensembles and forms round metal particles.

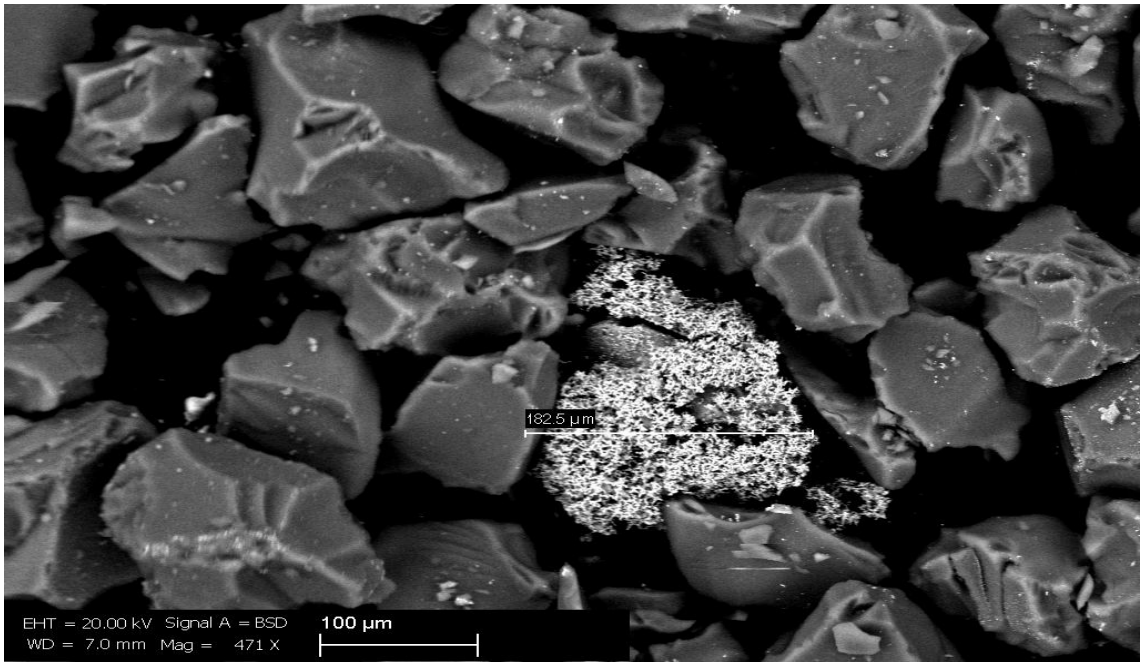

Figure 3.41 SEM image of Au/SiO_2 reduced in H_2 (C97893D)

The SEM image for the Au/SiO_2 catalyst reduced in H_2 (Figure 3.41) shows the formation of large gold ensembles of about 182 µm in size, in addition to some dispersed particles.

3.5.3.4 Sol immobilisation

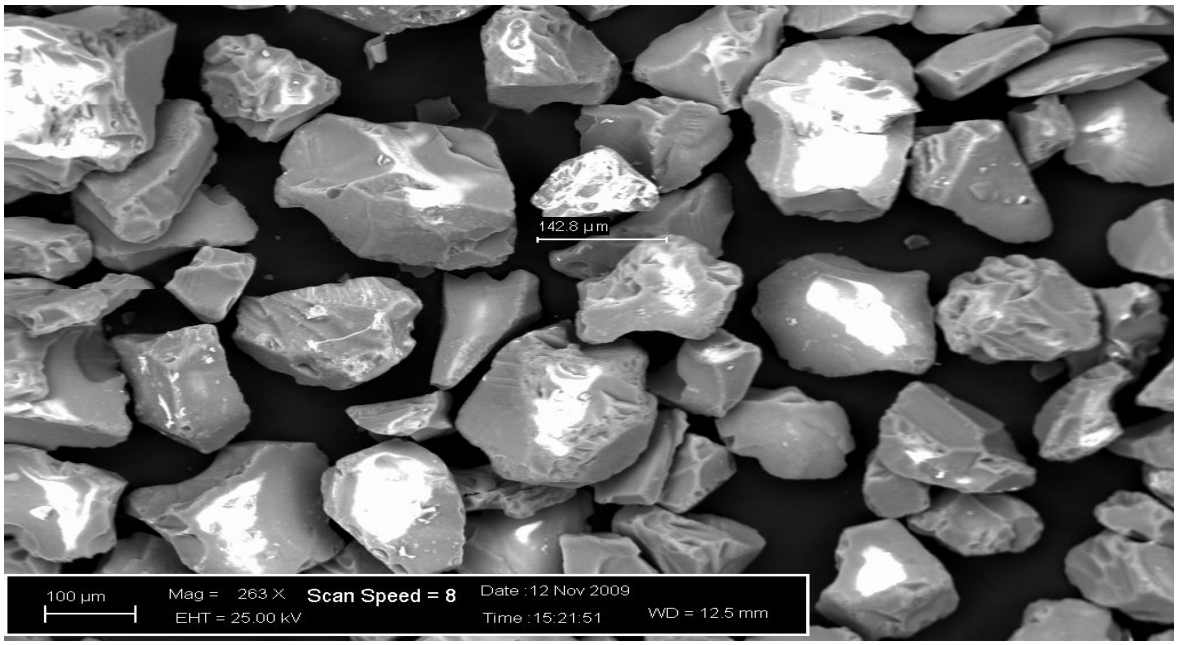

(a)

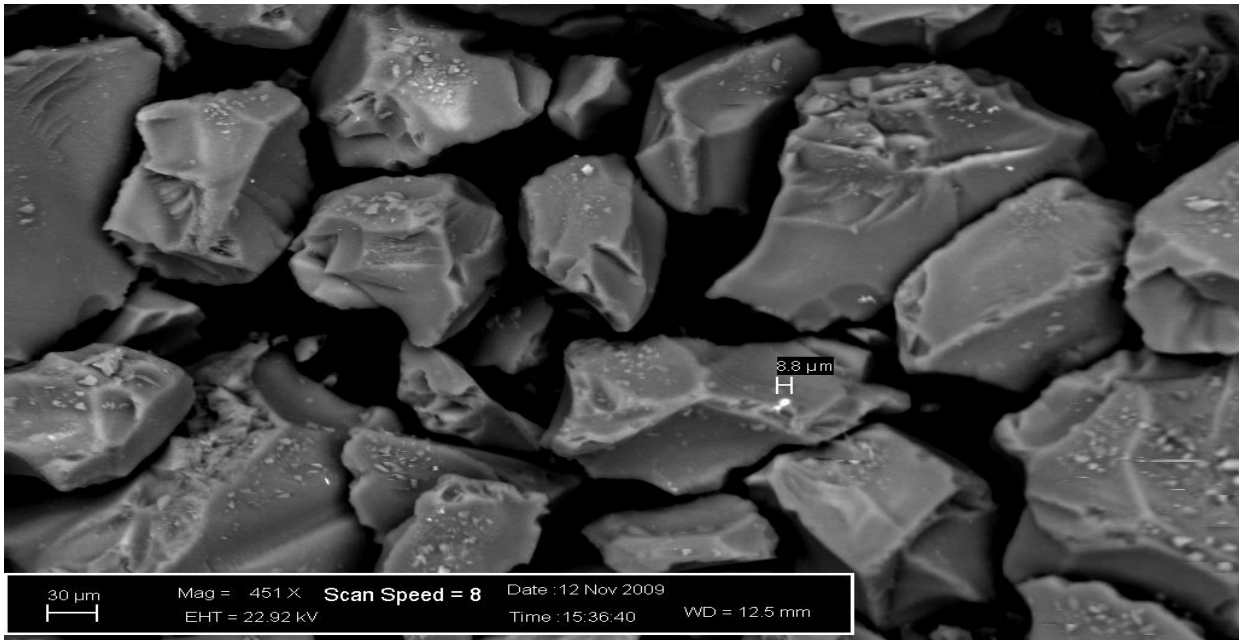

(b)

Figure 3.42 SEM image of (a) Au/SiO_2 (C978102) (b) $CuAu/SiO_2$ (C978103)

Sol immobilisation was used as another preparation method because it has been utilized by others to generate nanometer particles of gold, for use in size dependent reactions.[7] It is not very clear on the structure of the Au from the SEM image (Figure 3.42a) of the Au/SiO_2 catalyst, but we note the presence of Au regions on the support from the bright contrast in the image, which is due to the Au. The $AuCu/SiO_2$ SEM image (figure 3.42 b) shows highly dispersed metal particles on the support. However, smaller particles can not be seen by the SEM technique so TEM analysis has been carried out and discussed below.

3.6 TEM Analysis

This technique can identify if there are smaller active particles on the catalysts which are order of magnitudes smaller than the particles and clusters observed by SEM analysis.

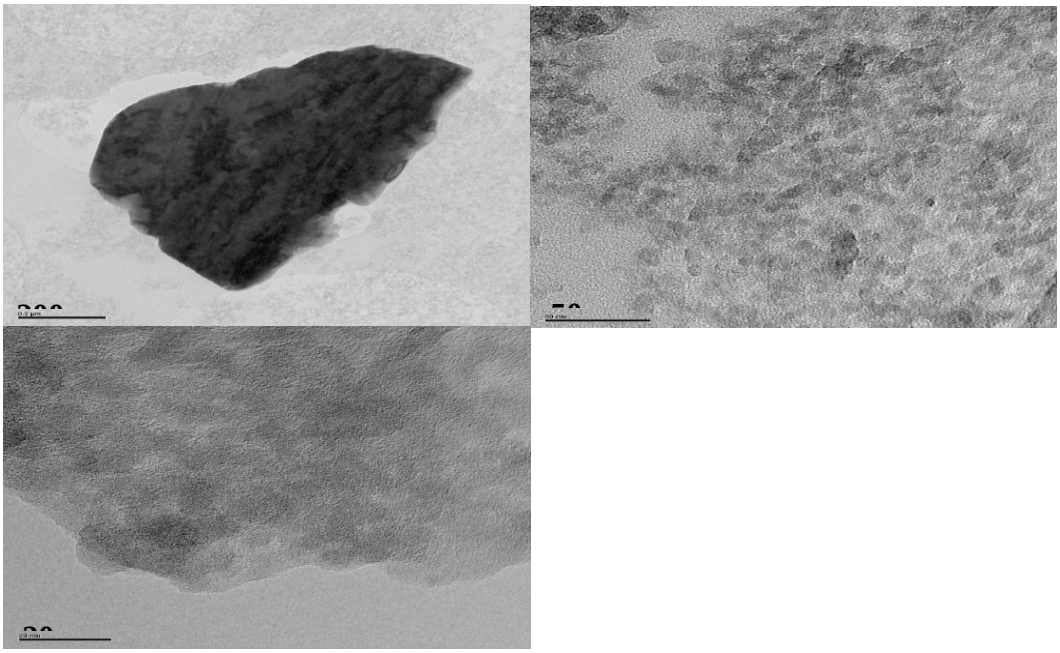

Figure 3.43 TEM images of 1:1 $CuAu/SiO_2$ calcined. (C978/19A)

TEM analysis was investigated for $CuAu/SiO_2$ calcined in air (Figure 3.43) and reveals large clusters on the support. EDX analysis (Figure 3.44) confirms that the large clusters are Au-rich although there is a small amount of Cu present.

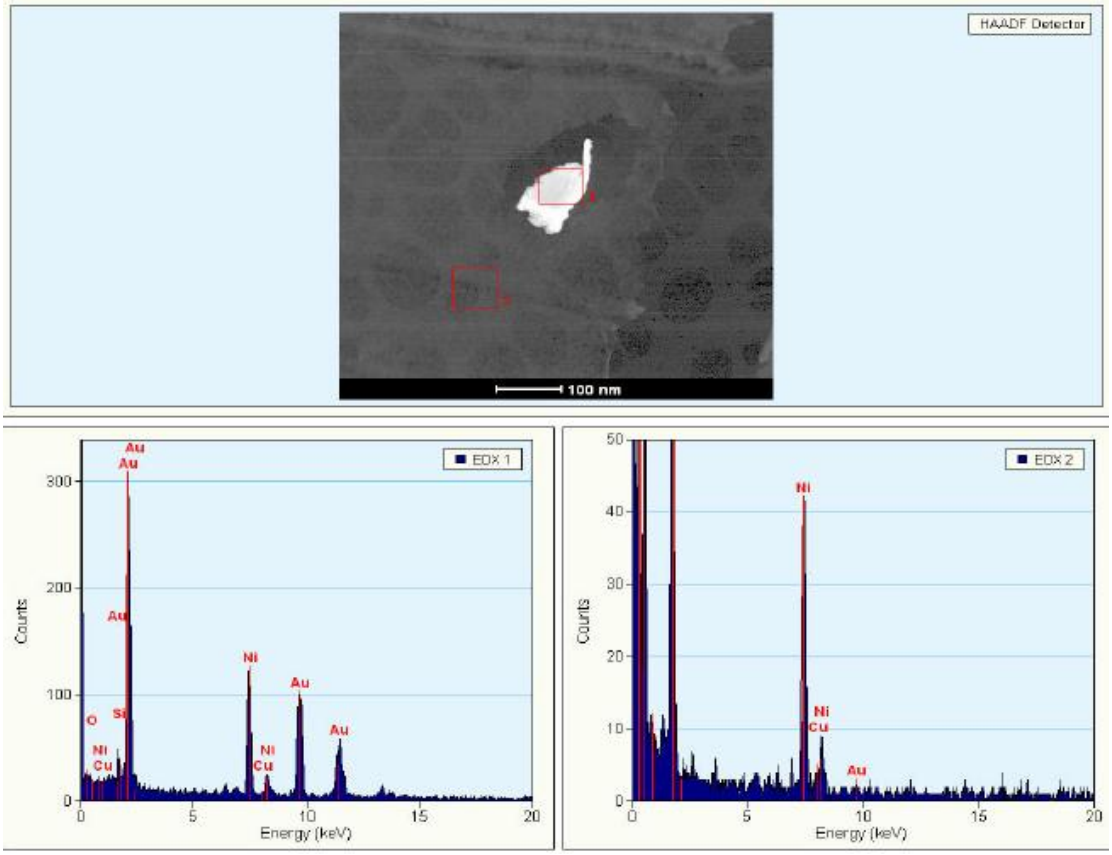

Figure 3.44 TEM/EDX analysis of calcined $CuAu/SiO_2$ (C978/19A). The background catalyst contains Cu. The Ni observed arises from the grid used to support the sample.

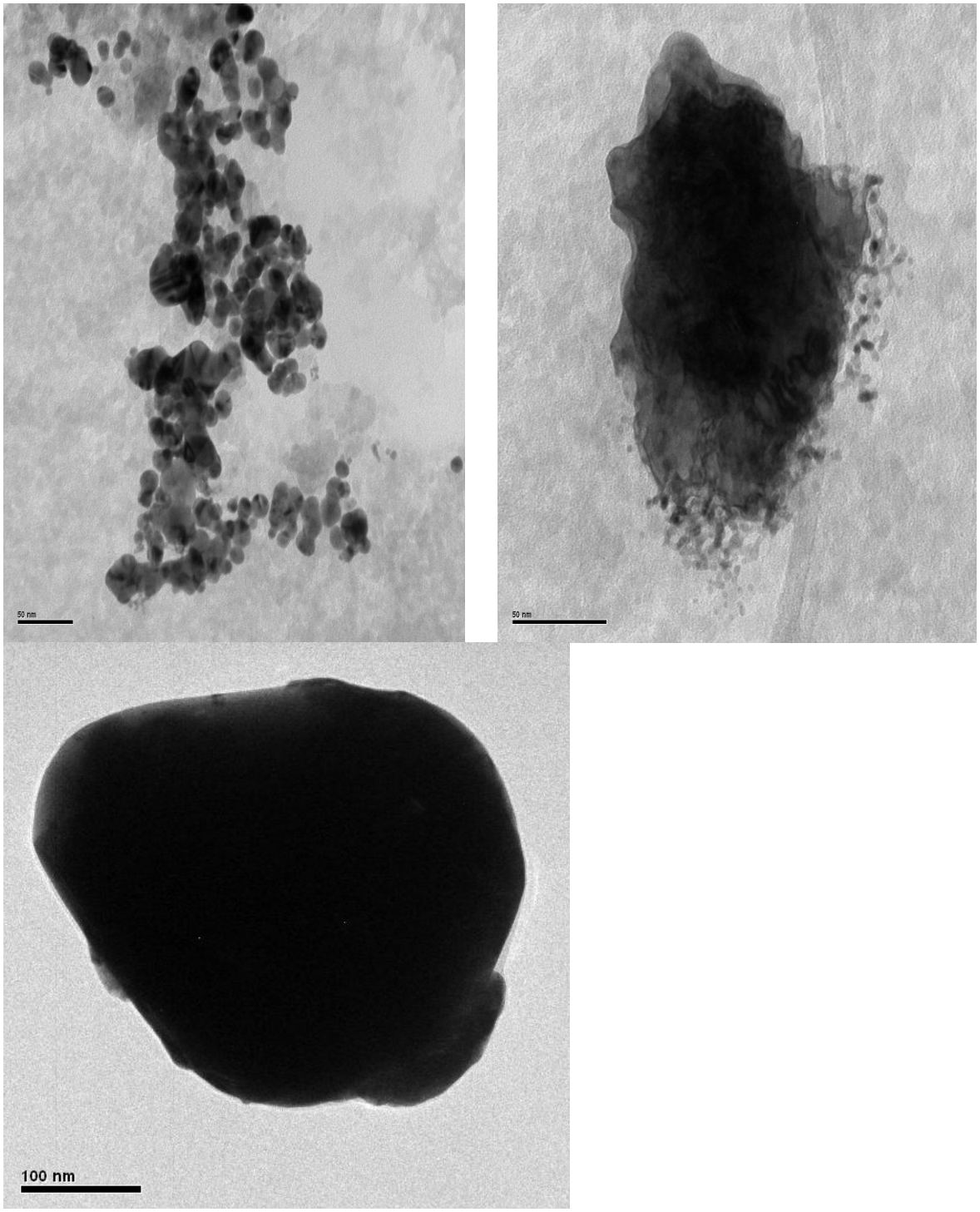

Figure 3.45 TEM images of $CuAu/SiO_2$ reduced only part of the Sinfelt method

(C978/101A)

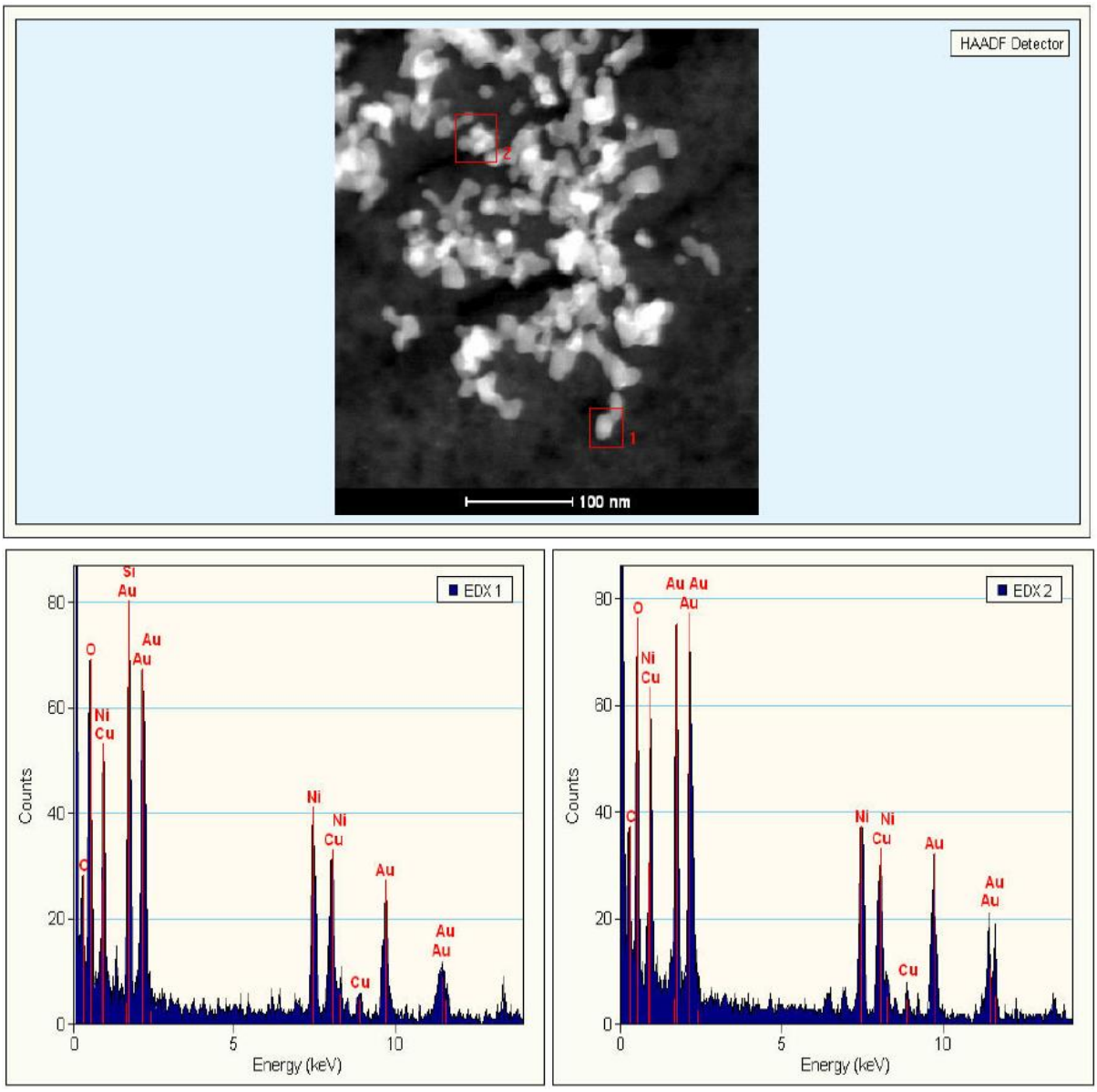

Figure 3.46 TEM/EDX analysis of reduced only part of the Sinfelt method for $CuAu/SiO_2$ (C987101A). The Ni is observed because it is the grid used to load sample.

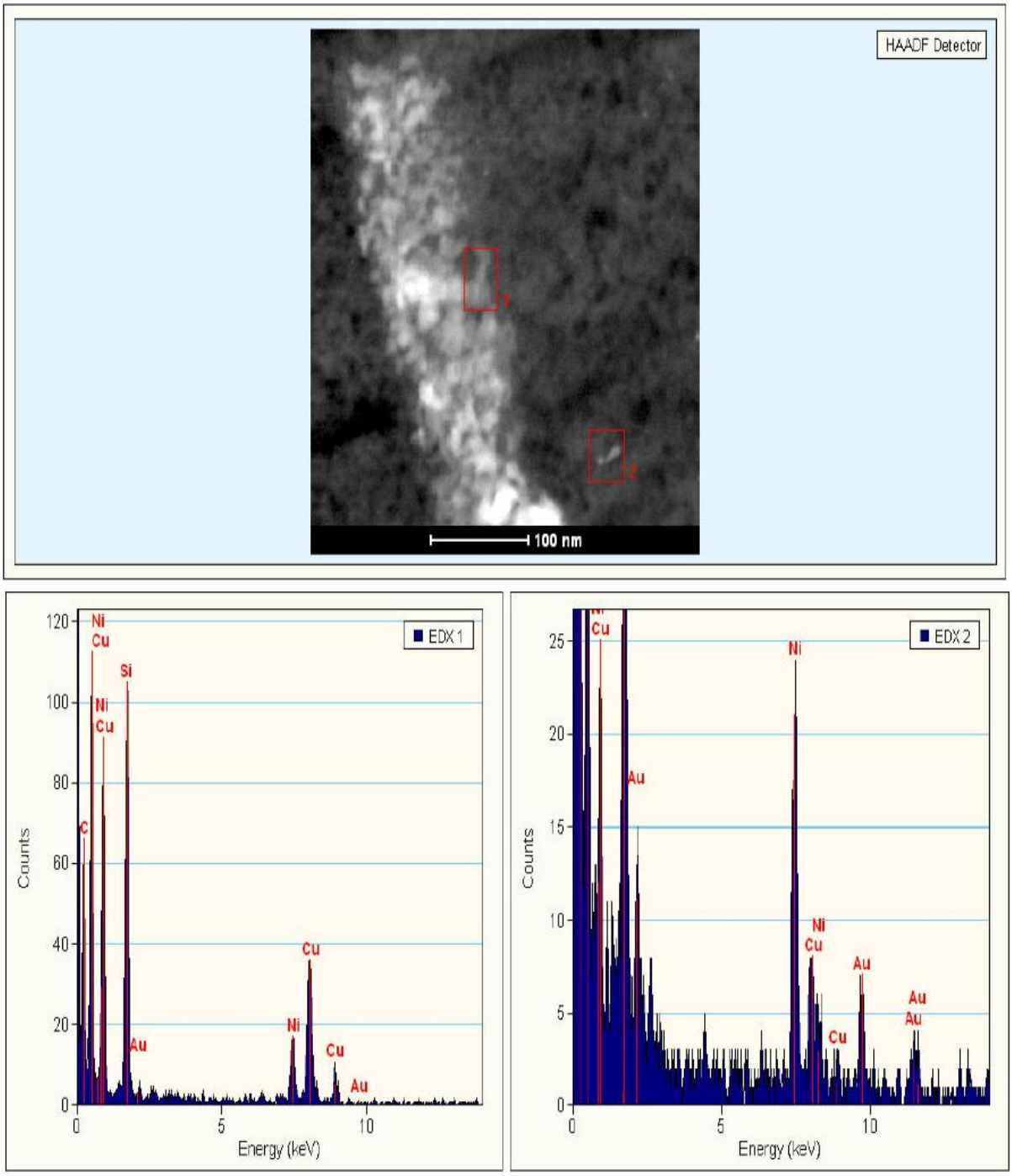

Figure 3.47 TEM/EDX analysis of reduced only part of the Sinfelt method for $CuAu/SiO_2$ (C978/101A). The Ni is observed because it is the grid used to load sample.

TEM images of $CuAu/SiO_2$ catalyst reduced at 315 ^oC for 2 h in H_2 showed the average particle size was 13 nm. The particles tended to exist in clusters that were fused to different

degrees (Figure 3.45). EDX analysis showed that the more open clusters contained both Cu and Au particles (Figure 3.46). However, the more compact clusters were rich in Cu content but only contained a little Au (Figure 3.47). TEM analysis showed that the interaction between copper and gold was high and that alloy formation was present as supported by the linescan (Figure 3.48). The EDX line scan clearly shows that some of the particles have surface layers of copper rich and their interior regions contain both Cu and Au.

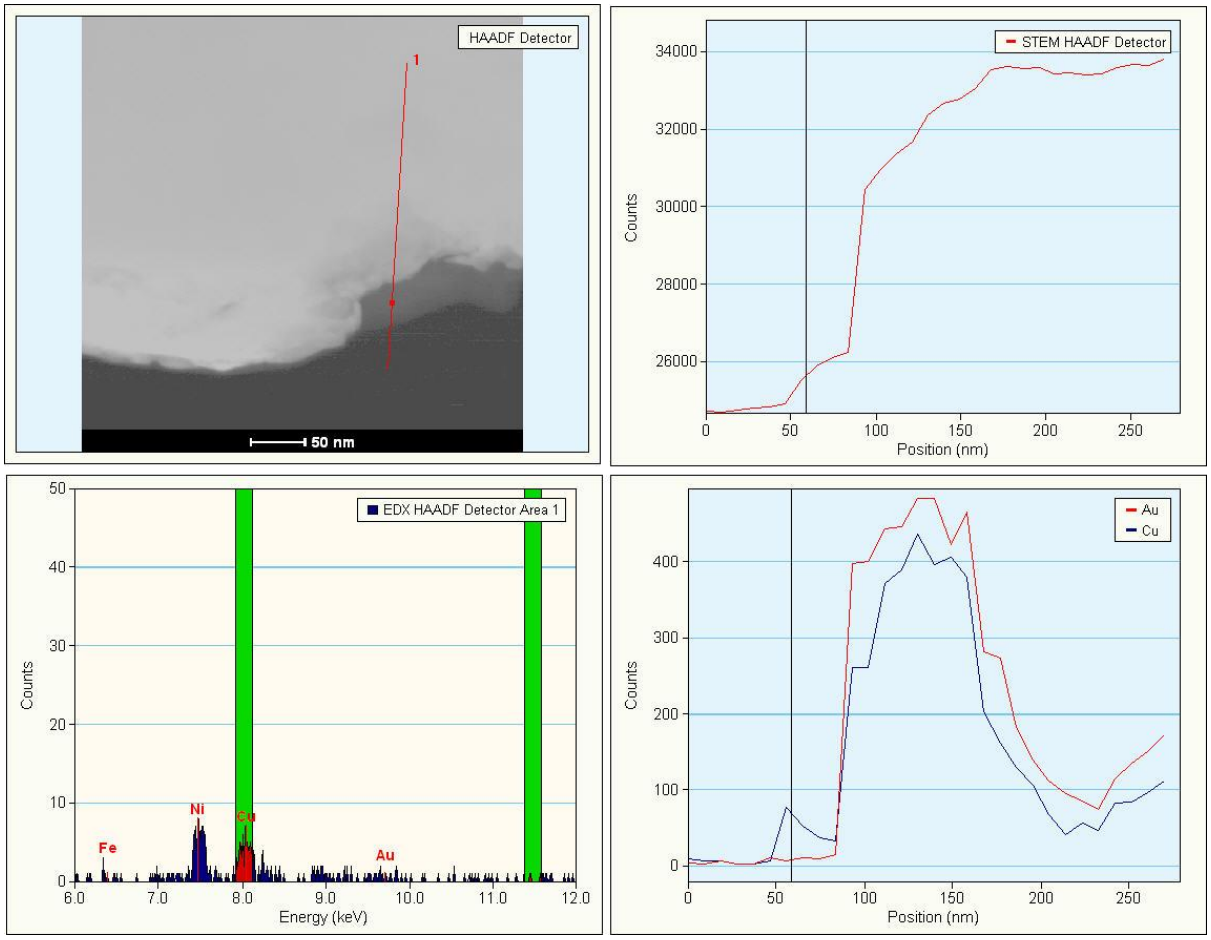

Figure 3.48 TEM/Linescan of reduced only $CuAu/SiO_2$ by Sinfelt method (C978/101A).

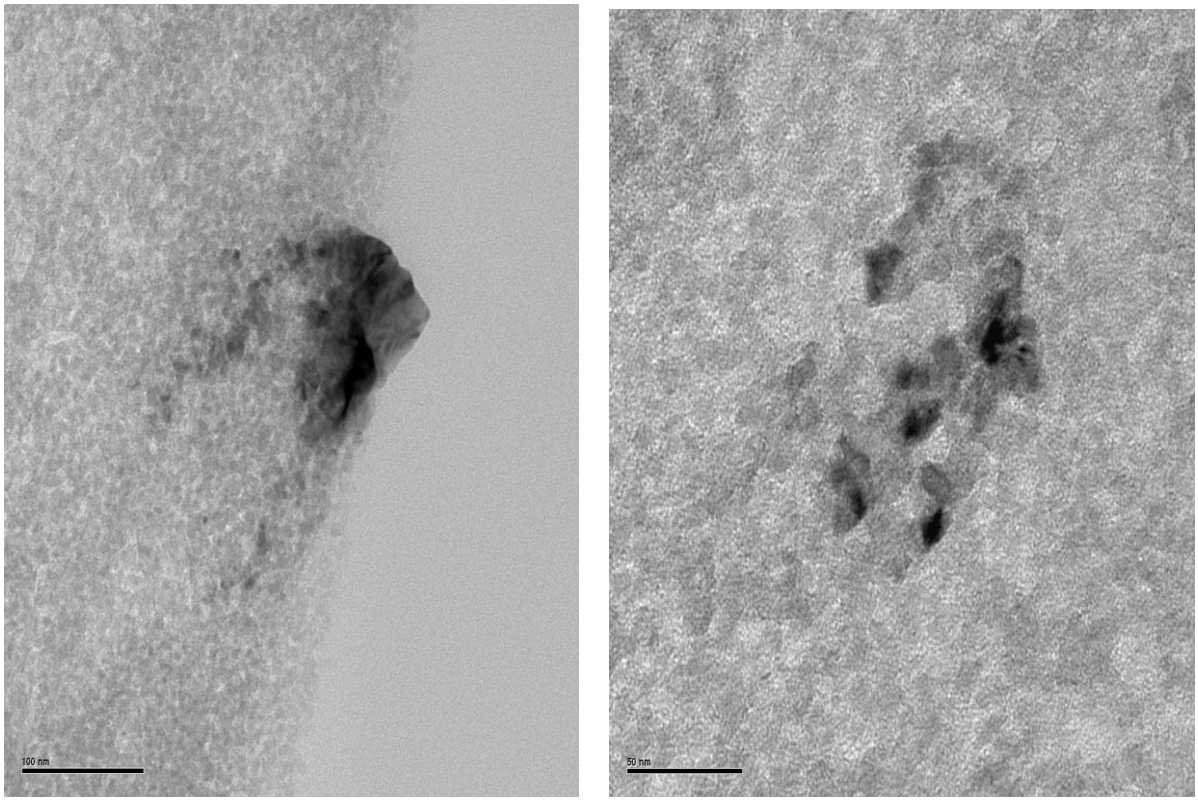

Figure 3.49 TEM images of $CuAu/SiO_2$ catalyst made by the Sinfelt method (C978/101A).

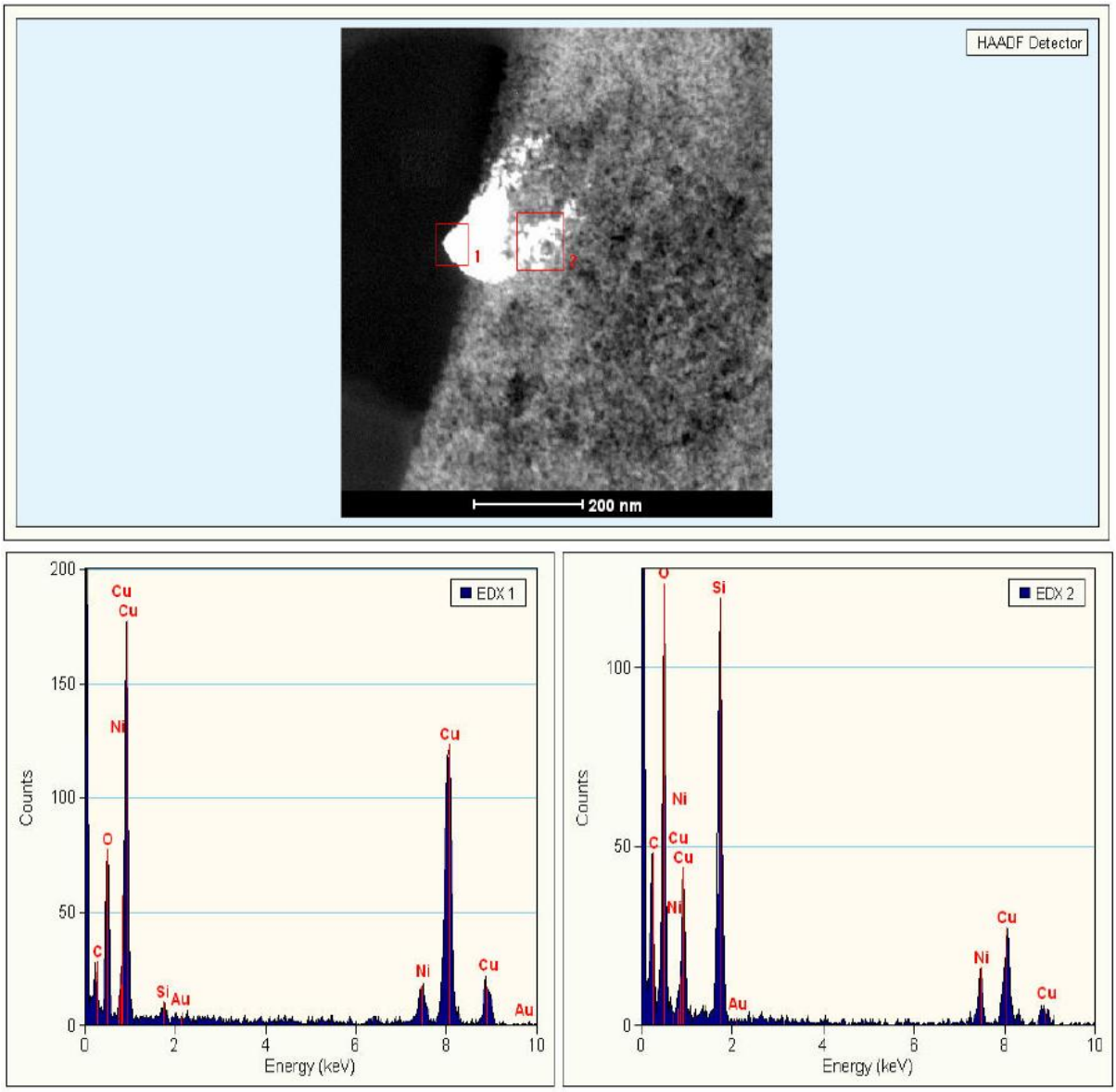

Figure 3.50 TEM/EDX $CuAu/SiO_2$ made by the Sinfelt method (C978/101A). The Ni is observed because it is the grid used to load sample.

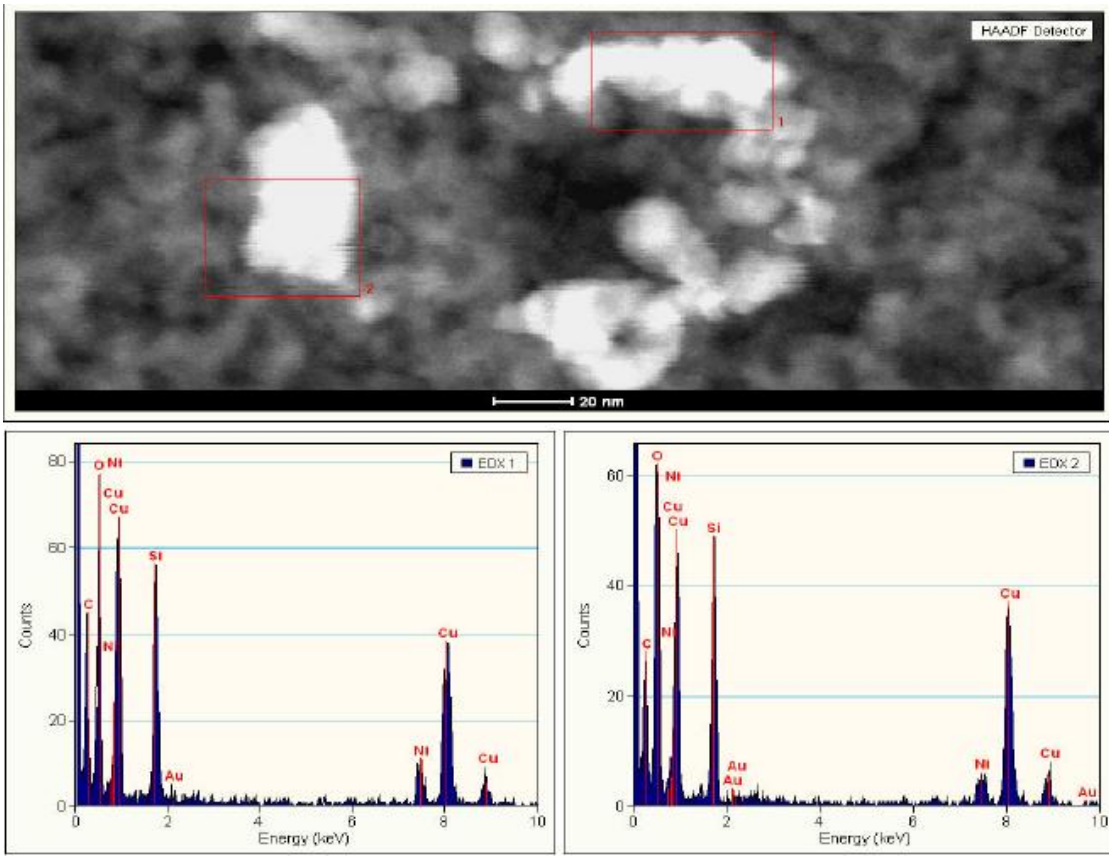

Figure 3.51 TEM-EDX analysis of CuAu/SiO_2 Sinfelt method (C978/101A). The supported material is predominantly Cu. The Ni observed arises from the grid used to support the sample.

TEM-EDX analysis shows that, after high temperature calcination the structure of the catalyst is different with irregular shaped copper particles of between 20-40 nm. The high temperature de-alloys the catalyst, leading to bimetallic Au and Cu particles. Clusters were observed which appeared to be rich in copper, as shown by the EDX analysis (Figure 3.50 and 3.51). The gold particles seem to have little interaction with the support.

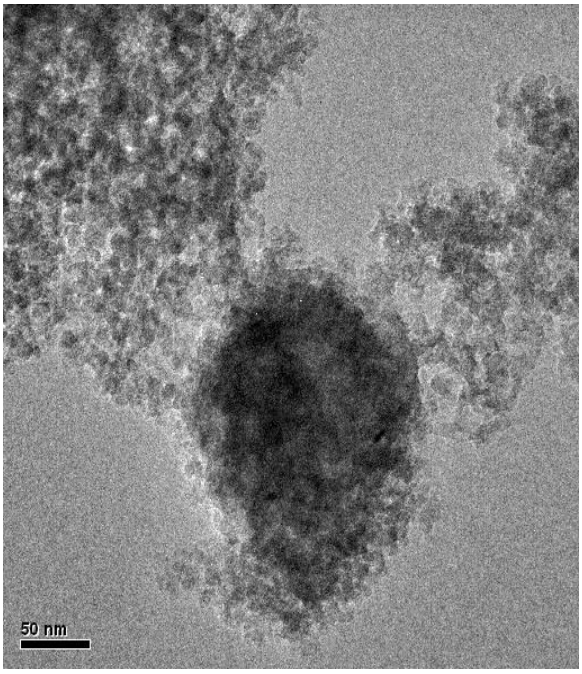

Figure 3.52 TEM image of $CuAu/SiO_2$ prepared by the Sinfelt method using a copper chloride precursor (C978/65A)

TEM analysis for a $CuAu/SiO_2$ catalyst by Sinfelt route but with copper nitrate replaced by copper chloride can be seen in Figure 3.52. CuAu alloy particles (Figure 3.53 and 3.54) can be found of micron size and the EDX line scan shows that some of the particles have surface layers that are copper rich, with their interior regions consisting of Cu and Au (Figure 3.55).

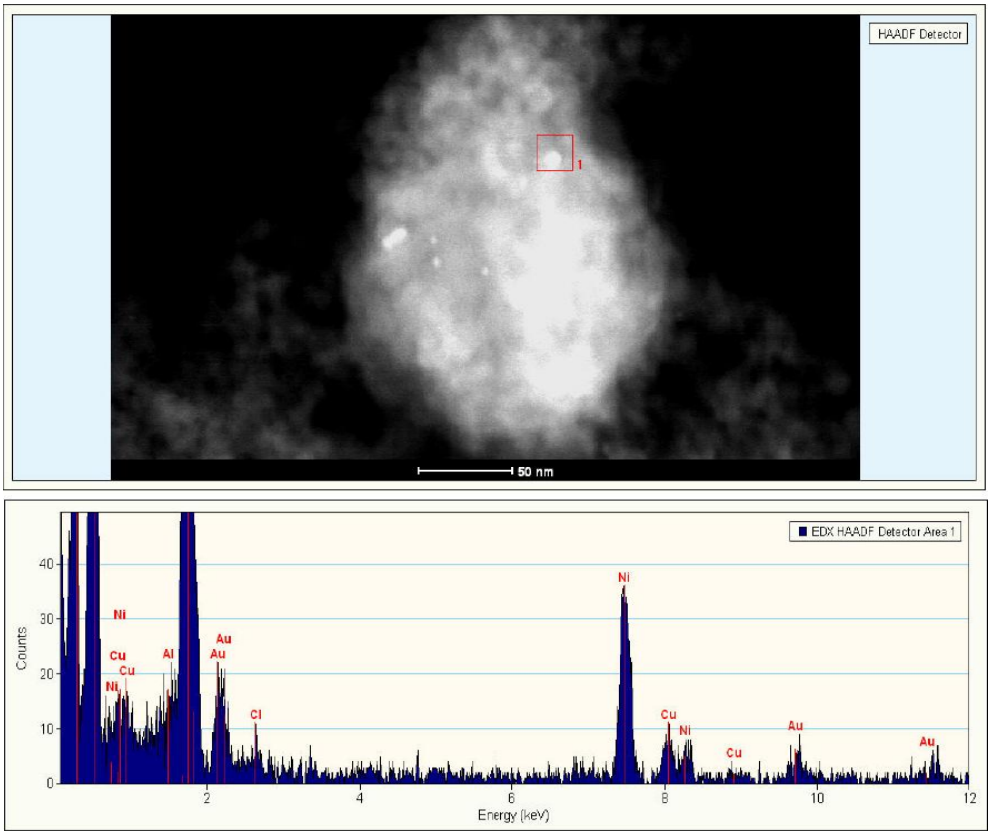

Figure 3.53 TEM/EDX analysis for $CuAu/SiO_2$ catalyst made by the Sinfelt route with copper chloride (C978/65A).

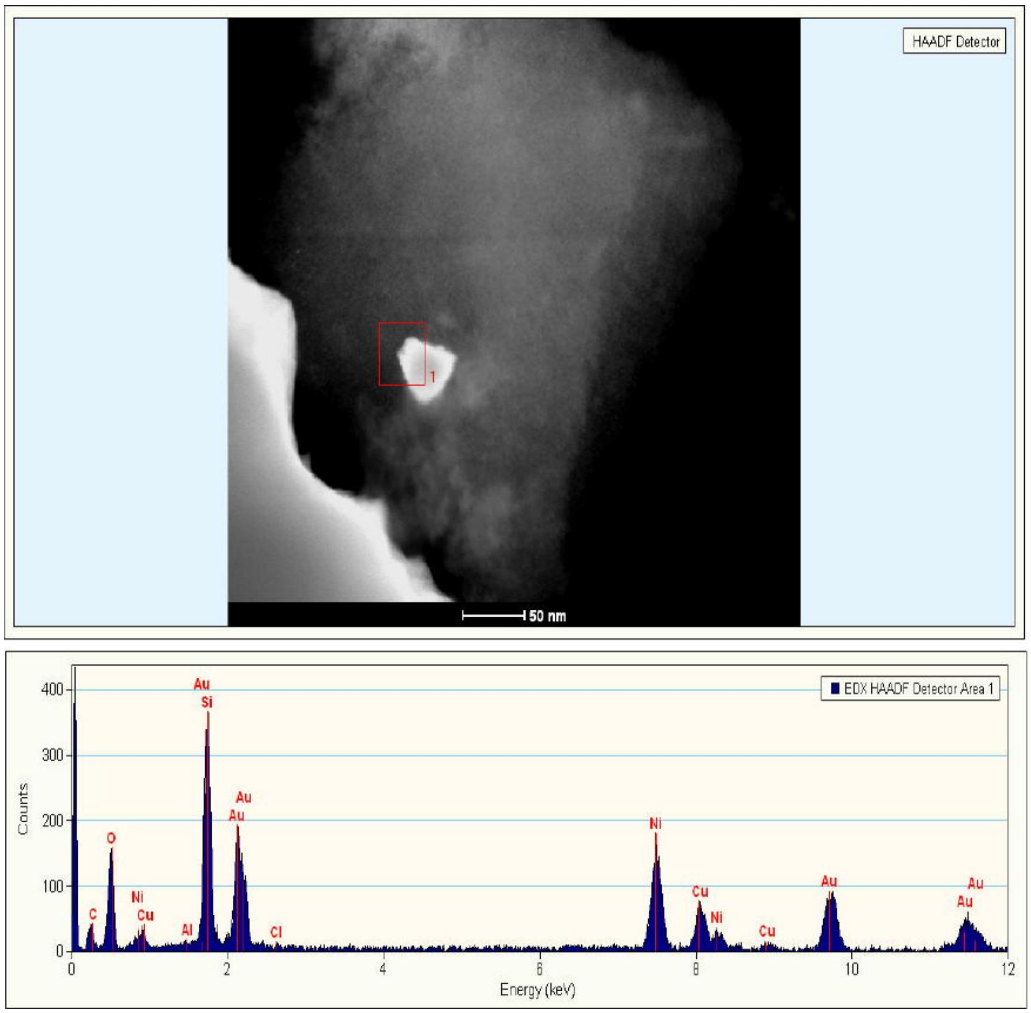

Figure 3.54 TEM/EDX analysis for $CuAu/SiO_2$ catalyst made by the Sinfelt route with copper chloride (C978/65A).

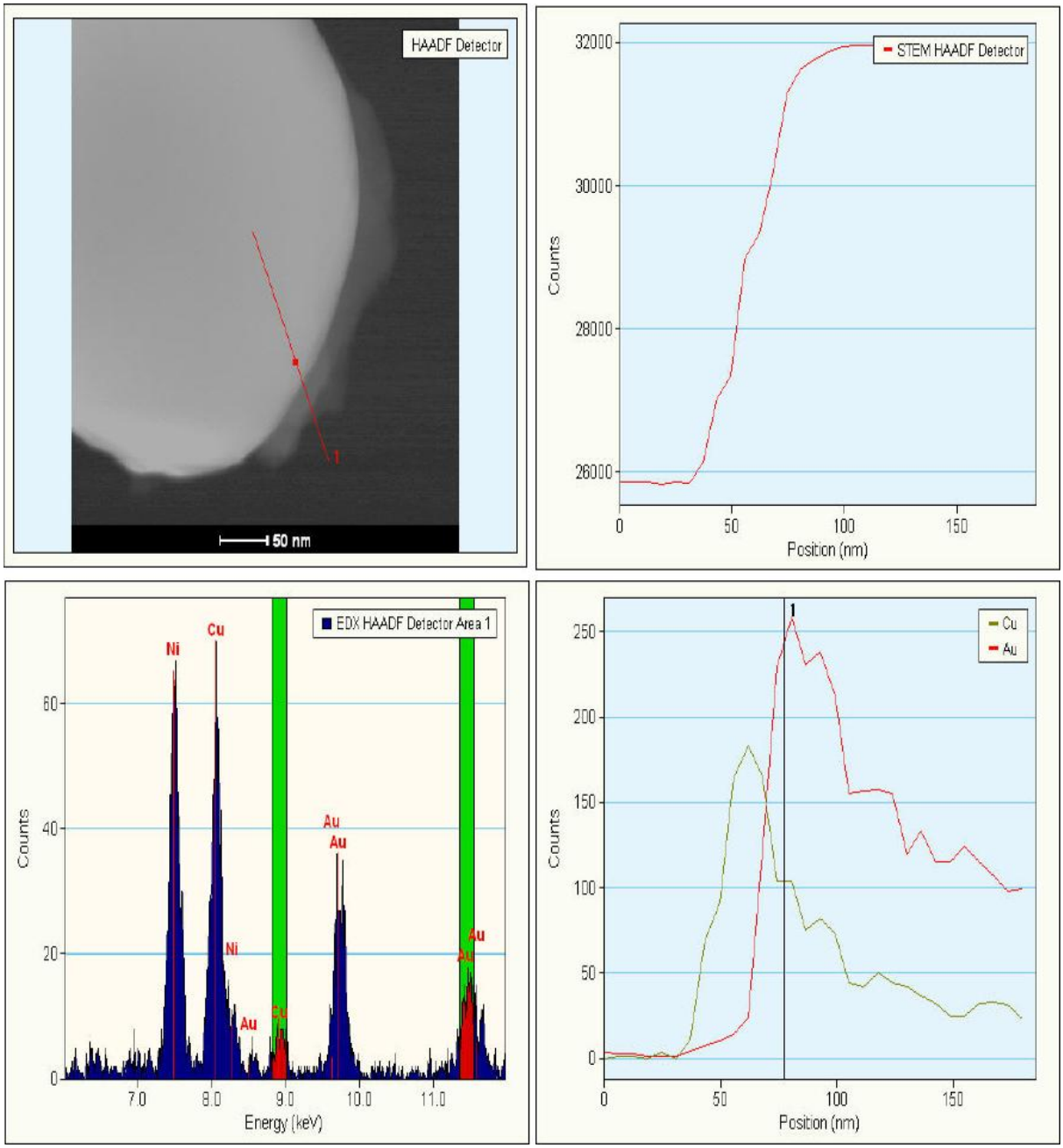

Figure 3.55 TEM/line scan analysis for CuAu/SiO_2 prepared by the Sinfelt method with copper chloride precursor (C978/65A).

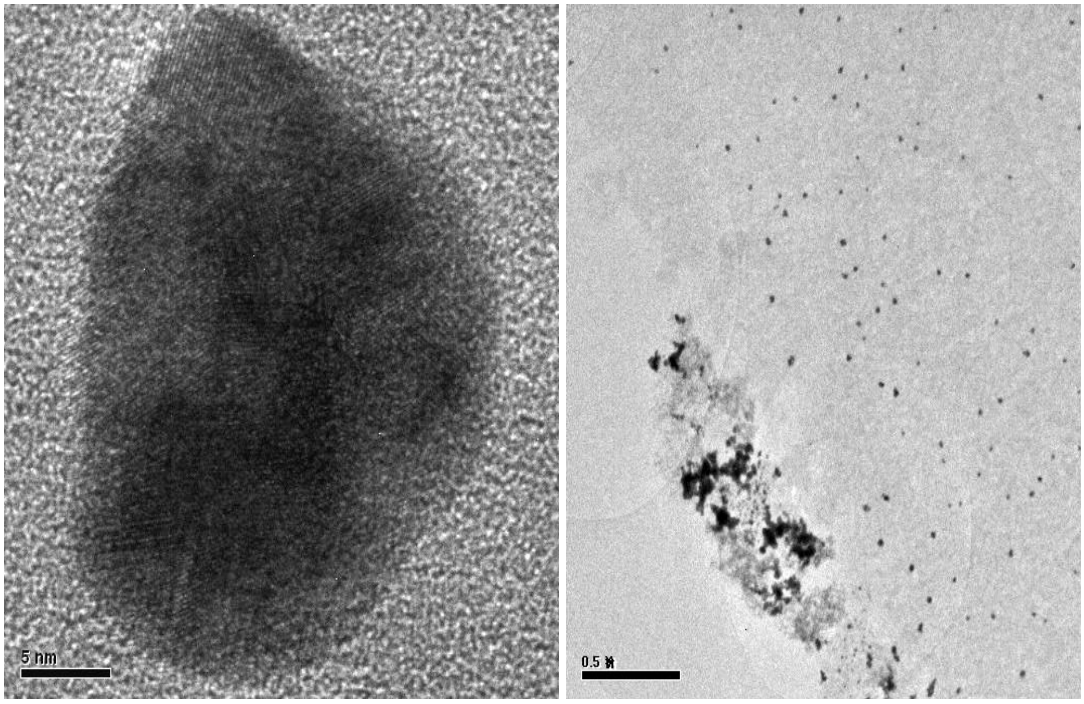

(a) (b)

Figure 3.56 TEM images of $CuAu/SiO_2$ reduced in $NaBH_4$ (C978/80A) (a) low magnification (b) at higher magnification

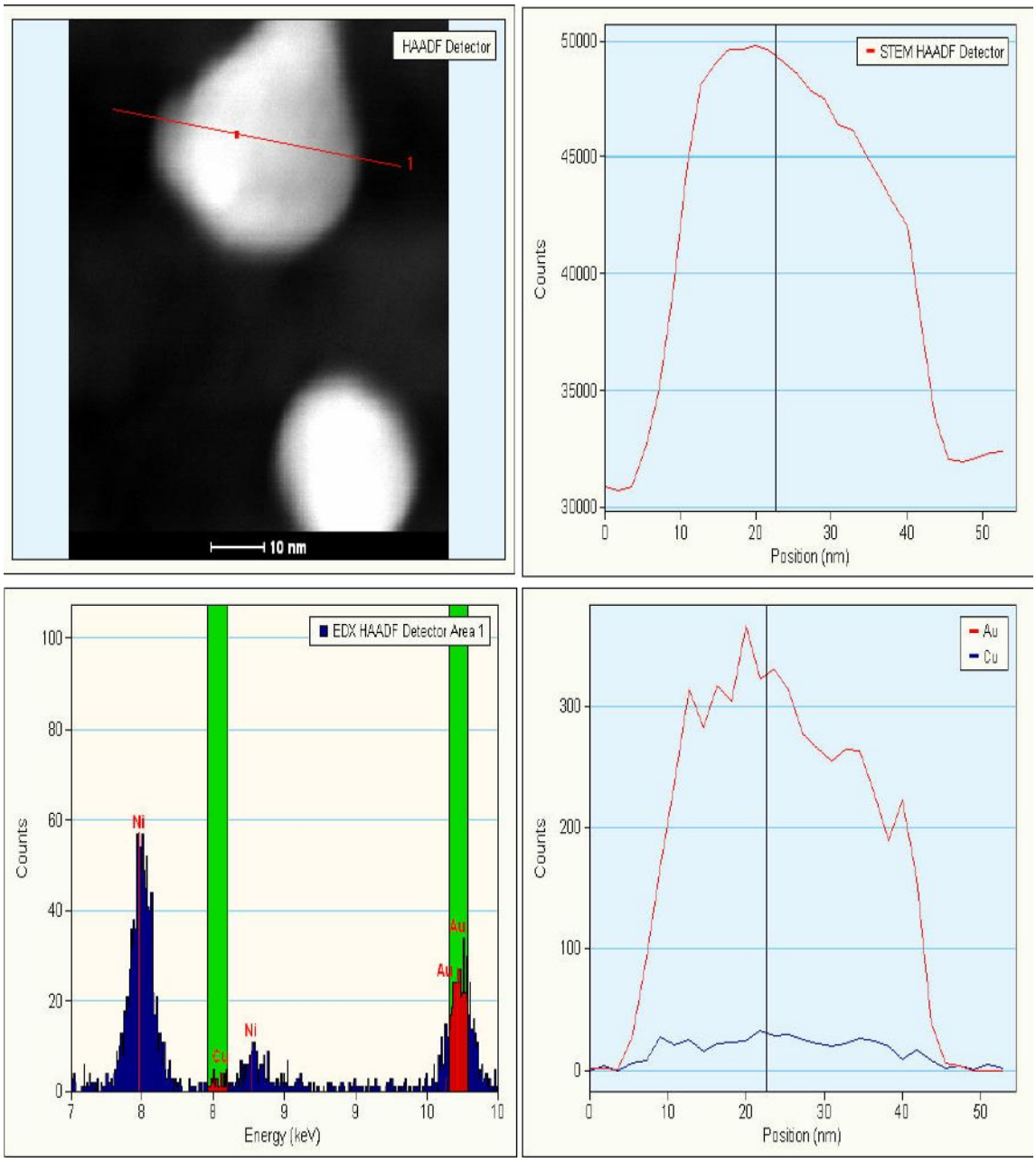

Figure 3.57 EDX HAADF and line scan for $CuAu/SiO_2$ reduced by $NaBH_4$ (C978/80A).

TEM analysis showed that there was alloy formation (Figure 3.57) but some particle illustrated Au concentration variation. Particle clusters (Figure 3.56 b) were seen occasionally on the surface of silica particle.

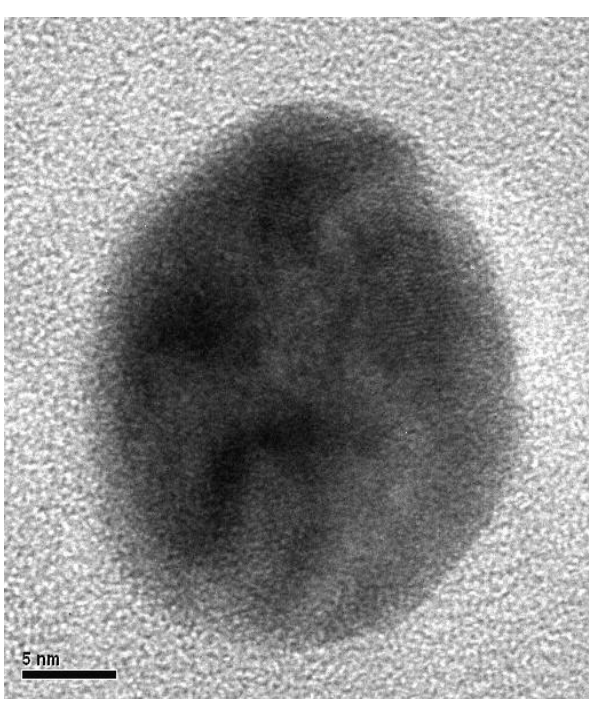

(a)

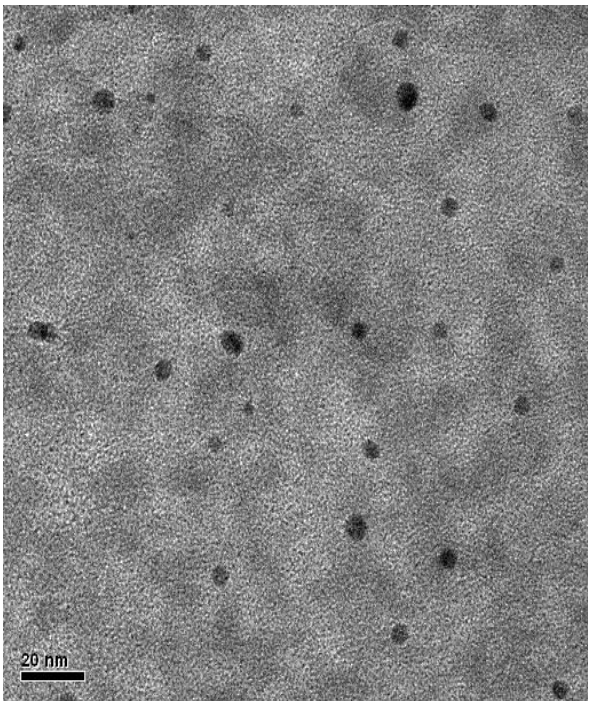

(b)

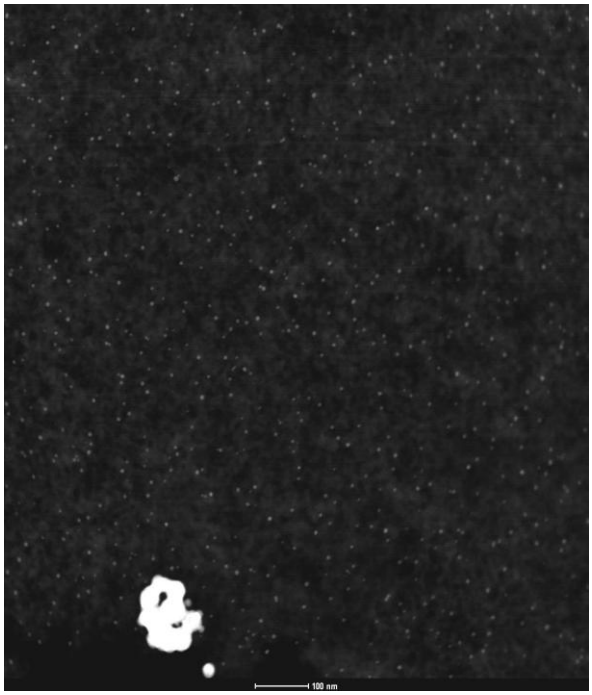

(c)

Figure 3.58 TEM images of HDC Cu + Au DP (C978/87) (a) at high magnification (b) at low magnication (c) at lower magnication

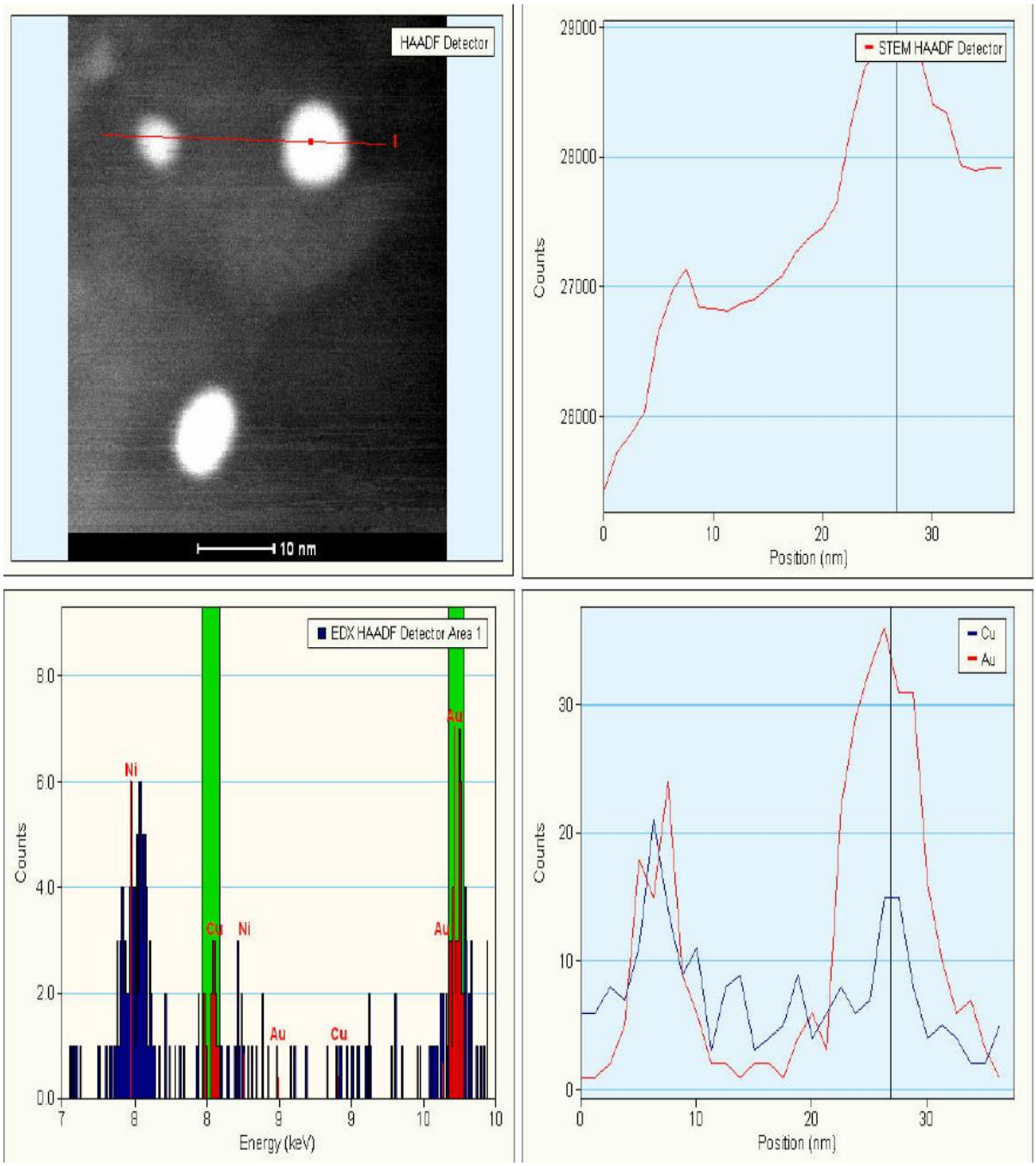

Figure 3.59 EDX HAADF and line scan for $CuAu/SiO_2$ made by HDC Cu + Au DP (C978/87).

Cu and Au form alloys as seen as well as clusters on the silica support. Some copper rich patches have been found (Figure 3.59) on the support silica. Moreover, the CuAu particle size distribution is bimodal. The majority of the particles are small but some particles are several times larger.

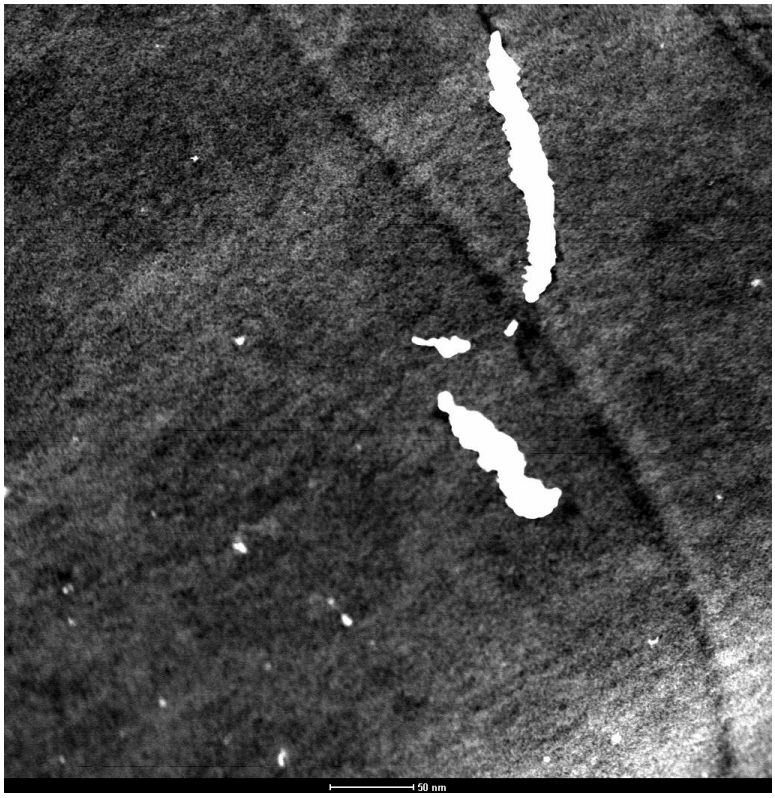

Figure 3.60 TEM image of $CuAu/SiO_2$ made by HDC Cu + Au IW (C978/90)

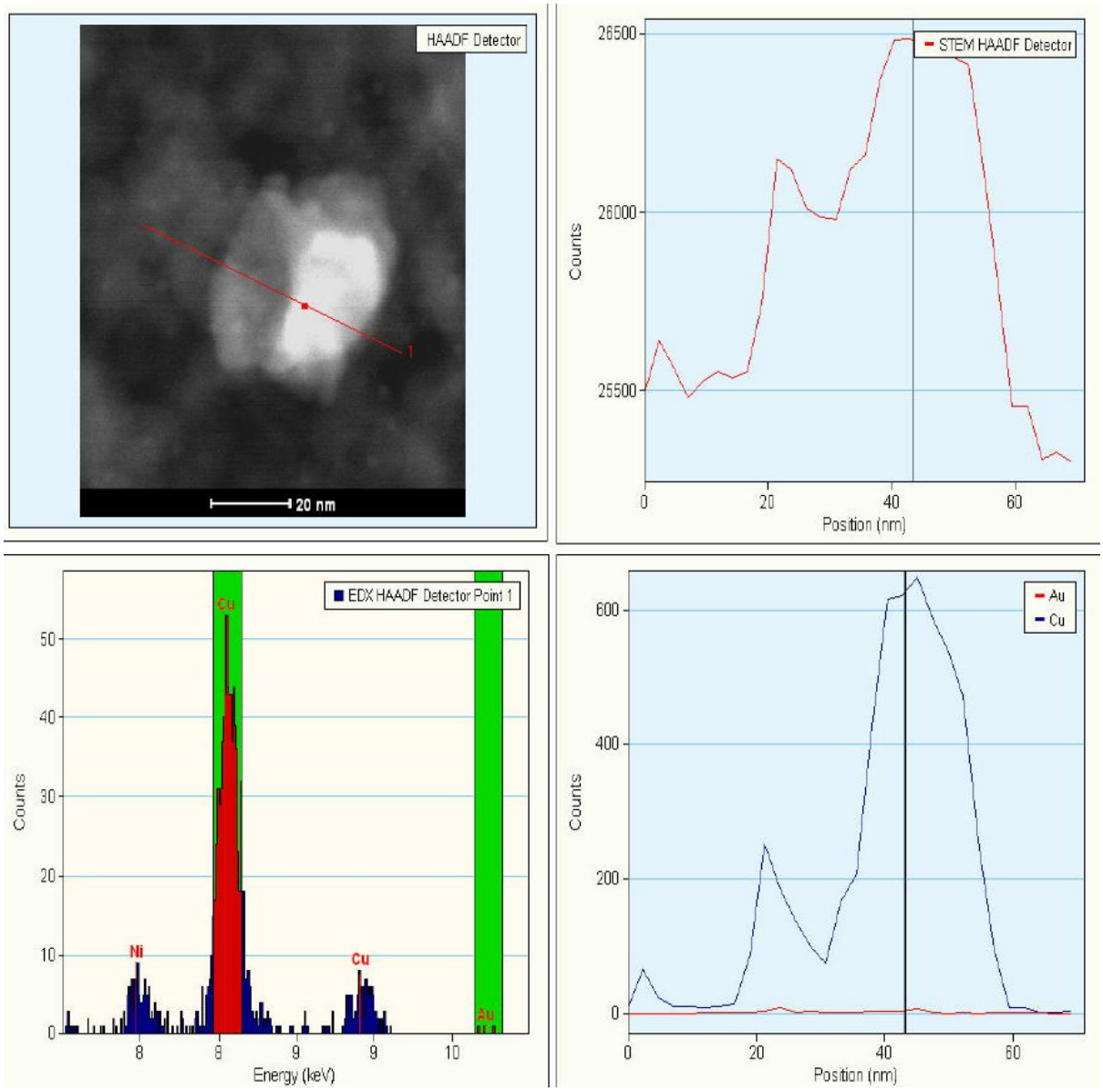

Figure 3.61 EDX HAADF and line scan for $CuAu/SiO_2$ made by HDC Cu + Au IW .(C978/90)

TEM analysis shows some pure Cu patches. Wormlike big CuAu particles (Figure 3.60) are common in addition to small alloy particles.

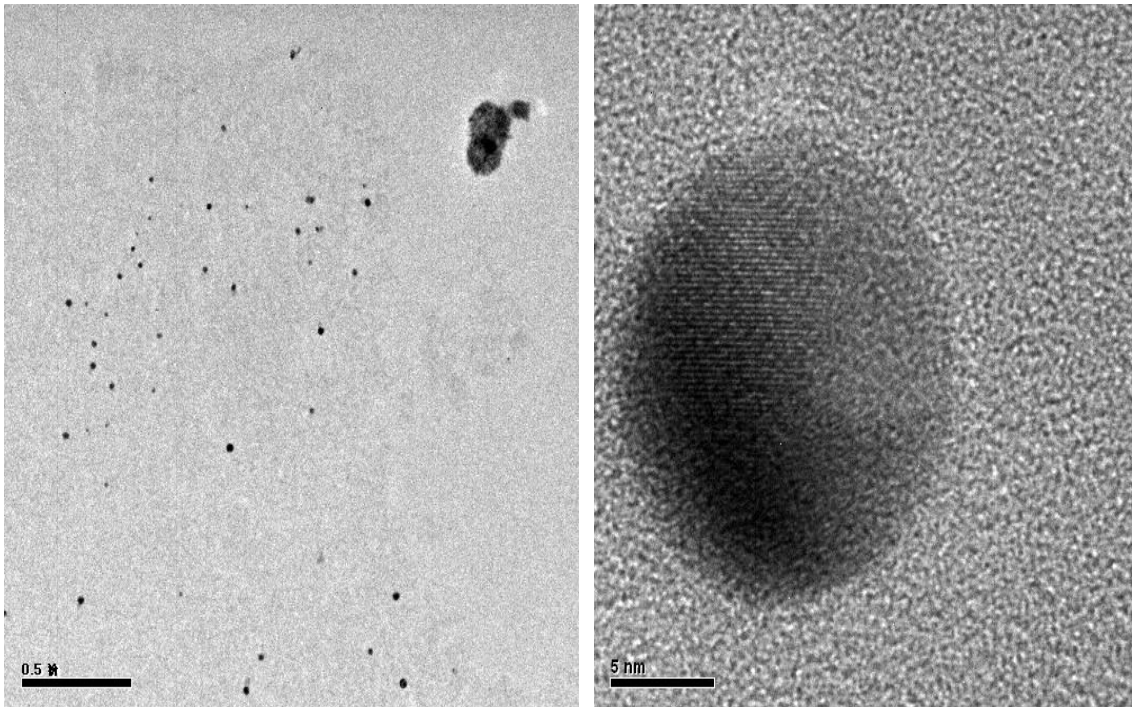

(a) (b)

Figure 3.62 TEM images of $CuAu/SiO_2$ reduced by $NaBH_4$ (C978/80A) and calcined in air.

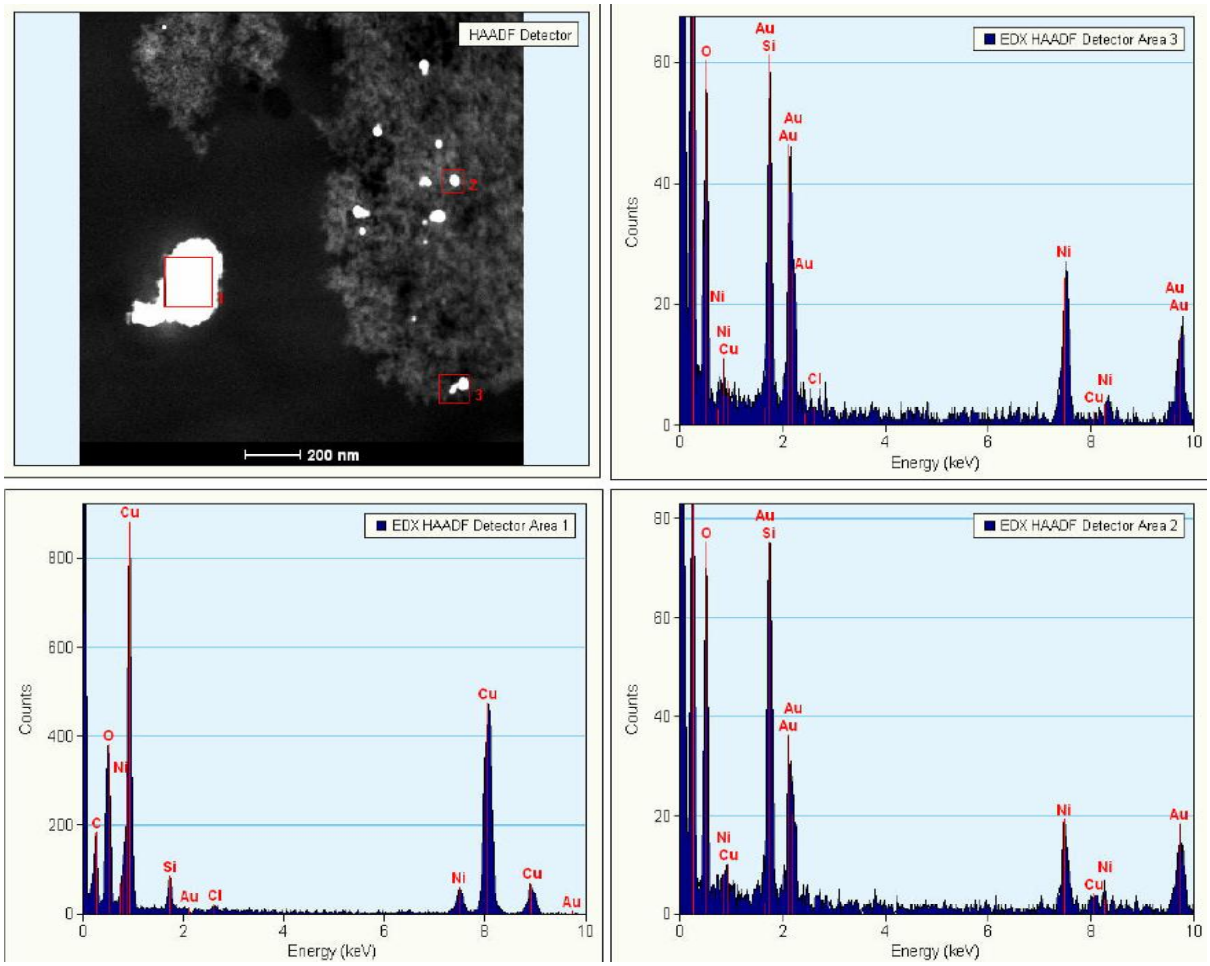

Figure 3.63 EDX for $CuAu/SiO_2$ reduced by $NaBH_4$ and calcined in air

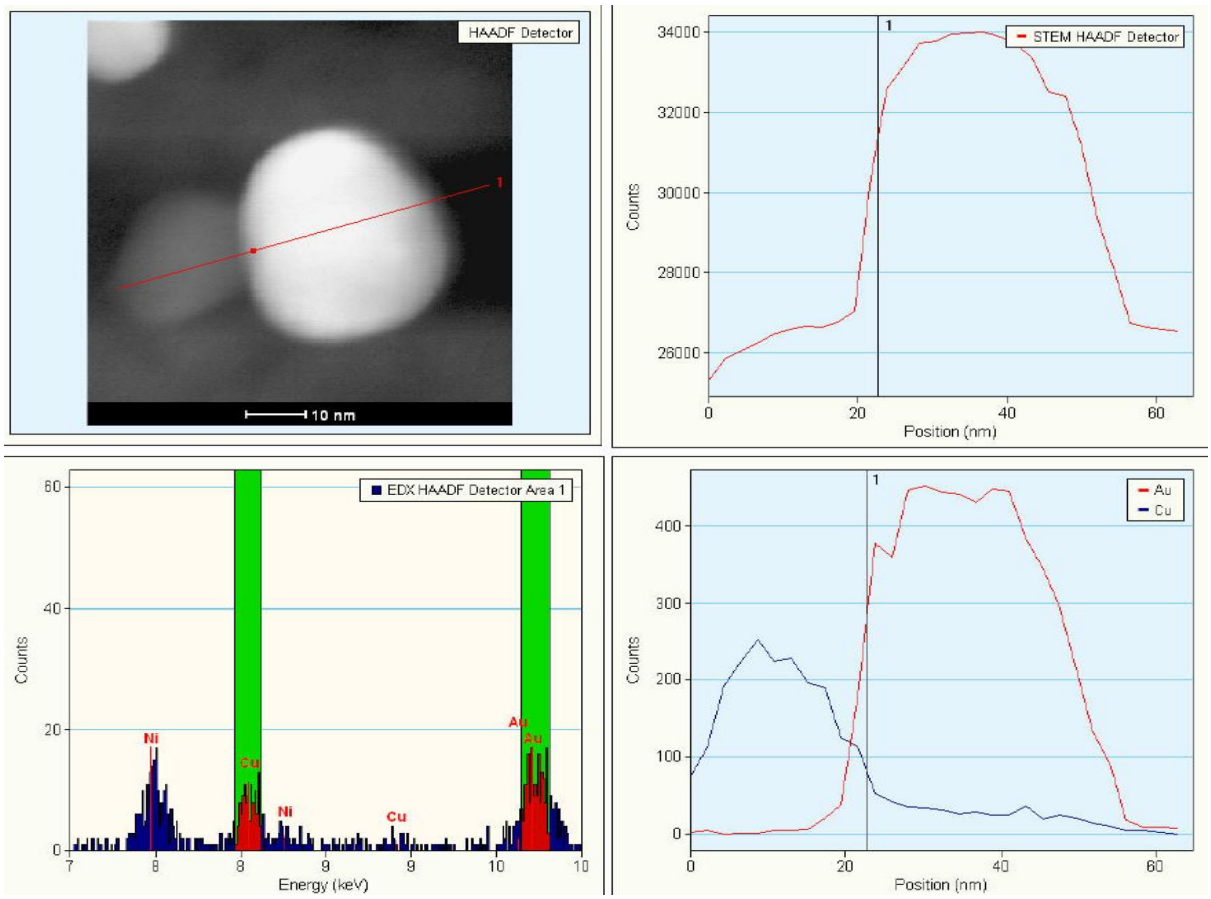

Figure 3.64 EDX HAADF and line scans for $CuAu/SiO_2$ reduced in $NaBH_4$ and calcined in air

TEM analysis of the $CuAu/SiO_2$ catalyst, reduced in $NaBH_4$ and calcined in air (Figure 3.63), showed that Cu and Au seemed to be separated as two phases, although some Cu particles were seen in contact with Au particles, as seen in the EDX line scan.

Sample	Mean	Minimum	Maximum
Reduced $NaBH_4$ (C978/80A)	24	11	42
HDC Cu + Au DP (C978/87)	9	2	71
HDC Cu + Au IW (C978/90)	11	3	107
Reduced $NaBH_4$ and calcined in air	24	11	33

Table 3.4 Particle size (nm) of different preparation methods

Table 3.4 displays the particle size variations for four different preparation methods. $CuAu/SiO_2$ catalyst reduced in $NaBH_4$ has the largest particle diameter of 24 nm. The smallest particle size is formed as a result of a high dispersion route for Cu followed by Au deposition precipitation method, with an average size of 9 nm. This agreed much better with the sizes observed by XRD which showed smaller particles compared with SEM which showed bigger particles and if bulk Au then they are probably not contributing to the catalytic activity. More than 500 particles were counted for TEM particle size data whilst for XRD analysis, more than 1000 particles were counted. It is important that many particles are measured for these characterization techniques so that statistically reliable mean size data can be presented.

3.7 XPS Analysis

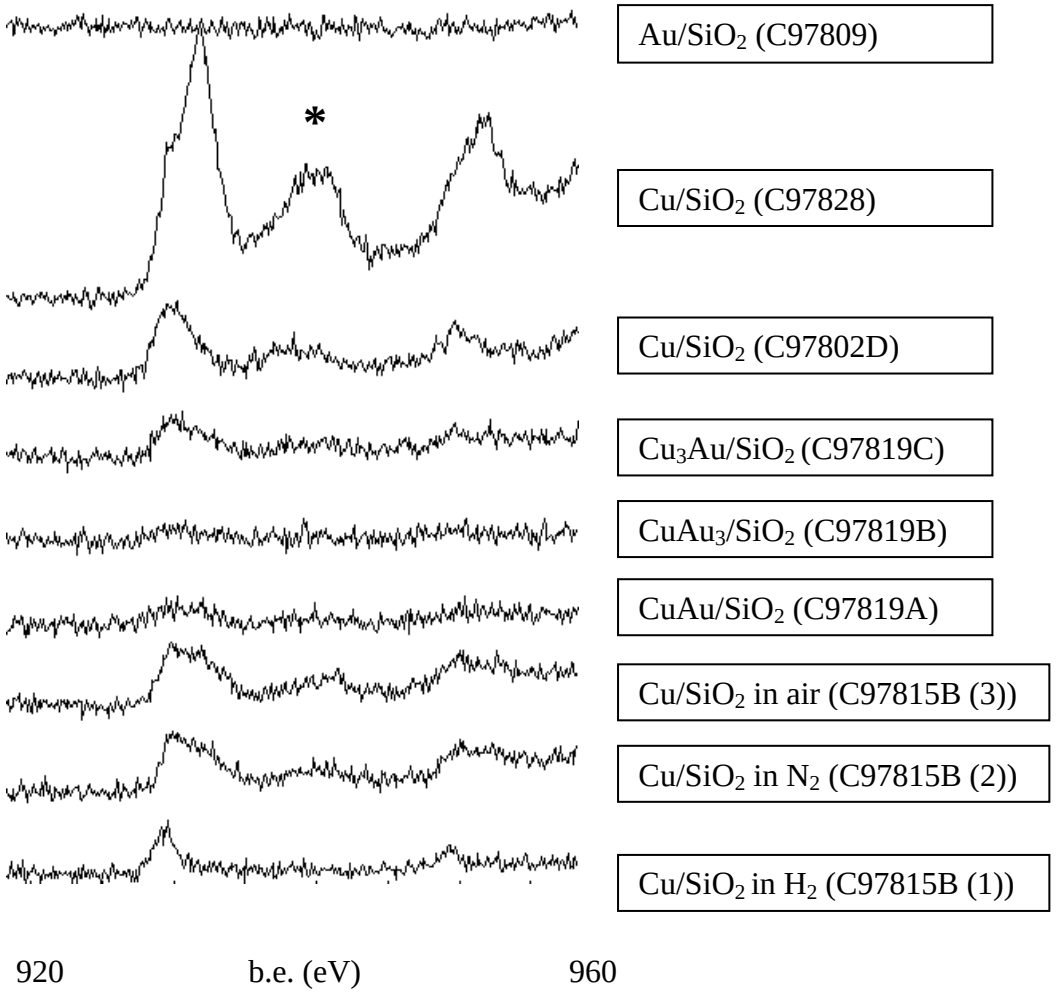

Figure 3.65 XPS spectra for series of catalysts in table 1 (appendix). The Cu^{2+} satellite peak is represented on spectra by *.

.

The XPS Cu(2p) spectra of a series of $AuCu/SiO_2$ catalysts as well as the Au and Cu only versions, have been analysed (Figure 3.65). The Cu/SiO_2 catalyst, made by a precipitation method (8), had the most intense spectrum which might suggest highly dispersed Cu on the silica support. This catalyst also clearly showed the presence of a Cu^{2+} species on surface. For directly calcined $AuCu/SiO_2$ (4) and Au_3Cu/SiO_2 (5) there did not appear to be a Cu^{2+} satellite peak, suggesting the presence of a Cu^{+} species. The Cu (2p3/2) peak was more

intense for the Cu_3Au/SiO_2. The directly calcined Cu/SiO_2 catalyst (7) confirmed the presence of Cu^{2+} species.

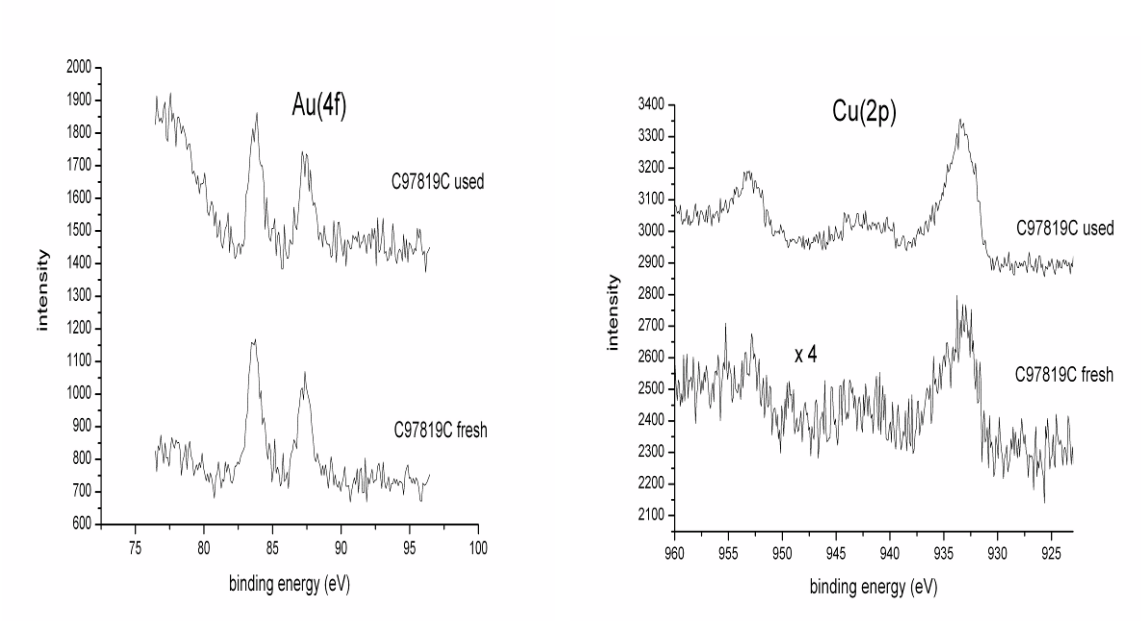

(a) **(b)**

Figure 3.66 XPS spectra for Cu_3Au/SiO_2 (C97819A) before and after propene oxidation (a) Au (4f) spectra (b) Cu (2p) spectra.

The Au(4f) and Cu(2p) XPS spectra for the Cu_3Au/SiO_2 catalyst before (fresh) and after propene oxidation are shown in Figure 3.66 a and b. These spectra suggest that the reduction in the Au:Cu ratio after use was due to an increase in the Cu(2p) signal (Cu(2p):Si(2p) ratio) rather than a loss in the Au.

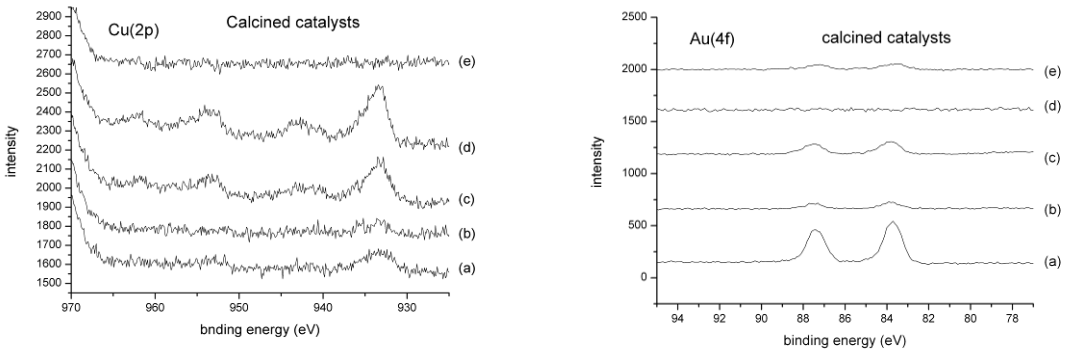

Figure 3.67 XPS analysis of calcined catalysts (C97819A-C, C97809, C97802D) showing (left) Cu(2p) and (right) Au(4f) spectra: (a) $CuAu_3/SiO_2$, (b) $CuAu/SiO_2$, (c) Cu_3Au/SiO_2, (d) Cu/SiO_2, (e) Au/SiO_2. The position of the Cu^{2+} satellite peak in the Cu(2p) spectra is marked with a dot.

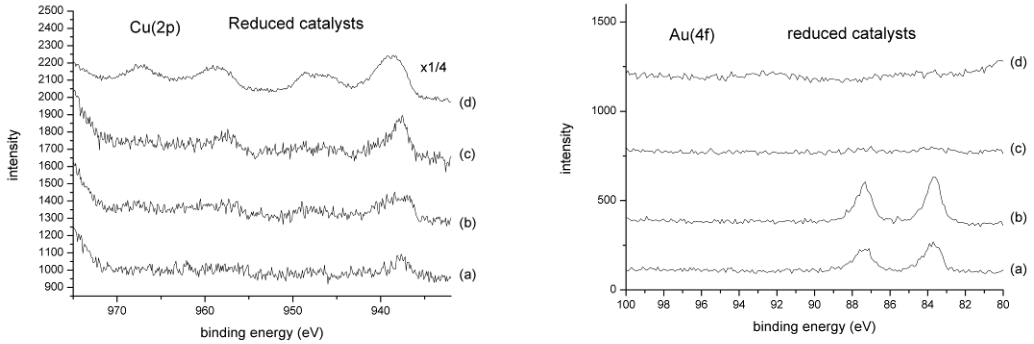

Figure 3.68 XPS analysis of reduced catalysts showing (left) Cu(2p) and (right) Au(4f) spectra: (a) $CuAu_3/SiO_2$, (b) $CuAu/SiO_2$, (c) Cu_3Au/SiO_2, (d) Cu/SiO_2, (e) Au/SiO_2 (C978/93A-E)

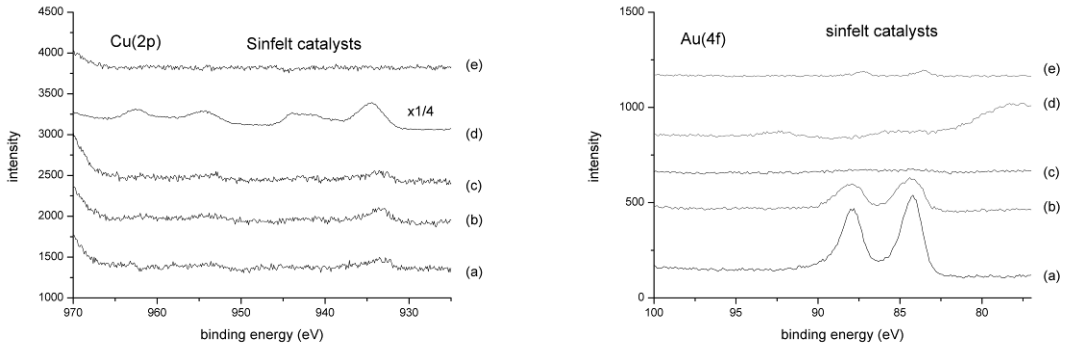

Figure 3.69 XPS analysis of reduced and calcined catalysts showing (left) Cu(2p) and (right) Au(4f) spectra: (a) $CuAu_3/SiO_2$, (b) $CuAu/SiO_2$, (c) Cu_3Au/SiO_2, (d) Cu/SiO_2, (e) Au/SiO_2 (C978/10A-E)

XPS spectra for the three molar ratios of $CuAu/SiO_2$ catalysts calcined in air are shown in Figure 3.67. The surface Cu:Au ratio increases monotonically with the expected bulk ratio (Table 3 appendix); however, there is a large increase in Cu enrichment. The XPS spectra of reduced catalysts are represented in Figure 3.68. The Cu(2p) spectra are extremely intense, when compared with the calcined catalyst spectra, which may be a consequence of higher Cu dispersion on the silica support caused by the reduction step. Cu^{2+} satellites are very weak as expected. The reduced Cu_3Au/SiO_2 catalyst has a significant enhancement in surface Cu concentration which could be explained by highly mobile metallic Cu (0) during the reduction method. Similar to the reduced catalysts, the XPS data for the Sinfelt catalysts (Figure 3.69) confirmed the presence of Cu^{+} species due to the absence of the Cu^{2+} satellite peak. However, unlike the directly calcined and reduced catalysts, the Sinfelt samples have Cu:Au ratios close to the expected bulk values, with the Cu rich composition being the only exception (appendix).

3.8 UV-Visible Plasmon analysis

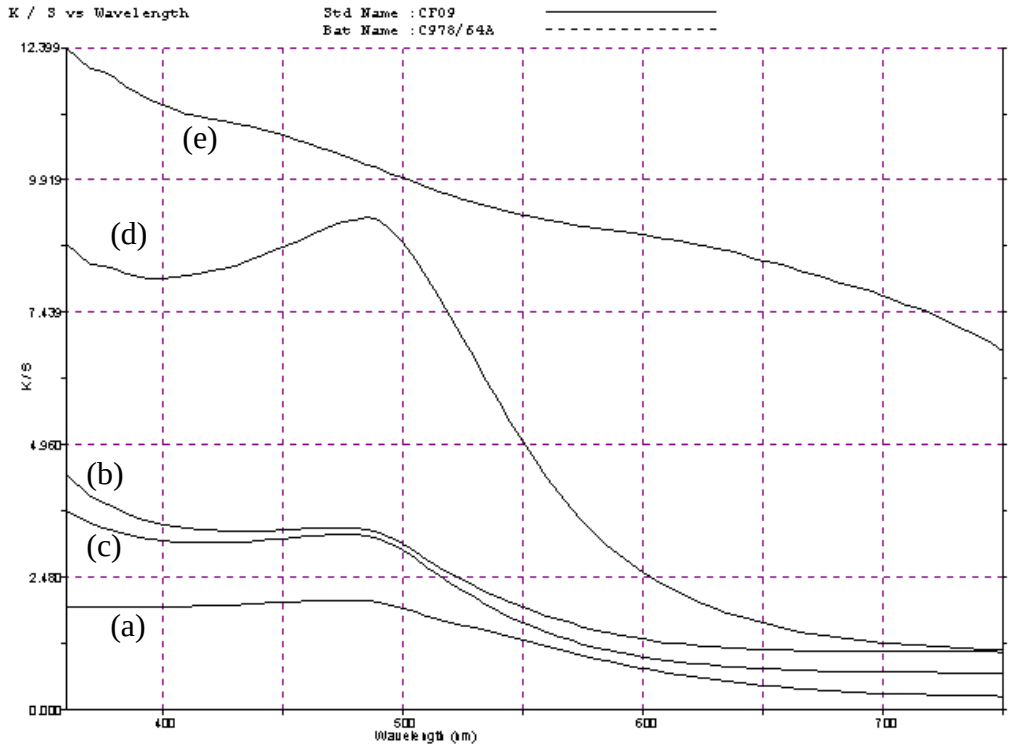

Figure 3.70 UV-Visible spectroscopy of calcined catalysts (C97819A-C, C97809, C97802D) (a) Au/SiO_2 (b) $CuAu3/SiO_2$ (c) $CuAu/SiO_2$ (d) Cu_3Au/SiO_2 and (e) Cu/SiO_2**.**

Visible spectroscopy has been used to investigate the interaction between gold and copper in the calcined catalysts (Figure 3.70). The spectra showed that the interaction between the metals was negligible, as the position of the plasmon bands was not shifted when the copper-gold ratio was changed.

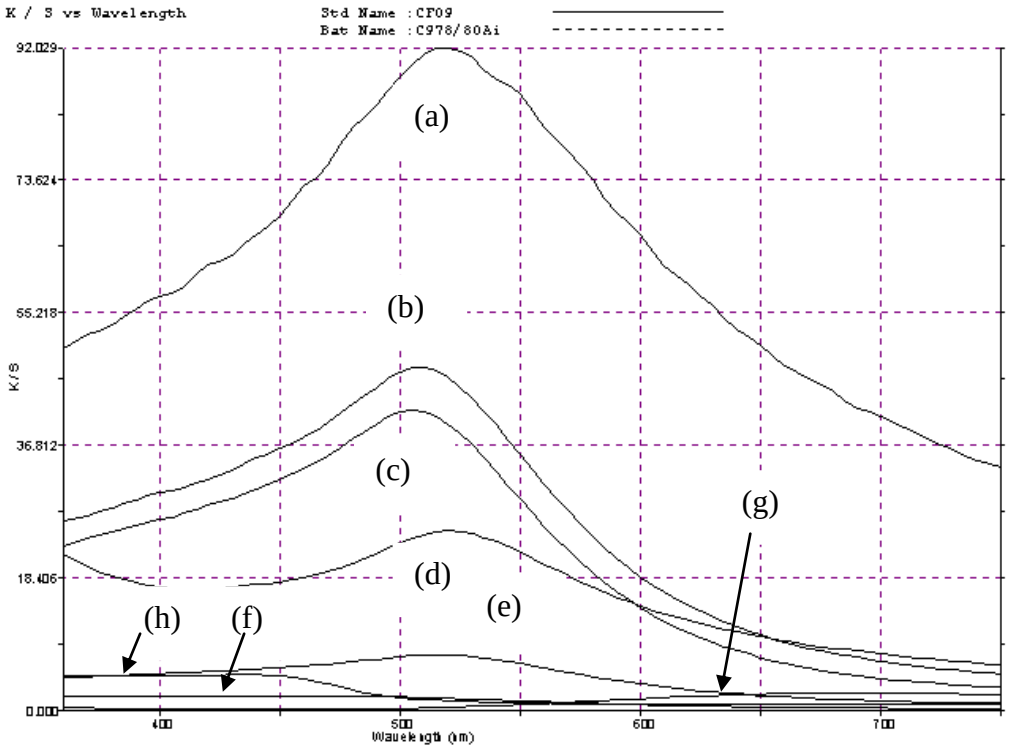

Figure 3.71 Plasmon bands for borohydride treated catalysts (C978/80A-E) (a) $AuCu/SiO_2$ (b) $AuCu/SiO_2$ with no ice treatment (c) $CuAu_3/SiO_2$ (d) Cu_3Au/SiO_2 (e) Au/SiO_2 (f) Cu only. Comparisons with other methods (g) HDC Cu dried only (CF128) (h) Au/SiO_2 direct calcination (C97809)

UV-Vis spectroscopy has been carried out for catalyst treated with $NaBH_4$ as a reducing agent instead of H_2 (Figure 3.71) and compared with Au/SiO_2 calcined in air (g) and HDC Cu dried only (f). All the $AuCu/SiO_2$ borohydride reduced catalysts shifted plasmon positions, suggesting a strong interaction between Cu and Au. Sodium borohydride reduction appeared to have an effect on the plasmon band as the Au only catalyst (e) had a different band width than the calcined in air Au sample (g). The more Cu rich the AuCu ratio, the further the peak maximum shifted to higher wavelength.

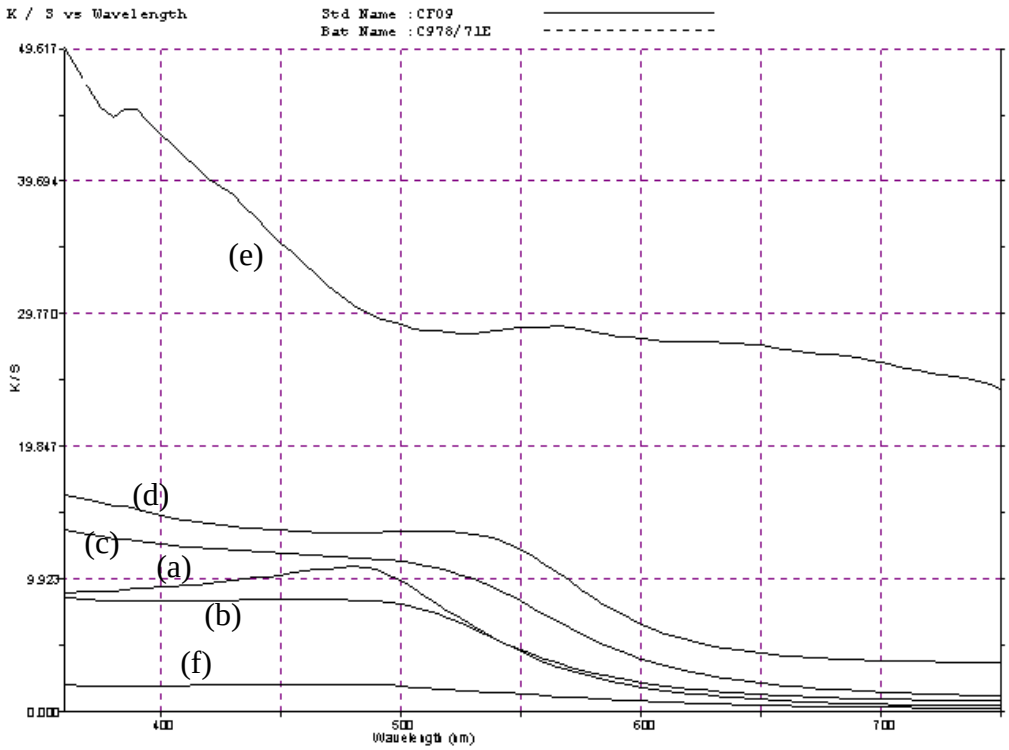

Figure 3.72 UV-Visible spectroscopy of reduced catalysts (C978/93A-E) (a) Au/SiO_2 (b) $CuAu_3/SiO_2$ (c) $CuAu/SiO_2$ (d) Cu_3Au/SiO_2 (e) Cu/SiO_2 and (f) Au/SiO_2 calcined.

Visible spectroscopy revealed the formation of bimetallic particles (Figure 3.72) as the position of the plasmon peak shifted away from the position of the gold as the copper-gold ratio changed. This was previously seen by Liu and co workers when their characterised borohydride reduced CuAu/SBA-15 catalysts by visible spectroscopy.[8]

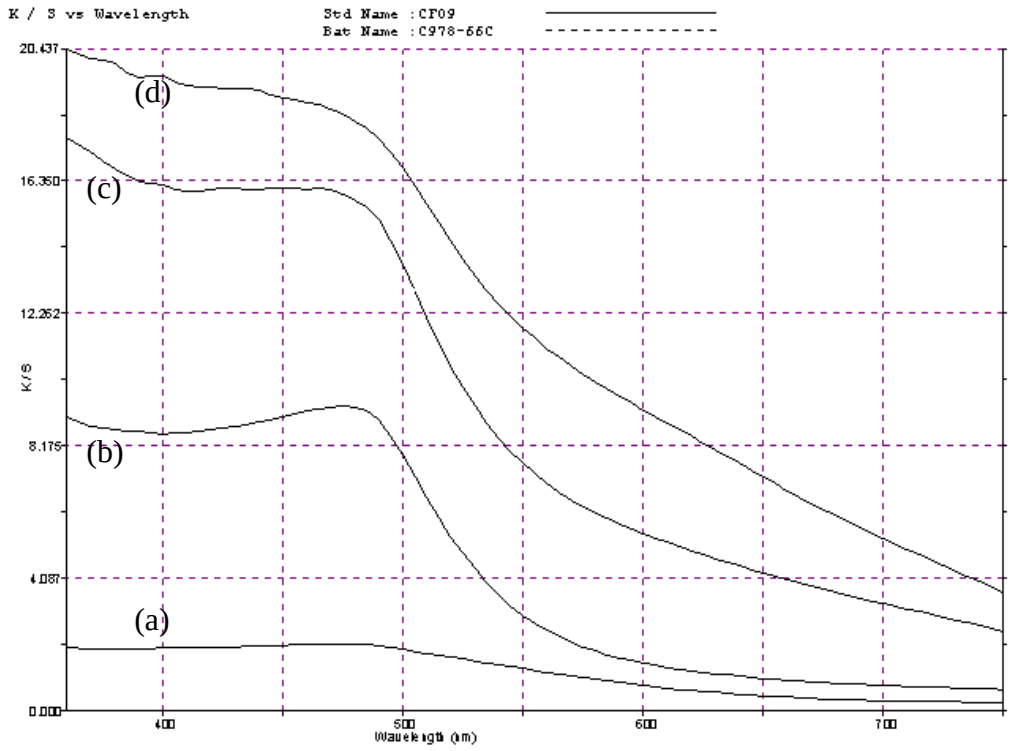

Figure 3.73 UV-Visible spectroscopy of reduced and calcined catalysts (C978/101A-E)(a) Au/SiO_2 (b) $CuAu_3/SiO_2$ (c) $CuAu/SiO_2$ (d) Cu_3Au/SiO_2

For the $CuAu/SiO_2$ catalysts prepared by a Sinfelt thermal treatment, the visible spectroscopy agrees with the TEM and XRD data as there does not appear to be much interaction between the gold and copper particles. This is suggested as there is not a shift in the plasmon peak when the copper-gold ratio is altered (Figure 3.73).

3.9 EGA Analysis

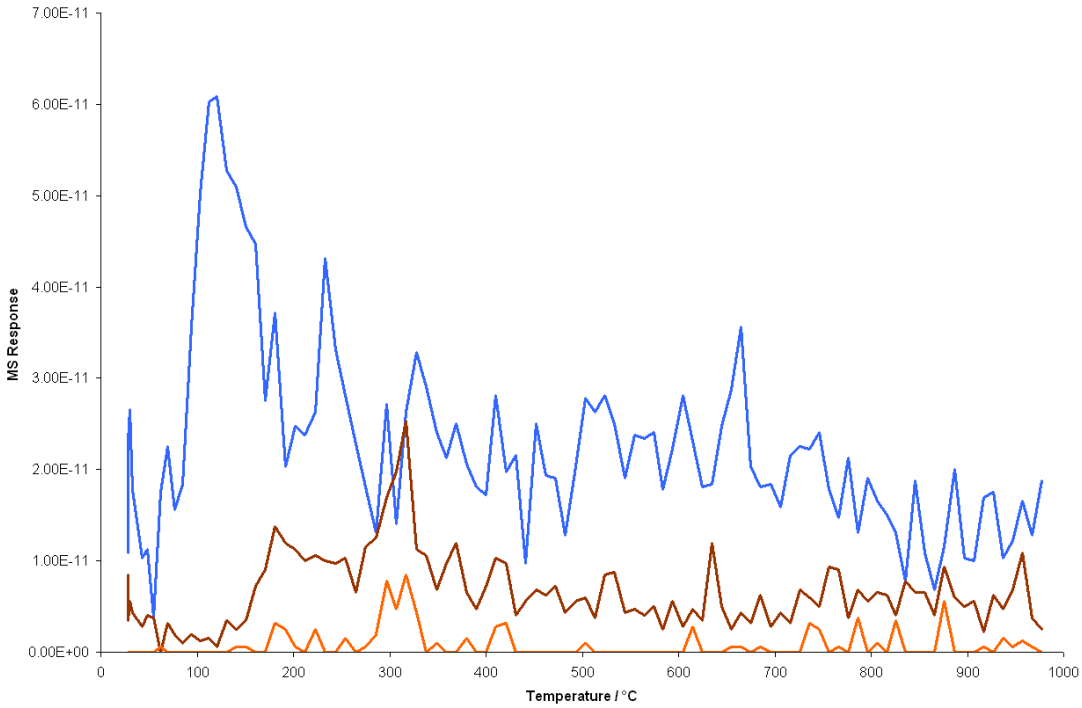

Figure 3.74 MS Profile of gases formed in the decomposition of the dried precursor under 5% O_2/He. Masses are 30 (NO, blue), 36 ($H^{35}Cl$, brown) and 38 ($H^{37}Cl$, orange).

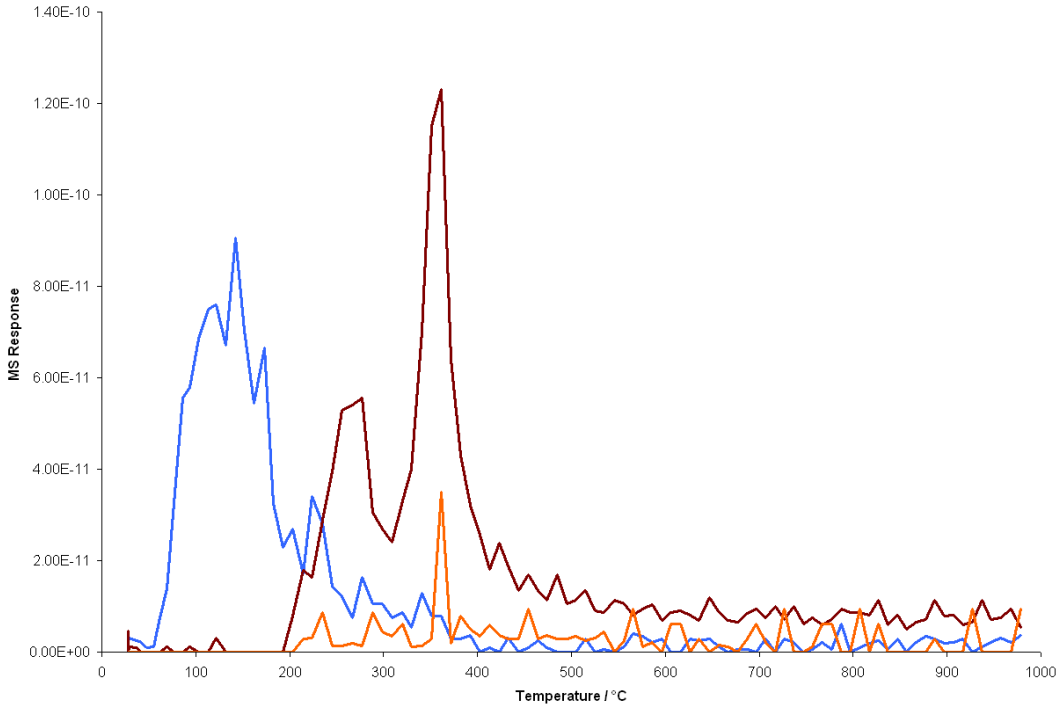

Figure 3.75 MS Profile of gases formed in the decomposition of the dried precursor under 5% H_2/N_2. Masses are 30 (NO, blue), 36 ($H^{35}Cl$, brown) and 38 ($H^{37}Cl$, orange).

To get a greater understanding of the $AuCu/SiO_2$ catalyst made, EGA analysis is of interest as it can help to explore the processes which lead to the different structures already suggested. When the catalysts are directly calcined in air, copper nitrate decomposes to copper oxide at a lower temperature and chloride is removed from the Au precursor (Figure 3.74). When the catalyst undergoes a reduction in H_2, the copper nitrate (Figure 3.75) is decomposed first with a major product loss of NO. But instead of forming copper oxide, as in the oxidation procedure, it forms copper metal.

3.10 The effect of sodium hydroxide reduction with metal salts

It has been well documented that metal boride impurities can be formed by the use of sodium borohydride reduction with metal salts. Sodium borohydride has been used in the preparation of copper and gold nanoparticles, and Schaak and group[9] prepared copper nanocomposites using the precursors $Cu(C_2H_3O_2)_2.H_2O$ and $HAuCl_4.3H_2O$ and added these to distilled water. After the mixture was stirred, $NaBH_4$ was added to form a mixture of copper and gold nanoparticles. XPS analysis was carried out for the AuCu and $AuCu_3$ samples and they concluded that there was no detection of impurities generated from the precursors. Boron, sodium and chloride were the main elements that were chosen to be checked, if present in the sample. ICP data confirmed that they were all absent.

Glavee and group [10] studied the aqueous and non aqueous reduction of Cu^{2+} as well as Fe^{3+}, Fe^{2+}, Co^{2+} and Ni^{2+}. The precursors $CuCl_2.2H_2O$ (Cu 2+(aq)) and $CuBr_2$ in Diglyme (Cu^{2+} (diglyme)) were reacted with $NaBH_4$. Glavee and group found that the light green Cu^{2+} solution changed to a yellow brown solution upon first addition of $NaBH_4$ and then went to a brown-black precipitate with gas evolution. The product was filtered and dried to form a powder. XRD analysis was performed on the powder and showed metallic copper with a crystallite size of 30 nm. Their work suggested that, because of the positive redox potential of copper, metallic copper was formed when reacted with $NaBH_4$ instead of the borohydride. A scheme was derived for this reaction:

$$2\ Cu^{2+}(aq) + 4\ BH^{4-}(aq) + 12\ H_2O \longrightarrow 2\ Cu(s) + 14\ H_2 + 4B(OH)_3$$

For the reaction with $CuBr_2$ in diglyme, vigorous gas evolution was seen and a coppery film on the walls of the glass was observed. XRD analysis detected metallic copper with a crystallite size of 24 nm. The group also studied reactions with cobalt and nickel, and found that boride compounds were formed which could be due to the more negative redox potentials. In the diglyme case, a colourless complex was formed when reacted with $NaBH_4$

but, upon thermal decomposition at 90 ^{o}C, a brown-black precipitate with gas evolution was generated. Glavee and group represented the reaction as:

$$2\,Cu^{2+}\,(diglyme) + 4BH_4^- \xrightarrow{Diglyme} 2\,Cu(BH_4)_2(diglyme)_n \xrightarrow{90\,^{\circ}C} 2\,Cu(s) + 2H_2 + 2B_2H_6$$

From the results in this thesis, after a sodium borohydride reduction, a brown-black colour change was observed and gas was evolved. However, from XPS and ICP analysis, no boron was detected in the catalysts. This appears to agree with a prior study carried out by Schaak and group[9]. For future work, the complete hydrolysis of the borohydride could be achieved rapidly by the addition of acid to the aqueous solution.

3.11 Discussion

Catalysts have been characterised by several techniques to try to determine their structure and the relationship between the preparation method and catalyst composition. Most catalysts for this study were made by incipient wetness impregnation, as it is a simple and reliable method for making supported catalysts. The only disadvantage to this technique is that the metal particles are not highly dispersed on the support, but are when made *via* deposition as observed from XRD. All catalysts were either calcined directly in air, reduced with either H_2 or $NaBH_4$ or reduced and calcined by the Sinfelt procedure[1] (315 ^{o}C in H_2/Ar followed by calcination at 676 ^{o}C in air). All the catalysts had high surface areas and gold and copper loadings were close to expected values.

Catalysts directly calcined in air were found to contain large ensembles of gold which were clearly shown in SEM images and on closer inspection, the ensembles were made up of smaller gold particles. The Au/SiO_2, directly calcined, catalyst also comprised these large ensembles, which suggested that there was a weak metal interaction due to the preparation method. XRD analysis also supported this finding, since strong reflections due to gold crystallites were present. These intense reflections overlapped with copper crystallites,

making them harder to observe in the XRD pattern. TEM and SEM analysis uncovered well-dispersed copper particles with large clusters that were gold rich. Gold metal and copper oxide were confirmed by XPS analysis for the copper only and Cu_3Au/SiO_2 catalyst, as a result of a distinctive satellite structure. Copper and gold interaction was weak and this was shown in the UV-vis spectrum, exhibiting no plasmon shift.

The TPR spectra for a typical Cu/SiO_2 catalyst prepared by impregnation with copper nitrate, followed by drying and direct calcination, revealed two copper species: bulk-like CuO and dispersed Cu^{2+} ions.[11] The relative amounts of these species and the degree of interaction with the support was influenced by factors, such as metal loading, solution pH and the nature of the silica used.[8,12,13] Both of these forms of Cu(II) reduced directly to copper metal but there was no evidence of Cu(I) intermediates.[11]

The TPR of our Cu/SiO_2 catalyst was in general agreement with the literature,[11] with peaks at 276 °C and 362 °C for Cu^{2+} ions and CuO particles respectively. There was also a shoulder at 237 °C which was tentatively assigned to small, easy-to-reduce CuO clusters.[13] However, the TPR was changed when gold was present in the catalyst. The peaks were all due to copper reduction. TPR showed that an Au/SiO_2 sample did not generate any peaks. XRD confirmed the presence of metallic gold in the samples after calcination. The major peak in the $CuAu/SiO_2$ catalysts was a broad peak at 227 °C, and a very broad peak or succession of peaks from 400-650 °C. These high temperature peaks were reminiscent of Cu^+ reduction in Cu/SiO_2 catalysts[12] and it might be that gold was able to stabilise this oxidation state.

A TEM study of the oxidation of bulk and nanoparticulate CuAu alloys found that islands of Cu_2O – rather than CuO – were produced[14,15] after vacuum annealing and oxidation in gaseous oxygen. The large low-temperature peak might be related to Au promotion of copper (II) by hydrogen spillover in the large Au-rich bimetallic particles. The hydrogen consumption for this study was calculated and the $CuAu/SiO_2$, $CuAu_3/SiO_2$ and Cu_3Au/SiO_2

catalyst had consumptions of 191, 738 and 638 μ mol/g respectively. One reason for the difference might be the introduction of chloride into the system *via* tetrachloroauric acid solution. That would decrease the pH of the impregnating solution and also potentially change the copper speciation. The TPR spectra were broadly similar to those observed for $CuAu/TiO_2$ catalysts, prepared by co-impregnation with copper chloride and gold chloride.[16] The peaks in that study were at higher temperature which may suggest an effect of changing the support used for the catalyst. However, the TiO_2-supported catalysts were reduced at 400ºC and then re-oxidised at 350 ºC prior to analysis, which could be responsible for the differences observed.

Reduction of the catalysts instead of calcination in air gave a different structure. The reduction step resulted in the formation of a CuAu alloy phase, which was present in the XRD analysis as a broad reflection, with the addition of some unalloyed gold reflections too. However, the broad reflection altered, depending on the Cu:Au ratio. The gold rich and $CuAu/SiO_2$ catalysts had a broad reflection with no structure, suggesting a variety of structures. But the copper rich catalyst had maxima in the broad reflection, implying that alloy formation was favoured. The formation of bimetallic particles was also confirmed from UV-vis spectroscopy as a consequence of the plasmon band peak maximum moving away from the gold plasmon band, as the Cu:Au ratio changed. This characterisation technique compared the reduction method with other pre-treatment conditions and determined that the strongest copper-gold interaction was after reduction only. A high temperature calcination de-alloyed the catalyst and showed no plasmon position change in the UV-vis spectrum. SEM analysis showed the formation of large clusters and well-dispersed smaller particles on the silica support. The EDX linescans revealed that the large clusters contained both copper and gold and that some of the particles had surface layers of pure copper, and their interior regions contained both copper and gold. Alloy formation was not 100% and there were some

monometallic particles observed by TEM. XPS spectra were also different when compared to the directly calcined samples, as their Cu (2p) spectra were much more intense, and it was concluded that the absence of the Cu^{2+} satellite peak proved the presence of Cu^{+} species as an outcome of the reduction procedure. The copper rich bimetallic catalyst had a significant enhancement in copper which could be due to highly mobile copper species on the support formed from the reduction step.

High temperature calcination of reduced catalysts caused major structural changes too. XRD analysis showed that the copper gold alloy phase changed to monometallic gold reflections. TEM analysis showed different structures than the calcined and reduced catalysts with irregularly shaped copper particles of about 20-40 nm in size. The high temperature calcination de-alloyed the copper and gold, leading to gold and copper bimetallic particles. Unlike the SEM images for the directly calcined catalysts, there were no large gold ensembles present, although rounded gold particles are observed. The copper-gold interaction was weaker compared to the reduced samples. As with the reduced catalysts, the Sinfelt samples had no Cu^{2+} satellite which suggested the presence of Cu^{+} species. This has been observed in other studies[15,17] as Au has been seen to stabilise the Cu_2O in alloy nanoparticles, which have been prepared by oxidation of a CuAu alloy. EGA analysis was carried out to explore the processes which led to the different structures observed. In the direct calcination samples, copper nitrate decomposed to copper oxide at a lower temperature than that at which the chloride was removed from gold. However, the gold and copper oxide did not interact, and so the gold formed large ensembles instead of highly dispersed CuO particles, due to the weak interaction with the silica support. When the decomposition occurred under hydrogen, again the copper was decomposed first, with the loss of NO as the major product. However, this led to the formation of copper metal, which interacts strongly with gold as it formed to give an alloy. The copper-gold alloy phase is very stable and needed calcination at high

temperatures to decompose it to copper oxide and gold metal. TPO analysis of a CuAu inter-metallic compound[1] found that the oxidation of the copper present proceeded between 650 ºC and 800 ºC, forming Au metal and CuO.

In situ XRD was studied for the $AuCu/SiO_2$ Sinfelt catalyst to investigate the changes in the metal species during the reduction and high temperature calcination. During the reduction step, the main reflections of gold metal were observed throughout the experiment. It was interesting to see that gold metal was already present at lower temperatures (<200 ^{o}C), maybe by decomposition in the drying step. This could be the source of the unalloyed Au particles observed. Changes to the preparation to reduce the copper at lower temperatures could lead to greater degrees of alloying and so better catalysts. EGA showed that NO was produced at 100 °C on reduction, with HCl from the decomposition of the gold precursor, observed above 200 °C. By XRD, however, broad reflections were observed at higher 2 theta than the gold reflection, starting from 275 °C. These were assigned to the formation of copper-gold alloy species. The reduced catalyst therefore contained a mixture of gold and copper-gold species. The intensity of the broad XRD reflection increased as the temperature and reaction time increased. It is possible that changes in the temperature and times of the reduction could be used to modify the CuAu nanoparticles produced. On oxidation, the alloy reflections disappeared and the final material contained crystalline gold. A copper (II) oxide reflection was also observed at the end of the high temperature calcination. XPS showed the presence of Cu^{+} on the surface of the catalyst. This has been observed before in Cu-based oxidation catalysis,[18] where a copper-ceria catalyst was found to contain Cu^{+} after contact with CO for thirty minutes.

Other preparation methods were also investigated to try and determine their structure and find out if the method of making a catalyst changed its structure. A sequential method for making $CuAu/SiO_2$ catalysts was created, where copper was deposited onto the support by high

dispersion, followed by gold deposited onto the support by deposition precipitation. XRD analysis was carried out on this sample and the fresh catalyst was amorphous, whereas the catalyst calcined in air had reflections for metallic gold. SEM images showed dispersed metal particles on the support. However, when the Au was deposited on the support by impregnation instead of deposition precipitation, larger ensembles of Au were apparent and more agglomeration of particles occurred.

TEM analysis for the HDC Cu + Au DP catalyst revealed alloy formation, as well as clusters on the silica support. Some pure copper patches were found in the silica support. Moreover, the CuAu particle size distribution was bimodal because the majority of the particles were small, but some particles were several times larger. TEM analysis of the HDC Cu + Au impregnation catalyst showed some pure copper patches. Wormlike big CuAu particles were common in addition to small alloy particles. This characterization technique also illustrated that, when gold was deposited by deposition precipitation instead of impregnation, smaller particles were detected (9 nm).

The XRD analysis for the Au/SiO_2 sol immobilisation catalyst was amorphous and showed no gold reflections. SEM analysis showed regions of Au on the support but the structure was unclear. The $AuCu/SiO_2$ catalyst, made by this method, displayed highly dispersed metal particles from the SEM images.

Sodium borohydride was used as an alternative to hydrogen for the reduction process and $CuAu/SiO_2$ catalysts was thermally treated with this reducing agent. UV-Visible spectroscopy showed that that there was a strong interaction between the gold and copper as the plasmon peak shifted, as the copper-gold ratio changed. The TEM analysis showed larger particles than those prepared by sequential HDC and either DP or impregnation methods. This technique also showed alloy formation but some particles illustrated Au concentration variation. Particle clusters could be seen occasionally on the surface of silica particles. From

the SEM images, large micron sized clusters were apparent, as well as some smaller dispersed particles. There was a difference observed in the XRD pattern for the catalysts reduced in $NaBH_4$, rather than H_2. Unlike the hydrogen reduced samples, no alloy species were detected and only metallic gold reflections were observed.

3.12 Conclusions

Monometallic and bimetallic copper and gold catalysts have been characterised by several techniques to determine their structure. This characterisation study has contributed to understanding relationships between the preparation method, reduction treatment or copper precursor and the nature of the supported catalyst. Analysis of the catalysts has shown the presence of a CuAu alloy phase as a result of a reduction step (315 ^oC for 2 h in H_2/Ar). De-alloying was observed when the catalyst was calcined at higher temperatures in air (676 ^oC for 15 h). Generally, catalysts that were directly calcined in air formed large ensembles on the support, whereas a reduction procedure still showed the presence of clusters; yet there were more highly dispersed particles on the support.

Other preparation methods were also carried out, such as sequential procedures, which involved the deposition of copper onto the support by high dispersion, followed by gold deposited onto the support by either deposition precipitation or impregnation. Copper-gold alloy particles were present in these catalysts and the preparation method of the gold seemed to suggest an effect on the structure of the catalyst. When the gold was deposited by deposition precipitation, smaller metal particles were observed than when impregnation was chosen.

References

1. H. Sinfelt and R.J. Baron, *US Pat* 3989674 (1976).

2. S. Kameoka and A.P. Tsai, *Catalysis Letters*, 121 (2008) 337.

3. R.J. Chimentao, F. Medina, J.L.G. Fierro, J. Llorca, J.E. Sueiras and Y. Cesteros, *Journal of Molecular Catalysis A: Chemical*, 274 (2007) 159.

4. H. Yang, F. Chang and L. S. Roselin, *Journal of Molecular Catalysis A: Chemical*, 276 (2007) 184.

5. X. Fang, S. Yao, Z. Qing and F. Li, *Applied Catalysis A*, 161 (1997) 129.

6. H. Lian, M. Jia, W. Pian , W. Zhang and Z. Jiang, *Chemical Research in Chinese University*, 22 (2006) 99.

7. F. Porta, L. Prati, M. Rossi, S. Coluccia and G. Martra, *Catalysis Today*, 61 (2000) 165.

8. X. Liu, A. Wang, X. Wang, C.Y. Mou and T. Zhang, *Chemistry Communications*, (2008) 3187.

9. R.E. Schaak, A.K. Sra, B.M. Leonard, R.E. Cable, J.C. Bauer, Y.F. Han, J. Means, W. Teizer, Y. Vasquez and E.S. Funck, *Journal of American Chemical Society*, 127 (2005) 3506.

10. G.N. Glavee, K.J. Klabunde, C.M. Sorensen and G.C. Hadjipanayis, *Langmuir*, 10 (1994) 4726.

11. J. Llorca, M. Dominguez, C. Ledesma, R.J. Chimentao, F. Medina, J. Sueiras, I. Angurell, M. Seco and O. Rossell, *Journal of Catalysis*, 258 (2008) 187.

12. R.J. Chimentao, F. Medina, J.L.G. Fierro, J. Llorca, J.E. Sueiras, Y. Cesteros and P. Salagre, *Journal of Molecular Catalysis A: Chemical*, 274 (2007) 159.

13. S. Kameoka and A.P. Tsai, *Catalysis Today*, 132 (2008) 88.

14. (a) Dutch Patent Application 6411608 (1964). (b) French Patent 1509768 (1967). (c) S.Wang, B. Shen and Q. Song, *Catalysis Letters*, 134 (2010) 102.

15. G.-W. Zhou, J.A. Eastman, R.C. Birtcher, P.M. Baldo, J.E. Pearson, L.J. Thompson, L. Wang and J.C. Yang, *Journal of Applied Physics*, 101 (2007) 033521.

16. T.A. Nijhuis, B.J. Huizinga, M. Makkee and J.A. Moulijn, *Industrial and Engineering Chemistry Research*, 38 (1999) 884.

17. K.Koga and D.Zubia, *Journal of Physical Chemistry C*, 112 (2008) 2079.

18. D.Gamarra, G.Munuera, A.B. Hungria, M. Fernandez-Garcia, J.C. Conesa, P.A. Midgely, X.Q.Wang, J.C. Hanson, J.A Rodriguez and A. Martinez-Arias, *Journal of Physical Chemistry C*, 11 (2007) 11026.

Chapter 4: Propene Oxidation

4.1 Introduction

Propene epoxidation is one of the most sought after goals in industrial chemistry. This reaction produces propene oxide, generating 7 million tons per year worldwide and is used in the production of polyethers and glycols. There are two current industrial processes already used:

1. Chlorohydrin process [1]
2. Hydroperoxide process [1]

The disadvantages of these reactions are that they are not environmentally favourable, as their by-products are harmful. Therefore, it would be highly desirable to find a catalyst that could produce propene oxide, using direct epoxidation with oxygen that forms environmentally friendly by-products. Silver catalysts have previously been used for epoxidation reactions.[1-3] However, Haruta *et al* [4] discovered that Au could be active for propene epoxidation. Lambert and co workers have also shown that copper can be an effective catalyst for this reaction.[5] Since gold is expensive, it would be beneficial to study its activity when alloyed with copper, as a possible catalyst, to achieve selective oxidation of propene.

4.2. Limitations of experiments and precision of data

Duplicate experiments were not performed in this study, due to time constraints. Therefore, the accuracy of the data collected in the absence and presence of hydrogen did have limitations. Future tests on the catalysts, using different feed ratios and compositions would be beneficial to get a better understanding of the results. Ideally, carbon balances should have been taken after every catalytic data set but, due to the time constraints carbon balances were only taken at certain times throughout reactor use.

Although repeat experiments were not carried out, the analysis each temperature point, during the propene tests, was carried out three times to give an average reading. The error for most of the catalysts was in the range ± 1-6% and therefore the results obtained are reasonably consistent and unless otherwise stated, the product distribution and conversions observed can be taken as fairly reliable for a single experiment. Although it must be noted, that repeat tests would have given more precise results and single experiments mean it is difficult to be certain how reproducible the results are.

4.3 Reaction products

There are several reaction products that can be formed from reactions using propene as a starting point (Figure 4.2); the main route of interest is epoxidation to produce propene oxide, which is one of the most challenging chemical reactions. The reason it is a difficult reaction is because of the allylic H atoms, which are easily removed, favouring combustion rather than selective oxidation. Propene oxide (CH_3-$CHCH_2$-O) was made as a result of activation of the carbon-carbon bond. Acrolein (CH_2=CH-CHO) was formed by the cleavage of the C-H bond. Complete combustion formed CO_2 and H_2O and a hydrogenation reaction formed propane (CH_3-CH_2-CH_3). Ethanal (CH_3-CHO) was a product produced by certain catalysts in this study and was produced from a C-C bond and from other possible side reactions.

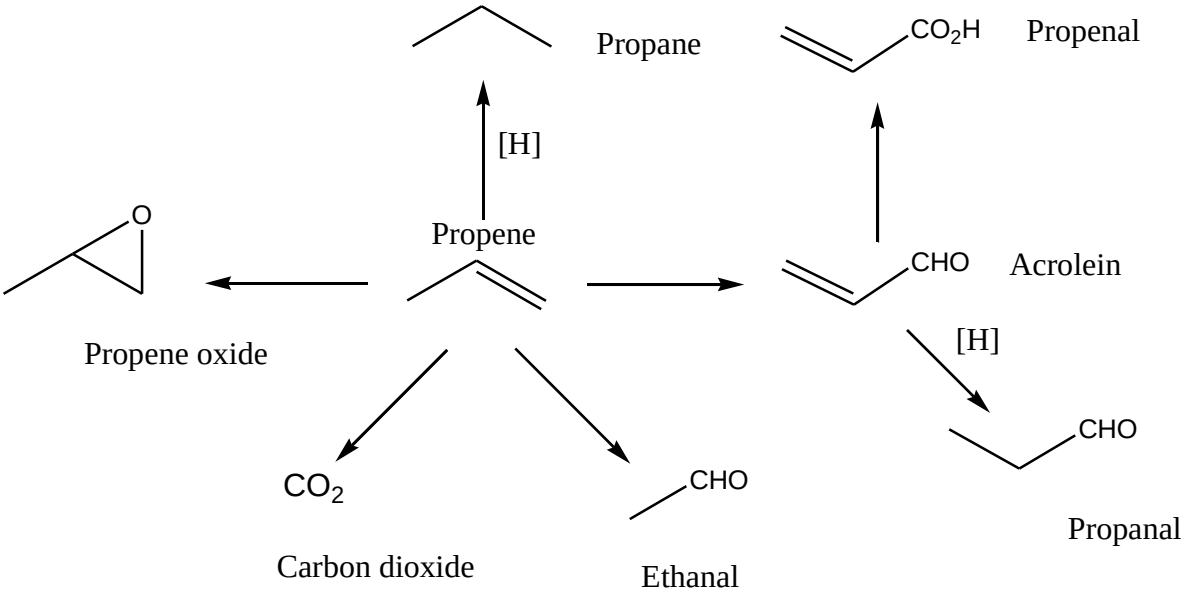

Figure 4.1 Reaction scheme of possible products from the oxidation of propene.

[H] represents hydrogenation reactions with H_2-O_2

4.4 Results

4.4.1 Effect of different catalyst preparation methods on propene oxidation

In this section, monometallic Cu/SiO_2 and Au/SiO_2 catalysts have been made mainly by impregnation but also by other routes such as precipitation and high dispersion. Their activity for propene oxidation was studied to determine if the catalytic activity was dependent on the preparation method. Sequential methods to form $CuAu/SiO_2$ catalysts involving high dispersion and either deposition precipitation (DP) or incipient wetness impregnation (IW) were also tested for propene oxidation. Sol immobilisation was also employed to form a $CuAu/SiO_2$ catalyst, and its activity is discussed in this section.

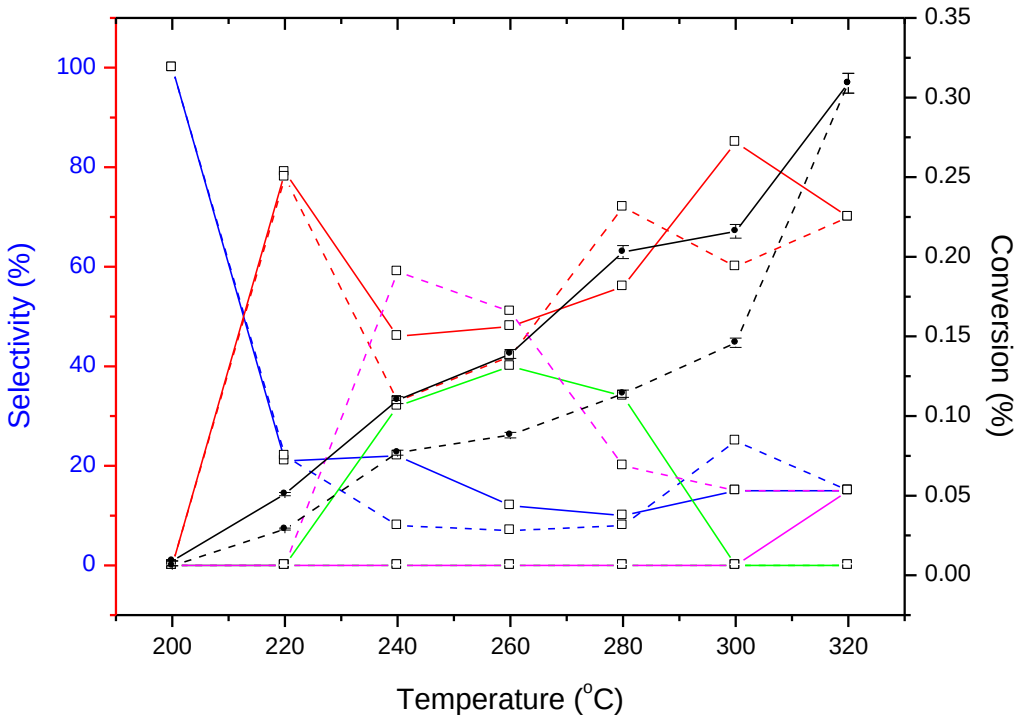

Figure 4.2 Copper nitrate /SiO_2 by impregnation and directly calcined (C97802D).

Propene oxidation with H_2: ____ Acrolein T $_{increase}$ - - - - Acrolein T$_{decrease}$ ____CO_2 T $_{increase}$ - - - - CO_2 T $_{decrease}$ ____ Propene oxide T $_{increase}$ - - - - Propene Oxide T $_{decrease}$ ____ Ethanal T$_{increase}$ - - - - Ethanal T$_{decrease}$ ____Conversion T $_{increase}$ - - - - Conversion T $_{decrease}$

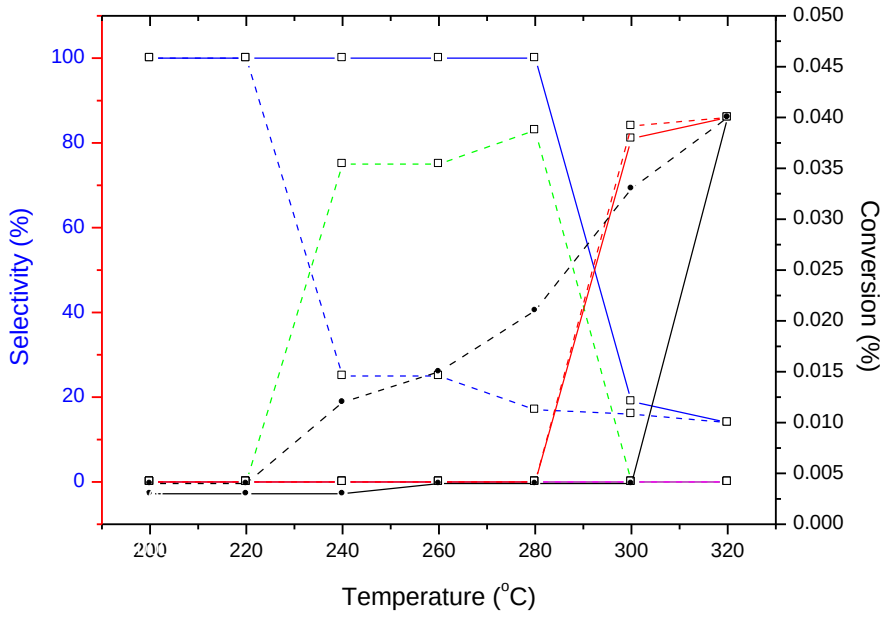

Figure 4.3 Copper nitrate /SiO_2 by impregnation directly calcined (C97802D). Propene oxidation without H_2 ____Acrolein T $_{increase}$ - - - - Acrolein T$_{decrease}$ ____CO_2 T $_{increase}$ - - - - CO_2 T $_{decrease}$ ____ Propene oxide T $_{increase}$ - - - - Propene Oxide T $_{decrease}$ ____ Ethanal T$_{increase}$ - - - - Ethanal T$_{decrease}$ ____Conversion T $_{increase}$ - - - - Conversion T $_{decrease}$

Impregnation was the standard preparation technique used for most of the propene oxidation experiments in this investigation. However, other features such as high dispersion catalysts and methods like deposition precipitation were carried out. Cu/SiO_2 catalysts made by impregnation, using copper nitrate and calcined in air at 400 ^{o}C for 2 h, were tested with (Figure 4.2) and without H_2 addition (Figure 4.3). Upon addition of hydrogen in the reactor feed the conversion was higher (0.32% ± 2% (0.3 – 0.34)) at 320 ^{o}C. However, due to the different feed ratios used for the presence of hydrogen experiments, there are limitations when comparing the results with and without hydrogen in the reactor feed throughout this study, as the feed ratios were not the same. It would be beneficial if experiments were done in the absence of hydrogen with the same feed ratios to identify if there was a real effect of

hydrogen on the catalysts performance. However, I am reasonable confident with the experiments carried out in the absence of hydrogen even with the low conversions i.e. 0.04% as there was little difference between the data collected for the 3 runs at each temperature. As the temperature of the experiment increased so did the conversion which was expected. The catalyst was selective to both acrolein and ethanal at higher temperatures in the presence of hydrogen. Propene oxide was also observed as the temperature increased between 240 and 280 ^{o}C, reaching about 40% selectivity at 260 ^{o}C. Without H_2, acrolein is only detected at 320 ^{o}C and the main products were CO_2, as the temperature increased and propene oxide, as the temperature decreased during the hysteresis. At each temperature three runs were taken and the error between these was low (±2%).

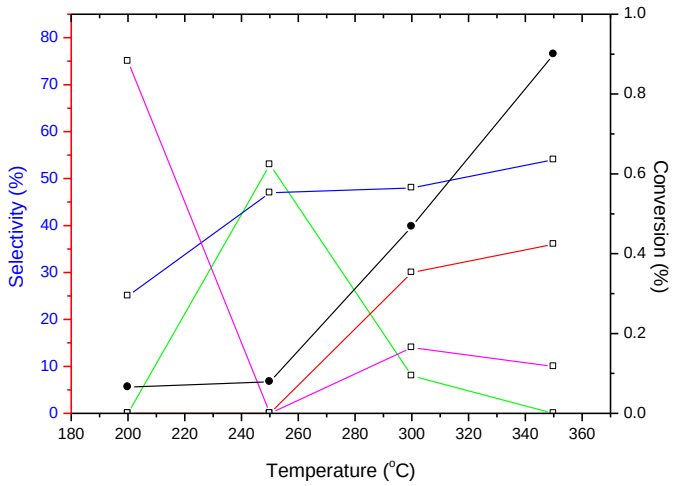

Figure 4.4 Cu/SiO_2 with copper chloride by impregnation with H_2 (C97802B)
Acrolein T $_{increase}$ CO_2 T $_{increase}$ Propene oxide T $_{increase}$ T $_{decrease}$
Ethanal T$_{increase}$ Conversion T $_{increase}$

A comparative Cu/SiO_2 catalyst was also studied which used copper chloride for the impregnation. (Figure 4.4) The reaction was carried out with H_2 and showed a conversion of 0.9% ± 1.4% which was higher than with a copper nitrate precursor, although no hysteresis experiment was done. At lower temperatures ethanal and propene oxide were formed, whilst at higher temperatures acrolein was also detected. For the copper nitrate catalyst, as the

temperature was increased acrolein was only detected at 300 ^{o}C (80%). As the temperature decreased during the hysteresis experiment propene oxide became the major product between 240 -280 ^{o}C (> 70%). Therefore, the choice of copper precursor used to make the catalyst could play a role in determining the product selectivity and conversion of propene.

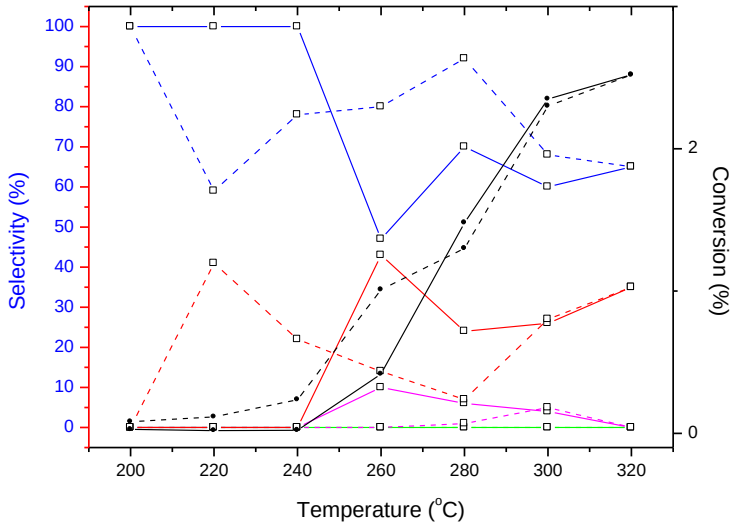

Figure 4.5 Copper nitrate /SiO_2 by Sinfelt treatment (C978/101E) Propene oxidation with H_2

Acrolein T $_{increase}$ Acrolein T$_{decrease}$ CO_2 T $_{increase}$ CO_2 T $_{decrease}$ Propene oxide T $_{increase}$ Propene Oxide T $_{decrease}$ Ethanal T$_{increase}$ Ethanal T$_{decrease}$ Conversion T $_{increase}$ Conversion T $_{decrease}$

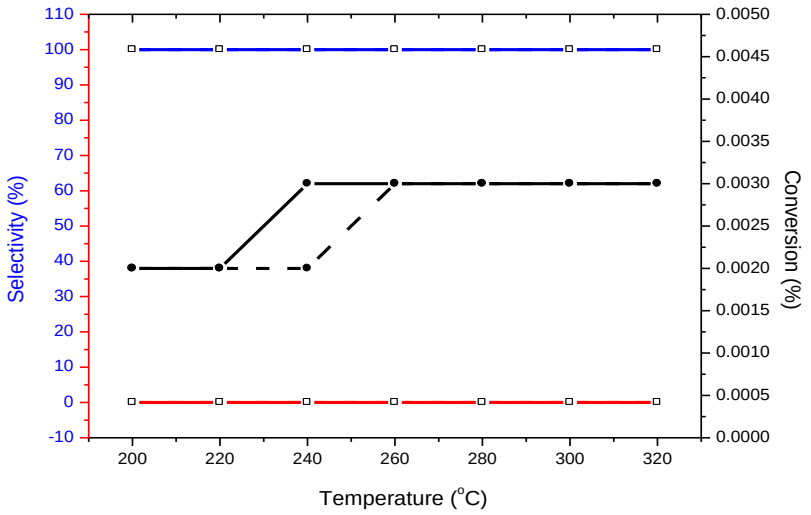

Figure 4.6 Copper nitrate /SiO_2 by Sinfelt treatment (C978/101E) Propene oxidation without H_2 Acrolein $T_{increase}$ Acrolein $T_{decrease}$ CO_2 $T_{increase}$ CO_2 $T_{decrease}$ Conversion $T_{increase}$ Conversion $T_{decrease}$

If a Cu/SiO_2 catalyst underwent a Sinfelt treatment (rather than direct calcination), which involved reduction in 5% H_2/Ar at 315 ^oC followed by a high temperature calcination of 676 ^oC for 15 h, the conversion and product distribution were different. Without H_2 (Figure 4.6) in the reactor, the conversion was lower than in the presence of H_2, which was seen with the other Cu/SiO_2 catalysts and CO_2 was virtually the only product observed across the temperature range. But, when H_2 was added (Figure 4.6), the catalyst became very active to propene oxidation (2% ± 1.8% conversion) and showed high selectivity towards acrolein. At 260 ^oC both ethanal and acrolein were observed, with selectivities of 8% ± 2.5% and 43% ± 2.5% respectively. This catalyst showed little hysteresis with temperature. When the same catalyst was tested without H_2 (Figure 4.6), selectivity was 100% towards CO_2 and was inactive with a conversion of 0.003% ± 3%.

The Sinfelt treatment does appear to have an effect on the catalyst's performance and this is similar to what was observed for the bimetallic Cu_3Au/SiO_2 catalysts, which are discussed

later in this chapter. For the directly calcined Cu_3Au/SiO_2 samples, with and without H_2, acrolein and propene oxide are both detected. However, when a Sinfelt treatment is used only acrolein is the major product with little hysteresis.

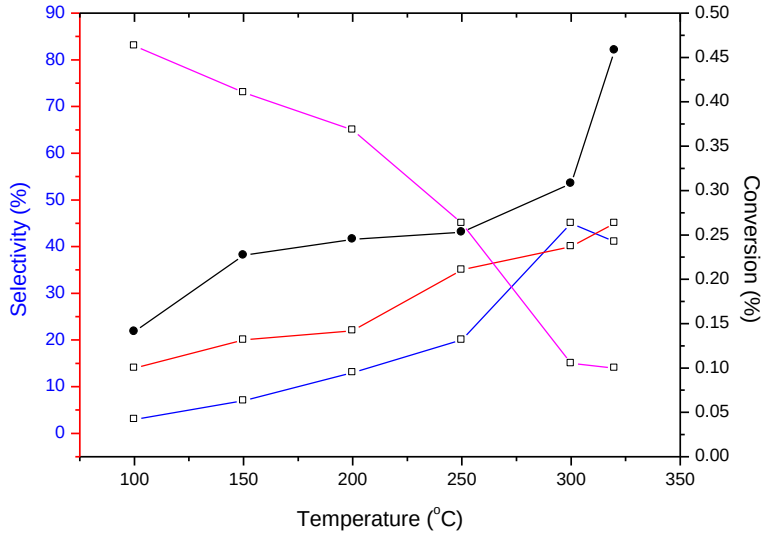

Figure 4.7 Copper nitrate /SiO_2 made by precipitation with (C97828). Propene oxidation with H_2

Acrolein T $_{increase}$ CO_2 T $_{increase}$ Propene oxide T $_{increase}$ T $_{decrease}$
Ethanal T$_{increase}$ Conversion T $_{increase}$

Precipitation was another preparation method used to form a Cu/SiO_2 catalyst, and this technique involved the use of copper nitrate and NaOH. For the precipitation catalyst, only propene oxidation with H_2 was tested for this method and no hysteresis data was collected. A propene conversion of 0.45% ± 1.5% observed (Figure 4.7) for this sample and at lower temperatures ethanal formation was favoured, whereas at higher temperatures acrolein and CO_2 were the major products.

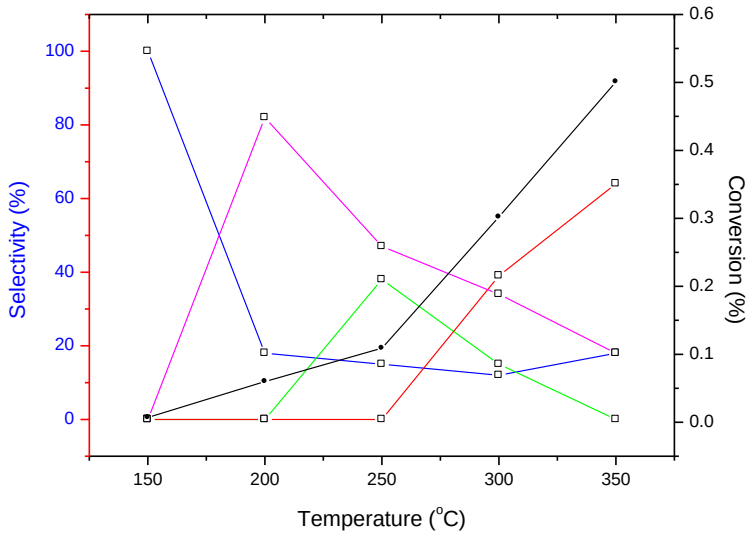

Figure 4.8 Cu/SiO_2 high dispersion route (CF128). Propene oxidation with H_2
Acrolein $T_{increase}$ CO_2 $T_{increase}$ Propene oxide $T_{increase}$
Ethanal $T_{increase}$ Conversion $T_{increase}$

When the Cu/SiO_2 catalyst had high dispersion (CF128) the product selectivity was altered (Figure 4.8). The catalyst was formed by using ammonium carbonate, copper hydroxycarbonate and water. The mixture was distilled and heated to obtain the catalyst. In the presence of hydrogen, the catalyst prepared this way gave a good activity with a conversion of 0.5% ± 3% at 350 ^oC and a selectivity towards acrolein (~65%) and ethanal (~20%). Propene oxide was detected with a selectivity of 40% at a temperature of 250 ^oC.

There was a significant change in propene conversion and selectivity to different products associated with the type of preparation method employed. The most active Cu/SiO_2 catalyst was made by impregnation followed by a Sinfelt treatment obtaining a 2% propene conversion although there was no propene oxide formation and selectivity to acrolein and ethanol was ~30% and ~7% respectively. Hydrogen addition into the reactor feed was crucial to obtain an active catalyst. Other methods like precipitation and high dispersion route were not as simple to carry out but they did give catalysts with a moderate selectivity.

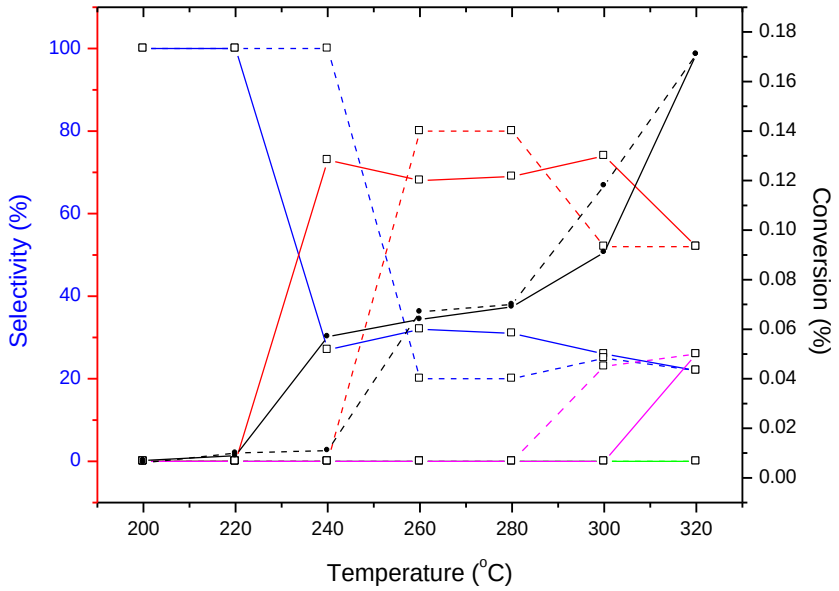

Figure 4.9 Au/SiO_2 by impregnation and direct calcination (C97809). Propene oxidation with H_2

Acrolein T $_{increase}$ Acrolein T$_{decrease}$ CO_2 T $_{increase}$ CO_2 T $_{decrease}$

Propene oxide T $_{increase}$ Propene Oxide T $_{decrease}$ Ethanal T$_{increase}$

Ethanal T$_{decrease}$ Conversion T $_{increase}$ Conversion T $_{decrease}$

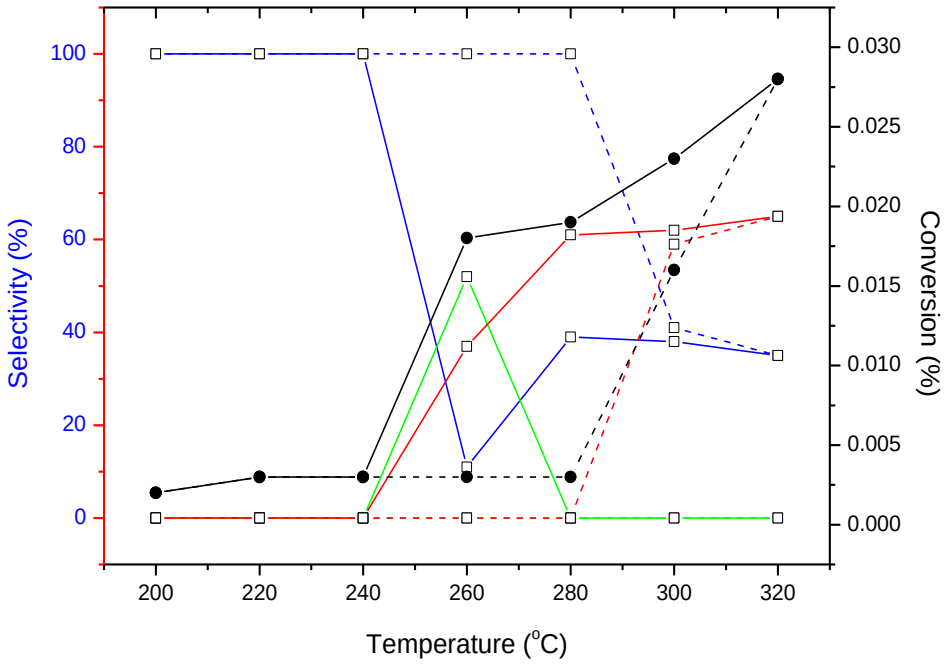

Figure 4.10 Au/SiO_2 by impregnation and direct calcination (C97809). Propene oxidation without H_2 addition. Acrolein $T_{increase}$ Acrolein $T_{decrease}$ CO_2 $T_{increase}$ CO_2 $T_{decrease}$ Propene oxide $T_{increase}$ Propene Oxide $T_{decrease}$ Ethanal $T_{increase}$ Ethanal $T_{decrease}$ Conversion $T_{increase}$ Conversion $T_{decrease}$

Monometallic Au/SiO_2 catalysts have been made mainly by impregnation as it was a simple technique, but other methods like deposition precipitation have also been utilized. An Au/SiO_2 catalyst, prepared by impregnation and followed by direct calcination in air at 400 ^oC for 2h, has been tested for propene oxidation (Figure 4.9 and 4.10). In the presence of H_2, a propene conversion of ~0.17% ± 3% (0.164 – 0.175) at 320 ^oC could be achieved. At this temperature, the catalyst was selective towards ethanal (~27%) and acrolein (50%). No propene oxide was formed and acrolein formation was quite stable, as the temperature increased. When there was no addition of hydrogen, the propene conversion was greatly diminished to ~ 0.024% ± 2% at 320 ^oC. However, propene oxide was detected at 260 ^oC at a

selectivity of 52% with a conversion of 0.019% ± 21%. As the error is larger for this result this experiment should be repeated for this catalyst at 260 ^{o}C.

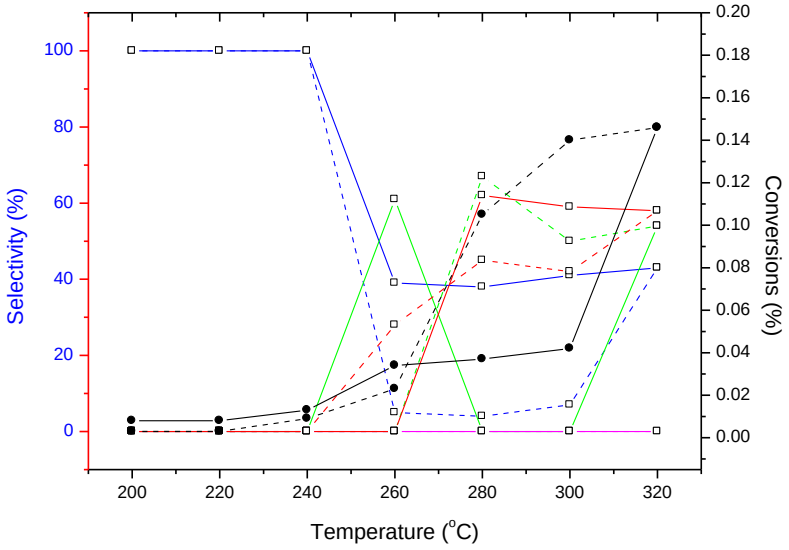

Figure 4.11 Au/SiO_2 by Deposition precipitation (C97836). Propene oxidation with H_2 addition.

Acrolein T $_{increase}$ Acrolein T$_{decrease}$ CO_2 T $_{increase}$ CO_2 T $_{decrease}$
Propene oxide T $_{increase}$ Propene Oxide T $_{decrease}$ Ethanal T$_{increase}$
Ethanal T$_{decrease}$ Conversion T $_{increase}$ Conversion T $_{decrease}$

If the preparation route was changed from impregnation to deposition precipitation (Figure 4.11) and an experiment run for propene oxidation in the presence of H_2, the propene conversion did not appear to alter much. However, propene oxide was formed at 260 ^{o}C with a selectivity of 60%. At 320 ^{o}C propene oxide had a selectivity of 57% but this result could be an anomaly due to a large error (± 17%) between the three readings at this temperature. Therefore, the presence of propene oxide at 320^{o}C may not be accurate and this experiment should be repeated. Acrolein formation was stable around 65% between 260 ^{o}C and 320 ^{o}C. No ethanal was formed using this catalyst.

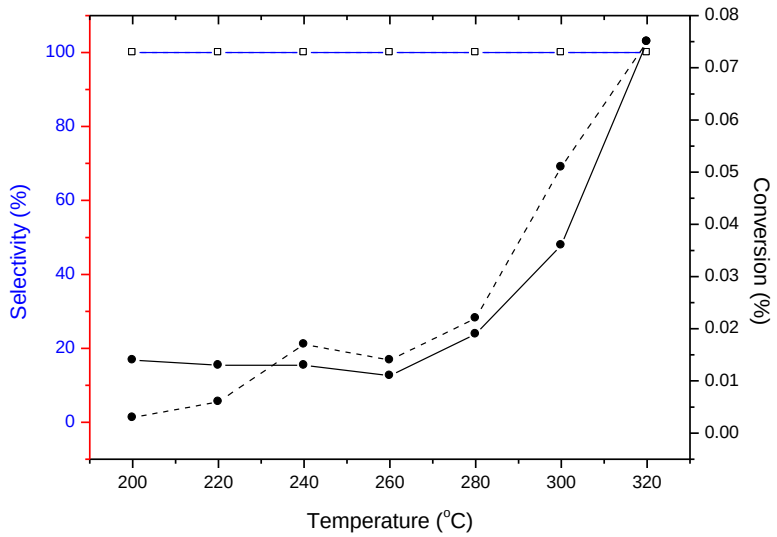

Figure 4.12 Au/SiO_2 Sinfelt (C978/101D). Propene oxidation with H_2

CO_2 T $_{increase}$ CO_2 T $_{decrease}$

Conversion T $_{increase}$ Conversion T $_{decrease}$

Unlike the Cu/SiO_2 catalyst, which was prepared by impregnation, followed by the Sinfelt treatment, there was little activity when this technique was applied to the Au/SiO_2 monometallic sample (Figure 4.12), and carbon dioxide was the only product formed.

Preparation techniques that incorporated two different methods were attempted to determine whether this route could lead to an active $AuCu/SiO_2$ catalyst for propene oxidation. These combined methods involved copper deposited onto the SiO_2 support by a high dispersion route (HDC) (which involved using copper hydroxycarbonate and ammonium carbonate and heating to 90-95^{o}C for 3hours), as this method previously showed good propene conversion in the oxidation reactions. Followed by a choice of gold being deposited by either impregnation or deposition precipitation.

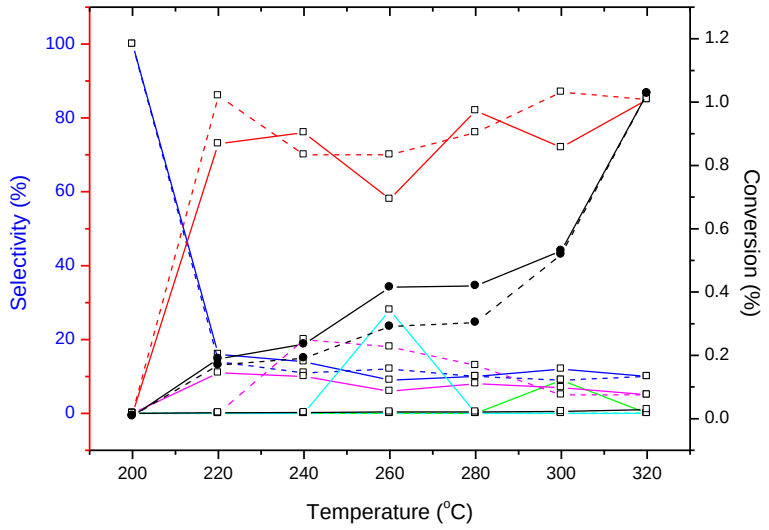

Figure 4.13 $CuAu/SiO_2$ HDC Cu + Au DP fresh catalyst (C978/87). Propene oxidation with H_2 addition. ____ Acrolein T $_{increase}$ - - - - Acrolein T$_{decrease}$ ____CO_2 T $_{increase}$ - - - - CO_2 T $_{decrease}$ ____ Propene oxide T $_{increase}$ - - - - Propene Oxide T $_{decrease}$ ____ Ethanal T$_{increase}$ - - - - - Ethanal T$_{decrease}$ ____Conversion T $_{increase}$ ---- Conversion T $_{decrease}$ ------ Acetone T $_{decrease}$ ____Acetone T $_{increase}$

The fresh $CuAu/SiO_2$ catalyst made by high dispersion (HDC) for Cu and deposition precipitation (DP) for Au was tested for propene oxidation in the presence of H_2 (Figure 4.13). No direct calcination or reduction was applied to this catalyst. A propene conversion of 1% ± 2% was observed at 320 ^{o}C with acrolein (80%) and a small amount of ethanal (6%) being detected at this temperature. Propene oxide was formed only at 300 ^{o}C with a selectivity of ~10%. Unlike any of the other propene oxidation experiments, acetone was another product observed in this reaction. The appearance of this product at 260 ^{o}C can be justified since the error was only ±3%.

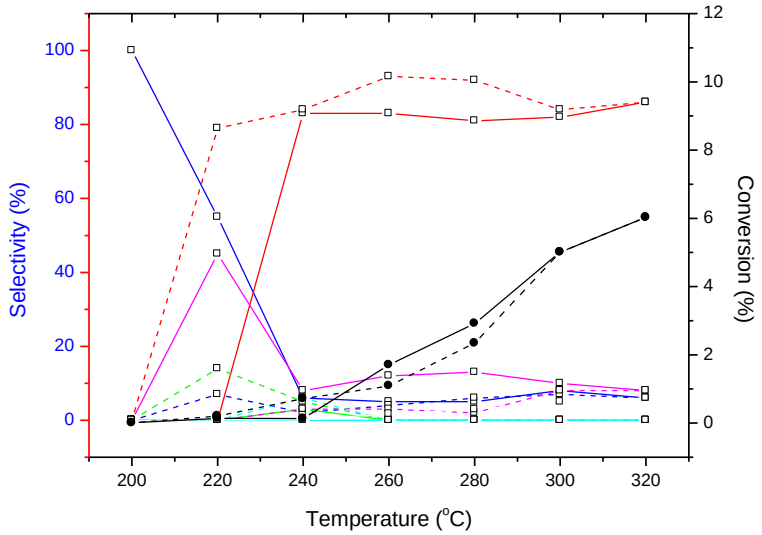

Figure 4.14 $CuAu/SiO_2$ HDC Cu + Au DP followed by a Sinfelt treatment . Propene oxidation with addition of H_2 ____ Acrolein T $_{increase}$ ---- Acrolein T$_{decrease}$ ____CO_2 T $_{increase}$ ---- CO_2 T $_{decrease}$ ____Ethanal T $_{increase}$ ---- Ethanal T $_{decrease}$ ____ Propene oxide T $_{increase}$ ---- Propene Oxide T $_{decrease}$ ____ Acetone T $_{increase}$ ---- Acetone T $_{decrease}$ ____Conversion T $_{increase}$ ---- Conversion T $_{decrease}$

When the $CuAu/SiO_2$ catalyst was treated by the Sinfelt method (Figure 4.14) its propene conversion went up dramatically to over 6% ± 1% which would be considered an active catalyst for this reaction. The hysteresis experiment showed that the catalyst was stable as the temperature increased and decreased, with the acrolein selectivity remaining between 80 to 90% between 220 ^{o}C and 320 ^{o}C. At higher temperatures, the catalyst was only selective towards acrolein but at temperatures lower than 220 ^{o}C it was selective towards propene oxide (14% ± 3%) and ethanal (45% ± 2%) which seemed to be a true result from the small error.

If this catalyst was directly calcined in air (Figure 4.15) rather than the Sinfelt treatment, the activity of the catalyst did not improved, compared to the freshly untreated catalyst. A propene conversion of 0.8% ± 2% was achieved. At higher temperatures, the catalyst was

selective to acrolein (80%) and propene oxide was detected at 300 ^{o}C with a selectivity of about 10%.

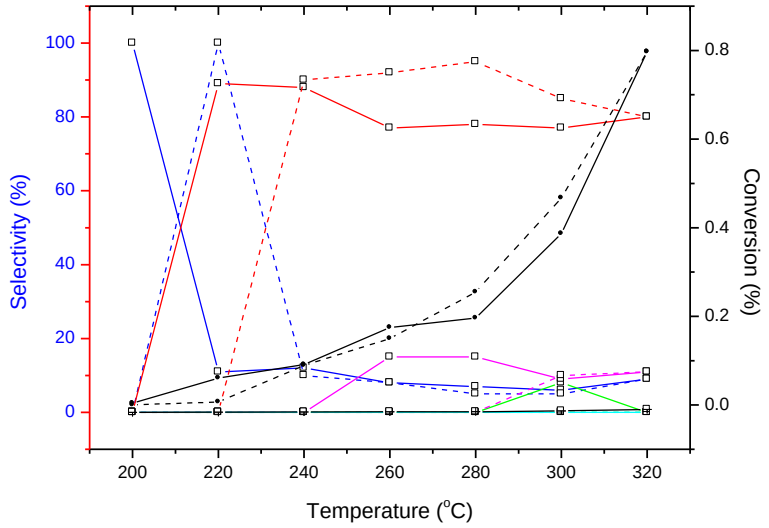

Figure 4.15 CuAu/SiO_2 HDC Cu + Au Dp calcined. Propene oxidation with H_2 addition.

Acrolein T $_{increase}$ Acrolein T$_{decrease}$ CO_2 T $_{increase}$ CO_2 T $_{decrease}$ Ethanal T $_{increase}$ Ethanal T $_{decrease}$ Propene oxide T $_{increase}$ Propene Oxide T $_{decrease}$ Conversion T $_{increase}$ Conversion T $_{decrease}$

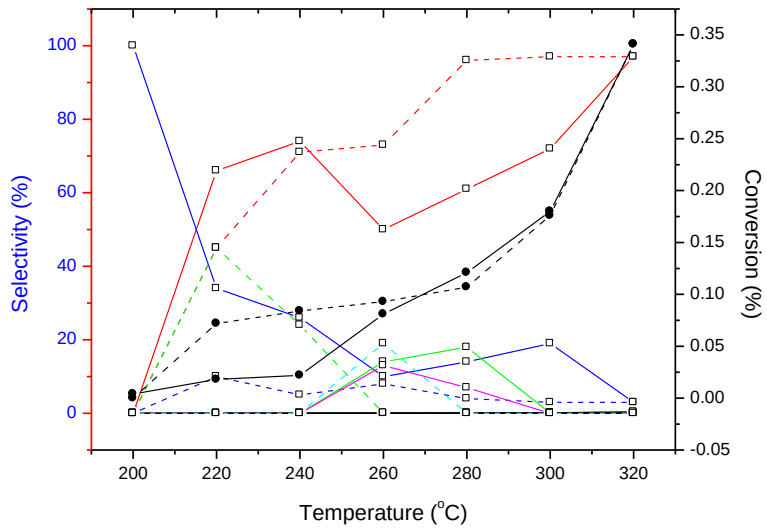

Figure 4.16 HDC Cu + Au Dp calcined. Propene oxidation without H_2 addition.

Acrolein T $_{increase}$ Acrolein T$_{decrease}$ CO_2 T $_{increase}$ CO_2 T $_{decrease}$

Ethanal T $_{increase}$ Ethanal T $_{decrease}$

Propene oxide T $_{increase}$ Propene Oxide T $_{decrease}$

Acetone T $_{increase}$ Acetone T $_{decrease}$ Conversion T $_{increase}$

Conversion T $_{decrease}$

Direct calcination of the HDC Cu and Au DP catalyst for propene oxidation without H_2 (Figure 4.16) was carried out to compare the catalyst activity in the absence of hydrogen. The propene conversion only reached half the value (0.4% ± 3%) at 320 ^{o}C that was produced in the presence of hydrogen. Propene oxide was between 260 ^{o}C and 280 ^{o}C with a selectivity of nearly 20% but the acrolein selectivity at higher temperatures was not as stable as when hydrogen was present.

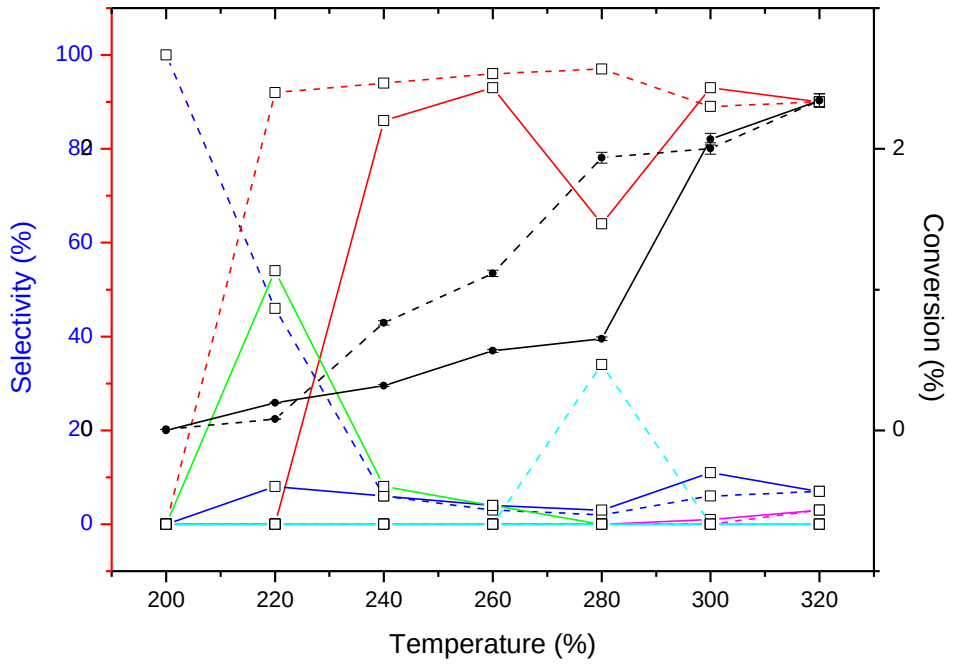

Figure 4.17 $CuAu/SiO_2$ by HDC Cu + Au Dp reduced in H_2. Propene oxidation with H_2 addition. Acrolein T $_{increase}$ Acrolein T$_{decrease}$ CO_2 T $_{increase}$ CO_2 T $_{decrease}$ Ethanal T $_{increase}$ Ethanal T $_{decrease}$ Propene oxide T $_{increase}$ Propene Oxide T $_{decrease}$ Acetone T $_{increase}$ Acetone T $_{decrease}$ Conversion T $_{increase}$ Conversion T $_{decrease}$

An alternative treatment of the $CuAu/SiO_2$ HDC and DP catalyst, being directly calcined or undergoing the Sinfelt treatment, is a direct reduction in H_2 at 400 ^oC for 2h. The $CuAu/SiO_2$ catalyst was reduced in this way and tested for propene oxidation with the addition of H_2 (Figure 4.17). A propene conversion of about 2.3% ± 1% was achieved at 320 ^oC and this catalyst was selective towards mostly acrolein at higher temperatures. At 220 ^oC, propene oxide was formed with a selectivity of 58% and acetone was observed at 280 ^oC (35%). Acetone was observed after each injection into the GC at 280 ^oC with this catalyst, and had an error of ± 2%. Therefore it can be taken as a reliable product at this temperature.

A $CuAu/SiO_2$ catalyst was prepared by the combined method, using high dispersion to deposit the copper. But, instead of deposition precipitation to deposit the gold onto the support, incipient wetness impregnation was employed. The catalyst was directly reduced in H_2 at 400 ^oC for 2h. The activity of this catalyst for propene oxidation was investigated (Figure 4.18) in the presence of H_2. Compared to when the gold was loaded onto the support by a DP method, using impregnation resulted in a lower propene conversion of 0.11% ± 3% at 320 ^oC. Acrolein (80% at 320 ^oC) and CO_2 are the only products that this catalyst was selective towards.

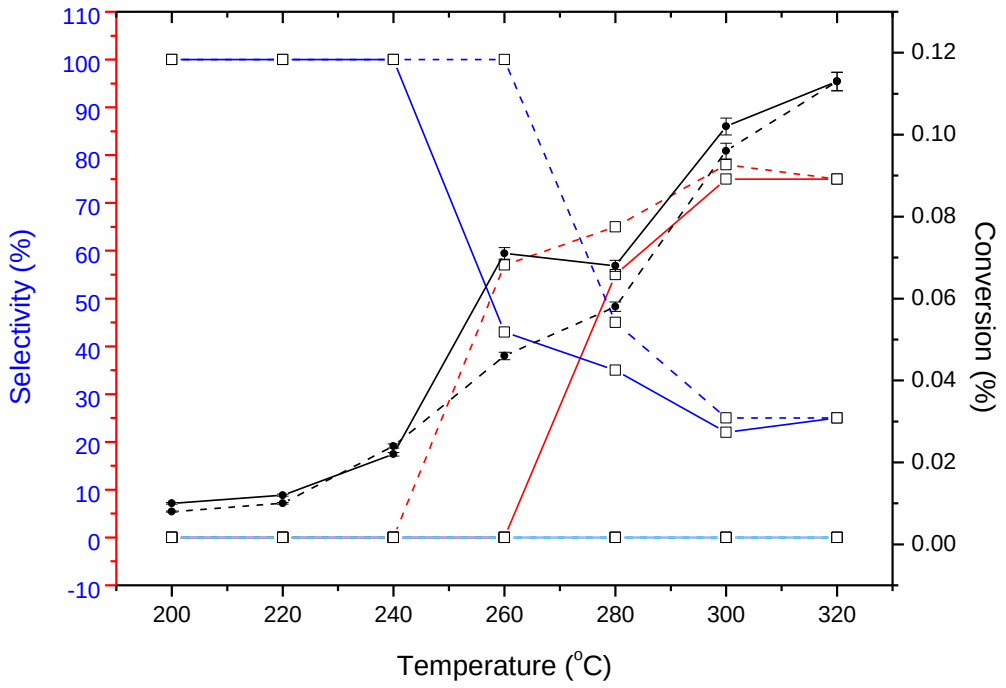

Figure 4.18 $CuAu/SiO_2$ HDC Cu + Au IW (C978/90) reduced in H_2. Propene oxidation with H_2 addition. ____Acrolein $T_{increase}$ - - - - Acrolein $T_{decrease}$ ____CO_2 $T_{increase}$ - - - - CO_2 $T_{decrease}$ ____Conversion $T_{increase}$ ---- Conversion $T_{decrease}$

If the $CuAu/SiO_2$ catalyst, made *via* HDC and incipient wetness impregnation, underwent a Sinfelt treatment (Figure 4.19) instead of a direct reduction in H_2, the propene conversion was increased to 0.27% ± 3% at 320 ^oC. Acrolein was still the major product formed at higher temperatures, but other products, were present; such as propene oxide, which was produced at 280 ^oC (~32%) and ethanal at 300 ^oC (~20%).

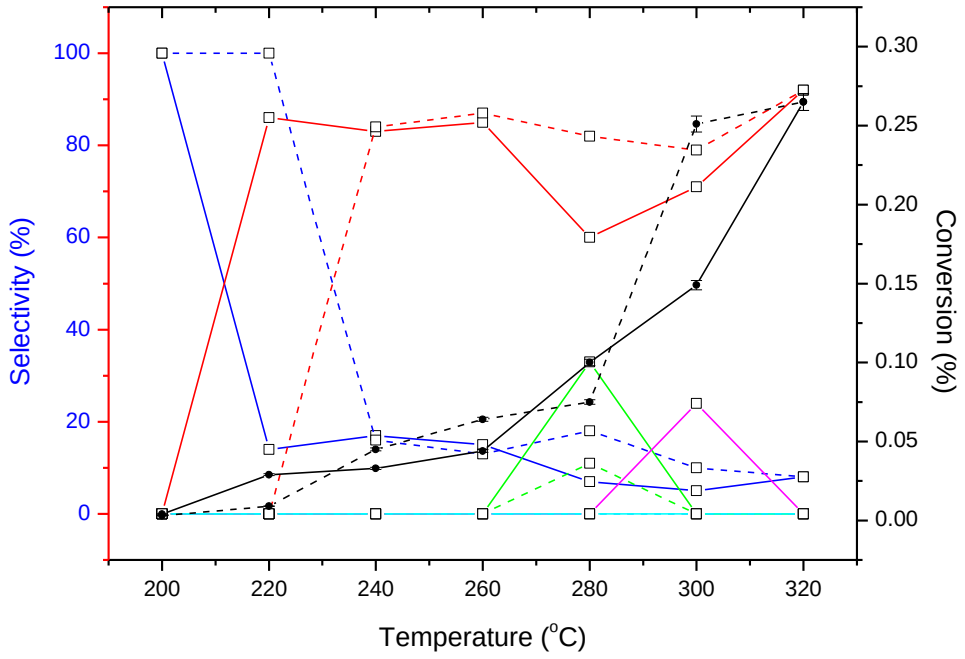

Figure 4.19 $CuAu/SiO_2$ HDC Cu + Au IW (C978/90) Sinfelt treatment. Propene oxidation with H_2 addition. ____Acrolein $T_{increase}$ ---- Acrolein $T_{decrease}$ ____CO_2 $T_{increase}$ ---- CO_2 $T_{decrease}$ ____Ethanal $T_{increase}$ ---- Ethanal $T_{decrease}$ ____ Propene oxide $T_{increase}$ ---- Propene Oxide $T_{decrease}$ ____Conversion $T_{increase}$ ---- Conversion $T_{decrease}$

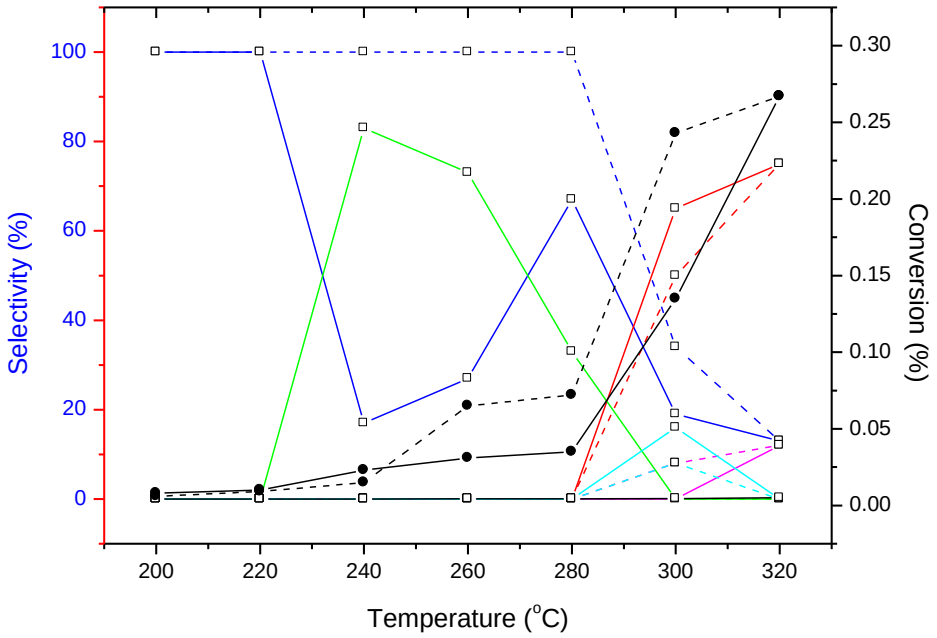

Figure 4.20 $AuCu/SiO_2$ by sol immobilisation fresh catalyst (C978/103) Propene oxidation with H_2 addition. Acrolein T $_{increase}$ Acrolein T$_{decrease}$ CO_2 T $_{increase}$ CO_2 T $_{decrease}$ Ethanal T $_{increase}$ Ethanal T $_{decrease}$ Propene oxide T $_{increase}$ Propene Oxide T $_{decrease}$ Acetone T $_{increase}$ Acetone T $_{decrease}$ Conversion T $_{increase}$ Conversion T $_{decrease}$

A new preparation method chosen was a sol immobilisation technique, which had been reported by other groups to form small metal particles in a narrow size-range.[6] A $AuCu/SiO_2$ catalyst was made by this route and analysed for propene oxidation in the presence of H_2. When the fresh catalyst was tested (Figure 4.20), a propene conversion of 0.27% ± 3% was reached at 320 ^{o}C. Acrolein (79%), ethanal (10%) and CO_2 (11%) were the only products observed at this temperature. Propene oxide was quite selective at lower temperatures between 260 ^{o}C and 280 ^{o}C (70-80%).

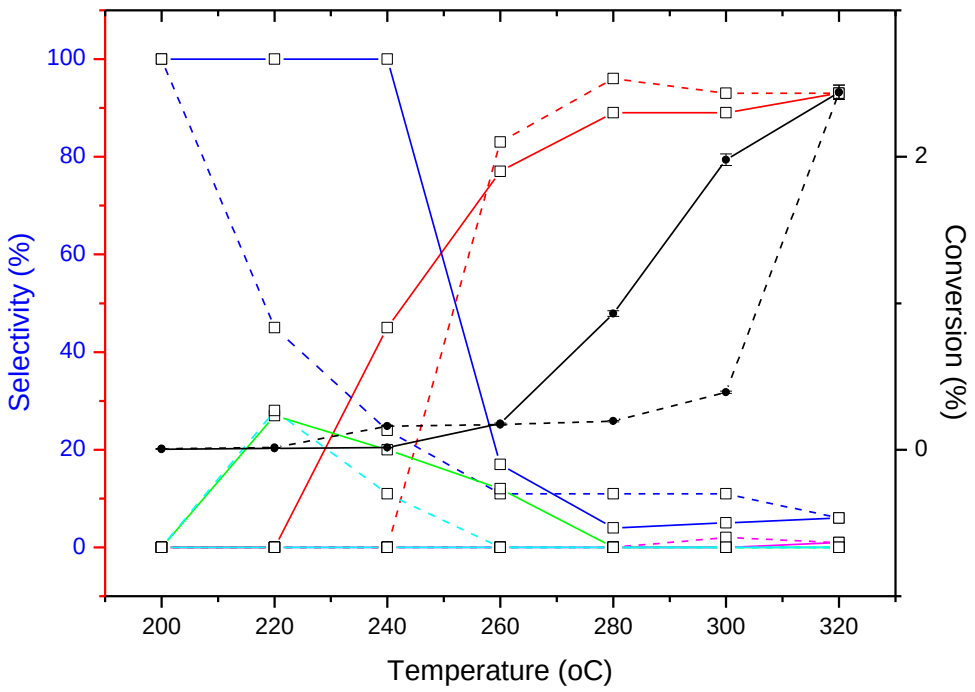

Figure 4.21 $AuCu/SiO_2$ by sol immobilisation (C978/103) calcined. Propene oxidation with H_2 addition. Acrolein $T_{increase}$ Acrolein $T_{decrease}$ CO_2 $T_{increase}$ CO_2 $T_{decrease}$ Ethanal $T_{increase}$ Ethanal $T_{decrease}$ Propene oxide $T_{increase}$ Propene Oxide $T_{decrease}$ Acetone $T_{increase}$ Acetone $T_{decrease}$ Conversion $T_{increase}$ Conversion $T_{decrease}$

The fresh $CuAu/SiO_2$ catalyst made by sol immobilisation method was directly calcined in air at 400 ^oC for 3h and then investigated for propene oxidation in the presence of H_2 (Figure 4.21). The direct calcination improved the propene conversion from 0.27% ± 3% to 2.5% ± 1% at 320 ^oC. At higher temperatures, the catalyst was very selective towards acrolein (80-90%) and was stable during the hysteresis experiment. Acetone was detected at 220 ^oC (29%) and propene oxide was formed between 220 ^oC and 260 ^oC (30% decreasing to 18%) and their presence could be justified as they had an error of ±2% and ± 2.7% respectively.

4.4.2 Effect of different copper precursors

In this section, copper chloride or copper nitrate has been used as the copper precursor to make CuAu, $CuAu_3$ and Cu_3Au, bimetallic catalysts supported on silica. Propene oxidation was investigated for all these catalysts in the presence and in the absence of hydrogen in the reactor feed. The type of copper precursor used as well as the preparation method was studied.

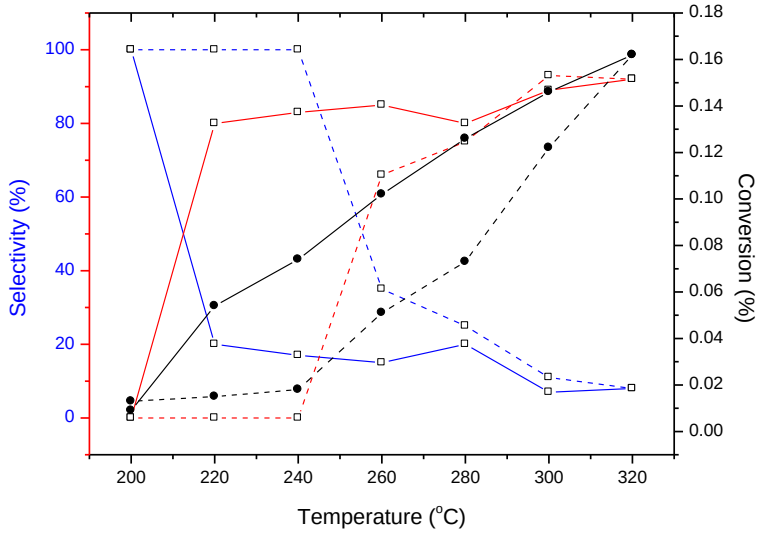

(a)

Figure 4.22 (a) $CuAu/SiO_2$ copper chloride direct calcination (C978/63A) Propene oxidation with H_2 ____Acrolein T $_{increase}$ - - - - Acrolein $T_{decrease}$ ____CO_2 T $_{increase}$ - - - - CO_2 T $_{decrease}$ ____ Propene oxide T $_{increase}$ - - - - Propene Oxide T $_{decrease}$ ____Conversion T $_{increase}$ - - - - Conversion T $_{decrease}$

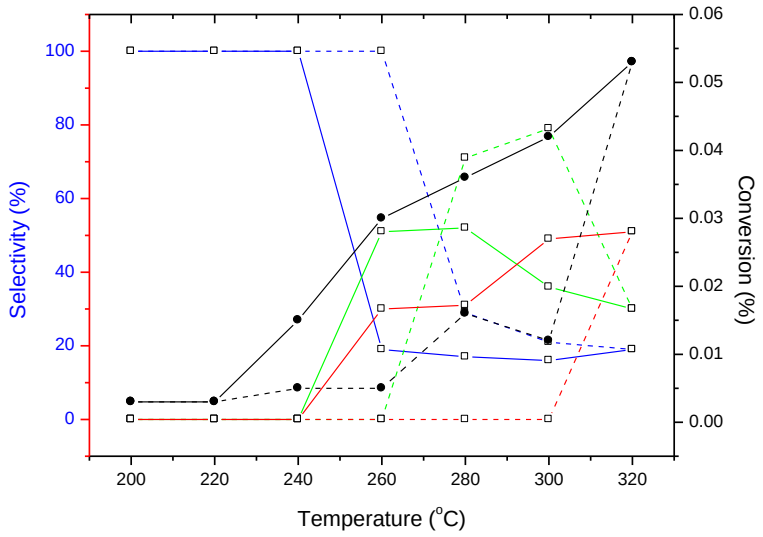

(b)

Figure 4.22 (b) $CuAu/SiO_2$ copper chloride direct calcination (C978/63A) Propene oxidation without H_2 . Acrolein $T_{increase}$ Acrolein $T_{decrease}$ CO_2 $T_{increase}$ CO_2 $T_{decrease}$ Propene oxide $T_{increase}$ Propene Oxide $T_{decrease}$ Conversion $T_{increase}$ Conversion $T_{decrease}$

The most obvious difference between the $CuAu/SiO_2$ catalyst, using copper chloride and directly calcined (Figure 4.22 (a) and 4.22 (b)) for propene oxidation with and without H_2, was that the conversion was greatly improved with the addition of H_2 (0.15% ± 3% at 320 ^oC). The only products formed in the presence of hydrogen were acrolein and CO_2. The selectivity towards acrolein remained quite stable as the temperature increased during the hysteresis (80%). In the absence of hydrogen, propene oxide was the major product but acrolein was still present.

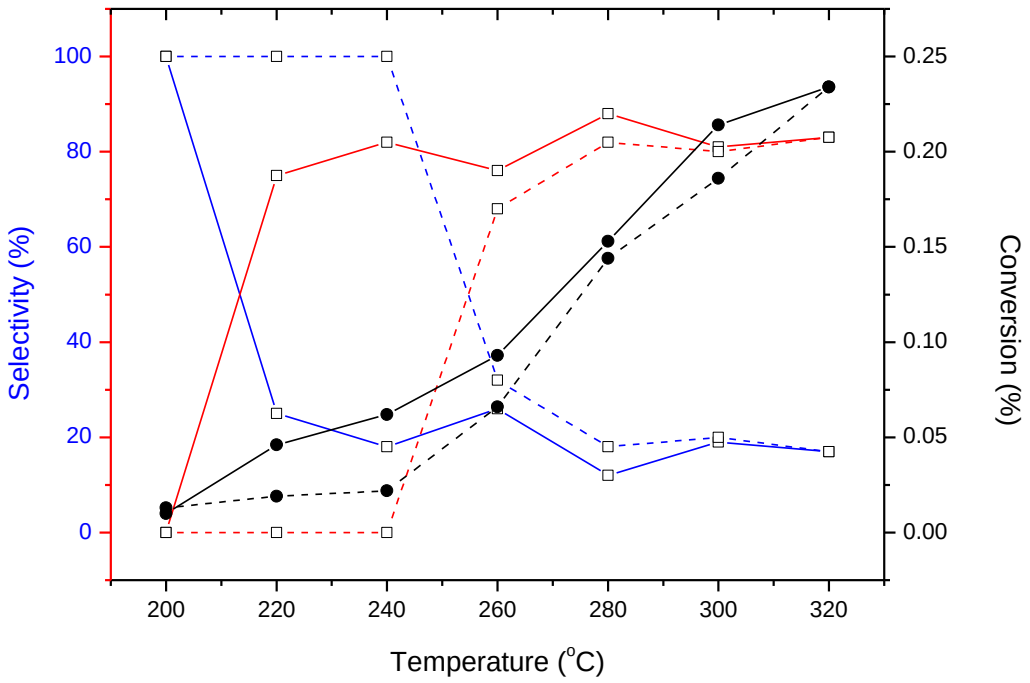

(a)

Figure 4.23 (a) $CuAu_3/SiO_2$ copper chloride direct calcination (C978/63B) Propene oxidation with H_2 ____Acrolein T $_{increase}$ - - - - Acrolein $T_{decrease}$ ____CO_2 T $_{increase}$ - - - - CO_2 T $_{decrease}$ ____ Propene oxide T $_{increase}$ - - - - Propene Oxide T $_{decrease}$ ____Conversion T $_{increase}$ - - - - Conversion T $_{decrease}$

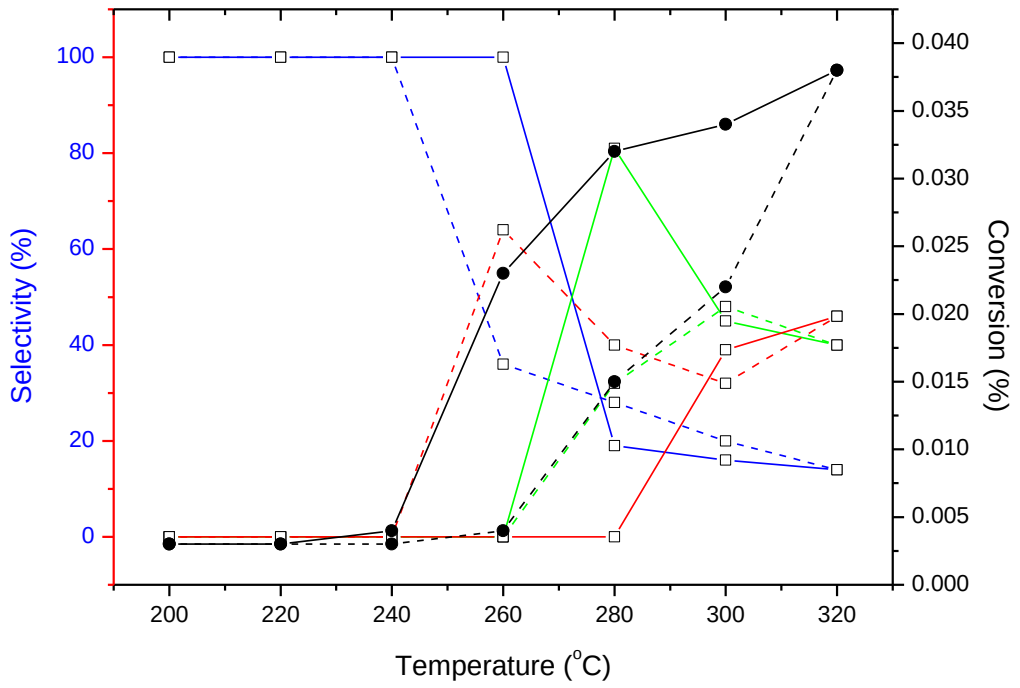

(b)

Figure 4.23 (b) $CuAu_3/SiO_2$ copper chloride direct calcination (C978/63B) Propene oxidation without H_2 addition ____Acrolein T $_{increase}$ ---- Acrolein T$_{decrease}$ ____CO_2 T $_{increase}$ ---- CO_2 T $_{decrease}$ ____ Propene oxide T $_{increase}$ ---- Propene Oxide T $_{decrease}$ ____Conversion T $_{increase}$ ---- Conversion T $_{decrease}$

Propene oxidation for the Au rich bimetallic catalyst ($CuAu_3/SiO_2$) with a copper chloride and a direct calcination (Figure 4.23 (a) and 4.23 (b)) was carried out. Again, like the $CuAu/SiO_2$ catalyst prepared the same way, acrolein and carbon dioxide were the only products in the presence of hydrogen. A propene conversion of 0.22% ± 3% was reached at 300 ^oC with an acrolein selectivity of 80%. The propene oxidation experiment without H_2 showed that propene oxide and acrolein were detected at higher temperatures. At 280 ^oC, propene oxide had a selectivity of 80% but at 300 ^oC that selectivity fell to 46% as acrolein is detected at 40%.

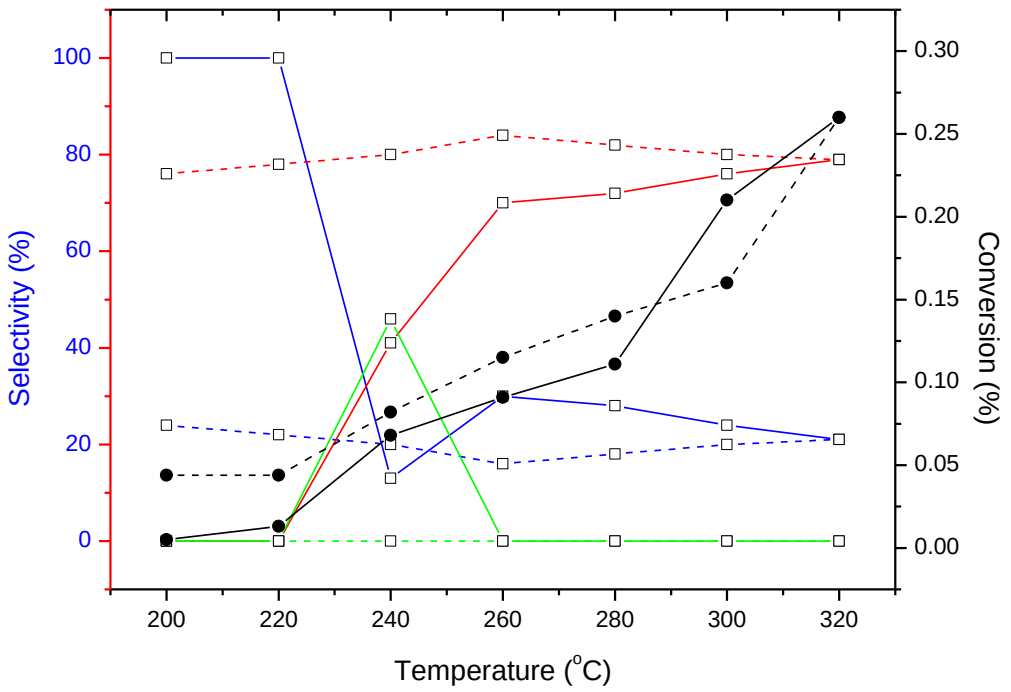

(a)

Figure 4.24 (a) Cu_3Au/SiO_2 copper chloride direct calcination (C978/63C).Propene oxidation with H_2 addition ____Acrolein T $_{increase}$ - - - - Acrolein T$_{decrease}$ ____CO_2 T $_{increase}$ - - - - CO_2 T $_{decrease}$ ____ Propene oxide T $_{increase}$ - - - - Propene Oxide T $_{decrease}$ ____Conversion T $_{increase}$ - - - - Conversion T $_{decrease}$

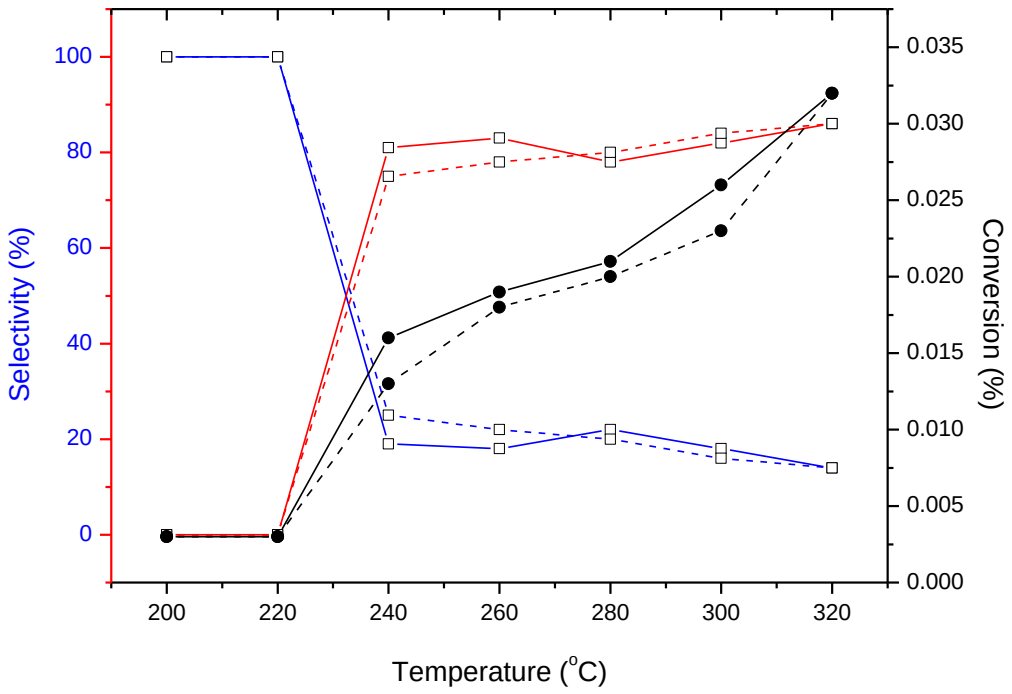

(b)

Figure 4.24 (b) Cu_3Au/SiO_2 copper chloride direct calcination (C978/63C).Propene oxidation without H_2 addition ____Acrolein T $_{increase}$ - - - - Acrolein T$_{decrease}$ ____CO_2 T $_{increase}$ - - - - CO_2 T $_{decrease}$ ____ Propene oxide T $_{increase}$ - - - - Propene Oxide T $_{decrease}$ ____Conversion T $_{increase}$ - - - - Conversion T $_{decrease}$

The Cu rich bimetallic catalyst Cu_3Au/SiO_2 had a different product selectivity than the CuAu and $CuAu_3$ catalysts (Figure 4.24 (a) and 4.24 (b)). In the presence of H_2, propene oxide was formed with a selectivity of nearly 50% at 240 ^oC. Acrolein was more selective at higher temperatures and reached 77% at 300 ^oC with a conversion of 0.21% ± 3%. Propene oxidation without hydrogen had a much lower propene conversion of 0.026% at 300 ^oC and was only selective towards acrolein and CO_2.

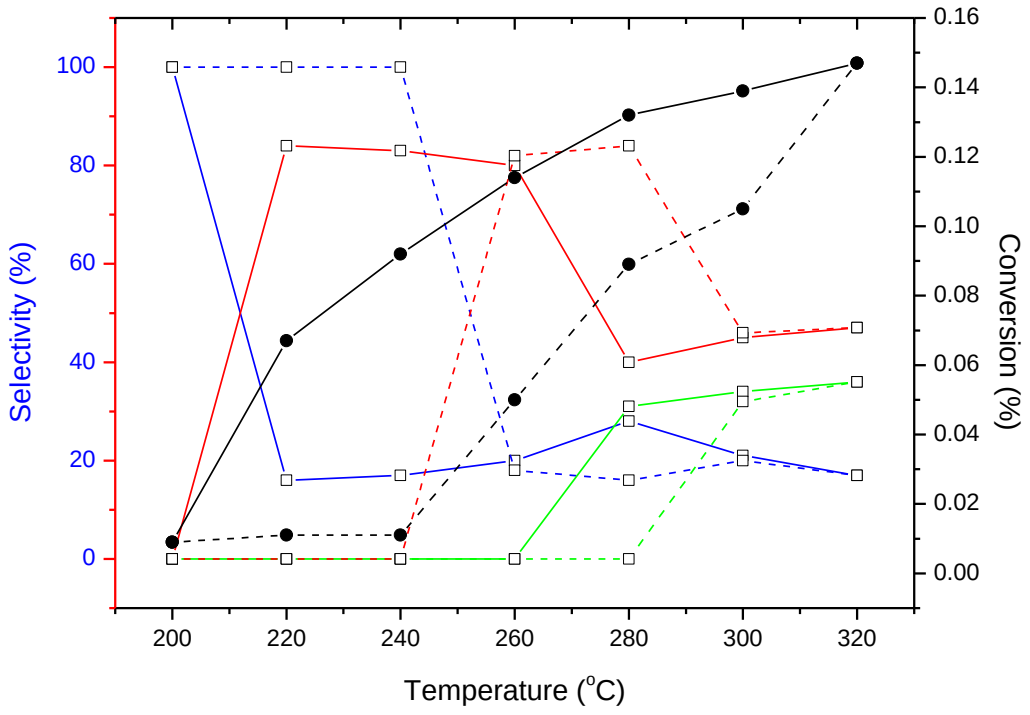

(a)

Figure 4.25 (a) CuAu/SiO_2 copper nitrate direct calcination (C97819A) Propene oxidation with H_2 ____Acrolein T $_{increase}$ - - - - Acrolein T$_{decrease}$ ____CO_2 T $_{increase}$ - - - - CO_2 T $_{decrease}$ ____ Propene oxide T $_{increase}$ - - - - Propene Oxide T $_{decrease}$ ____Conversion T $_{increase}$ - - - - Conversion T $_{decrease}$

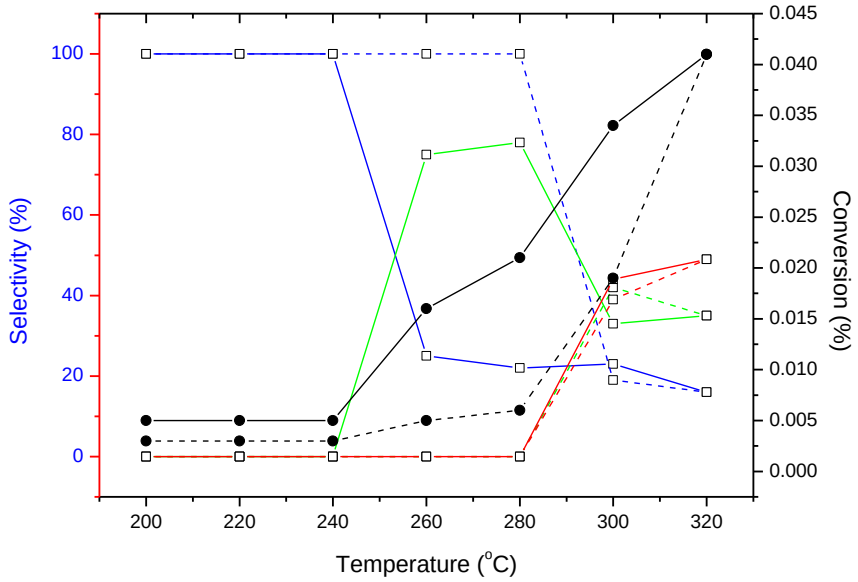

(b)

Figure 4.25 (b) CuAu/SiO_2 copper nitrate direct calcination (C97819A) Propene oxidation without H_2 ____Acrolein T $_{increase}$ - - - - Acrolein T$_{decrease}$ ____CO_2 T $_{increase}$ - - - - CO_2 T $_{decrease}$ ____ Propene oxide T $_{increase}$ - - - - Propene Oxide T $_{decrease}$ ____Conversion T $_{increase}$ - - - - Conversion T $_{decrease}$

The copper precursor was changed from copper chloride to copper nitrate and the material prepared the same way as the other catalysts, by direct calcination (Figure 4.25 (a) and 4.25 (b)). Propene oxidation for the CuAu/SiO_2 catalyst in the presence of H_2 showed a propene conversion of 0.14% ± 3% at 300 ^{o}C. Both propene oxide and acrolein were observed at higher temperatures between 280 ^{o}C and 300 ^{o}C. In the absence of H_2, propene oxide and acrolein were still seen but propene oxide was more selective at lower temperatures between 260 ^{o}C and 300 ^{o}C (78%).

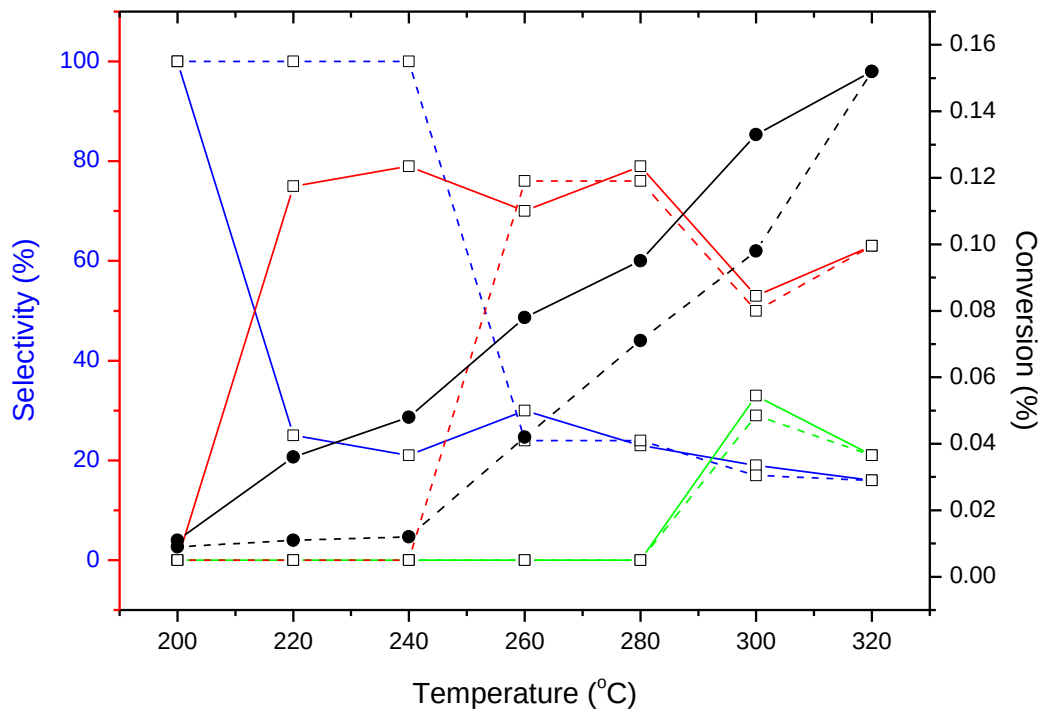

(a)

Figure 4.26 (a) $CuAu_3/SiO_2$ copper nitrate direct calcination (C97819B) Propene oxidation with H_2 ____Acrolein T $_{increase}$ - - - - Acrolein $T_{decrease}$ ____CO_2 T $_{increase}$ - - - - CO_2 T $_{decrease}$ ____ Propene oxide T $_{increase}$ - - - - Propene Oxide T $_{decrease}$ ____Conversion T $_{increase}$ - - - - Conversion T $_{decrease}$

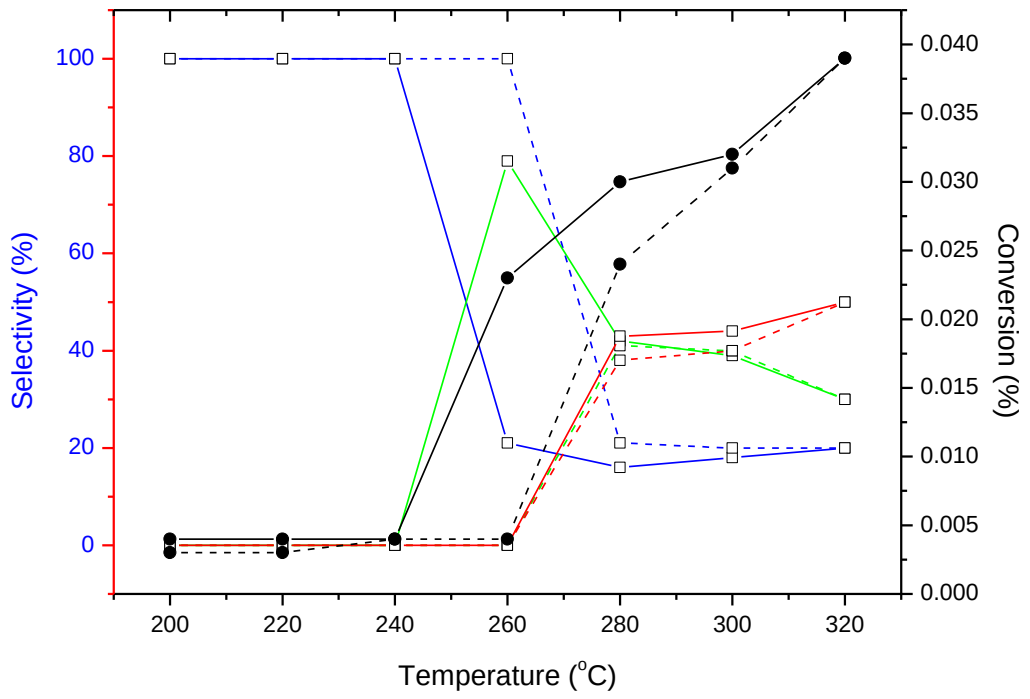

(b)

Figure 4.26 (b) $CuAu_3/SiO_2$ copper nitrate direct calcination (C97819B) Propene oxidation without H_2 ____Acrolein T $_{increase}$ - - - - Acrolein T$_{decrease}$ ____CO_2 T $_{increase}$ - - - - CO_2 T $_{decrease}$ ____ Propene oxide T $_{increase}$ - - - - Propene Oxide T $_{decrease}$ ____Conversion T $_{increase}$ - - - - Conversion T $_{decrease}$

Propene oxidation for directly calcined $CuAu_3/SiO_2$, using copper nitrate, was tested (Figure 4.26 (a) and 4.26(b)) and, in the presence of hydrogen, a propene conversion of 0.13% ± 3.5% was achieved at 300 ^oC. At this temperature, acrolein and propene oxide were formed with selectivities at 52% and 30% respectively. Without H_2, the conversion was much lower but still both propene oxide and acrolein were detected at 300 ^oC. Propene oxide was formed at 260 ^oC with a selectivity of 79% and this result appeared reliable as it was observed after each GC at 260 ^oC with an error of ±2%.

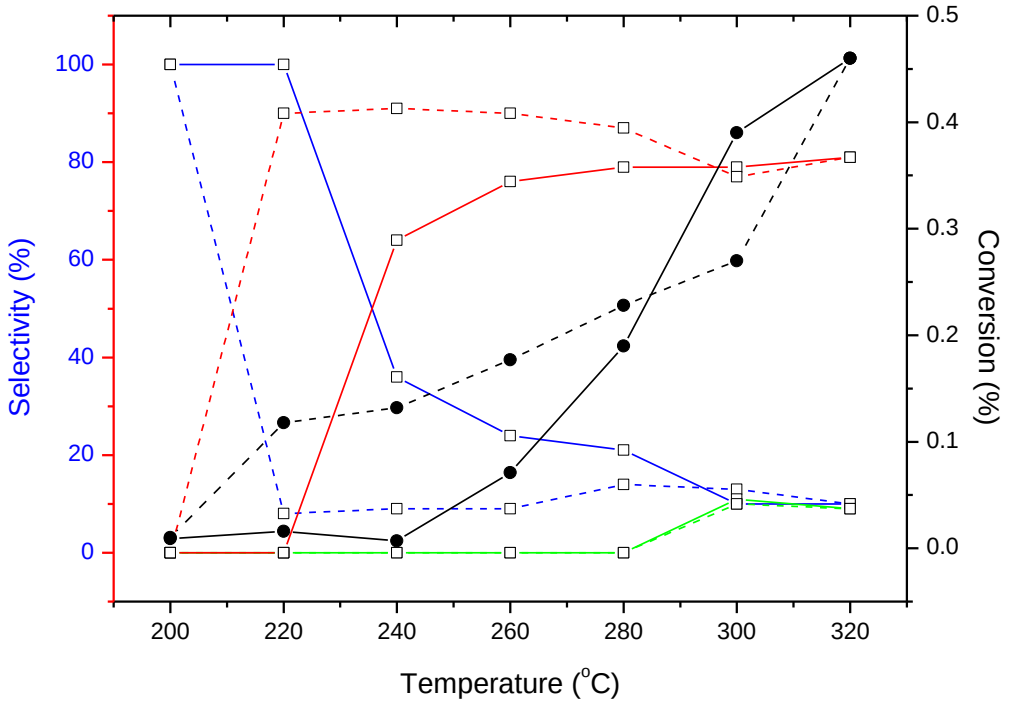

(a)

Figure 4.27 (a) Cu_3Au/SiO_2 copper nitrate direct calcination (C97819C). Propene oxidation with H_2 ____Acrolein T $_{increase}$ - - - - Acrolein $T_{decrease}$ ____CO_2 T $_{increase}$ - - - - CO_2 T $_{decrease}$ ____ Propene oxide T $_{increase}$ - - - - Propene Oxide T $_{decrease}$ ____Conversion T $_{increase}$ - - - - Conversion T $_{decrease}$

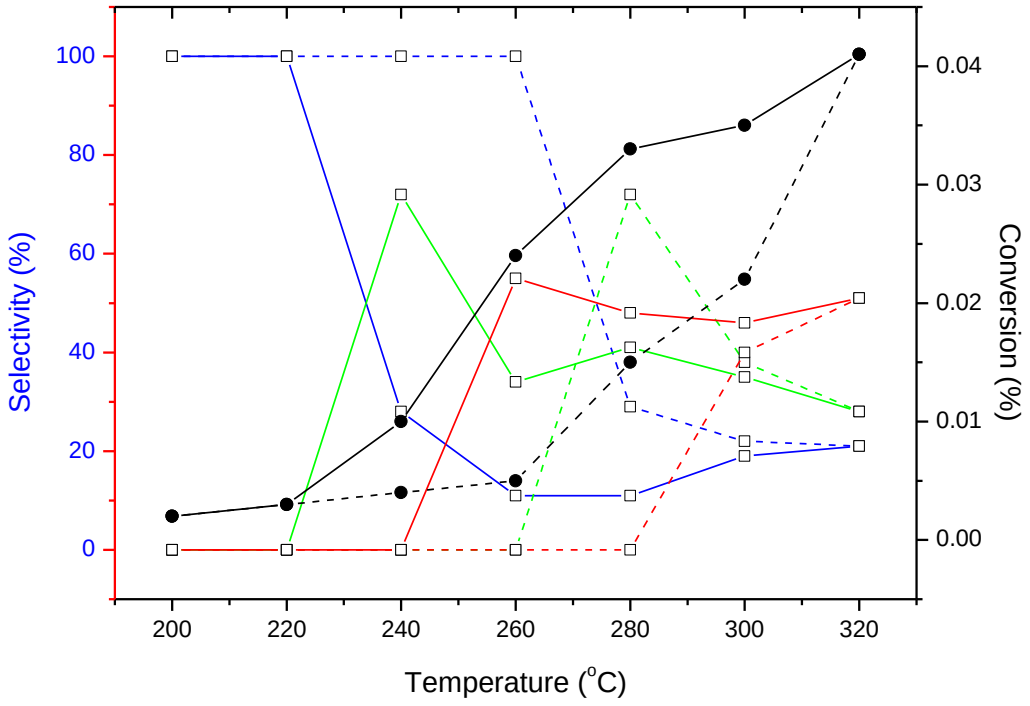

(b)

Figure 4.27 (b) Cu_3Au/SiO_2 copper nitrate direct calcination (C97819C). Propene oxidation without H_2 Acrolein T $_{increase}$ Acrolein T$_{decrease}$ CO_2 T $_{increase}$ CO_2 T $_{decrease}$ Propene oxide T $_{increase}$ Propene Oxide T $_{decrease}$ Conversion T $_{increase}$ Conversion T $_{decrease}$

The Cu rich Cu_3Au/SiO_2 catalyst had the highest propene conversion of 0.4% ± 1% at 300 ^oC in the presence of H_2 (Figure 4.27 (a)). This catalyst had a stable acrolein selectivity during the hysteresis and, as the temperature decreased, the acrolein selectivity increased to 90% at 220 ^oC. Acrolein was the major product but propene oxide was formed at 300 ^oC (10%). In the absence of hydrogen in the reactor feed, as with all the catalysts the conversion was much lower. Both propene oxide and acrolein were detected with propene oxide having a higher selectivity at lower temperatures and an error of ± 3%.

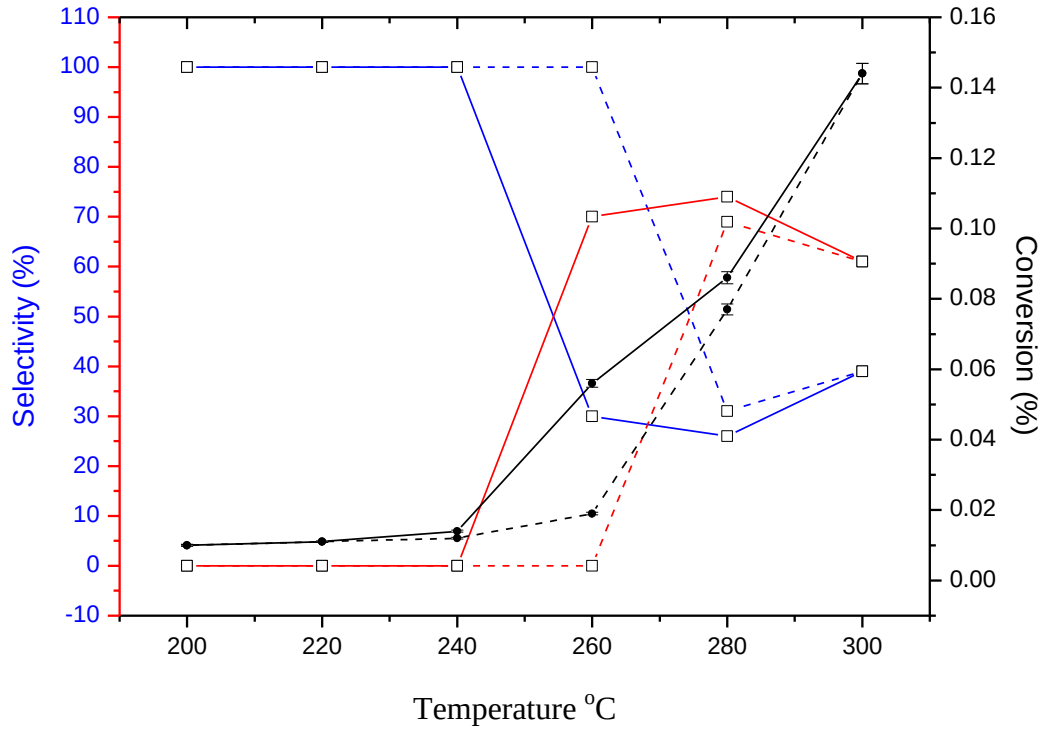

(a)

Figure 4.28 (a) $CuAu/SiO_2$ copper chloride Sinfelt (C978/65A) Propene oxidation with (a) and with H_2 ____Acrolein T $_{increase}$ - - - - Acrolein T$_{decrease}$ ____CO_2 T $_{increase}$ - - - - CO_2 T $_{decrease}$ ____ Propene oxide T $_{increase}$ - - - - Propene Oxide T $_{decrease}$ ____Conversion T $_{increase}$ - - - - Conversion T $_{decrease}$

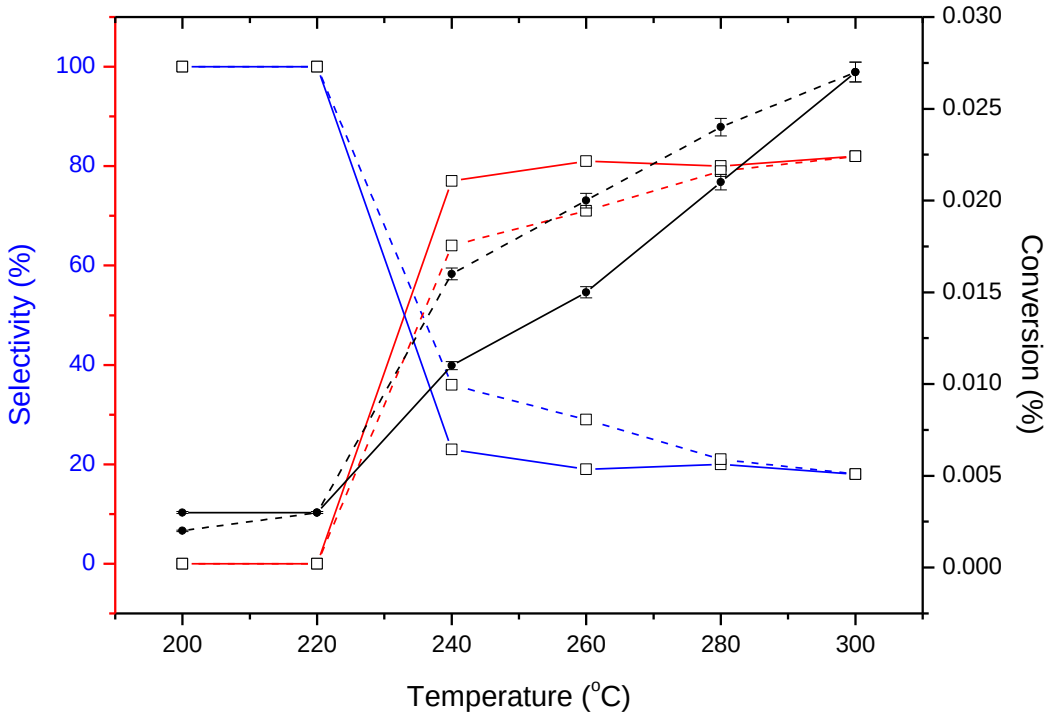

(b)

Figure 4.28 (b) $CuAu/SiO_2$ copper chloride Sinfelt (C978/65A) Propene oxidation with (a) and without H_2 ____Acrolein T $_{increase}$ - - - - Acrolein T$_{decrease}$ ____CO_2 T $_{increase}$ - - - - CO_2 T $_{decrease}$ ____ Propene oxide T $_{increase}$ - - - - Propene Oxide T $_{decrease}$ ____Conversion T $_{increase}$ - - - - Conversion T $_{decrease}$

The Sinfelt treatment (reduction at 315 ^{o}C for 2h in H_2/Ar followed by high temperature calcinations at 676 ^{o}C for 5h in air) was applied to the different molar ratios of $CuAu/SiO_2$ catalysts using copper chloride precursors. For the $CuAu/SiO_2$ sample, in the presence of hydrogen (Figure 4.29) and without H_2, only acrolein and carbon dioxide were produced. A propene conversion of nearly 0.15% ± 3% was observed with addition of hydrogen at 300 ^{o}C and a selectivity towards acrolein of 60%. The catalyst without H_2 in the reactor feed was stable and maintained an acrolein selectivity of 80%.

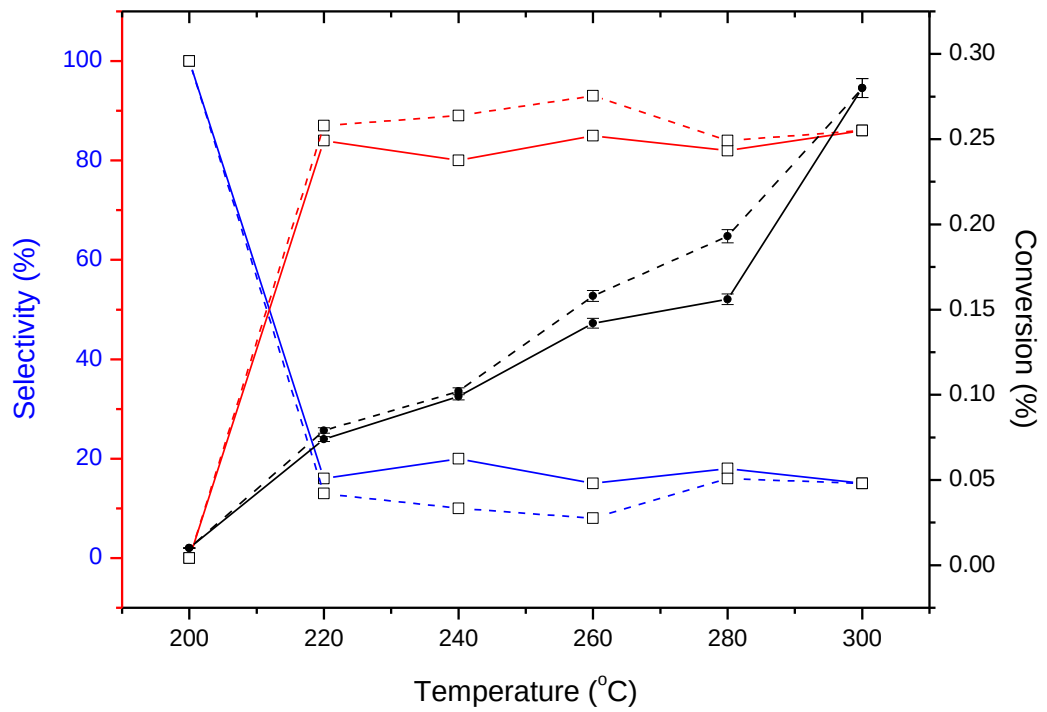

(a)

Figure 4.29 (a) $CuAu_3/SiO_2$ copper chloride Sinfelt (C978/65B). Propene oxidation with H_2

Acrolein T $_{increase}$ Acrolein T$_{decrease}$ CO_2 T $_{increase}$ CO_2 T $_{decrease}$

Propene oxide T $_{increase}$ Propene Oxide T $_{decrease}$ Conversion T $_{increase}$

Conversion T $_{decrease}$

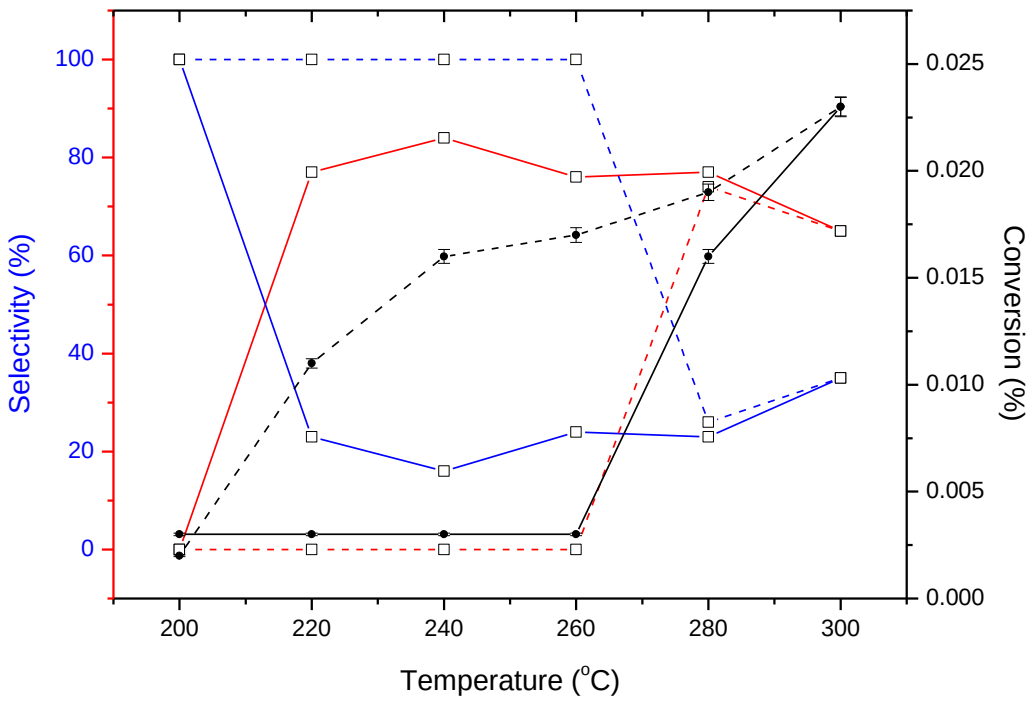

(b)

Figure 4.29 (b) $CuAu_3/SiO_2$ copper chloride Sinfelt (C978/65B). Propene oxidation without H_2

Acrolein T $_{increase}$ Acrolein T$_{decrease}$ CO_2 T $_{increase}$ CO_2 T $_{decrease}$

Propene oxide T $_{increase}$ Propene Oxide T $_{decrease}$ Conversion T $_{increase}$

Conversion T $_{decrease}$

The $CuAu_3/SiO_2$ catalyst prepared with a copper chloride precursor, followed by the Sinfelt treatment, showed a propene conversion of 0.28% ± 3% at 300 ^{o}C and an acrolein selectivity of 85%. This catalyst appeared stable during the hysteresis experiment. In the absence of H_2, acrolein and carbon dioxide were still the only products formed but the catalyst had a low stability. The propene conversion was much lower at 0.23% ± 3% at 300 ^{o}C.

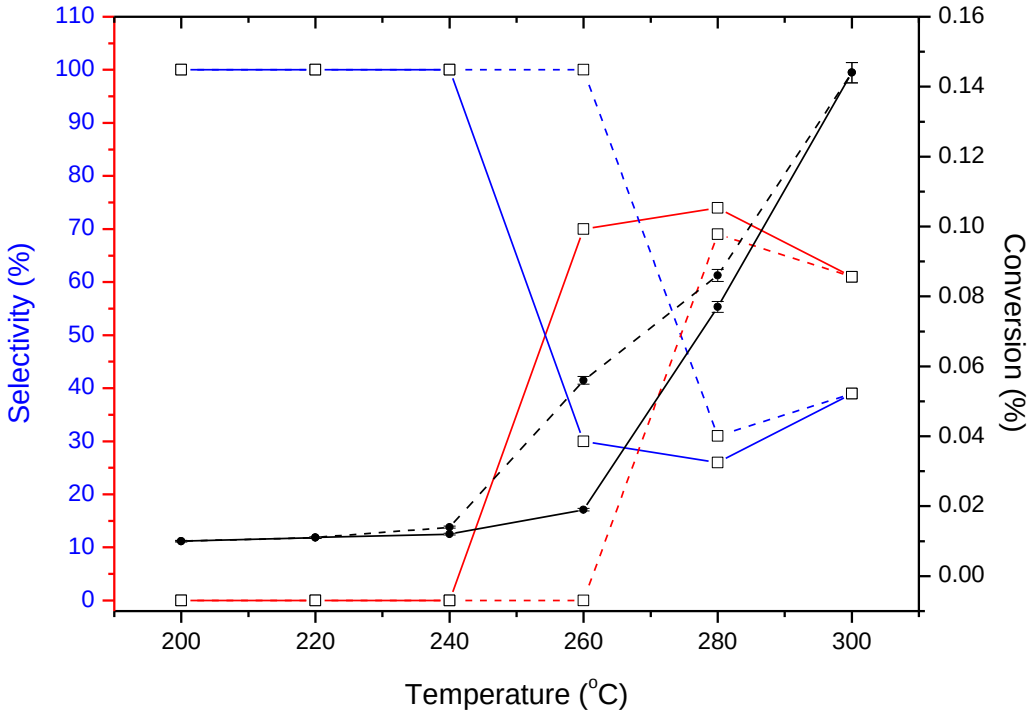

(a)

Figure 4.30 (a) Cu_3Au/SiO_2 copper chloride Sinfelt (C978/65C). Propene oxidation with H_2

Acrolein T $_{increase}$ Acrolein T$_{decrease}$ CO_2 T $_{increase}$ CO_2 T $_{decrease}$

Propene oxide T $_{increase}$ Propene Oxide T $_{decrease}$ Conversion T $_{increase}$

Conversion T $_{decrease}$

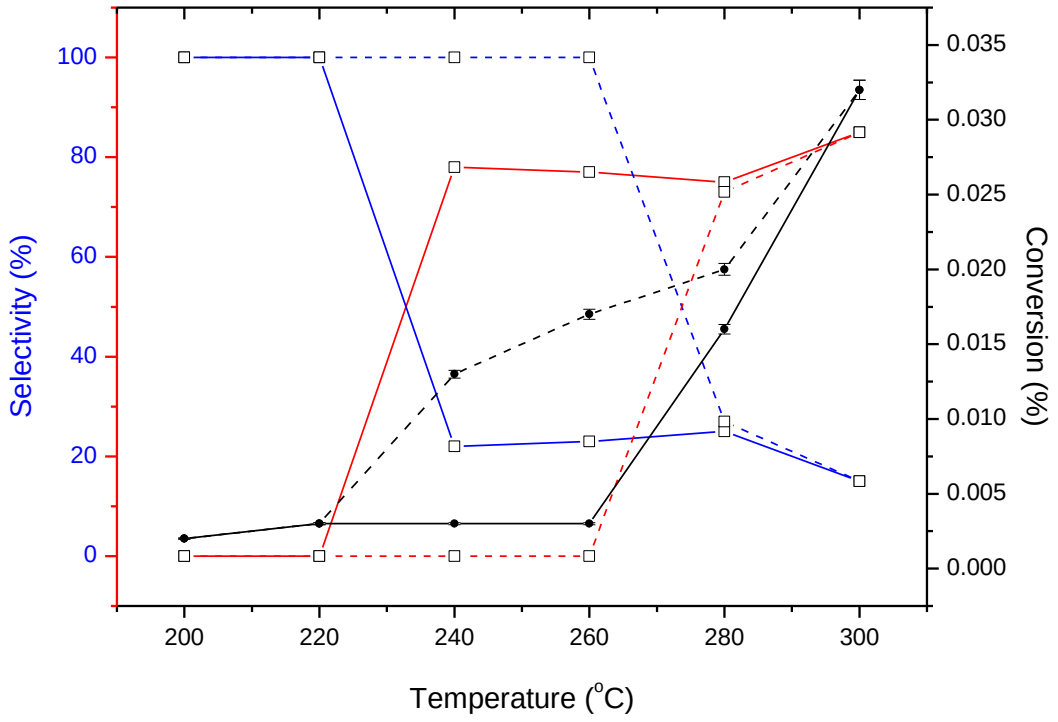

(b)

Figure 4.30 (b) Cu_3Au/SiO_2 copper chloride Sinfelt (C978/65C). Propene oxidation without H_2

Acrolein T $_{increase}$ Acrolein T$_{decrease}$ CO_2 T $_{increase}$ CO_2 T $_{decrease}$

Propene oxide T $_{increase}$ Propene Oxide T $_{decrease}$ Conversion T $_{increase}$

Conversion T $_{decrease}$

A similar trend was observed for the Cu rich Cu_3Au/SiO_2 catalyst made with a copper chloride precursor and the Sinfelt treatment (Figure 4.30 (a) and 4.30 (b)). With or without the presence of hydrogen in the reactor feed, the only products formed were acrolein and CO_2. A propene conversion of 0.15% ± 3% was obtained by the catalyst in the presence of H_2 at 300 ^oC.

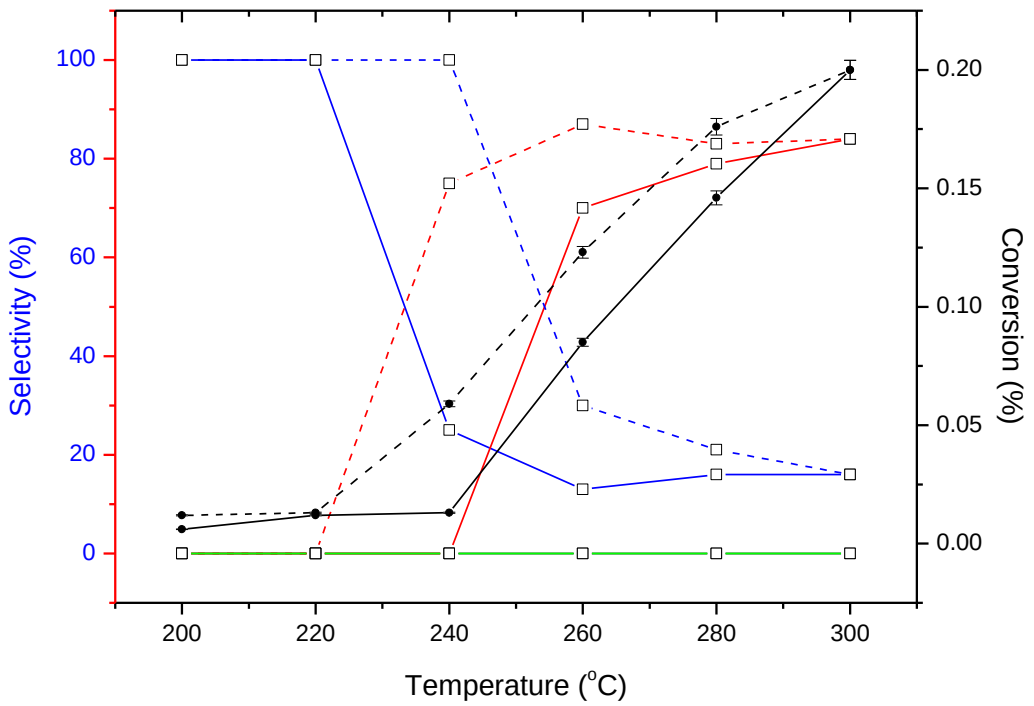

(a)

Figure 4.31 (a) CuAu/SiO_2 copper nitrate Sinfelt (C978/101A) Propene oxidation with H_2

Acrolein T $_{increase}$ Acrolein T$_{decrease}$ CO_2 T $_{increase}$ CO_2 T $_{decrease}$

Propene oxide T $_{increase}$ Propene Oxide T $_{decrease}$

Conversion T $_{increase}$ Conversion T $_{decrease}$

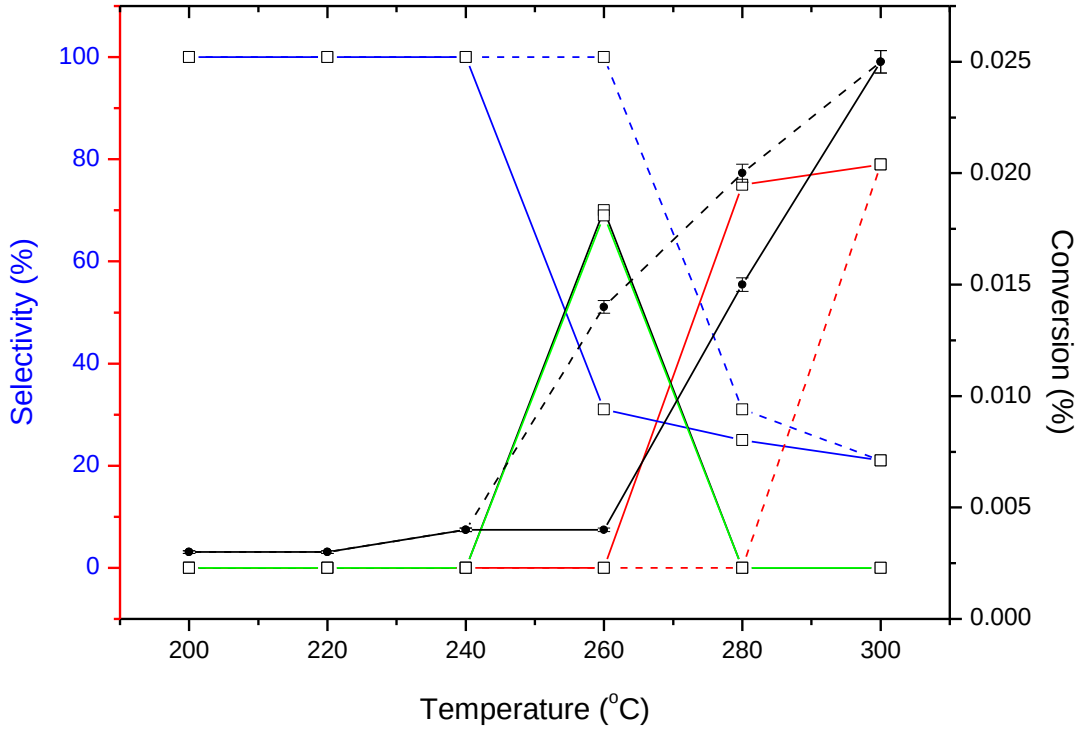

(b)

Figure 4.31 (b) $CuAu/SiO_2$ copper nitrate Sinfelt (C978/101A) Propene oxidation without H_2 . Acrolein $T_{increase}$ Acrolein $T_{decrease}$ CO_2 $T_{increase}$ CO_2 $T_{decrease}$ Propene oxide $T_{increase}$ Propene Oxide $T_{decrease}$ Conversion $T_{increase}$ Conversion $T_{decrease}$

$CuAu/SiO_2$ catalysts were prepared with copper nitrate, followed by the Sinfelt treatment (Figure 4.31 (a) and 4.31 (b)). Unlike the copper chloride catalysts prepared by this method, propene oxide was formed by this catalyst at 260 ^oC without the presence of H_2. A propene conversion of 0.2% ± 2 % at 300 ^oC was achieved with the addition of hydrogen. Only acrolein and CO_2 were produced in the presence of H_2.

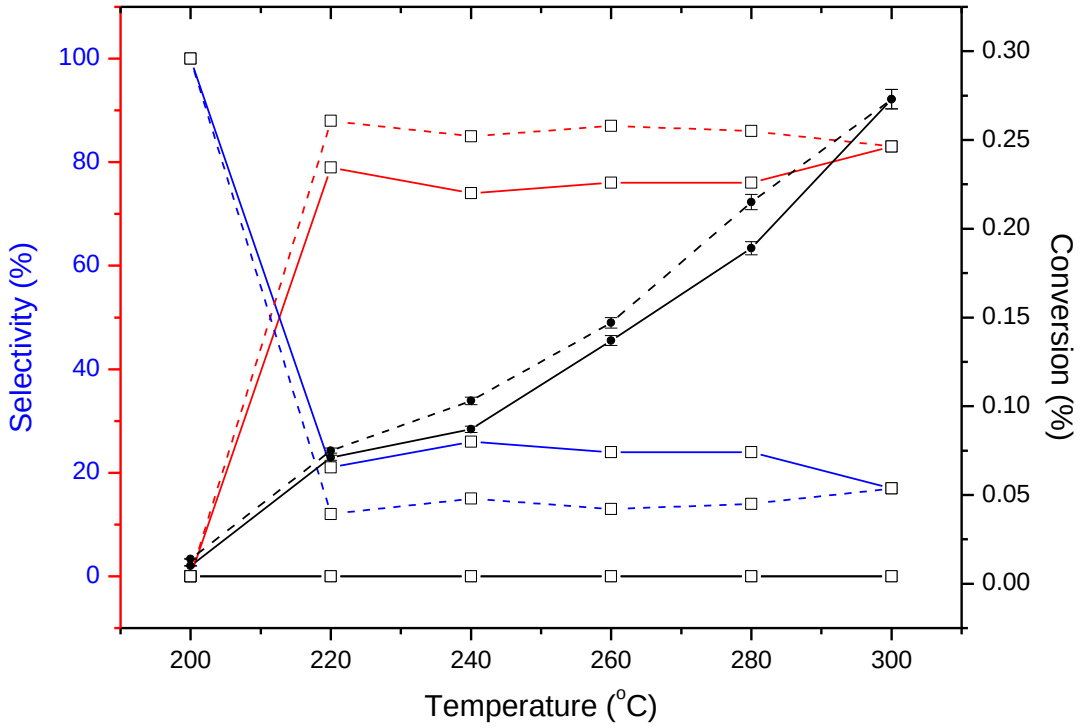

(a)

Figure 4.32 (a) $CuAu_3/SiO_2$ copper nitrate Sinfelt (C978/101B). Propene oxidation with H_2

Acrolein T $_{increase}$ Acrolein T$_{decrease}$ CO_2 T $_{increase}$ CO_2 T $_{decrease}$

Propene oxide T $_{increase}$ Propene Oxide T $_{decrease}$ Conversion T $_{increase}$

Conversion T $_{decrease}$

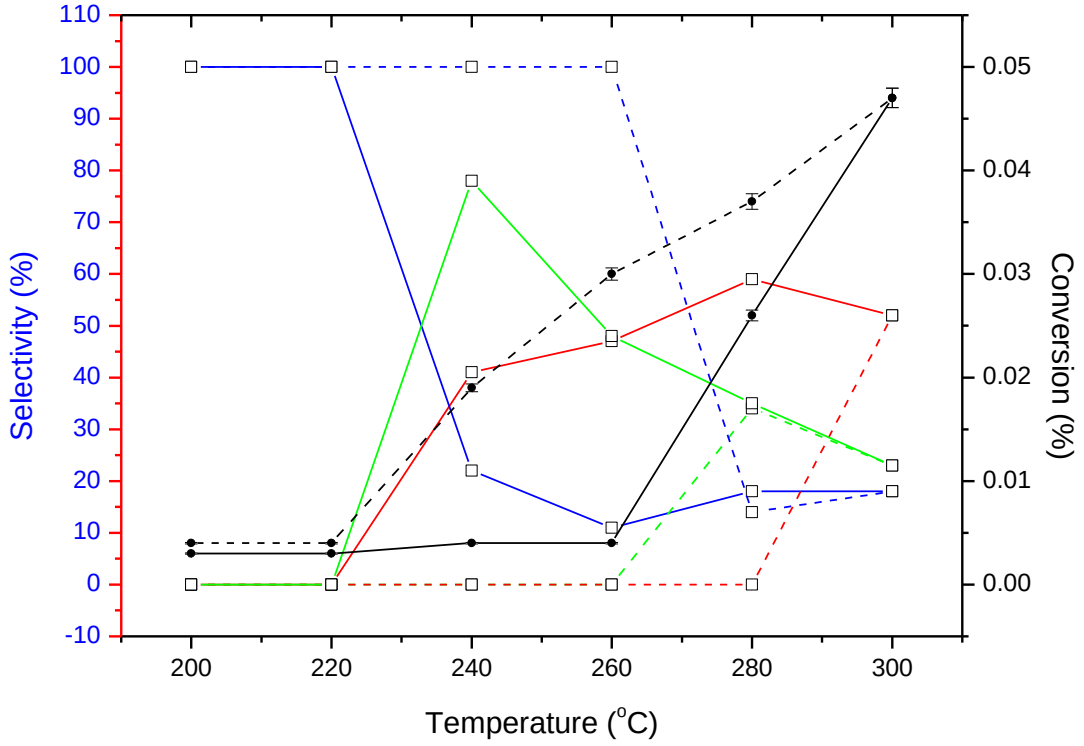

(b)

Figure 4.32 (b) $CuAu_3/SiO_2$ copper nitrate Sinfelt (C978/101B). Propene oxidation without H_2

Acrolein T $_{increase}$ Acrolein T$_{decrease}$ CO_2 T $_{increase}$ CO_2 T $_{decrease}$

Propene oxide T $_{increase}$ Propene Oxide T $_{decrease}$ Conversion T $_{increase}$

Conversion T $_{decrease}$

As with the $CuAu/SiO_2$ catalyst, the $CuAu_3/SiO_2$ sample, made with a copper nitrate precursor and Sinfelt treatment, formed propene oxide between 260 and 300 ^oC in the absence of H_2. Propene oxide was more selective at lower temperatures, whereas acrolein formation is favoured at higher temperatures. In the presence of H_2, the catalyst was quite stable with acrolein retaining its selectivity as the temperature decreased.

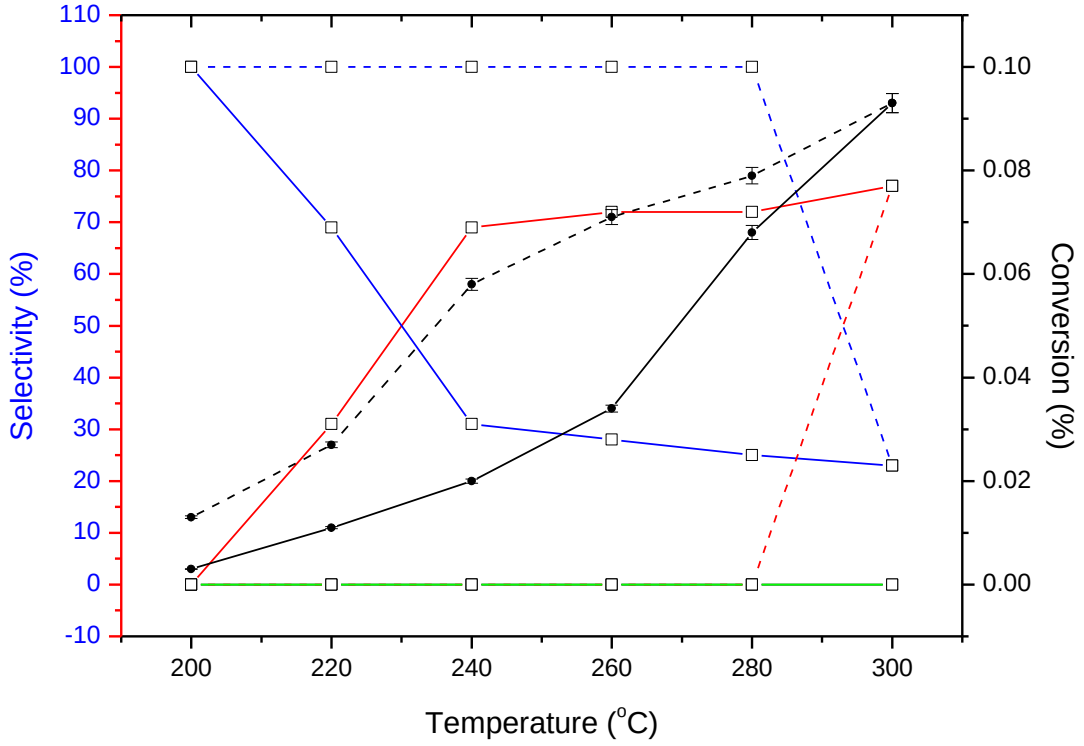

(a)

Figure 4.33 (a) Cu_3Au/SiO_2 copper nitrate Sinfelt (C978/101C). Propene oxidation with H_2

Acrolein T $_{increase}$ Acrolein T$_{decrease}$ CO_2 T $_{increase}$ CO_2 T $_{decrease}$

Propene oxide T $_{increase}$ Propene Oxide T $_{decrease}$

Conversion T $_{increase}$ Conversion T $_{decrease}$

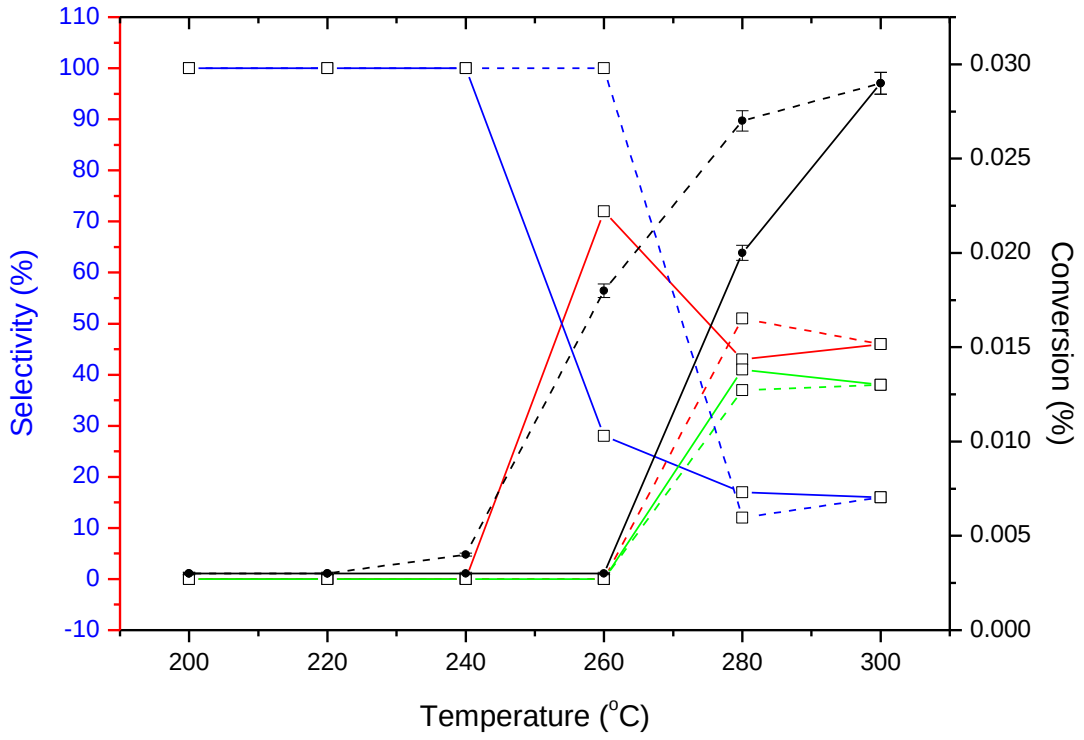

(b)

Figure 4.33 (b) Cu_3Au/SiO_2 copper nitrate Sinfelt (C978/101C). Propene oxidation without H_2 ____Acrolein T $_{increase}$ - - - - Acrolein T$_{decrease}$ ____CO_2 T $_{increase}$ - - - - CO_2 T $_{decrease}$ ____ Propene oxide T $_{increase}$ - - - - Propene Oxide T $_{decrease}$ ____Conversion T $_{increase}$ - - - - Conversion T $_{decrease}$

The copper rich Cu_3Au/SiO_2 catalyst prepared with a copper nitrate precursor and Sinfelt treatment (Figure 4.33 (a)) reached a propene conversion of 0.094% ± 2% in the presence of H_2 at 300 ^oC. As the temperature increased from 220 ^oC to 300 ^oC, the selectivity towards acrolein was around 70%. Without the addition of H_2, acrolein was more selective at lower temperatures (70% at 260 ^oC), whereas propene oxide is detected at temperatures above 260 ^oC.

4.4.3 Stability of the catalysts

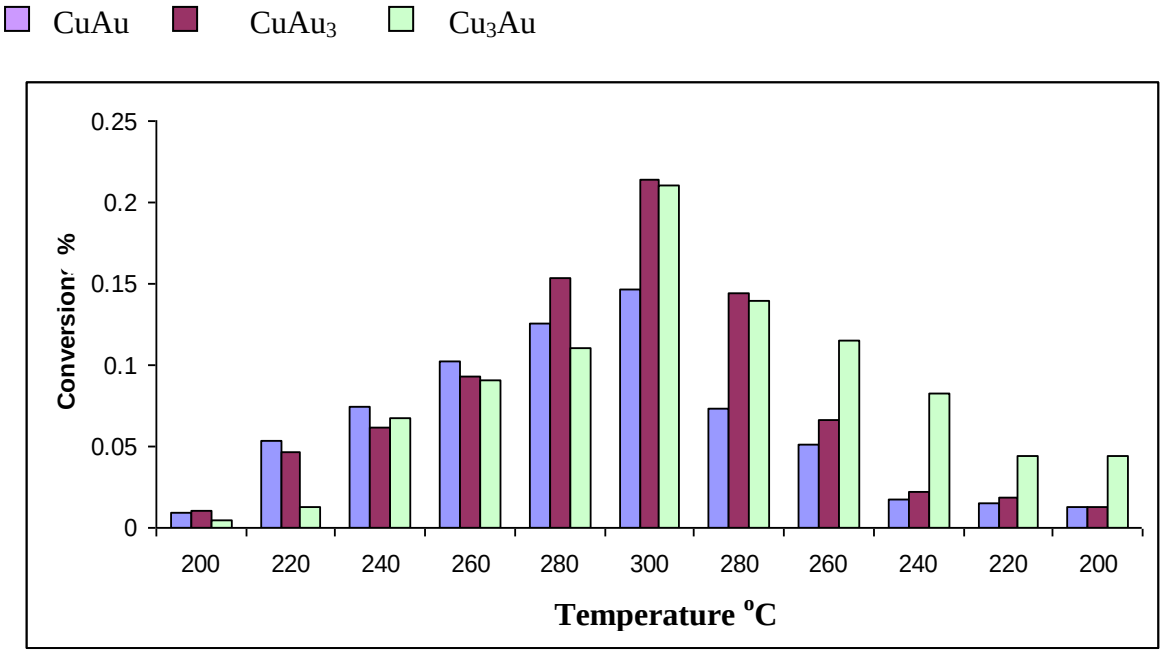

Figure 4.34 Prepared using copper chloride with direct calcination (C97863). Propene oxidation with H_2

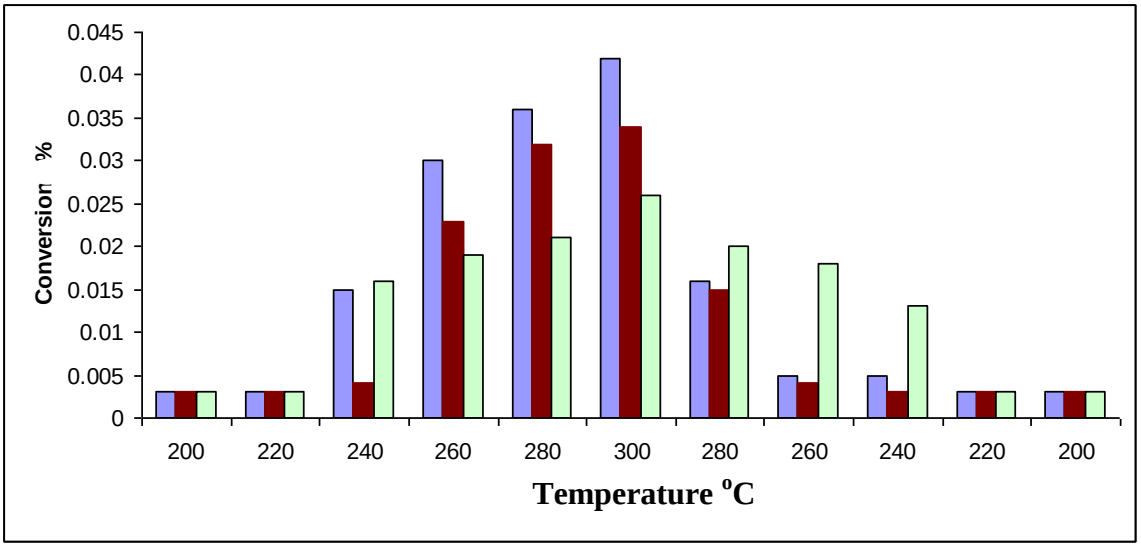

Figure 4.35 Prepared using copper chloride with direct calcination (C97863). Propene oxidation without H_2

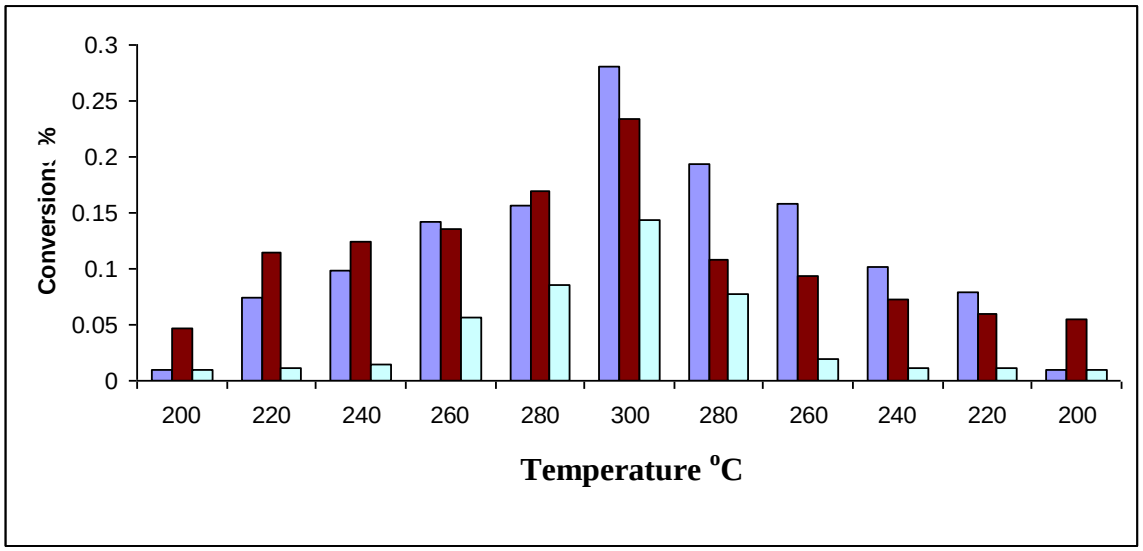

Figure 4.36 Prepared using copper chloride with Sinfelt treatment (C97865). Propene oxidation with H_2.

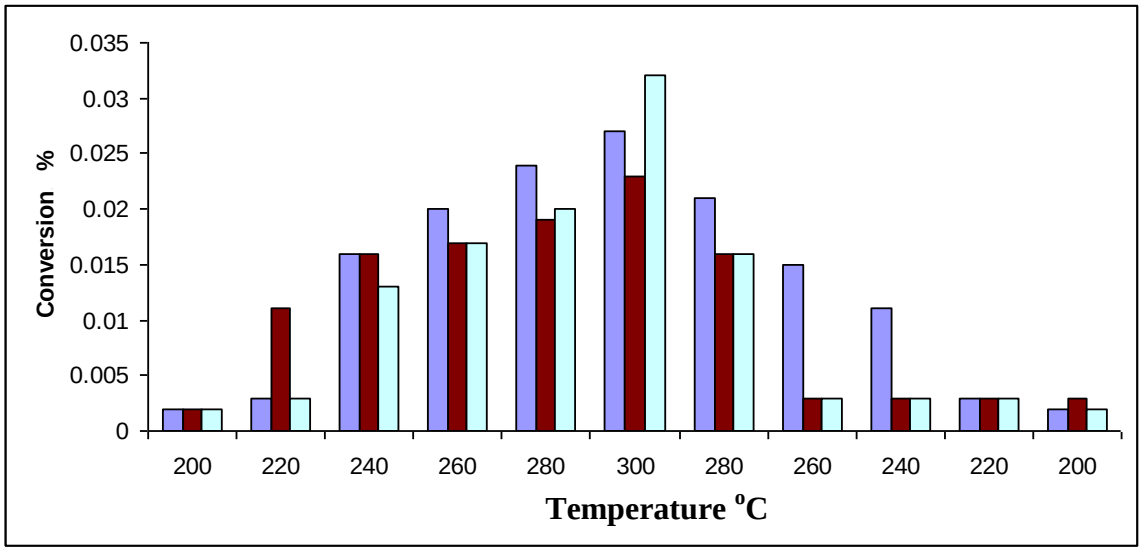

Figure 4.37 Prepared using copper chloride with Sinfelt treatment (C97865). Propene oxidation without H_2.

The conversion graphs above are examples of the general trend for all conversions for the catalysts studied in this section. The catalysts either have a copper nitrate or chloride precursor and are directly calcined or have a Sinfelt treatment. The most obvious difference is that in the presence of H_2 the conversions are much higher than without hydrogen. This suggests that the catalysts used with H_2 are more stable during the reaction. Another observation is that the equi molar ratios are less stable since their conversion fluctuate a

significant amount during the temperature increase and decrease. Whereas, catalysts that have conversions that gradually increase and decrease during their hysteresis can be considered more stable as they hold their activity better. The more copper rich the sample, the more durable the catalyst. The most stable catalyst appears to be the Sinfelt treated sample that uses a copper chloride precursor for propene oxidation in H_2 (Figure 4.37).

4.4.4 Effect of different reducing agents

Each catalyst was either reduced directly by hydrogen for 2h at 400 ^{o}C or with sodium borohydride. Monometallic Cu/SiO_2 and Au/SiO_2 catalysts were also prepared and reduced in the same way for comparison.

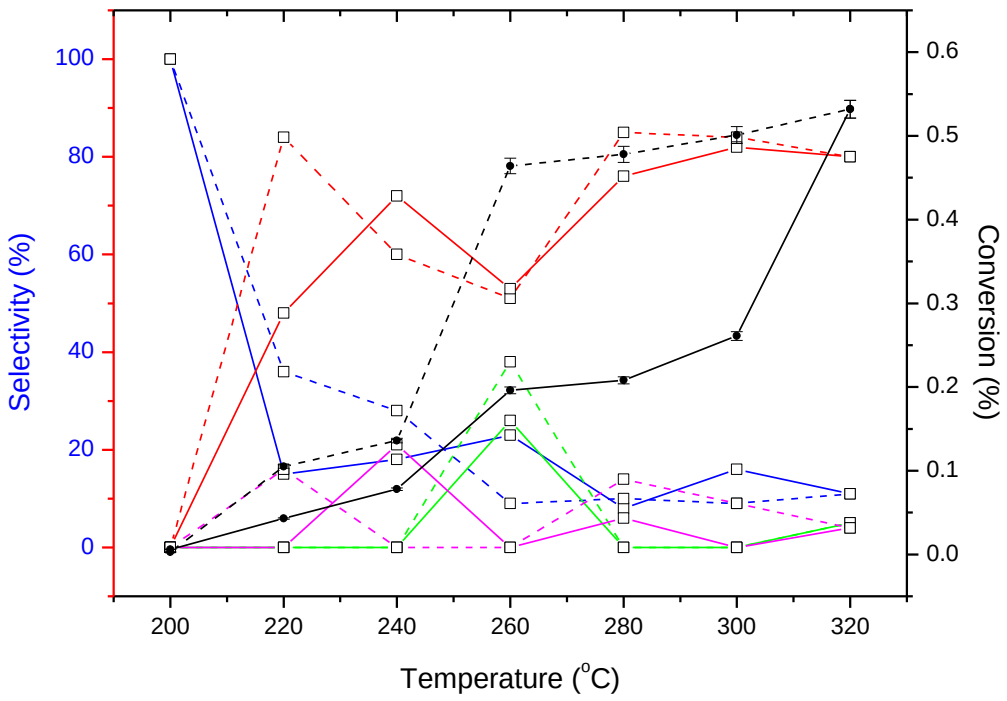

(a)

Figure 4.38 (a)_ CuAu/SiO_2 reduced with $NaBH_4$ (C978/80A) with H_2 addition

Acrolein $T_{increase}$ Acrolein $T_{decrease}$ CO_2 $T_{increase}$ CO_2 $T_{decrease}$ Propene oxide $T_{increase}$ Propene Oxide $T_{decrease}$ Ethanal $T_{increase}$ Ethanal $T_{decrease}$ Conversion $T_{increase}$ Conversion $T_{decrease}$

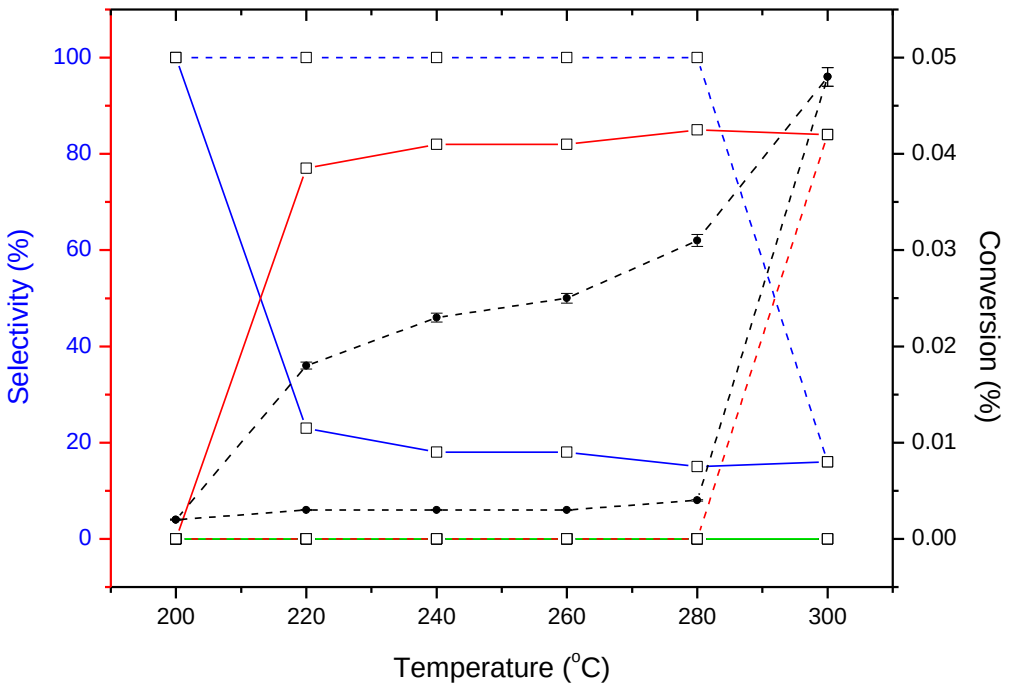

(b)

Figure 4.38 (b) $CuAu/SiO_2$ reduced with $NaBH_4$ (C978/80A) without H_2 addition. Acrolein $T_{increase}$ Acrolein $T_{decrease}$ CO_2 $T_{increase}$ CO_2 $T_{decrease}$ Propene oxide $T_{increase}$ Propene Oxide $T_{decrease}$ Ethanal $T_{increase}$ Ethanal $T_{decrease}$ Conversion $T_{increase}$ Conversion $T_{decrease}$

A $CuAu/SiO_2$ catalyst made by impregnation with copper nitrate and reduced in $NaBH_4$, has been tested for propene oxidation with and without H_2 (Figure 4.38 (a) and 4.38 (b)). In the presence of H_2, a propene conversion of 0.55% ± 1% could be reached at 320 °C. At this temperature acrolein (78%), CO_2 (15%), ethanal (3%) and propene oxide (4%) were formed. Propene oxide was most selective at 260 °C (26%). In the absence of H_2, acrolein (80%) and CO_2 were the only products formed with this catalyst.

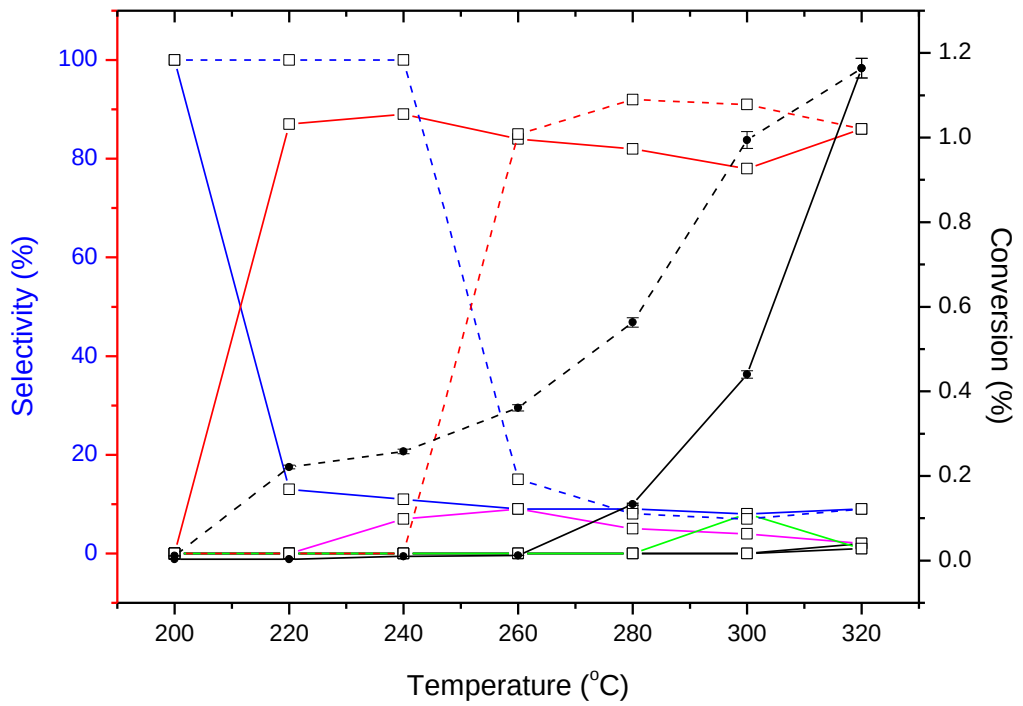

Figure 4.39 catalyst $CuAu/SiO_2$ reduced by $NaBH_4$ (C978/80A)with H_2 with 9000 GSHV

Acrolein $T_{increase}$ Acrolein $T_{decrease}$ CO_2 $T_{increase}$ CO_2 $T_{decrease}$ Propene oxide $T_{increase}$ Propene Oxide $T_{decrease}$ Ethanal $T_{increase}$ Ethanal $T_{decrease}$ Conversion $T_{increase}$ Conversion $T_{decrease}$

All of the propene oxidation reactions in the presence of H_2 had a gas hourly space velocity (GSHV) of 25,500h^{-1}. The GSHV of the reaction was altered to 9000h^{-1} for the $CuAu/SiO_2$ catalyst and the data collected (Figure 4.39). At 320 ^oC, only acrolein and CO_2 were detected but at 300 ^oC propene oxide was formed at ~10%. The conversion had increased to ~ 1.2% ± 1% and acrolein selectivity was more stable than when the GSHV is higher.

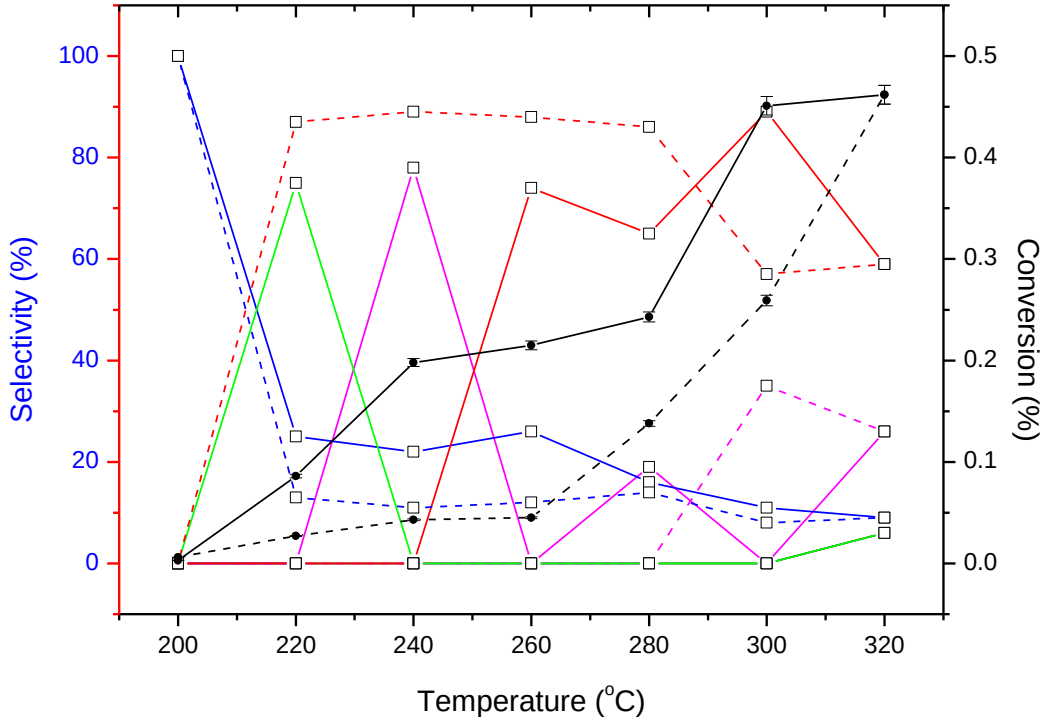

(a)

Figure 4.40 (a) $CuAu_3/SiO_2$ reduced with $NaBH_4$ (C978/80B) with H_2 addition

Acrolein T $_{increase}$ Acrolein $T_{decrease}$ CO_2 T $_{increase}$ CO_2 T $_{decrease}$ Propene oxide T $_{increase}$ Propene Oxide T $_{decrease}$ Ethanal $T_{increase}$ Ethanal $T_{decrease}$ Conversion T $_{increase}$ Conversion T $_{decrease}$

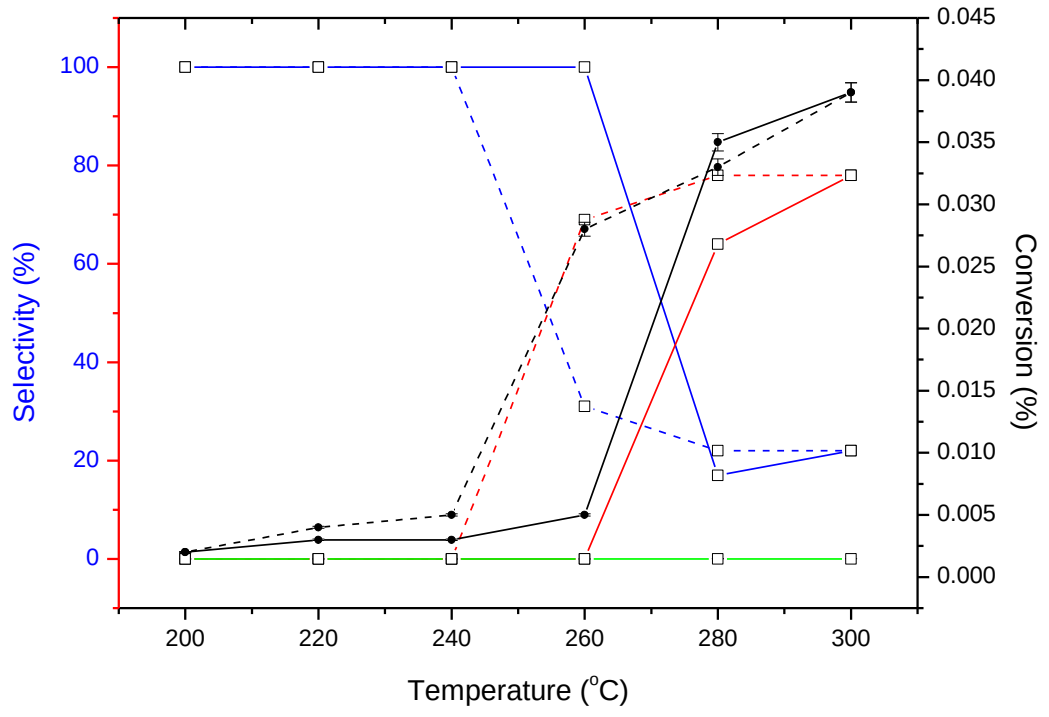

(b)

Figure 4.40 (b) $CuAu_3/SiO_2$ reduced with $NaBH_4$ (C978/80B) without H_2 addition.

Acrolein $T_{increase}$ Acrolein $T_{decrease}$ CO_2 $T_{increase}$ CO_2 $T_{decrease}$ Propene oxide $T_{increase}$ Propene Oxide $T_{decrease}$ Ethanal $T_{increase}$ Ethanal $T_{decrease}$ Conversion $T_{increase}$ Conversion $T_{decrease}$

In the presence of H_2, the Au rich $CuAu_3/SiO_2$ catalyst reduced by $NaBH_4$ had a propene conversion of ~0.44% ± 2% at 320 ^oC. Propene oxide had a high selectivity (77%) at 220 ^oC and similarly ethanal had a selectivity of 79% at 240 ^oC. Acrolein was only formed at temperatures higher than 240 ^oC

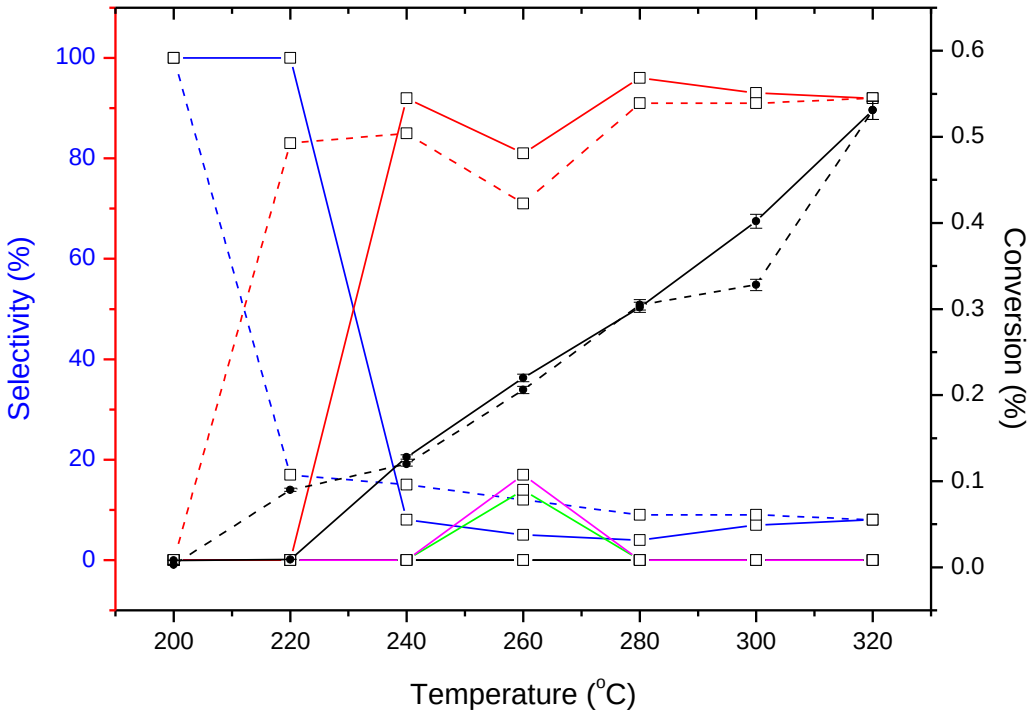

(a)

Figure 4.41 (a) Cu_3Au/SiO_2 reduced with $NaBH_4$ (C978/80C) with H_2 addition

Acrolein $T_{increase}$ Acrolein $T_{decrease}$ CO_2 $T_{increase}$ CO_2 $T_{decrease}$

Propene oxide $T_{increase}$ Propene Oxide $T_{decrease}$

Ethanal $T_{increase}$ Ethanal $T_{decrease}$ Conversion $T_{increase}$ ---- Conversion $T_{decrease}$

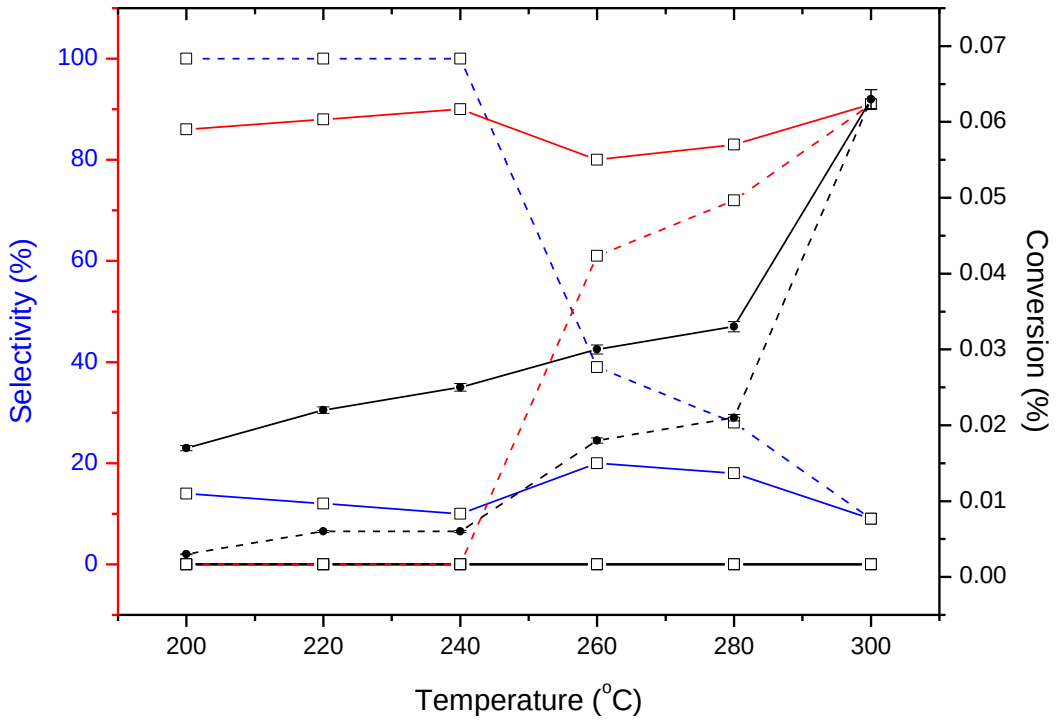

(b)

Figure 4.41 (b) Cu_3Au/SiO_2 reduced with $NaBH_4$ (C978/80C) without H_2 addition. Acrolein $T_{increase}$ Acrolein $T_{decrease}$ CO_2 $T_{increase}$ CO_2 $T_{decrease}$ Propene oxide $T_{increase}$ Propene Oxide $T_{decrease}$ Ethanal $T_{increase}$ Ethanal $T_{decrease}$ Conversion $T_{increase}$ Conversion $T_{decrease}$

In the presence of H_2, the Cu rich Cu_3Au/SiO_2 catalyst, reduced by $NaBH_4$, had a propene conversion of 0.53% ± 1% at 320 °C. Acrolein was the major product with this catalyst but propene oxide was also detected at 260 °C (12%). Without hydrogen in the reactor feed, propene conversion, as with all the catalysts, was much lower (0.063% ± 4%) at 320 °C. No propene oxide was formed when H_2 was not added and only acrolein and CO_2 were produced.

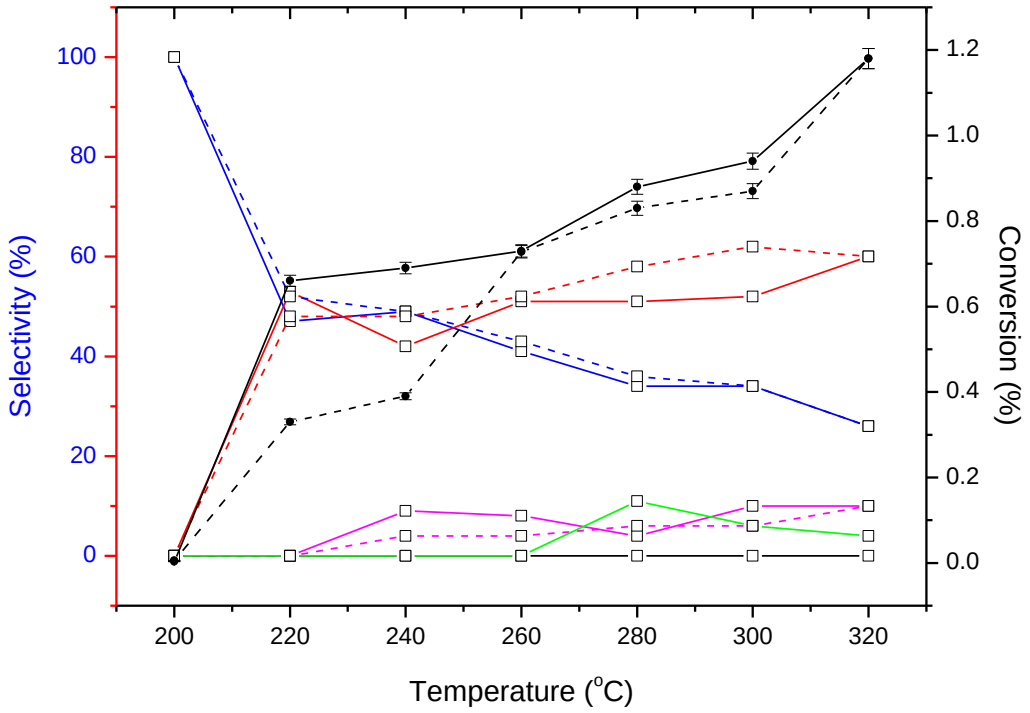

(a)

Figure 4.42 (a) Au/SiO_2 reduced in $NaBH_4$ (C978/80D) with H_2 addition.

Acrolein T $_{increase}$ Acrolein T$_{decrease}$ CO_2 T $_{increase}$ CO_2 T $_{decrease}$ Propene oxide T $_{increase}$ Propene Oxide T $_{decrease}$ Conversion T $_{increase}$ Conversion T $_{decrease}$

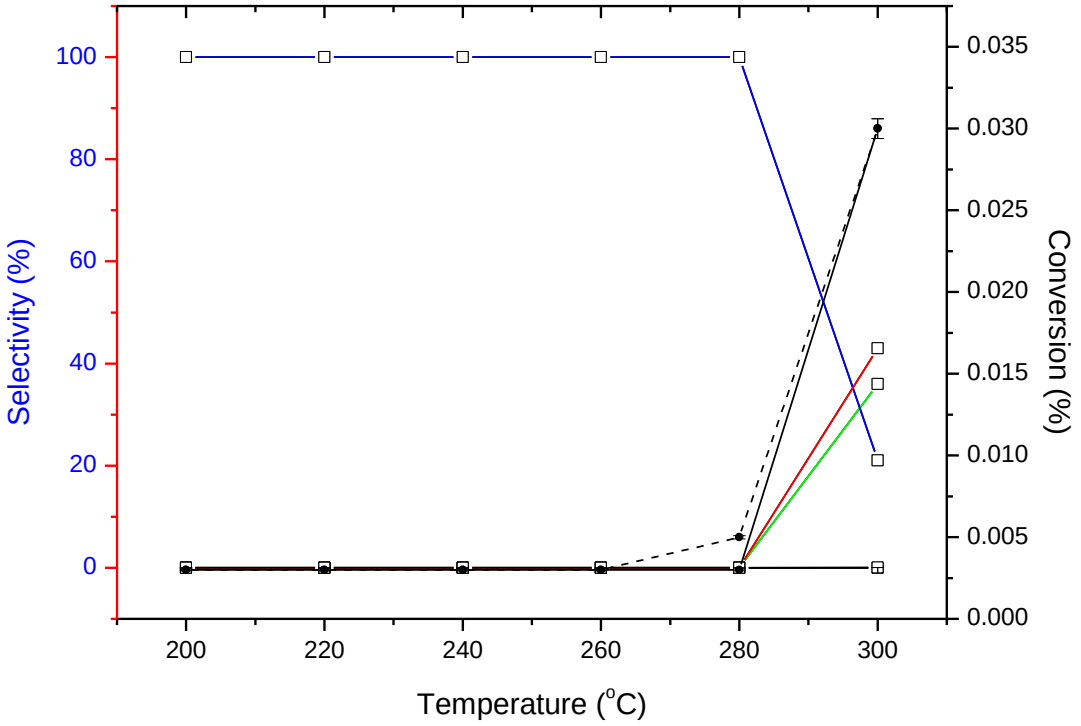

(b)

Figure 4.42 (b) Au/SiO_2 reduced in $NaBH_4$ (C978/80D) without H_2 addition.

Acrolein T $_{increase}$ Acrolein T$_{decrease}$ CO_2 T $_{increase}$ CO_2 T $_{decrease}$ Propene oxide T $_{increase}$ Propene Oxide T $_{decrease}$ Conversion T $_{increase}$ Conversion T $_{decrease}$

A monometallic Au/SiO_2 catalyst reduced by $NaBH_4$ was also prepared (Figure 4.42 (a) and 4.42 (b)) and with addition of H_2 there was a propene conversion of 1.2% ± 1% at 320 ^oC. At this temperature, acrolein (60%), CO_2 (27%), ethanal (10%) and propene oxide (3%) were formed. In the absence of H_2, a propene conversion of 0.03% ± 3% at 300 ^oC was observed. Both acrolein and propene oxide were produced at this temperature but the catalyst was not active at any other temperature.

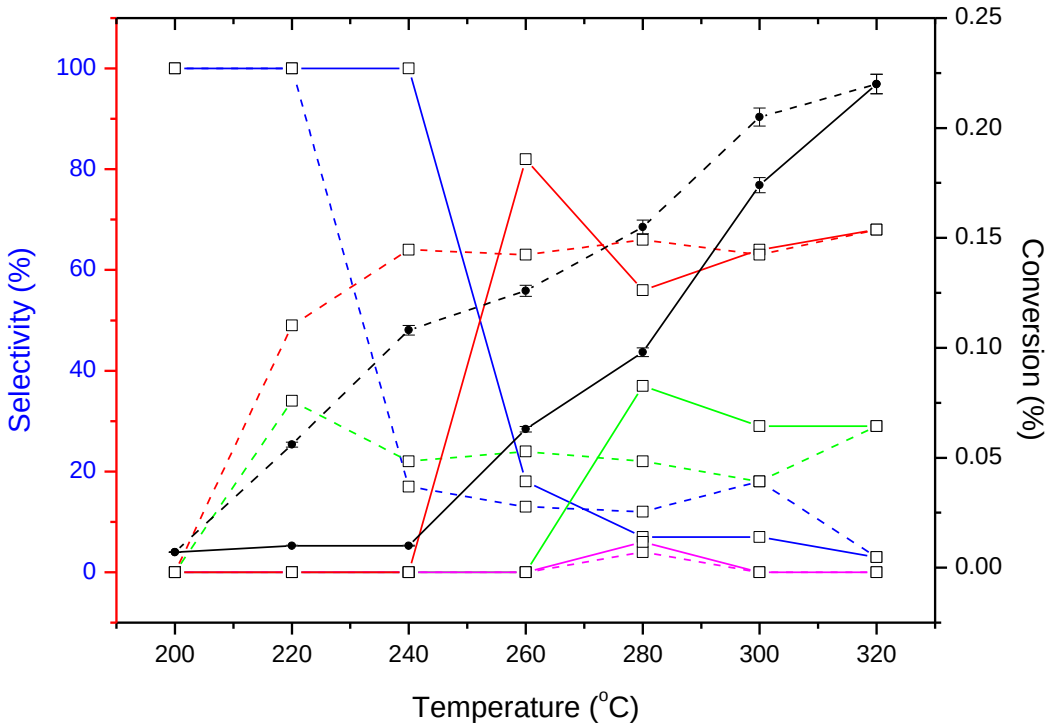

(a)

Figure 4.43 (a) Cu/SiO_2 reduced in $NaBH_4$ (C978/80E) with H_2 addition

Acrolein $T_{increase}$ Acrolein $T_{decrease}$ CO_2 $T_{increase}$ CO_2 $T_{decrease}$

Propene oxide $T_{increase}$ Propene Oxide $T_{decrease}$ Ethanal $T_{increase}$

Ethanal $T_{decrease}$ Conversion $T_{increase}$ Conversion $T_{decrease}$

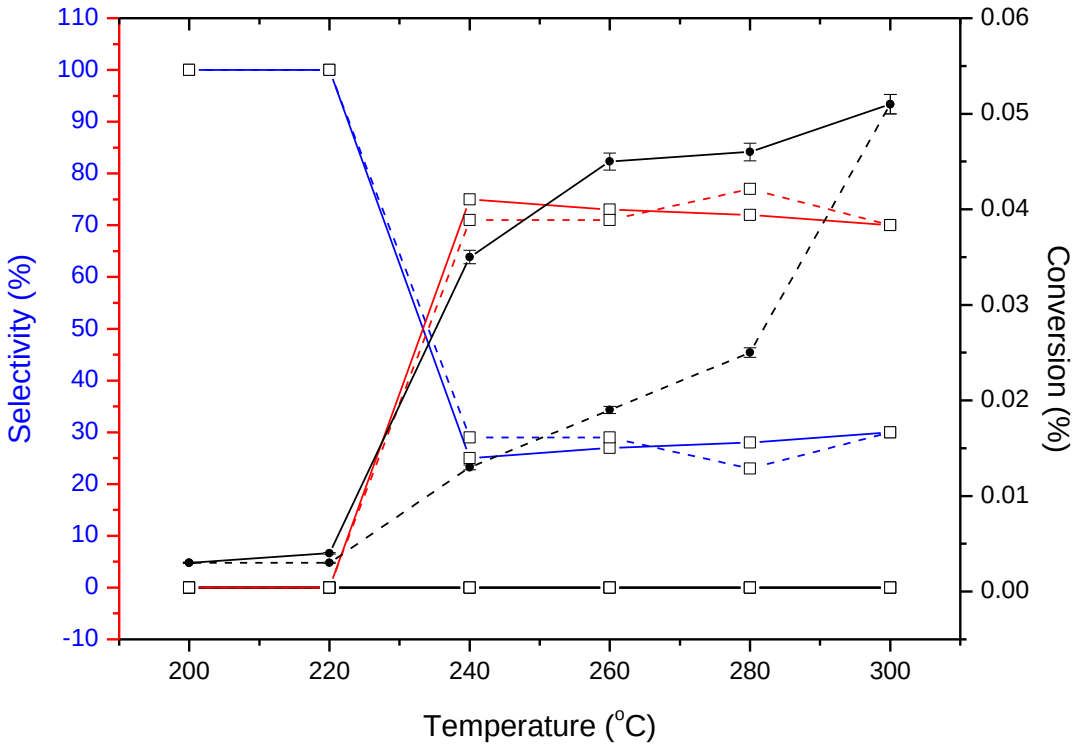

(b)

Figure 4.43 (b) Cu/SiO_2 reduced in $NaBH_4$ (C978/80E) without H_2 addition.

Acrolein $T_{increase}$ Acrolein $T_{decrease}$ CO_2 $T_{increase}$ CO_2 $T_{decrease}$

Propene oxide $T_{increase}$ Propene Oxide $T_{decrease}$ Ethanal $T_{increase}$

Ethanal $T_{decrease}$ Conversion $T_{increase}$ Conversion $T_{decrease}$

Cu/SiO_2 reduced by $NaBH_4$ (Figure 4.43 (a) and 4.43 (b)) was tested for propene oxidation with the addition of H_2. A propene conversion of 0.21% ± 3% at 320 ^oC was detected. Both acrolein (68%) and propene oxide (29%) were produced at this temperature. Without the presence of H_2, propene conversion was only 0.05% ± 4% at 300 ^oC. No propene oxide was formed. Only acrolein and carbon dioxide were observed.

4.4.5 Effect of Cu precursor for catalysts reduced by H_2

In this study, another set of catalysts relied on both copper chloride and copper nitrate as their precursors to make $CuAu/SiO_2$ catalysts by an impregnation procedure, followed by a reduction in H_2 for 2h at 400 ^oC. In this section, propene oxidation was investigated, with and without H_2, and the copper precursor was changed to identify whether any modification in product selectivity and conversion occurred.

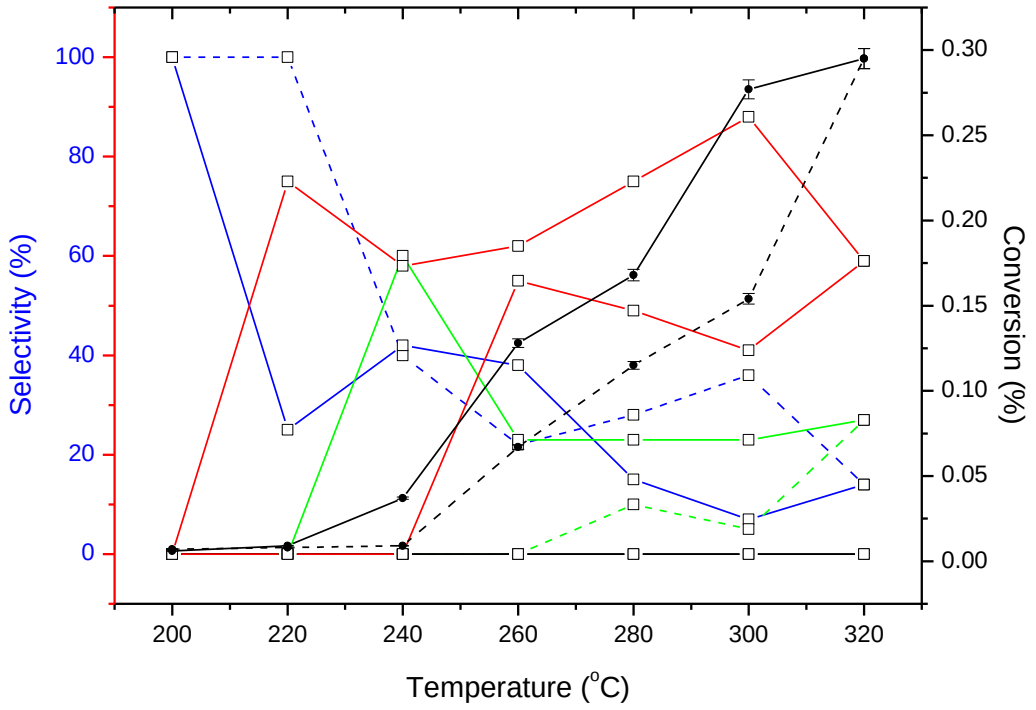

(a)

Figure 4.44 (a) $CuAu/SiO_2$ with copper nitrate precursor and reduced in H_2 (C978/93A) with H_2 addition ____Acrolein T $_{increase}$ - - - - Acrolein $T_{decrease}$ ____CO_2 T $_{increase}$ - - - - CO_2 T $_{decrease}$ ____ Propene oxide T $_{increase}$ - - - - Propene Oxide T $_{decrease}$ ____ Ethanal $T_{increase}$ - - - - Ethanal $T_{decrease}$ ____Conversion T $_{increase}$ ---- Conversion T $_{decrease}$

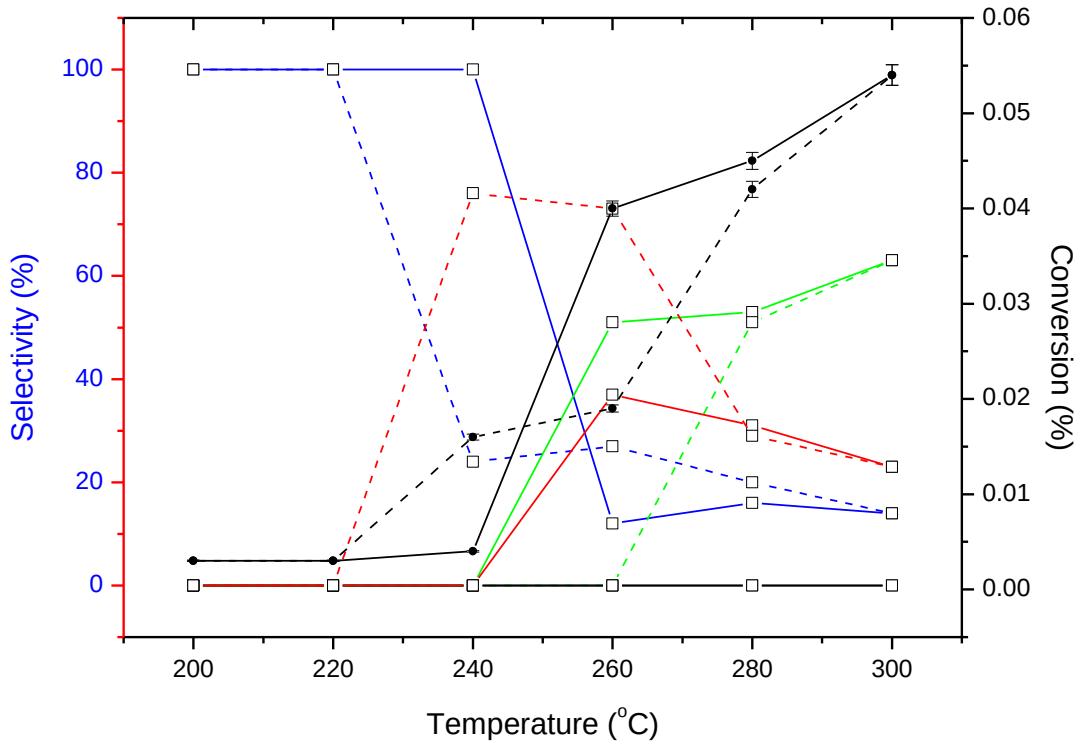

(b)

Figure 4.44 (b) $CuAu/SiO_2$ with copper nitrate precursor and reduced in H_2 (C978/93A) without H_2 addition ____ Acrolein $T_{increase}$ - - - - Acrolein $T_{decrease}$ ____ CO_2 $T_{increase}$ - - - - CO_2 $T_{decrease}$ ____ Propene oxide $T_{increase}$ - - - - Propene Oxide $T_{decrease}$ ____ Ethanal $T_{increase}$ - - - - - Ethanal $T_{decrease}$ ____ Conversion $T_{increase}$ ---- Conversion $T_{decrease}$

$CuAu/SiO_2$ prepared with a direct reduction, using copper nitrate (Figure 4.44 (a) and 4.44 (b)), had a propene conversion of 0.3% ± 2% at 320 °C with the presence of H_2. Both acrolein and propene oxide had selectivity. However, at 240 °C the error for the selectivity of propene oxide was ± 18% which would affect the reliability of this result. Therefore, there was some uncertainty with this result and repeat experiments at this temperature are necessary. Propene oxidation in the absence of H_2 for this catalyst gave a conversion of 0.055% ± 3% at 300 °C.

Propene oxide was more selective than acrolein as the temperature increased to 300 ^{o}C, whereas as the temperatures decreased, acrolein became more selective.

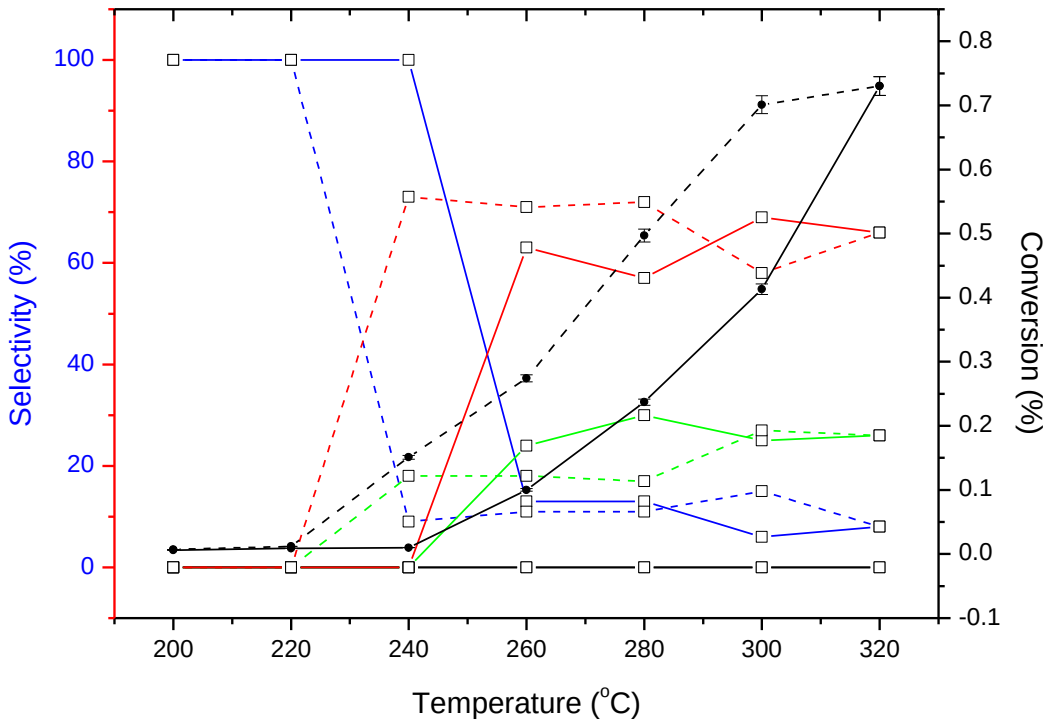

(a)

Figure 4.45 (a) $CuAu_3/SiO_2$ with copper nitrate precursor and reduced in H_2 (C978/93B) with H_2 addition ____Acrolein T $_{increase}$ - - - - Acrolein T$_{decrease}$ ____CO_2 T $_{increase}$ - - - - CO_2 T $_{decrease}$ ____ Propene oxide T $_{increase}$ - - - - Propene Oxide T $_{decrease}$ Ethanal T$_{decrease}$ ____Conversion T $_{increase}$ - - - - Conversion T $_{decrease}$

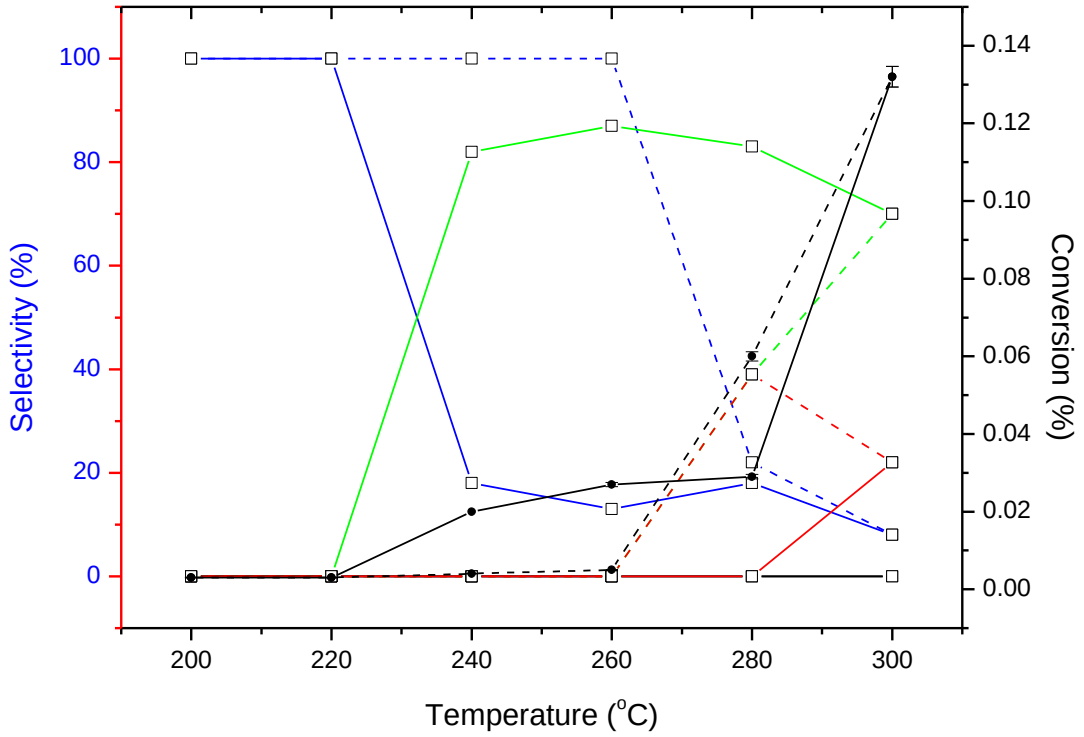

(b)

Figure 4.45 (b) $CuAu_3/SiO_2$ with copper nitrate precursor and reduced in H_2 (C978/93B) without H_2 addition ____ Acrolein T $_{increase}$ - - - - Acrolein T$_{decrease}$ ____CO_2 T $_{increase}$ - - - - CO_2 T $_{decrease}$ ____ Propene oxide T $_{increase}$ - - - - Propene Oxide T $_{decrease}$ Ethanal T$_{decrease}$ ____Conversion T $_{increase}$ - - - - Conversion T $_{decrease}$

The $CuAu/SiO_2$ had an effective propene conversion of 0.75% ± 1% at 320 ^{o}C. Acrolein (67%) and propene oxide (28%) were produced at this temperature. In the absence of H_2, the conversion reached 0.13% ± 2% which was much higher than other catalyst tested without H_2. Propene oxide was the product most selective under these conditions but acrolein was also detected at 300 ^{o}C (22%).

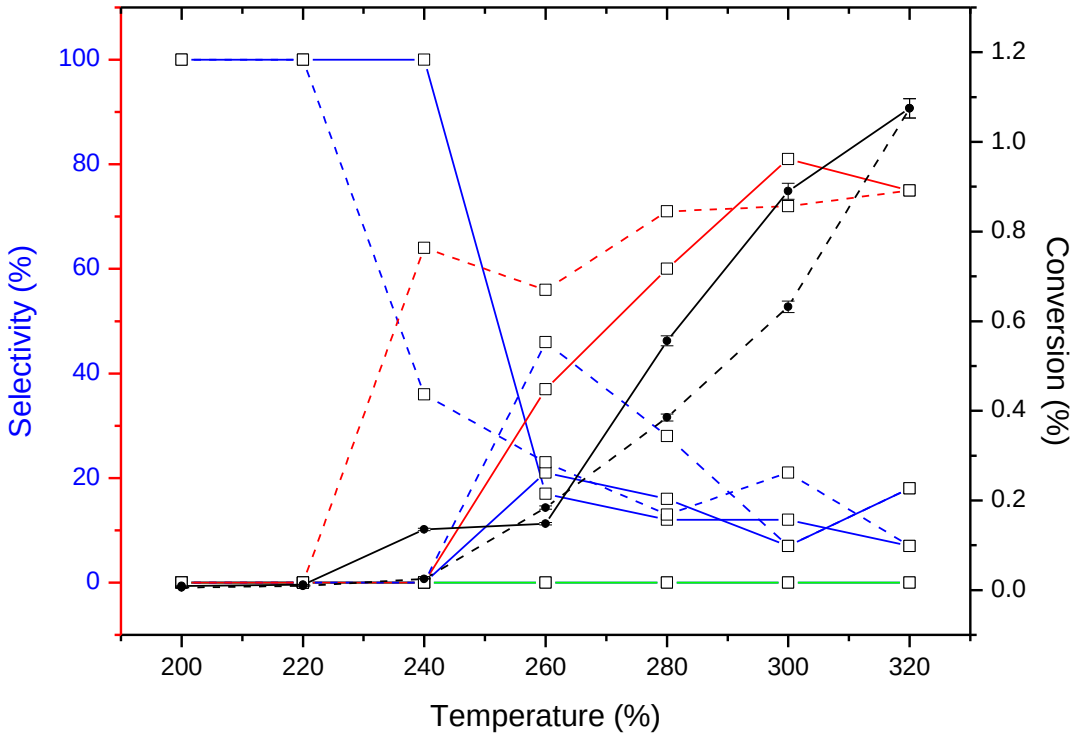

(a)

Figure 4.46 (a) Cu_3Au/SiO_2 with copper nitrate precursor, reduced H_2 (C978/93C). Propene oxidation with H_2 addition

Acrolein T $_{increase}$ Acrolein T$_{decrease}$ CO_2 T $_{increase}$ CO_2 T $_{decrease}$

Propene oxide T $_{increase}$ Propene Oxide T $_{decrease}$ Conversion T $_{increase}$

Conversion T $_{decrease}$

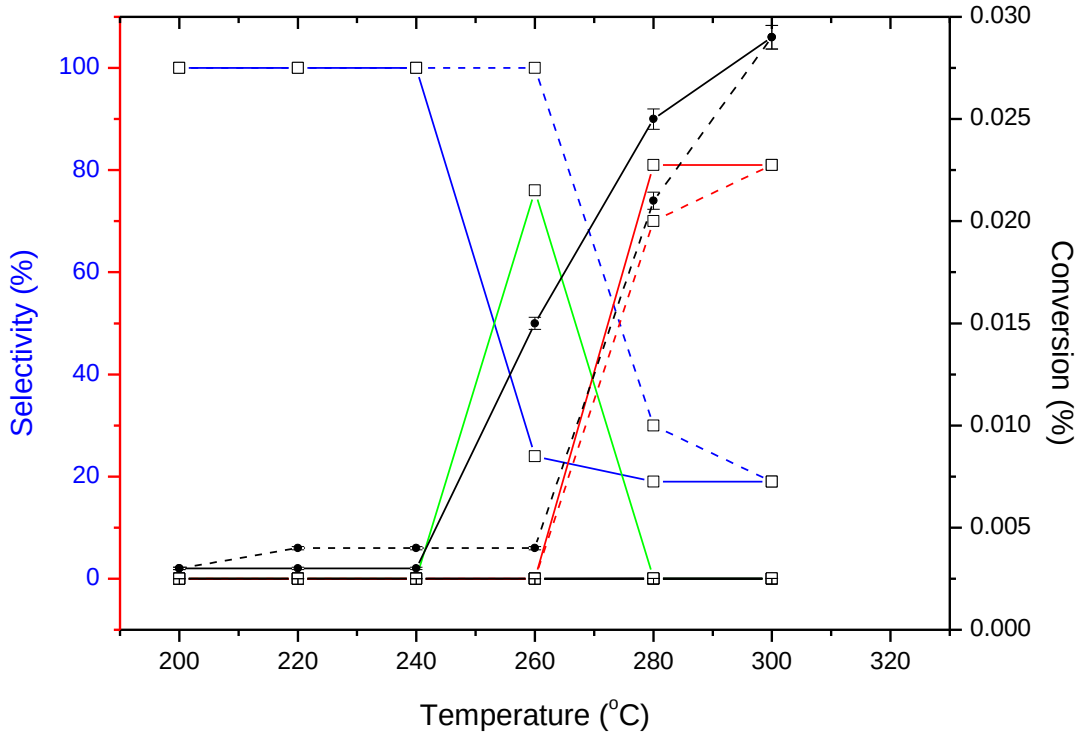

(b)

Figure 4.46 (b) Cu_3Au/SiO_2 with copper nitrate precursor, reduced H_2 (C978/93C). Propene oxidation without H_2 addition

Acrolein T $_{increase}$ Acrolein T$_{decrease}$ CO_2 T $_{increase}$ CO_2 T $_{decrease}$

Propene oxide T $_{increase}$ Propene Oxide T $_{decrease}$ Conversion T $_{increase}$

Conversion T $_{decrease}$

A Cu_3Au/SiO_2 catalyst reduced directly by H_2 was studied for propene oxidation, with and without H_2 (Figure 4.46 (a) and 4.46 (b)). With the addition of H_2, a propene conversion of 1.1% ± 1% was obtained at 320 ^oC, which was the highest activity for catalysts prepared under these conditions. Acrolein and propene oxide were both detected. Without H_2 in the reactor feed, the propene conversion was about 0.03% ± 3% at 300 ^oC and only acrolein and CO_2 were formed at this temperature. Propene oxide was very selective at 260 ^oC (78%). No ethanal was observed with this catalyst.

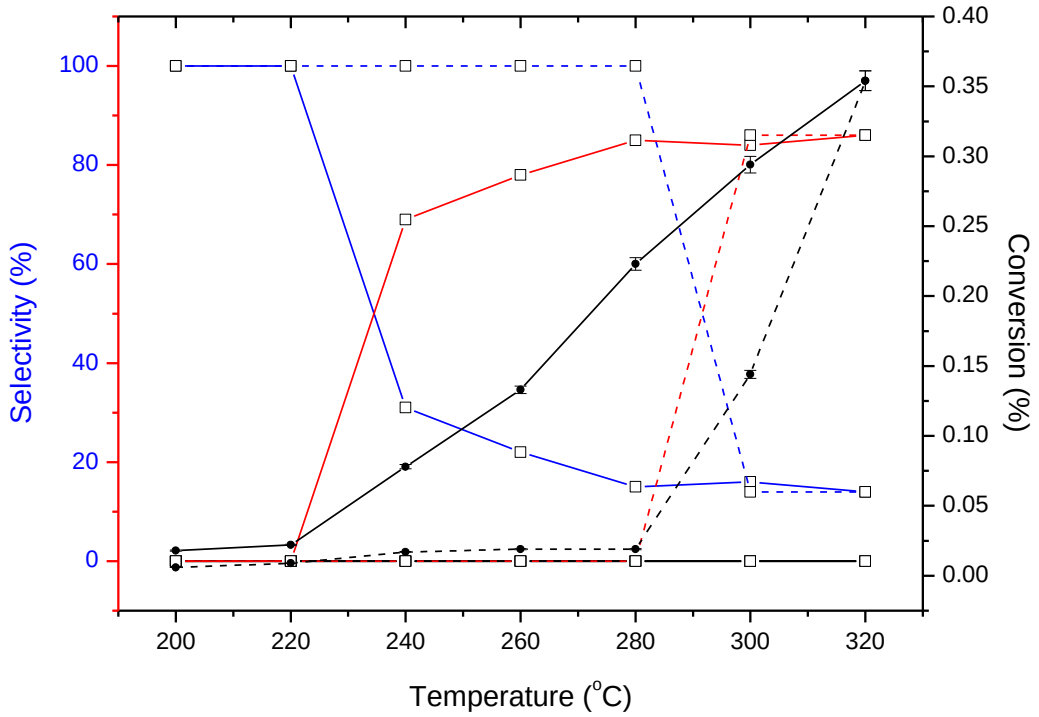

(a)

Figure 4.47 (a) Au/SiO_2 with copper nitrate precursor, reduced H_2 (C978/93D) with H_2 addition ____Acrolein T $_{increase}$ - - - - Acrolein T$_{decrease}$ ____CO_2 T $_{increase}$ - - - - CO_2 T $_{decrease}$ ____ Propene oxide T $_{increase}$ - - - - Propene Oxide T $_{decrease}$ ____Conversion T $_{increase}$ - - - - Conversion T $_{decrease}$

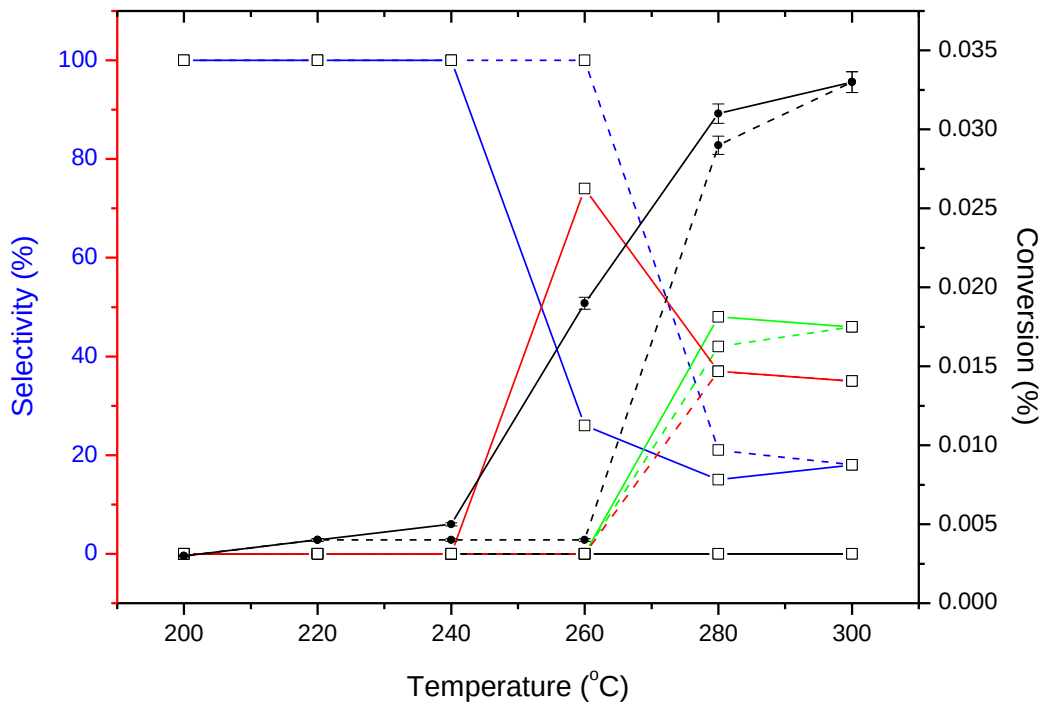

(b)

Figure 4.47 (b) Au/SiO_2 with copper nitrate precursor, reduced H_2 (C978/93D) without H_2 addition ____Acrolein T $_{increase}$ - - - - Acrolein T$_{decrease}$ ____CO_2 T $_{increase}$ - - - - CO_2 T $_{decrease}$ ____ Propene oxide T $_{increase}$ - - - - Propene Oxide T $_{decrease}$ ____Conversion T $_{increase}$ - - - - Conversion T $_{decrease}$

In the presence of H_2, the propene conversion for an Au/SiO_2 catalyst was 0.35% ± 2% at 320 ^oC. Acrolein and CO_2 were the only products that were formed with this catalyst. In the absence of H_2, acrolein and propene oxide were both produced but acrolein was most selective at 260 ^oC (72%).

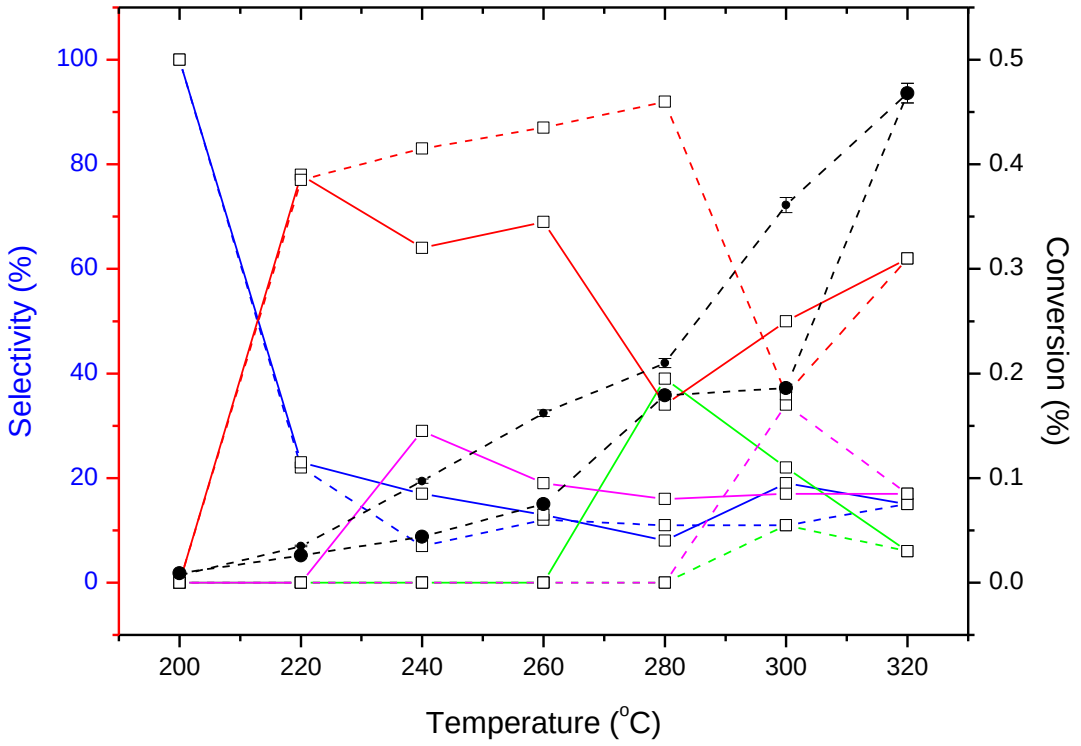

(a)

Figure 4.48 (a) Cu/SiO_2 with copper nitrate precursor, reduced H_2 (C978/93E) with H_2 addition ____ Acrolein $T_{increase}$ - - - - Acrolein $T_{decrease}$ ____ CO_2 $T_{increase}$ - - - - CO_2 $T_{decrease}$ ____ Propene oxide $T_{increase}$ - - - - Propene Oxide $T_{decrease}$ ____ Ethanal $T_{increase}$ - - - - Ethanal $T_{decrease}$ ____ Conversion $T_{increase}$ - - - - Conversion $T_{decrease}$

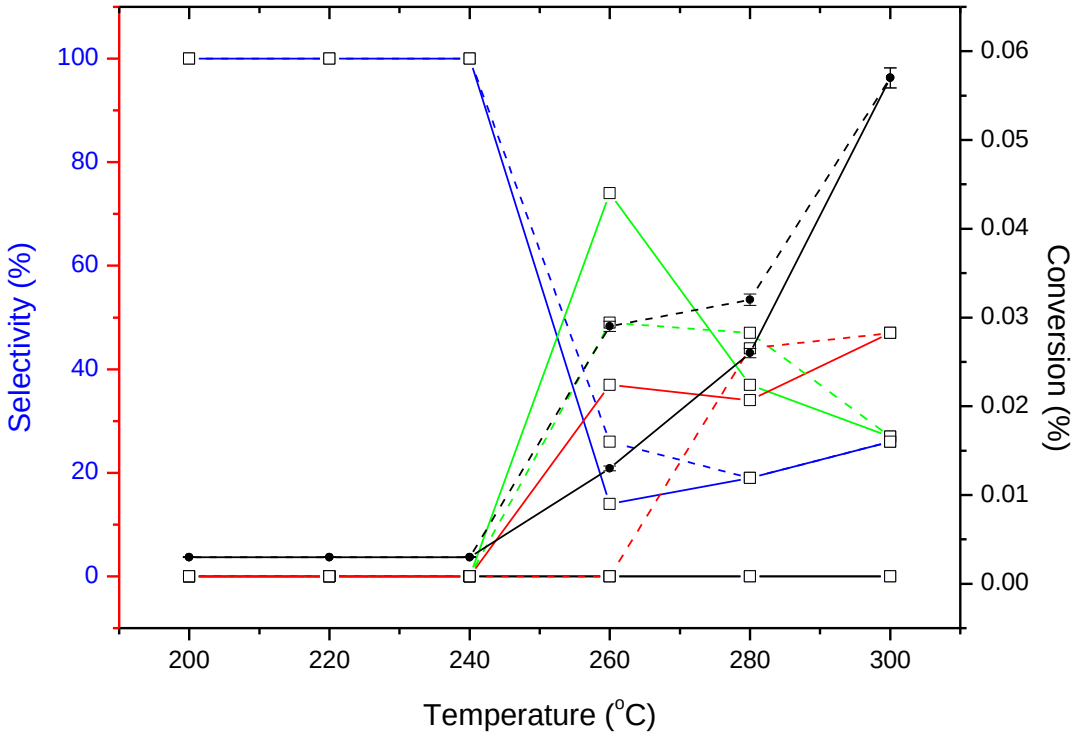

(b)

Figure 4.48 (b) Cu/SiO_2 with copper nitrate precursor, reduced H_2 (C978/93E) without H_2 addition. ____Acrolein $T_{increase}$ - - - - Acrolein $T_{decrease}$ ____CO_2 $T_{increase}$ - - - - CO_2 $T_{decrease}$ ____ Propene oxide $T_{increase}$ - - - - Propene Oxide $T_{decrease}$ ____ Ethanal $T_{increase}$ - - - - Ethanal $T_{decrease}$ ____Conversion $T_{increase}$ - - - - Conversion $T_{decrease}$

In the presence of H_2, the Cu/SiO_2 catalyst had a propene oxidation of 0.48% ± 2% at 320 °C. Acrolein, CO_2 and propene oxide were all detected at this temperature. Without H_2, the conversion dropped to 0.06% ± 5% at 300 °C and acrolein and propene oxide were observed between 260 and 300 °C.

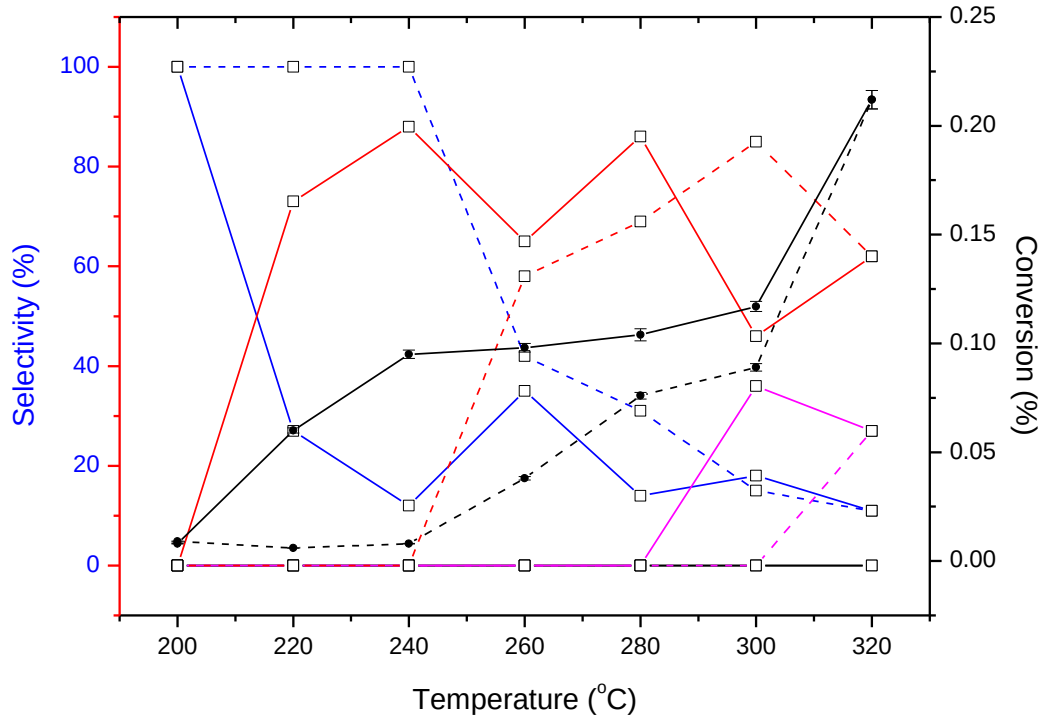

(a)

Figure 4.49 (a) CuAu/SiO_2 with copper chloride precursor, reduced in H_2 (C978/99A) with H2 addition (b) ____Acrolein T $_{increase}$ - - - - Acrolein T$_{decrease}$ ____CO_2 T $_{increase}$ - - - - CO_2 T $_{decrease}$ ____ Propene oxide T $_{increase}$ - - - - Propene Oxide T $_{decrease}$ ____ Ethanal T$_{increase}$ - - - - Ethanal T$_{decrease}$ ____Conversion T $_{increase}$ - - - - Conversion T $_{decrease}$

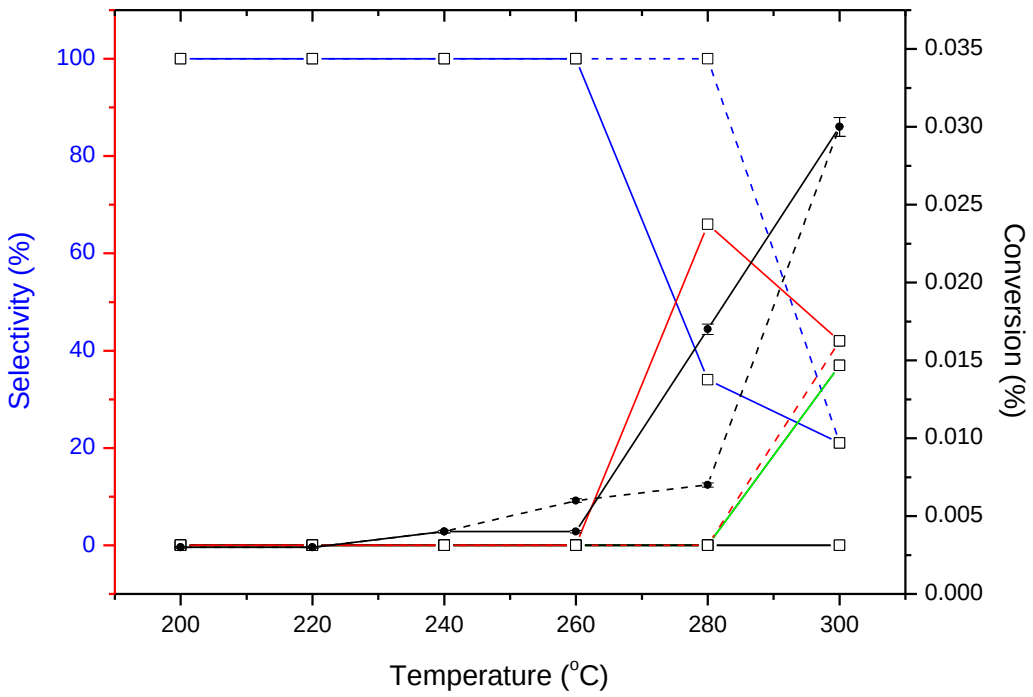

(b)

Figure 4.49 (b) CuAu/SiO_2 with copper chloride precursor, reduced in H_2 (C978/99A) without H_2 addition. ____Acrolein T $_{increase}$ - - - - Acrolein $T_{decrease}$ ____CO_2 T $_{increase}$ - - - - CO_2 T $_{decrease}$ ____ Propene oxide T $_{increase}$ - - - - Propene Oxide T $_{decrease}$ ____ Ethanal $T_{increase}$ - - - - - Ethanal $T_{decrease}$ _____Conversion T $_{increase}$ ---- Conversion T $_{decrease}$

CuAu/SiO_2 reduced by H_2 was tested for propene oxidation (Figure 4.49 (a) and 4.49 (b)) but the copper precursor was changed to copper chloride. In the presence of H_2, a propene conversion of 0.22% ± 3% was obtained at 320 ^{o}C. Propene oxide was not detected and only acrolein. CO_2 and ethanal were selective. In the absence of H_2, propene oxide and acrolein were produced but the catalyst had little activity, the conversion being low as anticipated.

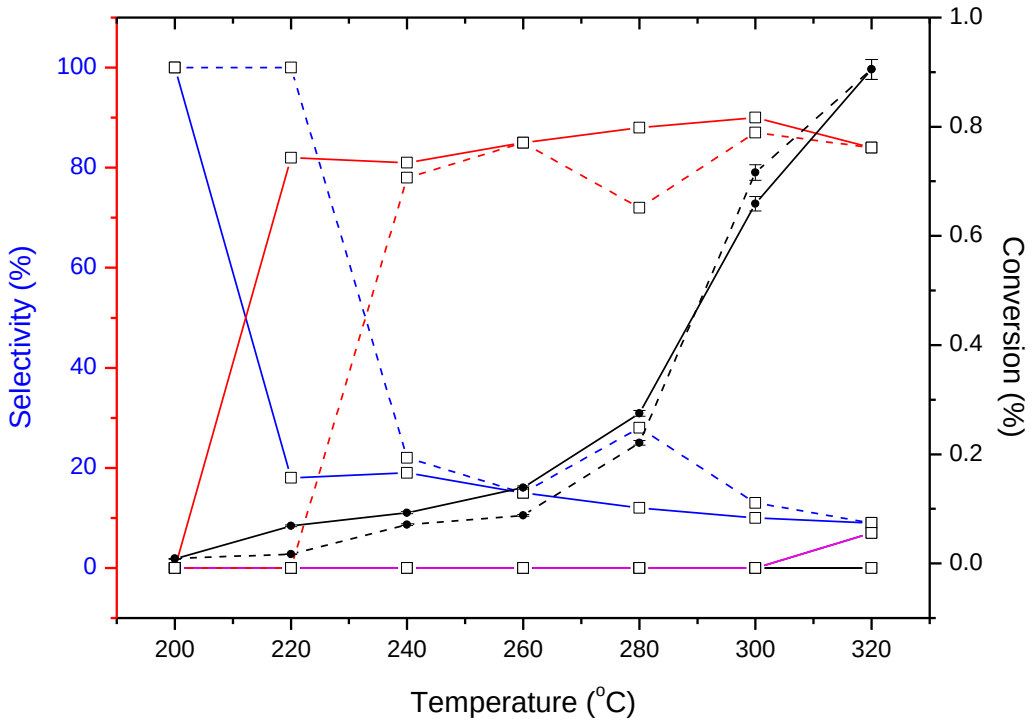

(a)

Figure 4.50 (a) $CuAu_3/SiO_2$ with copper chloride precursor, reduced in H_2 (C978/99B) with H_2 addition ____Acrolein $T_{increase}$ - - - - Acrolein $T_{decrease}$ ____CO_2 $T_{increase}$ - - - - CO_2 $T_{decrease}$ ____ Propene oxide $T_{increase}$ - - - - Propene Oxide $T_{decrease}$ ____ Ethanal $T_{increase}$ - - - - Ethanal $T_{decrease}$ ____Conversion $T_{increase}$ - - - - Conversion $T_{decrease}$

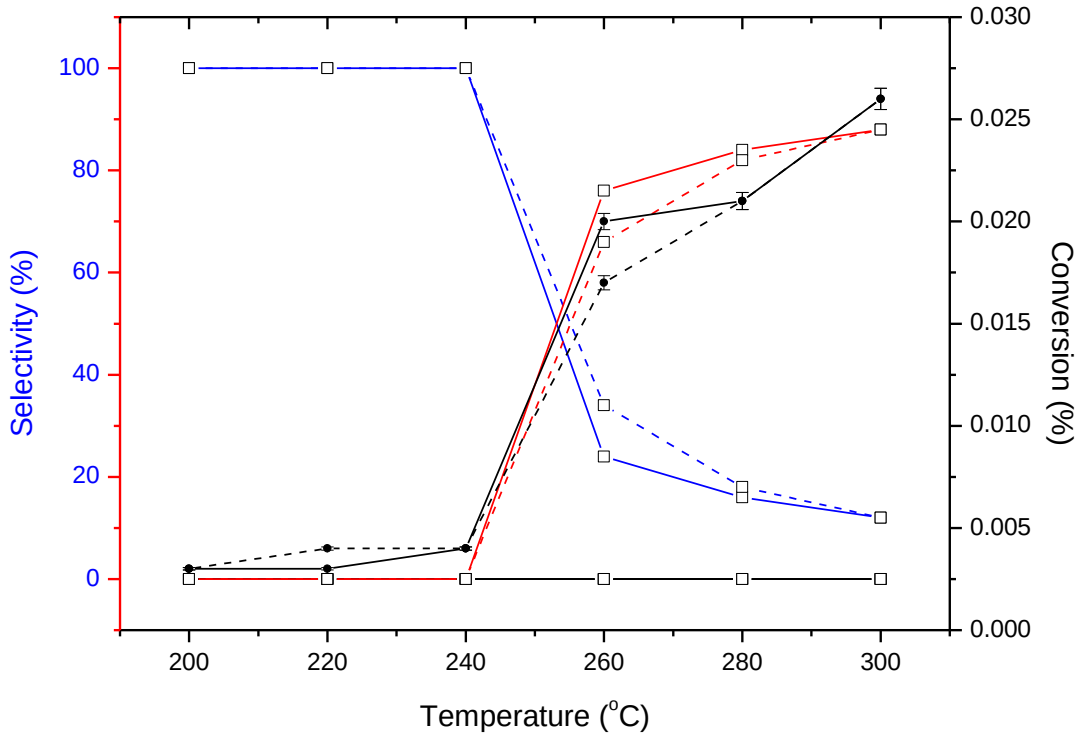

(b)

Figure 4.50 (b) $CuAu_3/SiO_2$ with copper chloride precursor, reduced in H_2 (C978/99B) without H_2 addition. ____Acrolein T $_{increase}$ - - - - Acrolein $T_{decrease}$ ____CO_2 T $_{increase}$ - - - - CO_2 T $_{decrease}$ ____ Propene oxide T $_{increase}$ - - - - Propene Oxide T $_{decrease}$ ____ Ethanal $T_{increase}$ - - - - Ethanal $T_{decrease}$ ____Conversion T $_{increase}$ - - - - Conversion T $_{decrease}$

The Au rich $CuAu_3/SiO_2$ catalyst, reduced in H_2 with copper chloride, had a propene conversion of 0.9% ± 2% at 320 ^oC, which was higher than when copper nitrate precursor was used. Acrolein was the most selective product (90% at 300 ^oC). Without H_2, only acrolein and CO_2 were observed at 300 ^oC.

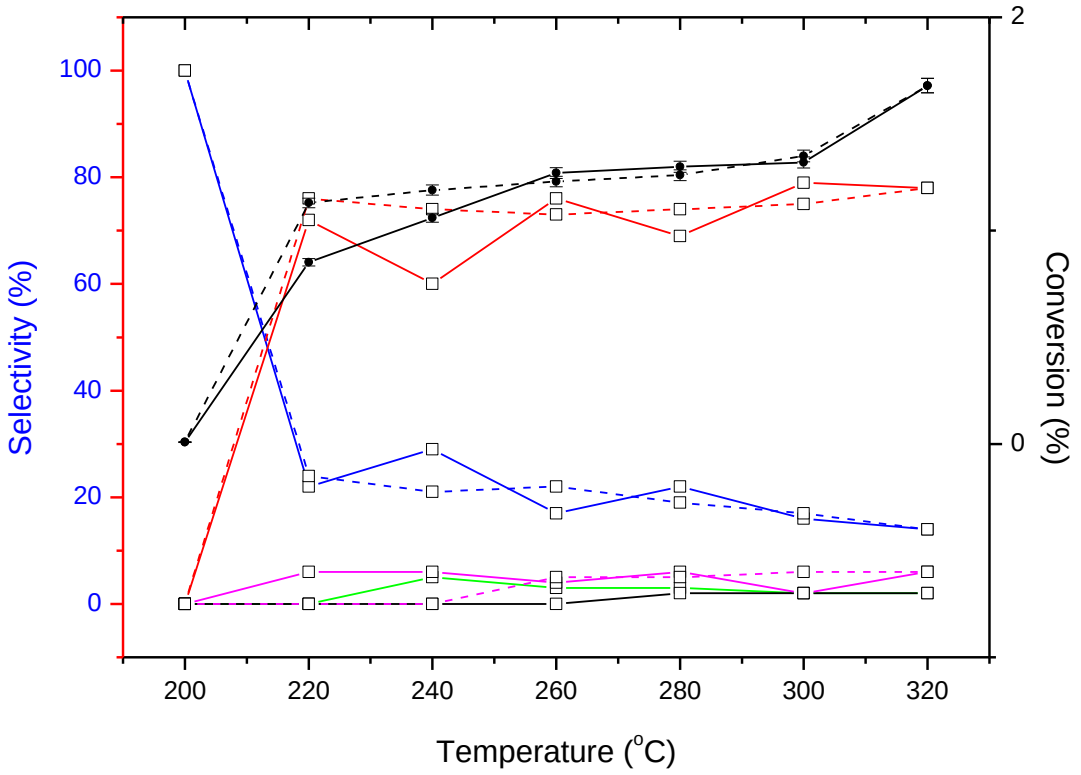

(a)

Figure 4.51 (a) Cu_3Au/SiO_2 with copper chloride precursor, reduced in H_2 (C978/99C) with H_2 addition ____ Acrolein T $_{increase}$ - - - - Acrolein $T_{decrease}$ ____CO_2 T $_{increase}$ - - - - CO_2 T $_{decrease}$ ____ Propene oxide T $_{increase}$ - - - - Propene Oxide T $_{decrease}$ ____ Ethanal $T_{increase}$ - - - - Ethanal $T_{decrease}$ ____Conversion T $_{increase}$ - - - - Conversion T $_{decrease}$

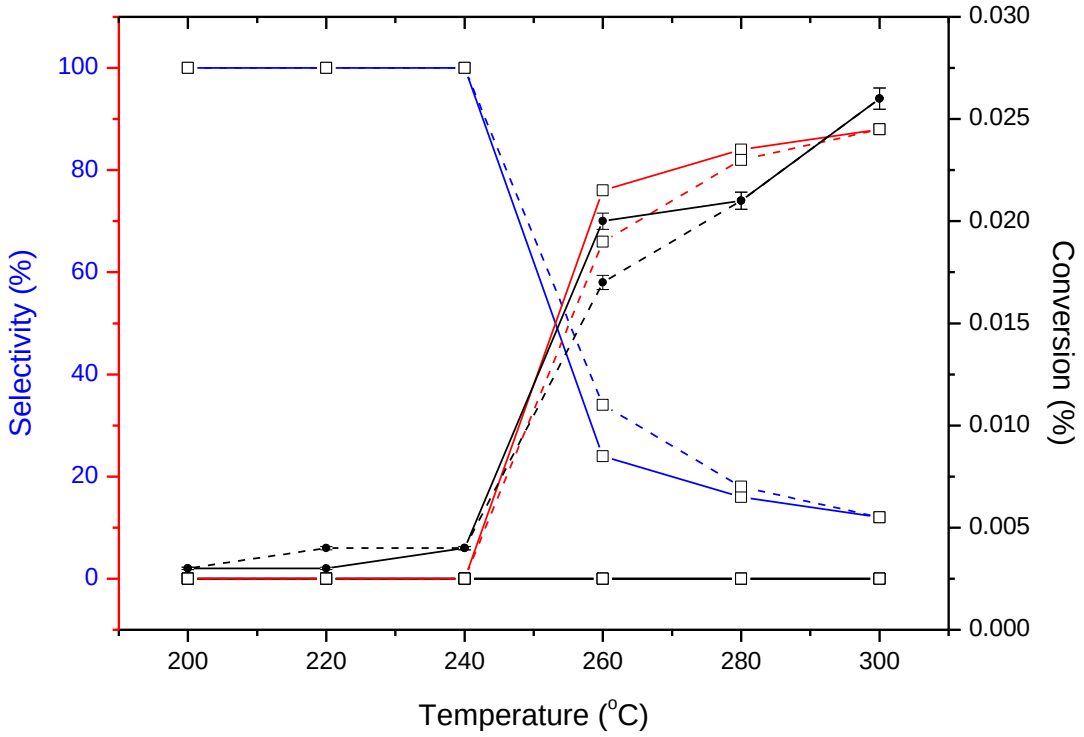

(b)

Figure 4.51 (b) Cu_3Au/SiO_2 with copper chloride precursor, reduced in H_2 (C978/99C) without H_2 addition. ____Acrolein T $_{increase}$ - - - - Acrolein T$_{decrease}$ ____CO_2 T $_{increase}$ - - - - CO_2 T $_{decrease}$ ____ Propene oxide T $_{increase}$ - - - - Propene Oxide T $_{decrease}$ ____ Ethanal T$_{increase}$ - - - - Ethanal T$_{decrease}$ ____Conversion T $_{increase}$ - - - - Conversion T $_{decrease}$

The Cu rich Cu_3Au/SiO_2 catalyst, reduced in H_2 with copper chloride, had a higher propene conversion (1.7% ± 1%) than when copper nitrate was used (0.7% ± 1.6%). Acrolein was the most selective product but ethanal was also detected at about ~5%. In the absence of H_2 only acrolein and carbon dioxide were formed, whereas when copper nitrate was used propene oxide was also observed.

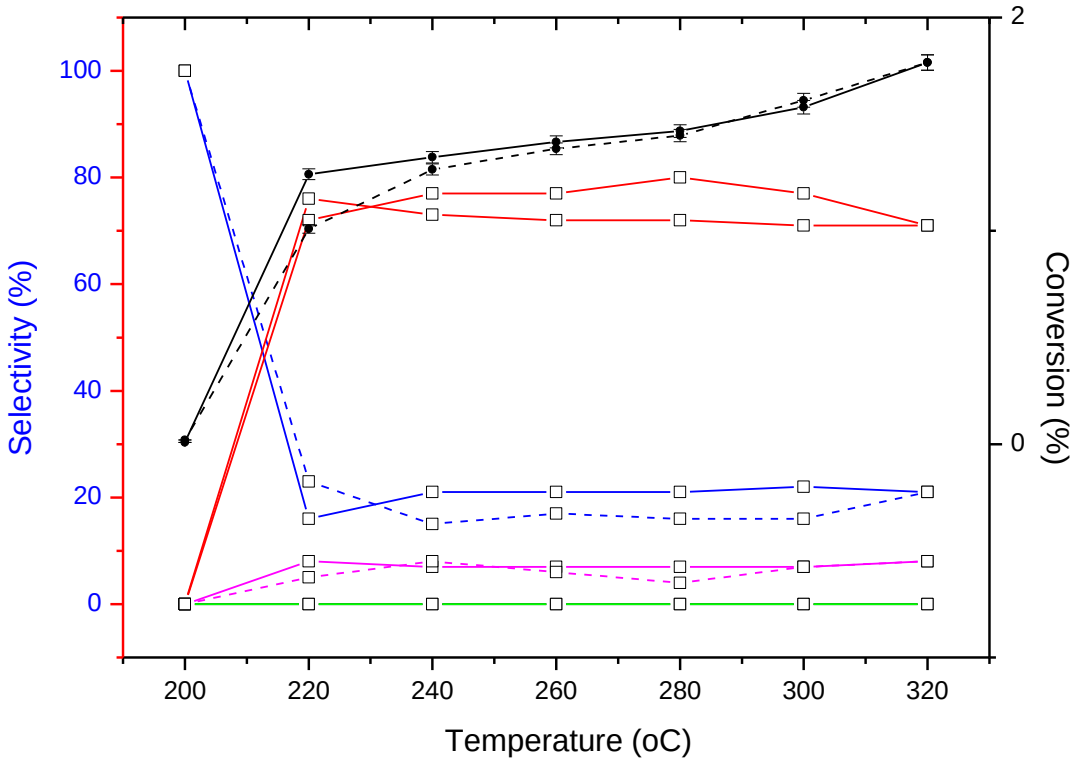

(a)

Figure 4.52 (a) Cu/SiO_2 with copper chloride precursor, reduced in H_2 (C978/99D) with H_2 addition ____ Acrolein T $_{increase}$ - - - - Acrolein $T_{decrease}$ ____ CO_2 T $_{increase}$ - - - - CO_2 T $_{decrease}$ ____ Propene oxide T $_{increase}$ - - - - Propene Oxide T $_{decrease}$ ____ Ethanal $T_{increase}$ - - - - Ethanal $T_{decrease}$ ____ Conversion T $_{increase}$ - - - - Conversion T $_{decrease}$

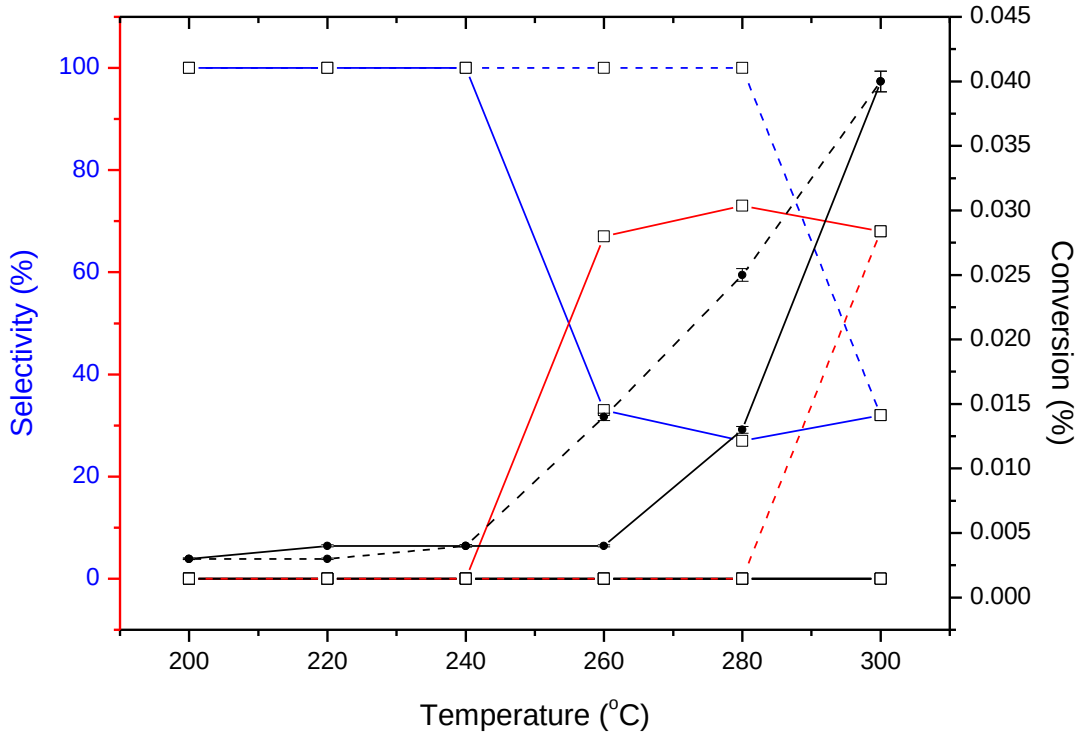

(b)

Figure 4.52 (b) Cu/SiO_2 with copper chloride precursor, reduced in H_2 (C978/99D) without H_2 addition. ____Acrolein $T_{increase}$ - - - - Acrolein $T_{decrease}$ ____CO_2 $T_{increase}$ - - - - CO_2 $T_{decrease}$ ____ Propene oxide $T_{increase}$ - - - - Propene Oxide $T_{decrease}$ ____ Ethanal $T_{increase}$ - - - - Ethanal $T_{decrease}$ ____Conversion $T_{increase}$ ---- Conversion $T_{decrease}$

Cu/SiO_2 was also prepared with copper chloride and reduced in H_2 (Figure 4.52 (a) and 4.52 (b)). In the presence of H_2, a propene conversion of 1.8% ± 1% was obtained at 320 ^oC which was the most active out of all the catalysts made under these conditions. This catalyst had a stable activity with acrolein selectivity of about 70 to 80% between 220 to 320 ^oC. No propene oxide was observed but ethanal was detected between 220 ^oC and 320 ^oC at about 10% selectivity. In the absence of H_2, acrolein and CO_2 were the only products obtained whereas, when copper nitrate was used, propene oxide was also produced.

4.4.6 Product selectivity and conversion for different preparation methods

The presence or absence of hydrogen for the propene oxidation experiments had a significant effect on the propene conversion. The choice of copper precursor and the preparation conditions could also affect the product selectivity. In this section, bar charts have been used to illustrate the selectivity and conversions of different catalysts, which were all made by impregnation, and either reduced by H_2 or $NaBH_4$ and which had different copper precursors.

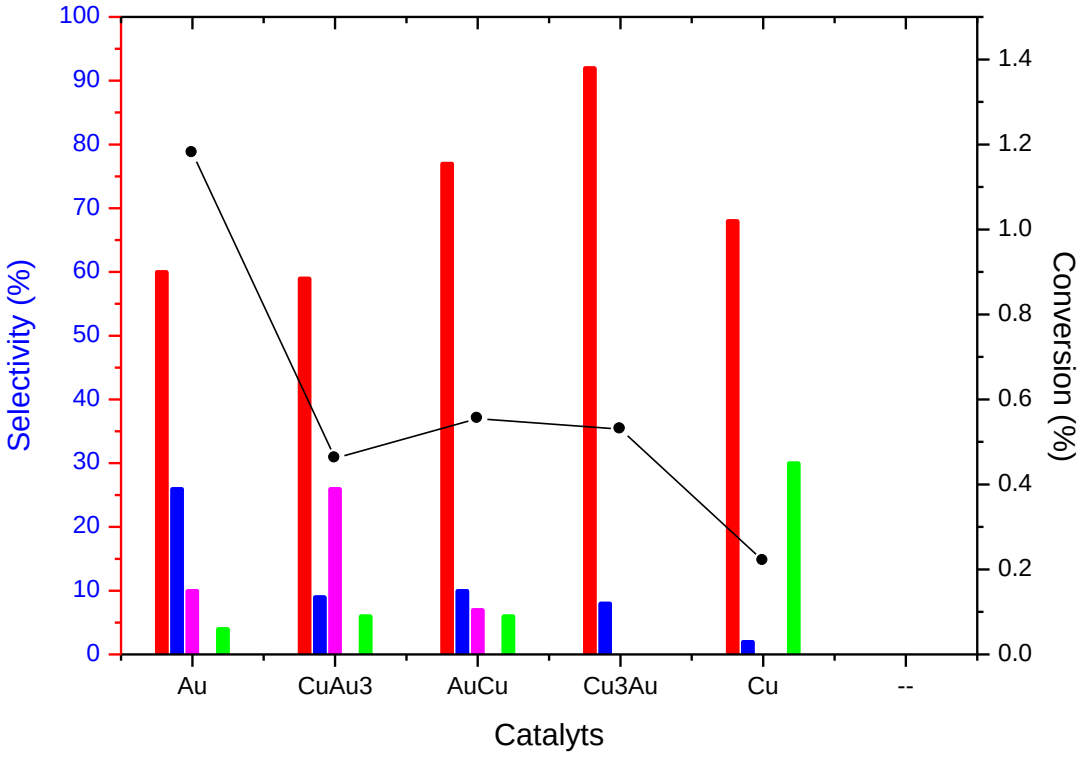

Figure 4.53 Catalysts reduced with $NaBH_4$ (C978/80A-E) with H_2 addition at 320 ^oC.
Acrolein CO_2 Propene oxide Ethanal Conversion

For all the catalysts prepared by impregnation using copper nitrate and reduced in $NaBH_4$, acrolein was the main product of propene oxidation in the presence of H_2 at a temperature of 320 ^oC. No propene oxide was detected for the copper rich Cu_3Au/SiO_2 catalyst. Propene

oxide was most selective for the monometallic Cu/SiO_2 catalyst and ethanal was only seen in the Au/SiO_2, $CuAu_3/SiO_2$ and $AuCu/SiO_2$ samples tested. Propene conversion was the highest for the Au/SiO_2 catalyst (1.2% ± 1%) and lowest for the Cu/SiO_2 catalyst (0.2% ± 3%).

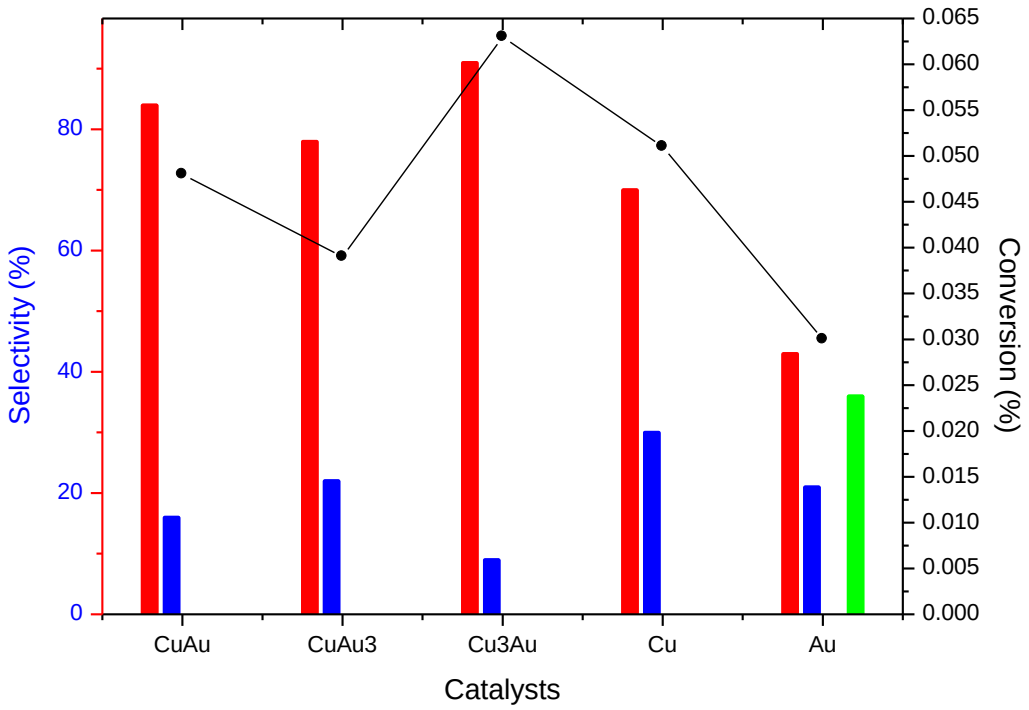

Figure 4.54 Catalysts reduced with $NaBH_4$ (C978/80A-E) without H_2 addition at 320 ^oC.
Acrolein CO_2 Propene oxide Ethanal Conversion

When the catalysts were used for propene oxidation without H_2 (Figure 4.54), the most notable effect was that the conversion was greatly reduced. All the catalyst were still selective towards acrolein, as they were in the presence of H_2. However, Au/SiO_2 was the only catalyst selective towards propene oxide and no catalyst produces ethanal.

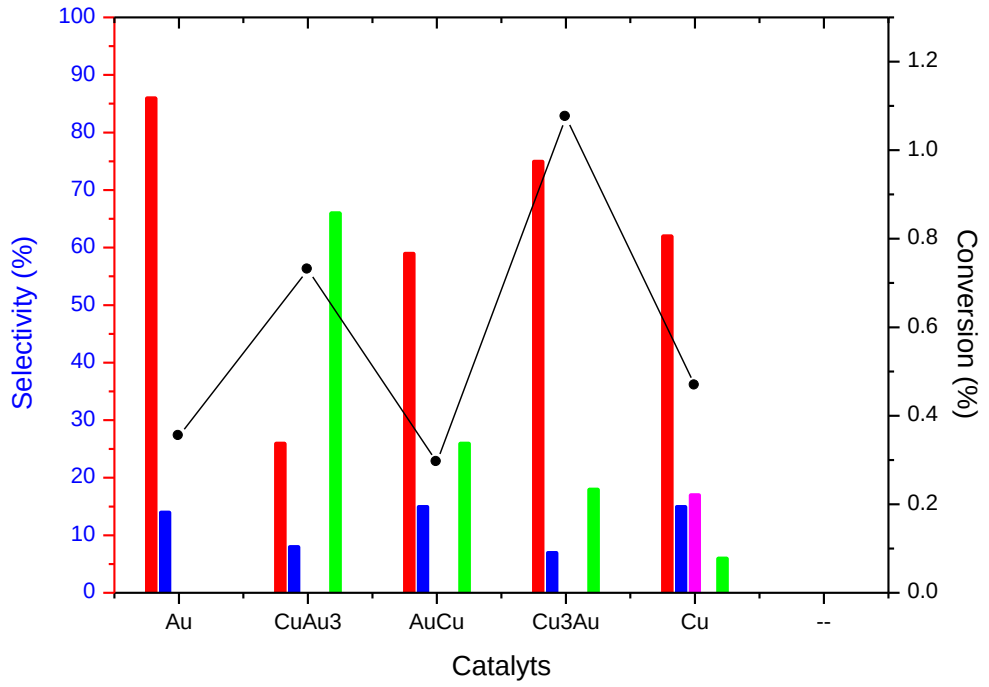

Figure 4.55 Catalysts made with a copper nitrate precursor by impregnation, reduced in H_2 (C978/93A-E).

Acrolein CO_2 Propene oxide Ethanal Conversion

If the catalysts were reduced in H_2, instead of $NaBH_4$, then the selectivities of the products are changed (Figure 4.55). All the series of catalyst were selective towards acrolein. Apart from the Au/SiO_2 catalyst, all the other samples were selective to propene oxide. Ethanal was only one with selectivity for the Cu/SiO_2 catalyst. The Cu rich Cu_3Au/SiO_2 had the highest conversion of 1.1% ± 1%.

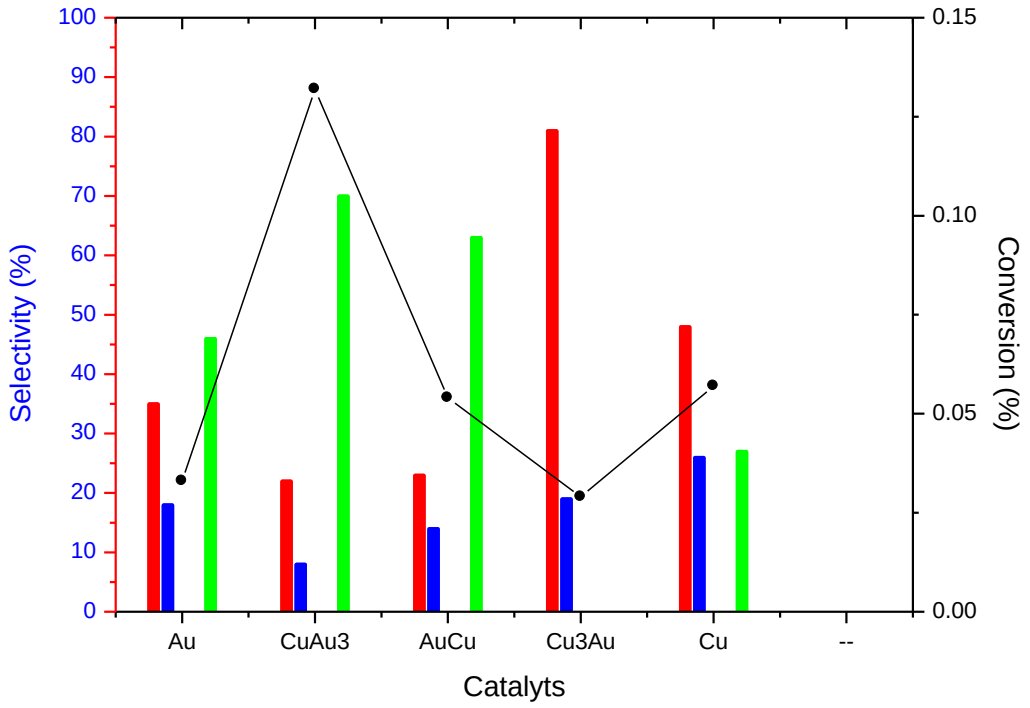

Figure 4.56 Catalyst made with a copper nitrate precursor reduced in H_2 (C978/93A-E). Propene oxidation at 300 ^{o}C without H_2.
Acrolein CO_2 Propene oxide Ethanal Conversion

When H_2 was not present in the reactor feed, all the catalyst were selective to both acrolein and propene oxide, except for the Cu_3Au/SiO_2. The Au rich bimetallic catalyst had the highest propene conversion of 0.13% ± 4%.

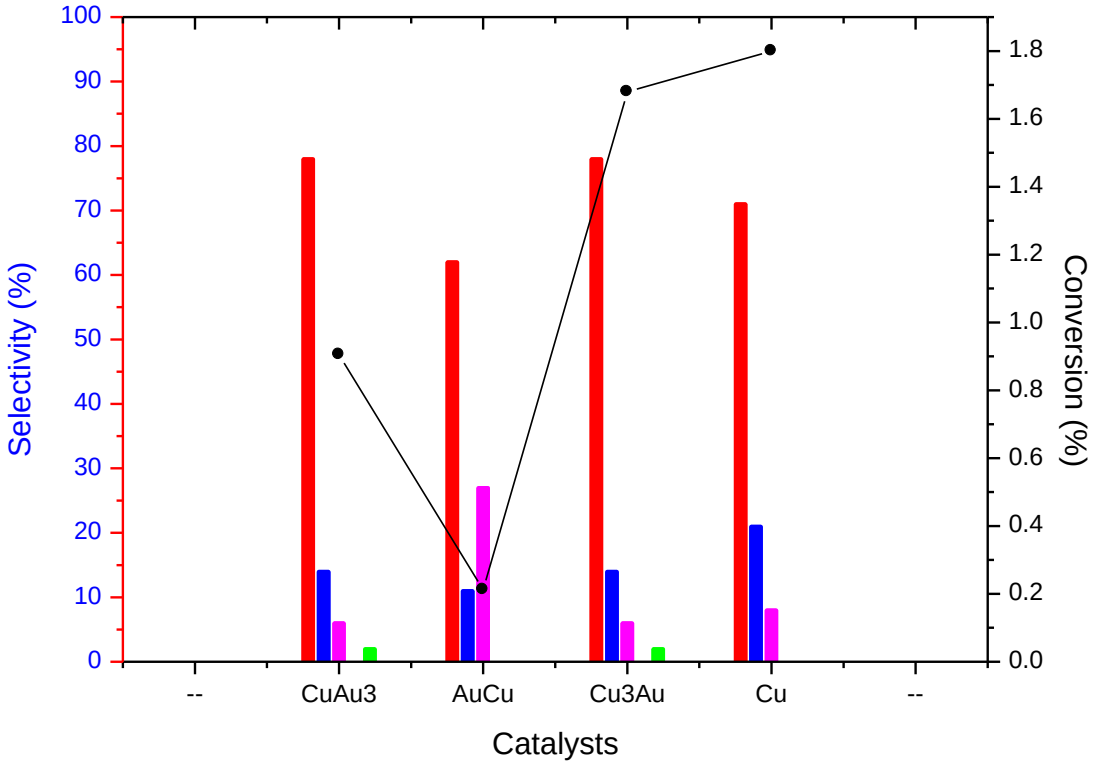

Figure 4.57 Catalysts made with a copper chloride precursor by impregnation, reduced in H_2 (C978/99A-D). Propene oxidation at 320 ^{o}C with H_2.
Acrolein CO_2 Propene oxide Ethanal Conversion

If the copper precursor was changed from copper nitrate to copper chloride, then all the catalysts were selective towards ethanal and acrolein. Only the Cu rich and Au rich catalysts formed propene oxidation. The Cu_3Au/SiO_2 and the Cu/SiO_2 catalyst had higher conversions than the Au rich Cu_3Au/SiO_2 and Au/SiO_2.

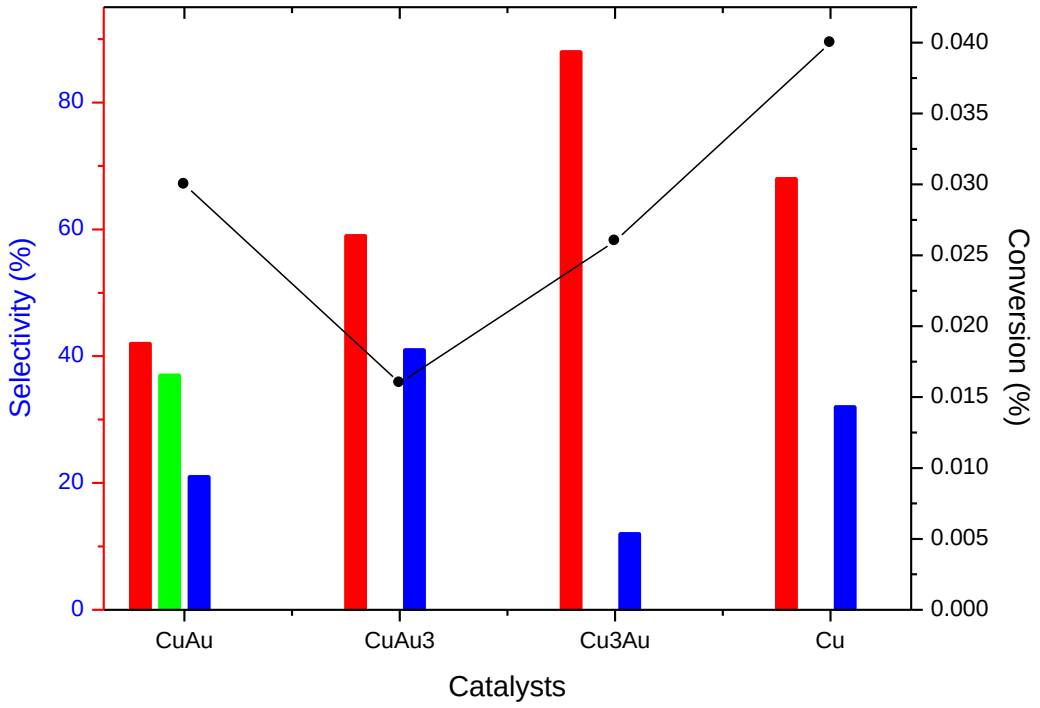

Figure 4.59 Catalysts made with a copper chloride precursor reduced in H_2. (C97899A-D). Propene oxidation at 300 ^{o}C without H_2.
Acrolein CO_2 Propene oxide Ethanal Conversion

If the catalyst had first been reduced in H_2 and a copper chloride precursor used (Figure 4.58) then, in the absence of H_2, only the $CuAu/SiO_2$ catalyst was selective towards acrolein and propene oxide. The Cu/SiO_2 catalyst had the highest propene conversion of 0.04% ± 6%.

4.5 Discussion

For all the catalysts tested for propene oxidation only single experiments were carried out due to time constraints. However, for each experiment three injections were used at each temperature to give an average result. Unless otherwise stated, the error was in the range of between ±1- 6% of the value quoted which gave data that could be justified, as long as the limitations from the absence of repeat experiments were taken into account. Duplicate experiments would be required to confidently confirm the findings in this study.

The activity and selectivity of the catalysts studied for propene oxidation with and without hydrogen addition, showed that they could be affected by their composition and thermal treatment. Most of the catalysts possessed low propene conversions, compared with past catalysts used to test for this reaction. This was due to the high gas space velocity used in the experiments. Gas space velocity can affect the catalyst performance and this has been observed by Zhan and group.[7] They found that with increasing space velocity the propene conversion decreased but the selectivity towards propene oxide increased. This could be explained because with the space velocity increasing, the contact time of propane and propylene with the catalyst became short and therefore part of them left the catalyst surface without reacting. Therefore, propane conversion decreased. Different gas feed ratios for reactions with and without hydrogen were used and this may have an effect on the catalyst's performance. Therefore, it was difficult to compare the results in the absence versus presence of hydrogen, as the reaction conditions varied and caused limitations with the results.

Effect of different catalyst preparation and copper precursor

Different preparation methods and the use of either copper chloride or copper nitrate precursors were used to make monometallic Cu/SiO_2 catalysts. A simple Cu/SiO_2 catalyst prepared by impregnation with copper nitrate and directly calcined, was investigated for

propene oxidation. With the addition of hydrogen, a propene conversion of 0.3% (at 320 ^{o}C) was obtained with a selectivity to only acrolein and ethanal. In the absence of hydrogen, the conversion was much lower and propene oxide was detected as the temperature of the hysteresis experiment decreased. XPS analysis for the directly calcined Cu/SiO_2 catalyst confirmed the presence of Cu^{2+} species. Modifying the catalyst, so that the copper chloride was the chosen precursor used, led to a much higher propene conversion of 0.9% ± 1.4% (320 ^{o}C) with the addition of H_2. This catalyst was selective to acrolein at higher temperatures and propene oxide at lower temperatures, which was the general trend for most of the catalysts tested. Instead of a direct calcination in air, some catalysts had the Sinfelt thermal treatment applied (reduction at 315 ^{o}C for 2h in 5% Ar/H_2 followed by high temperature calcination at 676 ^{o}C for 15h in air). This thermal treatment was used for a Cu/SiO_2 catalyst and analysed for propene oxidation. With the addition of hydrogen, the copper catalyst was active with a propene conversion of 2.3% ± 1% (at 320 ^{o}C). The main product was acrolein, although ethanal was detected at 260 ^{o}C (10%). When hydrogen was not present in the reactor feed, there was little activity and only CO_2 was formed. The XPS data for the Sinfelt catalysts confirmed the presence of Cu^{+} species due to the absence of the Cu^{2+} satellite peak. Whereas for the directly calcined $AuCu/SiO_2$ and Au_3Cu/SiO_2 there did not appear to be a Cu^{2+} satellite peak, suggesting the presence of a Cu^{+} species.

XRD analysis showed that there were differences between directly calcined and Sinfelt treated catalysts. All the Sinflet $CuAu/SiO_2$ compositions (1:1, 1:3 and 3:1) had metallic gold and copper oxide – *Tenorite* phases. For all the directly calcined bimetallic catalysts, Au metal was present but for the $CuAu/SiO_2$ sample a copper chloride hydroxide phases were also observed. For the $CuAu_3/SiO_2$ sample sodium chloride was detected, whereas copper chloride hydroxide and copper oxide –*Tenorite* were observed for the Cu_3Au/SiO_2 catalyst. There was also a trend with the copper crystallite sizes calculated by the Scherrer equation.

Directly calcined bimetallic catalysts were smaller in size than the Sinfelt treated samples. However the directly calcined samples had Au particles slightly larger (42-45nm) compared to the Sinfelt bimetallic catalysts (27-37nm). The different copper phases and crystallite sizes could account for the enhanced performance of the Sinfelt catalysts compared to the directly calcined treatments.

From looking at the characterisation and the activity for copper catalysts with different preparation treatments it can be suggested that the best oxidation state for the copper is Cu(I). In this state an increased propene conversion can be observed. Also a Sinfelt treatment in most cases increased the activity and made the catalysts more stable with less hysteresis compared to the directly calcined samples.

Making a Cu/SiO_2 catalyst by precipitation gave a propene conversion of 0.4% ± 3% (320 ^oC) and a selectivity towards acrolein at higher temperatures and ethanal at lower temperatures. The diffraction pattern indicated that the sample was mainly composed of a major amount of amorphous material and a trace amount of poorly crystalline copper oxide – *Tenorite.* The copper oxide crystallite size of 3.8 nm was calculated. The Cu/SiO_2 catalyst, made by a precipitation method had the most intense XPS spectrum which might suggest highly dispersed Cu on the silica support. This catalyst also clearly showed the presence of a Cu^{2+} species on surface

A high dispersion route was also employed to generate a Cu/SiO_2 catalyst and, in the addition of hydrogen, this catalyst gave an activity similar to the precipitation method (0.5% ± 3%). However, propene oxide was favoured at lower temperatures and acrolein at higher temperatures. Another $CuAu/SiO_2$ catalyst, prepared by a sequential preparation method that consisted of high dispersion for copper and incipient wetness impregnation for gold, was also analysed for propene oxidation. In the presence of hydrogen, only acrolein and carbon dioxide were observed, with acrolein reaching a selectivity of ~74% between 300 – 320 ^oC

and a propene conversion of 0.12% ± 3% (320 ^{o}C). XRD analysis only revealed metallic gold phases. From the SEM study large ensembles of gold as well as highly dispersed particles could be seen on the support. There was also evidence of small CuAu alloy particles. When the catalyst was Sinfelt treated, propene oxide was detected at 280 ^{o}C (30%) and ethanal at 300 ^{o}C (~20%). Acrolein was the major product using this catalyst. A propene conversion of 0.25% ± 3% (at 320 ^{o}C) was achieved in the presence of hydrogen, which was higher than when the catalyst was directly reduced in hydrogen. The Sinfelt treatment appears to make the particles more disperse which improves their activity for propene oxidation.

Generally, directly calcined CuAu/SiO_2 catalysts showed a modest activity when compared to other catalysts that were investigated, which increased with the co-feeding of hydrogen. The type of copper precursor used and the composition of the catalyst used had a consequence on the product selectivity and conversion. SEM analysis showed no major difference between copper nitrate and chloride precursors. For the directly calcined bimetallic catalysts, the CuAu and $CuAu_3$ samples both showed the presence of large gold ensembles whereas the Cu_3Au/SiO_2 catalyst had small spherical particles of copper and gold. All catalysts were more active in the presence of hydrogen. For the CuAu and $CuAu_3$ catalysts made with a copper chloride precursor, only acrolein and CO_2 were formed, whereas propene oxide was also detected for the Cu rich Cu_3Au catalyst. If the precursor was changed to copper nitrate, all of the CuAu compositions were selective towards both acrolein and propene oxide but the copper rich catalyst was the most active, with a propene conversion of 0.4% ± 3% (at 320 ^{o}C). Altering the thermal treatment also affected the selectivity. All the catalysts that were Sinfelt treated showed moderate activity and only formed acrolein and CO_2 independent of the copper precursor used. The nitrate precursor catalysts were also selective to propene oxide in the absence of hydrogen. In the presence of hydrogen, unlike the trend seen with the catalysts that were directly calcined, the copper rich bimetallic sample had the lowest

conversion of 0.095% ± 4% (at 320 ^{o}C). With exception of the copper rich composition, the high temperature calcination of the Sinfelt procedure did not decrease the activity of the catalysts, as might have been expected.

Comparing all the $AuCu/SiO_2$ catalysts (1:1, 1:3 and 3:1) either directly calcined or Sinfelt treated showed differences with their XRD and SEM analysis which could be linked to their catalytic performance. For the Sinfelt treated bimetallic catalysts metallic gold and copper oxide – *Tenorite* were detected whereas for the directly calcined samples copper chloride hydroxide was detected which was undesirable and chloride could act as a poison or a promoter on the catalytic activity. Referring to the propene activity the Sinfelt catalyst performed better which could be due to the absence of this chloride phase which some of the bimetallic catalysts possessed.

Both the $AuCu/SiO_2$ and Au_3Cu/SiO_2 directly calcined compositions had large gold ensembles from SEM analysis whereas the $AuCu_3/SiO_2$ catalyst had smaller spherical metal particles. This different feature of the catalyst could account for changes in the activity because the absence of these large clusters in the copper rich bimetallic sample resulted in the highest propene conversion.

Effect of monometallic versus bimetallic catalysts

Monometallic Au/SiO_2 was also prepared by various methods. When the catalyst was prepared by impregnation and tested for propene oxidation with the addition of H_2, a propene conversion of 0.18% ± 3% (320 ^{o}C) was achieved. This catalyst was selective to acrolein and ethanal but did not form propene oxide. SEM analysis showed the presence of large gold clusters which was a result of a weak metal support interaction. In the absence of H_2, propene conversion was low at 0.024% ± 2% (300 ^{o}C). Acrolein was formed between 260 ^{o}C to 300 ^{o}C, whereas propene oxide was observed at 260 ^{o}C (50%). Deposition precipitation was

another procedure used to prepare an Au/SiO_2 catalyst and a propene conversion of 0.15% ± 3% (320 ^oC) was produced. At higher temperatures, acrolein was formed and at 260 ^oC propene oxide was formed, although it was also detected at 320 ^oC (48%). The Sinfelt thermal treatment did not improve the activity of an Au/SiO_2 catalyst and, instead, the only product formed was carbon dioxide.

Procedures to form effective $CuAu/SiO_2$ bimetallic catalysts were implemented for this study and one route was to combine the use of two sequential methods. One example that formed $CuAu/SiO_2$, was to firstly deposit copper onto the support *via* a high dispersion pathway, followed by depositing Au onto the support by deposition precipitation. The untreated catalyst was tested for propene oxidation, along with a catalyst subjected to different thermal treatments. The fresh catalyst was quite active with a propene conversion of 1% (320 ^oC) with the addition of hydrogen in the reactor feed and the main product was acrolein. Acetone was produced at 260 ^oC (30%) and propene oxide was formed at 300 ^oC (10%). TEM/EDX analysis was carried out on this sample and showed that copper and gold formed alloy as well as some clusters on the support. The majority of the particles were small but there were some larger particles present, the mean diameter was 9nm. When the fresh catalyst had the Sinfelt treatment applied to it, its activity went up greatly (6% ± 1% at 320 ^oC) and became an effective catalyst for propene oxidation in the presence of hydrogen. This thermal treatment appeared to help improve the dispersion of the metal particles and this was key for an effective propene activity. Acrolein was selective around 80% at lower temperatures and maintained its selectivity, increasing to 90% as the temperature decreased. Ethanal had a selectivity at 240 ^oC (~45%). Directly calcining the catalyst gave a lower conversion of 0.8% ± 2% with the addition of hydrogen. Acrolein, again, was the major product and ethanal and propene oxide were detected at higher temperatures as well. In the absence of hydrogen, the directly calcined catalyst had a lower conversion of 0.35% ± 3% which, although low, was

considerably better without the addition of hydrogen in the experiment. In addition to acrolein, acetone and propene oxide were also produced. A direct reduction in H_2 gave an improved conversion of 2.3% ± 1% (320 ^{o}C) with selectivity towards acrolein, acetone (~35% at 280 ^{o}C) and propene oxide (~53% 220 ^{o}C).

$CuAu/SiO_2$ catalysts prepared by high dispersion method (HDC) for copper followed by gold deposition precipitation were compared to catalysts made by HDC copper and gold incipient wetness impregnation. SEM analysis showed that the metal particles were much more dispersed and smaller in size when gold was deposited by deposition precipitation. Whereas, large clusters and some smaller particles were observed for the impregnation gold method. The existence of more highly dispersed particles could have accounted for the larger propene conversion (1% at 320^{o}C) for the Au DP (fresh catalyst) sequential method compared to the Au IW preparation (0.12% at 320^{o}C).

It was concluded that the best method for making an effective catalyst for propene oxidation was from the $AuCu/SiO_2$ catalyst made from copper prepared by a high dispersion route followed by deposition precipitation of gold onto the support. The above characterisation and catalytic activity showed that this method had the most promise because the fresh catalyst even before thermal treatment had a 1% conversion at 320^{o}C. The fresh catalyst had a copper-gold alloy present which was confirmed from TEM and EDX analysis. Utilizing the Sinfelt thermal treatment (315^{o}C in H_2/Ar for 2h and calcined in air at 676^{o}C for 15h), the activity improved to 6% at 320^{o}C. From TEM analysis, it appeared that after the high temperature calcination at 676^{o}C for 15h de-alloying occurred leaving small gold and copper metal particles and these particles appear to be the most active towards acrolein formation out of all the catalysts prepared for this thesis.

Effect of different reducing agents

For the bimetallic catalysts reduced by $NaBH_4$, the product selectivity was not generally changed as acrolein, propene oxide and ethanal were observed, except for the case of the copper rich sample which did not produce ethanal. The activity of the catalysts was improved with the directly calcined and Sinfelt treated catalysts. A TEM study showed that alloy formation was present for the $CuAu/SiO_2$ catalyst reduced by $NaBH_4$. If this sample was calcined in air, copper and gold appeared to be separated into two phases. TEM analysis revealed that the mean diameter was 24nm and calcination in air had no effect on the size. The monometallic Au/SiO_2 catalyst was the least active (0.12% ± 3% at 320 ^oC). In general, in the absence of hydrogen, only acrolein and CO_2 were detected.

When catalysts were reduced in H_2 and then tested for propene oxidation, the product selectivity for the nitrate-containing samples seemed to be unaffected by the absence or not of hydrogen in the reactor feed. Only the monometallic Au and Cu catalysts had a slight variation in selectivity that was dependent on the addition of hydrogen. All the bimetallic catalysts with a nitrate precursor were selective to acrolein and propene oxide, the most active catalyst being the copper rich sample (1.1% ± 1% at 320 ^oC). If the nitrate precursor was substituted for the chloride equivalent, then ethanal was formed. SEM characterisation showed the presence of large gold ensembles for the $CuAu/SiO_2$ and Au rich bimetallic catalysts. But for the Cu rich bimetallic sample no large clusters were seen and only round metal particles were detected. The copper rich bimetallic catalyst ($CuAu_3/SiO_2$) was the most active bimetallic catalyst but the monometallic sample had the overall highest activity.

Effect of hydrogen co- feeding

A key observation from the results of this study showed that the addition of hydrogen increased the propene conversion and in some cases changed the product distribution.

However, the different gas feed ratios with and without hydrogen need to be noted and to definitively support this observation experiments in the absence of hydrogen with a ratio of 1:1:7 propene: oxygen: helium should be carried out.

The effect of hydrogen co-feeding was also investigated and, regardless of the preparation method or thermal treatment, all the catalysts had a large increase in activity. This could possibly be due to more active oxidising species on the surface, when there is the addition of hydrogen in the system. The presence of hydrogen might allow the formation of a hydroperoxide (OOH) species[8] which might then react with the propene directly or decompose before the reaction into another active oxidising species. The active oxidising species in the absence of hydrogen could be similar to the one involved for carbon monoxide (atomic oxygen).[9,10] The role of the hydrogen could be to dissociate molecular oxygen and leave water, as well as an active oxygen species, at the catalyst's surface.

However, the reactive oxygen species appeared to be dependent on the catalyst. Sometimes, similar selectivity to products, with and without hydrogen was observed. This observation could be attributed to the hydroperoxide species decomposing to atomic oxygen, before the reaction with propene and therefore acting like a catalyst without hydrogen. When the selectivity was different with the addition of hydrogen, different oxidising intermediates could be formed to those generated in its absence.

Potential active sites

The catalytic investigation of propene oxidation suggested the presence of several different types of active site for the reaction. A copper (I) active site was observed for the three molar ratios of Sinfelt treated $CuAu/SiO_2$ catalysts. These catalyst had a high stability which was represented by little hysteresis. This active site had a high selectivity towards acrolein which has be shown before.[11] Zhu and group found that K-promoted monometallic Cu/SiO_2 a Cu(I)

species and this improved the selectivity towards propene oxide over acrolein at 250-300 ^{o}C.[12] The group suggested the reason for this was that Cu (I) was not as active for the oxidation of propene oxide to acrolein and other products.

A copper (II) active site was linked to low activity and selectivity towards acrolein and propene oxide. This could possibly be the active site for the CuAu/SiO_2 catalysts calcined directly with air and for the Sinflet treated Cu/SiO_2 catalyst, as they exhibited low selectivity and favoured combustion. This has been noted in work carried out by others[11] which suggests that CuO leads to the combustion of propene. The addition of hydrogen and promotion of gold increased the selectivity to acrolein in the bimetallic catalysts. A CuAu alloy active site was associated with the reduced CuAu bimetallic catalyst which generated a variety of products. The mixed selectivity could also be linked to the possible presence of some Cu (I) in the catalyst. The presence of hydrogen in the reactor feed significantly increased the activity of these catalysts. A mixed selectivity was also seen by Llorca and co workers[13] who made CuAu/TiO_2 catalysts with thiol-stabilised nanoparticles. The more copper rich catalysts were more active which concurred with the results in this study, even though they used N_2O instead of O_2 or O_2 and H_2 as their oxidant. A metallic gold active site was observed for the reduced, directly calcined and Sinfelt treated monometallic catalyst and, generally, led to more combustion than the copper sites. This was enhanced by hydrogen in the reactor feed. However, this was not found by Haruta and team [4] and the difference could be accounted for by the functionality of the support. The Cu/SiO_2 catalyst reduced directly in H_2 had a metallic Cu(0) active site which gave a low conversion and a wide product selectivity. This result was confirmed in the work by Vaughan *et al* [5] who prepared a Cu/SiO_2 catalyst with selectivity towards acrolein, propene oxide and CO_2, when the catalyst was reduced. However, they made their catalyst by a different method (microemulsion) which could justify any differences in results, since this technique produced a more highly dispersed catalyst.

The active site which gives the best catalytic structure was the Cu(I) active site which was present when the bimetallic catalysts were Sinfelt treated. This thermal treatment produced highly dispersed small metal particles which gave a stable activity towards acrolein formation. Propene conversion was higher for the Sinfelt bimetallic catalysts when compared to the directly calcined samples which had a Cu(II) active site. Monometallic catalysts didn't perform as well as the bimetallic catalysts suggesting that there was a possible synergy between the copper and gold in the bimetallic catalysts which improved its activity.

4.6 Conclusion

Monometallic and bimetallic copper and gold catalysts were tested for propene oxidation in the presence and absence of hydrogen in the reactor feed. The effect of different preparation methods, copper precursors and reduction conditions were investigated to determine if there was a change in the performance of the catalyst. The most catalytically active sample was made by a sequential method, which involved copper deposited onto the support by a high dispersion route, followed by gold being deposited by deposition precipitation. A thermal Sinflet treatment (reduction in H_2/Ar at 315 ^oC for 2h and calcination at 676 ^oC for 15h in air) was carried out on this catalyst before it was tested for propene oxidation. This step played an important role in the improved activity of the catalyst. From SEM analysis the thermal treatment appeared to make the catalyst particles more dispersed compared to the directly calcined catalysts that had large clusters of particles present. TPR characterisation showed only a single reduction peak for the reduction of CuO to Cu metal. However, for the directly calcined samples two peaks were observed suggesting a two step reduction with the major peak representing CuO to metallic Cu and the other peak for Cu(II)O to Cu(I). A propene conversion of over 6% was achieved at 320 ^oC in the presence of hydrogen. This catalyst was mainly selective towards acrolein at higher temperatures and propene oxide and ethanal at

lower temperatures. Hydrogen co-feeding increased the activity for all experiments and was needed to produce reasonable conversions. In the absence of hydrogen, all catalysts showed very low conversions of propene (<1%). There were limitations in this study because time constraints meant it was not possible to repeat the experiments. Furthermore, different reactor feed ratios were used, with and without hydrogen for propene oxidation.

From this thesis, the catalyst with the highest activity for propene oxidation was a $AuCu/SiO_2$ catalyst made by a high dispersion route for copper followed by gold prepared by deposition precipitation (figure 4.15). A Sinfelt thermal treatment was carried out on this catalyst and gave a conversion of over 6% at 320^{o}C in the presence of hydrogen in the co-feed. Loading copper onto the catalyst by a high dispersion route followed by gold by deposition precipitation improved the catalysts activity when compared to the standard impregnation method. However, there was not enough characterisation carried out on this particular catalyst preparation to get a full understanding of its structure and activity. Therefore, future studies into this route would be beneficial to better understand what features of this catalyst give it enhanced performance over the other catalysts. Compared to the literature the propene conversion was close to the commercially desirable 7% obtained by Haruta[14] from a sol-gel method. However, in our study acrolein was the major product with a selectivity over 80% between 240^{o}C and 320^{o}C, whereas for Haruta's work a selectivity towards propene oxide greater than 90% was achieved.

The most effective catalysts appeared to benefit from the Sinfelt thermal pre-treatment and from TEM analysis of the $CuAu/SiO_2$ catalyst made *via* impregnation and Sinfelt treated, alloy formation was seen after the reduction in hydrogen. But after the high temperature calcination de-alloying occurred which resulted in the presence of bimetallic gold and copper particles. The Sinfelt method appeared to generate highly dispersed small metal particles that were the most stable and had the least hysteresis for propene oxidation. Cu(I) was suggested

as the possible active site for the Sinfelt bimetallic catalysts and gave better activity than the directly calcined bimetallic catalysts.

4.7 References

1. A. Takahashi, N. Hamakawa and I. Nakamura, *Applied Catalysis A General*, 294 (2005) 34.

2. X.W. Guo, R.P. Wang and X.S. Wang, *Catalysis Today*, 211 (2003) 211.

3. M.F. Luo, J.Q. Lu and C. Li, *Catalysis Letters*, 86 (2003) 43.

4. T. Hayashi, K. Tanaka and M. Haruta, *Journal of Catalysis*, 178 (1998) 566-75.

5. O.P.H. Vaughan, G. Kyriakou, N. Macleod, M. Tikhov and R.M Lambert, *Journal of Catalysis*, 236 (2005) 401-404.

6. F. Porta, L. Prati, M. Rossi, S. Coluccia and G. Martra, *Catalysis Today*, 61 (2000) 165.

7. G. Zhan, M. Du, D. Sun, J. Huang, X. Yang, Y. Ma, A-R Ibrahim and Q. Li, *Industrial and Engineering Chemistry Research*, 50 (2011) 9019.

8. P. Landon, P.J. Collier, A.J. Papworth, C.J. Kiely and G.J. Hutchings, *Chemical Communications*, (2002) 2058.

9. B.K. Min and C.M. Friend, *Chemistry Reviews*, 107 (2007) 2709.

10. D. Gamarra, C. Belver, M. Fernadez-Garcia and A. Martinez-Arias, *Journal of American Chemical Soc*iety, 129 (2007) 12064.

11. J.B. Reitz and E.I. Solomon, *Journal of American Chemical Society*, 120 (1998) 11467.

12. W. Zhu, Q. Zhong and Y. Wang, *Journal of Physical Chemistry C*, 112 (2008) 7731.

13. J. Llorca, M. Dominguez, C. Ledesma, R.J. Chimentao, F. Medina, J. Sueiras, I. Angurell, M. Seco and O. Rossell, *Journal of Catalysis*, 259 (2008) 187.

14. A. K. Sinha, S. Seelan, M. Okumura, T. Akita, S. Tsubota and M. Haruta, *Journal of Physical Chemistry B*, 109 (2005) 3956.

Chapter 5: Other reactions with CuAu catalysts

5.1 Introduction

Oxidation is an important method for the synthesis of chemical intermediates. Using oxygen from air for catalytic reactions is favoured as it is environmentally benign and is often used in 'green' chemistry. Gold catalysts have shown promise for the synthesis of hydrogen peroxide[1,2] and alcohol oxidation.[3,4] Au nano-crystalline materials have been found to be highly effective for selective and total oxidation. Supported gold catalysts have recently shown 100% selectivity towards glyceric acid in the oxidation of glycerol when NaOH is used in the reaction.[5-7] Benzyl alcohol oxidation has also been linked to the use of Au/SiO_2 catalysts and demonstrated a high selectivity (greater than 95%) for benzyl alcohol oxidation with air with conversions between 50-75%.[8]

Copper catalysts have not been studied greatly for most of the preliminary reactions. However, in contrast, gold catalysts have been studied for all of these reactions. Copper and gold have been used together for benzyl alcohol oxidation to make $CuAu/SiO_2$ bimetallic catalysts.[9] A yield of 98% and selectivity towards benzylaldehyde of 99% were attained from this catalyst. They also reported a synergy between the copper and gold which contributed to the increase in activity, compared to the monometallic catalysts. Cu-Cr catalysts have been used for glycerol oxidation and have shown a high selectivity and activity.[10] The catalysts have been made by a non-alkoxide sol-gel method and could achieve a glycerol conversion of 52% and selectivity towards 1,2- propanediol above 88% at 210 ^{o}C and 4.15 MPa H_2 pressure. A copper complex has also been used for the oxidation of glycerol under mild conditions.[11] In this study, tetracopper(II) triethanolaminate complex was reacted with t-BuOOH, TBHP and water in a homogeneous system for the oxidation of glycerol to dihydroxyacetone.

Huang and co-workers [12] have used highly dispersed copper silica catalysts (CuO/SiO_2) for glycerol hydrogenolysis and the paper concluded that catalysts prepared by a precipitation-gel method were more active than catalysts made *via* an impregnation route.

In this chapter, the study of a few preliminary reactions is presented to uncover if any of the catalysts prepared were active for reactions other than propene oxidation. The reactions investigated were: hydrogen peroxide synthesis and hydrogenation, glycerol oxidation and benzyl alcohol oxidation. These reactions were chosen because gold catalysts have shown potential or are already active for these reactions.

5.2 Results

5.2.1 Hydrogen peroxide synthesis and hydrogenation reactions

5.2.1.1 Introduction

Highly dispersed Au catalysts have been reported to be active for many significant reactions in the chemical industry such as oxidation reactions. Hydrogen peroxide synthesis is of commercial interest and its production has been studied by Dissanayake and co-workers [13,14] from Pd catalysts. Au, Pd and Pd-Au catalysts have also been prepared and successfully used for hydrogen peroxide synthesis in liquid phase at low temperatures [15,16] between 1-2 ^oC.

In the past, Pd has attracted a lot of interest for this reaction but a major disadvantage of using supported Pd catalysts is that they are also active for the hydrogenation reactions. [17,15] Previously, additives have been used which has caused concern, as their removal is not environmentally friendly. Au has recently been added to Pd catalysts and has increased the activity and selectivity for hydrogen peroxide formation. [18-20] The support used has been shown to have an effect on the size of the Au-Pd nanoparticles, as well as their shape.[21,22] In general, carbon supports have demonstrated a much better activity than TiO_2 supports.[21]

However, Au-Pd/TiO_2 catalysts have been prepared that have an activity equivalent to highly dispersed carbon supported catalysts by changing preparation parameters.[23]

Hydrogen peroxide decomposition performance has been greatly affected for Pd supported catalysts due to the presence of additives such as halides [17] and their oxidation.[24-27] A study on the factors affecting the activity of the decomposition of hydrogen peroxide by Pd/carbon and other supports has been discussed. [28] But these Pd studies have not been investigated fully, which has led to detailed work on factors affecting the decomposition [29] and the effect of using different mineral acids in addition to other factors, like the presence or absence of different halide anions and/or protons, concentration of acid (protons) and/or halide anions and different reaction temperatures.[30]

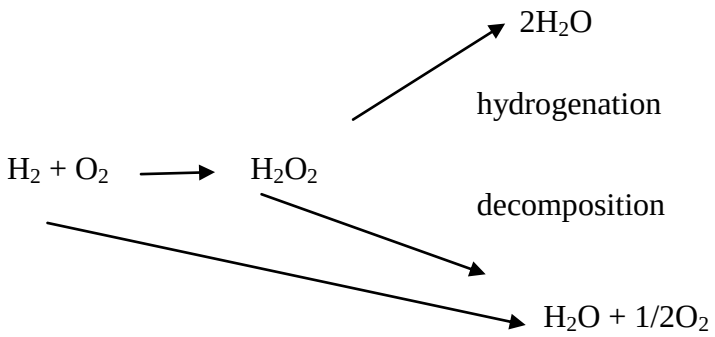

Figure 5.1 Reaction involved in the synthesis of H_2O_2

5.2.2 H_2O_2 Synthesis results

Catalyst	mmol/h/mol Au	Average mmol/h/mol Au
Au:Cu/SiO_2 (C97819A)	581	
	583	582
Au_3Cu/SiO_2 (C97819B)	508	
	602	532
	485	
$AuCu_3/SiO_2$ (C97819C)	1069	984
	898	
Au/SiO2 DP (C97836)	545	
	325	435
	434	

Table 1 Hydrogen peroxide synthesis of Au and AuCu silica supported catalysts. See appendix (Table 1) for catalyst codes.

Catalysts were tested for H_2O_2 synthesis and their activity was low, compared to conventional catalysts used in this reaction. Supported Au catalysts are active for the direct synthesis of hydrogen peroxide and in depth studies have been carried out.[31] From Table 1, the $AuCu_3/SiO_2$ prepared by direct calcination in air, had the highest productivity per mole of Au (984 mmol/h/mol Au), whereas, the catalyst prepared *via* the deposition precipitation method had the lowest activity (435 mmol/h/mol Au). The H_2O_2 synthesis reactions seemed to suggest a trend which was unexpected. The Au/SiO_2 only catalyst made via the deposition precipitation had the lowest productivity of 435 mmol/h/mol, but, as the Cu content increased in the catalyst, the activity increased. The $AuCu/SiO_2$ had a productivity of 582 mmol/h/mol and rose significantly to 984 mmol/h/mol for the $AuCu_3/SiO_2$ catalyst. This was unexpected because Cu/SiO_2 are not commonly used for this reaction because they have low activity, [32] and Au only catalysts have been shown to achieve good productivity for H_2O_2.[31] These results suggest a possible AuCu active site for the bimetallic catalysts but can only be speculated on in this study. The accuracy for these experiments was poor as the results did deviate quite a bit after each run and therefore averages of the results were taken with large

differences. These initial experiments gave us a general feel for how the catalyst might react but more experiments would be needed to give accurate productivity that can be reproduced for each catalyst.

5.2.3 Hydrogenation results

Catalyst	Standard wt% H_2O_2 before hydrogenation	Average wt% H_2O_2 after hydrogenation	Wt% decrease
Cu_3Au/SiO_2(C97819C)	4.2	4.0	0.2
$CuAu_3/SiO_2$(C97819B)	4.2	3.9	0.3
$CuAu/SiO_2$(C97819A)	4.2	3.6	0.6
Au/SiO_2 (C97809)	4.2	3.7	0.5
Cu/SiO_2(C97802D)	4.2	3.9	0.3
Au/SiO_2 DP(C97836)	4.2	3.5	0.7
Cu/SiO_2 in H_2 (C97815B1)	4.9	3.6	1.3
Cu/SiO_2 in N_2 (C97815B2)	4.9	4.5	0.4
Cu/SiO_2 in air (C97815B3)	4.9	4.6	0.3
Cu_3Au/SiO_2 (C97819C) fired at 900^{o}C	4.9	4.5	0.3
$CuAu_3/SiO_2$ (C97819B) fired at 900^{o}C	4.9	4.7	0.2

Table 2 Hydrogenation data. See appendix (Table 1) for catalyst codes.

Copper supported on SiO_2 and other supports were shown to be an effective catalyst for hydrogenation reactions.[33] Out of all the catalysts tested for hydrogen peroxide hydrogenation (table 2), Cu/SiO_2 (1.3%) was the most productive catalyst that was prepared using copper (II) chloride, made by impregnation and reduced at 400 ^{o}C in H_2. The lowest activity (0.2 wt%) was observed from the Au_3Cu/SiO_2 sample calcined in air at 400 ^{o}C and 900 ^{o}C. These

results seem promising because the Cu/SiO_2 catalyst performed better than any of the Au/SiO_2 catalysts. Samples with more Cu content were more active than ones with less Cu, when fired at 900 ^oC in air. Catalysts calcined at 400 ^oC in air showed a different trend as the $CuAu/SiO_2$ catalyst achieved the best hydrogenation activity.

There has been a trend, where a catalyst that is active for H_2O_2 synthesis will not perform well for the hydrogenation reaction ($H_2O_2 + H_2 + Cat \rightarrow 2H_2O$). From Table 1, showing the hydrogen peroxide synthesis activity, the Cu_3Au/SiO_2 had the highest productivity (984 mmol/h/mol) but had one of the lowest hydrogenation results. Furthermore, the Au/SiO_2 catalyst, made via deposition precipitation, had the lowest hydrogen peroxide synthesis activity but had a higher hydrogenation activity than all the other catalysts that were tested for H_2O_2 synthesis.

5.3 Glycerol and Benzyl Alcohol Oxidation

5.3.1 Introduction

For glycerol oxidation, there are several factors that can affect the direction of the oxidation pathway from either the primary or secondary hydroxyl group, which are: temperature, pH or metal loading. Primary oxidation is favoured over secondary when using platinum catalysts supported on active charcoal and the major product is glyceric acid (55% at 90% conversion). Au-Pt bimetallic catalysts have a 72% selectivity to glyceric acid at 50% conversion and 31% at 100% conversion.[34] It has been found [35] that basic reaction conditions are essential for the gold catalysis, since the initial step of the oxidation and the dehydrogenation of glycerol cannot proceed in the absence of a base. In the presence of a base, the H^+ is readily abstracted from one of the primary hydroxy groups to form glyceric acid. The oxidation products of glycerol can be converted into products for polymers or biodegradable emulsifiers and glyceric acid can be used for skin disorders.

The oxidation of benzyl alcohol in air, in a vapour phase process, gave a high selectivity and yield of benzaldehyde using 1% Au-Cu/SiO_2.[9] One of the most efficient catalysts for this reaction was a AuCu/SiO_2 sample with AuCu ratio of 4 : 1 by weight (approximately 4 : 3 molar ratio) and a total metal loading of 1% which gave a benzaldehyde yield of 98%. The catalysts were made by incipient wetness impregnation of SiO_2 with $HAuCl_4$ and $CuCl_2$ and reduced with $NaBH_4$. Chen and co workers have also investigated the oxidation of benzyl alcohol but without the presence of a solvent.[36] The study revealed that the Au–Pd bimetallic catalysts had an enhanced catalytic performance compared to the Au and Pd monometallic catalysts. The highest turnover frequency of 8667 h^{-1} was achieved over a bimetallic catalyst with Au:Pd molar ratio of 1:5. It was also suggested that a synergetic effect between Au and Pd nanoclusters could have accounted for the better catalytic activity of bimetallic catalysts.

5.3.2 Results

5.3.2.1 Glycerol Oxidation

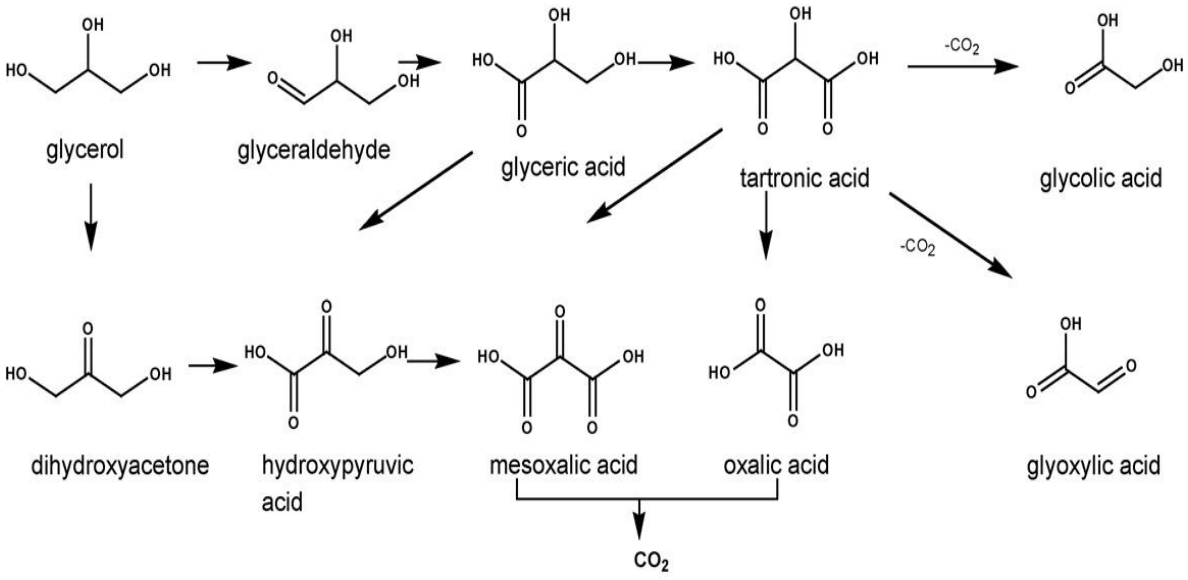

Figure 5.2 Scheme of possible pathways from glycerol starting material

From Table 3 (appendix) it can be deduced that $CuAu/SiO_2$ catalyst prepared by Sinfelt treatment had a conversion to glycerol that increased from 2.01 to 2.36% after 3h but then decreases back to 2.05% at the end of the reaction. The oxalic acid selectivity increases from 0.57% after 30 mins to 0.97% after 4 h. Formic acid selectivity also increases from 8.6 to 11% after 4h. Glyceric acid is the product observed with highest selectivity for glycerol oxidation using this catalyst (65-66%) followed by glycolic acid (21%-24%).

The $CuAu/SiO_2$ catalyst directly calcined gave a glycerol conversion that was lower than the previous Sinfelt sample and dropped from 1.77 to 1.46% after 4 h. Oxalic acid selectivity increased from 0.77 to 0.81% and formic acid increased from 4.37 to 13.75 % after 4 h. Glyceric acid was the most selective product for this reaction and had the highest selectivity after 2 h (65%).

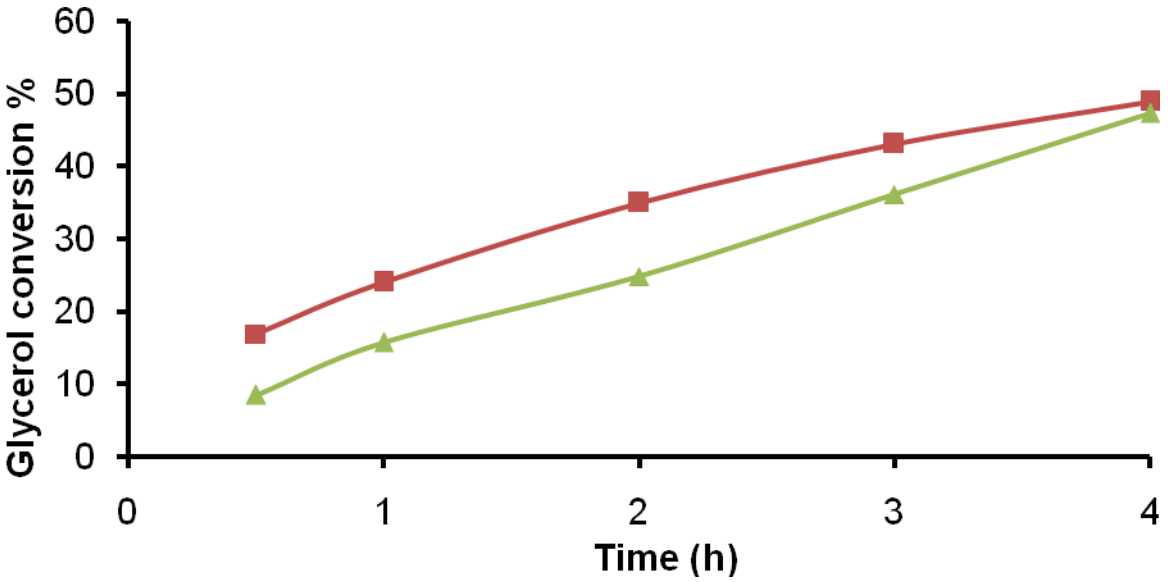

Figure 5.3 Glycerol oxidation at 60 ^{o}C (green line) and 100 ^{o}C (red line) with Au/SiO_2 catalyst sol catalyst (C978102)

A monometallic Au/SiO_2 catalyst made by a sol immobilisation method was tested for glycerol oxidation (Figure 5.3). This reaction was carried out at two temperatures: 60 and 100 ^{o}C for 4 h. Both reaction temperatures formed a glycerol conversion of nearly 50% after 4 hours, although the Au/SiO_2 catalyst tested at the lower temperature reached higher

conversions quicker. Therefore, when the catalyst was made via this route, its activity was enhanced, although it didn't perform as well as platinum catalysts previously studied by others.[35] The sol immobilisation technique is an effective way of controlling the size of the nano particles [37] and this factor could be the reason this catalyst is much more active than the catalysts made by impregnation independent of calcination or reduction treatments.

5.3.2.2 Benzyl Alcohol Oxidation

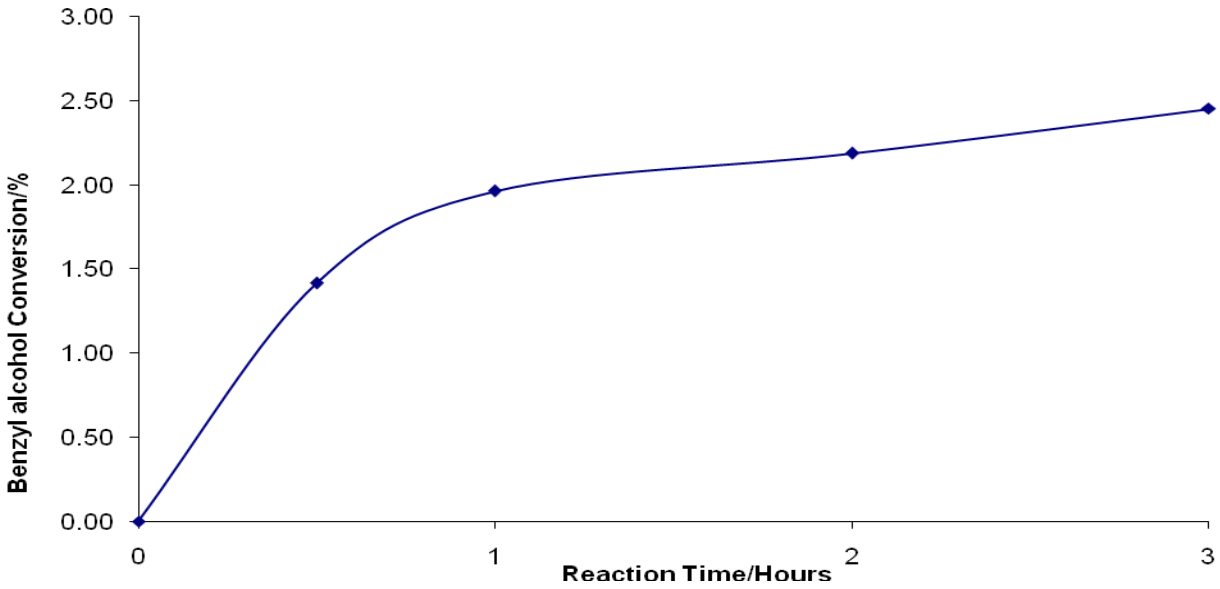

Figure 5.4 Benzyl alcohol conversion with Au/SiO_2 sol catalyst (C978102)

The Au/SiO_2 catalyst prepared by sol immobilisation, was also analysed for benzyl alcohol oxidation (Figure 5.4). After 3 hours a conversion of 2.5% was acheived which is low compared to $AuCu/SiO_2$ [38] and Au/Pd catalysts.[39]

5.4 Discussion

A few preliminary reactions were chosen to be investigated using selected catalysts. Catalysts tested for hydrogen peroxide synthesis showed low activity, but there was a trend observed. The more Cu rich the bimetallic catalysts, the more active the catalyst was towards formation of hydrogen peroxide. The catalyst made by decomposition precipitation was the least active. However, in the hydrogenation reactions for hydrogen peroxide, the opposite was true. The Au/SiO_2 catalyst prepared by deposition precipitation had the highest activity for the decomposition of hydrogen peroxide. The Cu_3Au/SiO_2 catalyst which showed the best performance during hydrogen peroxide synthesis had one of the lowest productivities for hydrogenation. This trend was expected and has been suggested previously.

The oxidation of glycerol was tested for $AuCu/SiO_2$ catalysts directly calcined or treated by Sinfelt thermal conditions. Both these catalysts showed low glycerol conversion and the major products were glyceric and glycolic acid. However, an Au/SiO_2 catalyst, prepared by a sol immobilisation method, was also analysed for this reaction. At temperatures of 60 ^oC and 100 ^oC, conversions of almost 50% were observed after 4 hours. This is very promising, as it shows that when a catalyst is made in an alternative way, the Au particles perform differently to those made by a simple impregnation method. From the characterisation data in Chapter 3, SEM analysis didn't appear to show many visible metal particles, which suggested the presence of smaller particles that could be detected by TEM analysis. However, both the $CuAu/SiO_2$ catalysts, either calcined directly or treated by the Sinfelt method (reduction at 315 ^oC in H_2/Ar followed by calcination at 676 ^oC for 15 h in air), formed large clusters of gold particles, observed by SEM analysis. For the $CuAu/SiO_2$ catalyst treated by the Sinfelt procedure, the average particle size was 13 nm, which is larger than would be expected for a catalyst prepared by a sol immobilisation method. The sol immobilisation method has been compared with deposition precipitation for Au/TiO_2 catalysts and tested for glycerol

oxidation.[40] That study revealed that the reduction method and the use of protective agents (PVA) affected the catalytic performance. The highest activity was observed for an Au/TiO_2 catalyst with a low temperature reduction that was prepared by deposition precipitation. It has been shown by Porta *et al.* [41] that the sol preparation method can form particles, with particle size ranges between 4 and 6 nm, and can possess active sites that are active for total oxidation. However, the impregnation method gave a better catalytic performance for propene oxidation (conversion of 33–32% for impregnation method versus 17% for sol preparation method). The group stated that a reason for the lower activity, when using sol immobilisation, could be due to the presence of PVA or boron derivatives poisoning the active sites for the reaction. A study on the particle size effect on glycerol oxidation has been reported [37] and an increase in the particle size from 2 to 16 nm decreased the activity of this reaction. Therefore, a possible explanation for the increased activity for glycerol oxidation with a sol immobilisation catalyst may be due to the presence of smaller particles.

Benzyl alcohol oxidation was also tested using this Au/SiO_2 catalyst, but showed very little activity towards benzyladehyde reaching a conversion of 2.5% after 3 hours. Benzyl alcohol oxidation has been previously studied using an Au supported catalyst prepared by sol immobilisation.[42] The technique formed Au particles that were small in size with narrow size distribution, which resulted in a high selectivity and activity for benzyl alcohol oxidation. They concluded that the type of support and heat pre-treatment affected the performance. The best activity was seen when using Au/carbon, and heat treating this catalyst beforehand enhanced its activity. Therefore, a reason for the Au/SiO_2 catalyst not showing a high activity towards benzylaldehyde could be due to the silica support used and the absence of any heat pre-treatment.

The preliminary studies in this thesis have shown that monometallic and bimetallic $CuAu/SiO_2$ catalysts aren't very active for hydrogen peroxide synthesis and hydrogenation.

However, a trend was observed with the catalysts presented. For hydrogen peroxide synthesis, the most copper rich (Cu_3Au/SiO_2) catalyst was the most active, whilst the Au/SiO_2 sample prepared by deposition precipitation was the least active. The opposite pattern was observed for the hydrogenation reactions, since the Au/SiO_2 catalyst showed the best performance, whereas the copper rich (Cu_3Au/SiO_2) catalyst had one of the lowest performances for this reaction. Glycerol oxidation and benzyl oxidation were tested using a Au/SiO_2 catalyst prepared by the sol immobilisation method. Benzyl alcohol performance was low with this catalyst but, for glycerol oxidation, this catalyst reached a reasonable conversion of nearly 50% after 4 hours at 60 ^{o}C. Out of all the reactions investigated, the Au/SiO_2 sol catalyst had the best potential. Bimetallic Au/Pd catalysts have been tested for glycerol oxidation, prepared by sol immobilisation.[37,43] The use of bimetallic catalysts, compared to monometallic samples, increased the activity. Therefore, it would be beneficial for the $CuAu/SiO_2$ bimetallic catalyst, prepared by sol immobilisation, to be tested for this reaction.

5.5 Conclusion

Hydrogen peroxide synthesis and hydrogenation reactions were chosen to test a select few catalysts. Both reactions showed low activity overall but there was a trend observed between the two reactions. The Au/SiO_2 catalyst prepared by deposition precipitation was the least active for hydrogen peroxide synthesis but had the highest performance when tested for hydrogenation. However, the $CuAu/SiO_2$ copper rich catalyst had the best activity towards hydrogen peroxide synthesis and, therefore, had the lowest activity for the hydrogenation reaction.

Benzyl oxidation was studied on the Au/SiO_2 catalyst prepared by sol immobilisation but unfortunately showed a low activity (2.5% conversion after 3 hours) towards benzylaldeyhde.

This reaction had been previously tested on catalysts made by this technique, [42] but other studies used different supports and pre-treatments which could have influenced the catalyst's performance.

Glycerol oxidation was used to test the activity for a few of the $CuAu/SiO_2$ catalysts, either prepared by direct calcination or the Sinfelt treatment. Similarly, these catalysts showed little activity. However, the Au/SiO_2 catalyst, made by the sol immobilisation method, was also tested for this reaction and, at temperatures of 60 ^{o}C and 100 ^{o}C, a conversion of ~ 50% was observed after 4 hours. The performance of this catalyst has potential, as the sol immobilisation technique can form small particles in narrow size ranges and has already been used in other glycerol oxidation studies.[41]

5.6 References

1. A.M. Joshi, N.W. Delgass and K.T. Thomson, *Journal of Physical Chemistry C,* 111 (2007) 7384.

2. D.P. Dissanayake and J.H. Lunsford, *Journal of Catalysis*, 206 (2002) 173.

3. S. Biella, L. Prati and M. Rossi, *Inorganica Chimica Acta*, 349 (2003) 253.

4. S. Biella, L. Prati and M. Rossi, *Journal of Catalysis*, 206 (2002) 242.

5. S. Carrettin, P. McMorn, P. Johnston, K. Griffin, C.J. Kiely, G.A. Attard and G.J. Hutchings, *Topics in Catalysis*, 27 (2004) 131.

6. S. Carrettin, P. McMorn, P. Johnston. K. Griffin and G.J. Hutchings, *Chemical Commun*ications, 7 (2002) 696.

7. S. Carrettin, P. McMorn, P. Johnston. K. Griffin and G.J. Hutchings, *Physical Chemistry Chemical Physics*, 5 (2003) 1329.

8. S. Biella and M. Rossi, Chemical Communications, 378 (2003) 21.

9. C. Della Pina, E. Falletta and M. Rossi, *Journal of Catalysis*, 260 (2008) 384.

10. Z. Ma, Z. Xiao, J.A. Bokhoven and C. Liang, *Journal of Material Chemistry*, 20 (2010) 755.

11. M.V. Kirillova, A.M. Kirillov, D. Mandelli, W.A. Carvalho, A.J.L. Pombeiro, G.B. Shulpin, *Journal of Catalysis*, 272 (2010) 9.

12. Z. Huang, F. Cui, H. Kang, J. Chen, X. Zhang and C. Xia, *Chemistry of Materials*, 20 (2008) 5090.

13. D.P. Dissanayake and J.H. Lunsford, *Journal of Cataysis*, 206 (2002) 173.

14. D.P. Dissanayake and J.H. Lunsford, *Journal of Catalysis*, 214 (2003) 113.

15. P. Landon, P.J. Collier, A.J. Papworth, C.J. Kiely, G.J. Hutchings, *Chemical Communications*, 18 (2002) 2058.

16. P. Landon, P.J. Collier, A.F. Carley, D. Chadwick, A.J. Papworth, A. Burrows, C.J. Kiely, G.J. Hutchings, *Journal of Physical Chemistry Chemical Physics*, 5 (2003) 1917.

17. V.R. Choudhary, C. Samanta and A.G. Gaikwad, *Chemical Communications*, 18 (2004) 2054.

18. J.K. Edwards, B. Solsona, P. Landon, A.F. Carley, A. Herzing, M. Watanabe, C.J. Kiely and G.J. Hutchings, *Journal of Materials Chemistry*, 15 (2005) 4595.

19. J.K. Edwards, B. Solsona, P. Landon, A.F. Carley, A. Herzing, C.J. Kiely and G.J. Hutchings, *Journal of Catalysis*, 236 (2005,) 69.

20. J.K. Edwards, A.F. Carley, A. Herzing, C.J. Kiely and G.J. Hutchings, *Faraday Discussions*, 138 (2008) 225.

21. G. Li, J.K. Edwards, A.F. Carley and G.J. Hutchings, *Catalysis Today*, 122 (2007) 361

22. J.K. Edwards, B. Solsona, E. Ntainjua, A.F. Carley, A.A. Herzing, C.J. Kiely and G.J. Hutchings, *Science*, 323 (2009) 1037.

23. J. Pritchard, Q. He, E.N. Ntainjua, M. Piccinini, J.K. Edwards, A.A. Herzing, A.F. Carley, J.A. Moulijn, C.J. Kiely and G.J. Hutchings, *Green Chemistry*, 12 (2010) 915.

24. V.R. Choudhary, A.G. Gaikwad, S.D. Sansare, *Angewande Chemie International Edition*, 40 (2001) 1776.

25. V.R. Choudhary, A.G. Gaikwad, S.D. Sansare, *Catalysis Letters*, 83 (2002) 235.

26. A.G. Gaikwad, S.D. Sansare, V.R. Choudhary, *Journal of Molecular Catalysis A: Chemical*, 181 (2002) 143.

27. V.R. Choudhary, C. Samanta, T.V. Choudhary, *Applied Catalysis A: General*, 308 (2006) 128.

28. T.V. Choudhary, C. Samanta, V.R. Choudhary, *Journal of Molecular Catalysis A*, 260 (2006) 115.

29. V. R. Choudhary, C. Samanta, P. Jana, *Applied Catalysis A: General*, 332 (2007) 70.

30. V. R. Choudhary, C. Samanta, P. Jana, *Applied Catalysis A: General*, 317 (2007) 234.

31. M. Okumura, Y. Kitagawa, K. Yamagcuhi, T. Akita, S. Tsubota and M. Haruta, *Chemistry Letters*, 32 (2003) 822.

32. G. Li, J. Edwards, A.F. Carley and G.J. Hutchings, *Catalysis Communications*, 8 (2007) 247.

33. R.S. Rao, A.B. Walters, and M.A. Vannice, *Journal of Physical Chemistry B*, 109 (2005) 2086.

34. A. Behr, J. Eilting, K. Irawadi, J. Leschinski and F. Lindner, *Green Chemistry*, 10 (2008) 13.

35. S. Carrettin, P. McMorn, P. Johnston, K. Griffin, C.J. Kiely and G.J. Hutchings, *Physical Chemistry Chemical Physics*, 5 (2003) 1329.

36. Y. Chen, H. Lim, Q. Tang, Y. Gao, T. Sun, Q. Yan, Y. Yang, *Applied Catalysis A: General*, 380 (2010) 55.

37. N. Dimitratos, J.A. Lopez-Sanchez, D. Lennon, F. Porta, L. Prati and A. Villa, *Catalysis Letters*, 108 (2006) 3.

38. N. Dimitratos, J.A. Lopez-Sanchez, D. Morgan, A. Carley, L. Prati, G.J. Hutchings, *Catalysis Today*, 122 (2007) 317.

39 N. Dimitratos, F. Porta, L. Prati, *Applied Catalysis A: General*, 291 (2005) 210.

40. N. Dimitratos, A. Villa, C.L. Bianchi, L. Prati, M. Makkee, *Applied Catalysis A: General*, 311 (2006) 185.

41. F. Porta, L. Prati, M. Rossi, S. Coluccia, G. Martra, *Catalysis Today*, 61 (2000) 165.

42. J.A. Lopez-Sanchez, N. Dimitratos, P. Miedziak, E. Ntainjua, J.K. Edwards, D. Morgan, A.F. Carley, R. Tiruvalam, C.J. Kiely and G.J. Hutchings, *Physical Chemistry Chemical Phys*ics, 10 (2008) 1921.

43. N. Dimitratos, J.A. Lopez-Sanchez, J.M. Anthonykutty, G. Brett, A.F. Carley, R.C. Tiruvalam, A.A. Herzing, C.J. Kiely, D.W. Knight and G.J. Hutchings, *Physical Chemistry Chemical Physics*, 11 (2009) 4952.

Chapter 6: Conclusions and future work

6.0 Conclusions

Copper and gold are metals that have had many uses in catalysis. Heterogeneous copper catalysts are well known hydrogenation and oxidation catalysts. The use of nanoalloys in catalysis is a rapidly expanding field. There has been immense interest in the use of supported gold nanoparticles as catalysts and bimetallic catalysts, containing gold in combination with other metals, represent an emerging field of research. Therefore, the aim of this thesis was to try and determine the structure and nature of the gold and copper catalysts prepared, and to reveal any promising catalytic performance for propene oxidation.

Monometallic and bimetallic $AuCu/SiO_2$ catalysts were prepared, mainly by an impregnation method. Other techniques, such as deposition precipitation, high dispersion, sol immobilisation and sequential procedures, involving the combination of two preparation pathways, have been utilised. These catalysts were characterised by several techniques, such as XRD, BET, XPS, TEM, SEM and UV visible spectroscopy to try to determine the structure of the catalysts. The catalysts were tested for propene oxidation in the presence and absence of hydrogen to investigate their activity and selectivity towards acrolein and propene oxide. Other preliminary reactions, such as hydrogen peroxide synthesis and glycerol oxidation, were also analysed for the purpose of suggesting other potential reactions that could be further investigated.

Different thermal treatments of the dried copper and gold precursors on the silica were studied. The different thermal treatments gave catalysts with significantly different structures and properties. Direct calcination gave a $CuAu/SiO_2$ catalyst which contained very large gold ensembles with minimal interaction with the copper particles. The presence of copper-gold particles, containing some copper with copper (II) ions on the silica support, was also observed. EGA analysis showed copper nitrate precursor decomposed to copper oxide. These

catalysts generally had a low activity with a selectivity towards acrolein, CO_2 and propene oxide. A hydrogen reduction led to the formation of copper-gold alloy particles. The difference from the direct calcination procedure was that the copper reduced to copper metal straight after decomposition, followed by interaction with reduced gold. Successive high temperature calcination in air (at 676 ^oC for 15 h) resulted in the de-alloying of the copper from the gold. There was some evidence that the presence of gold in the catalyst stabilised the formation of Cu^+ against further oxidation. These catalysts showed moderate activity but were selective to acrolein, especially in the presence of hydrogen in the reactor feed. The conversion of the catalysts for propene oxidation was greatly altered in the presence or absence of hydrogen. With the addition of hydrogen, the conversion was greatly enhanced. The presence of hydrogen increased the catalytic activity, possibly because the surface coverage of oxygen species increased. The selectivity towards different products was probably due to the presence of different oxidising species involved.

The most active $CuAu/SiO_2$ catalyst was made by a sequential method (Figure 4.15), which involved copper being deposited on the silica support by high dispersion, followed by gold deposited by deposition precipitation. TEM analysis suggested the presence of copper-gold alloy particles. The above characterisation and catalytic activity showed that this method had the most promise because the fresh catalyst even before thermal treatment had a 1% conversion at 320 ^oC. A thermal treatment, that involved a reduction in H_2/Ar for 2 h at 315 ^oC followed by a high temperature calcination at 676 ^oC for 15 h in air (Sinfelt method), produced a propene conversion of nearly 6% and 320 ^oC in the presence of hydrogen. This catalyst had a high selectivity towards acrolein and carbon dioxide.

Another interesting feature of the reduced and calcined catalysts were there stability, as there was little hysteresis observed, with the reaction temperature systematically increased and decreased. In most cases, propene oxide was only detected at lower temperatures (200 to 260

^{o}C) and, if it was observed at higher temperatures, it only had a low selectivity. This could be because of the fundamental instability of propene oxide. When the temperature was increased, the propene conversion also increased, as might be expected, but it produced less selectivity towards the epoxidation of propene and favoured acrolein formation.

The different products formed for propene oxidation in this thesis were a consequence of different surface reactions. Acrolein, propene oxide and carbon dioxide were the major products in this study. Acrolein was a result of C-H cleavage, whereas propene oxide was formed by the activiation of the C=C bond. Carbon dioxide was formed by the total oxidation of propene and required both the C-C bonds to be broken without the release of any intermediates. Catalysts that had high selectivity towards carbon dioxide, like the Au/SiO_2 catalyst reduced with $NaBH_4$ in the absence of hydrogen for propene oxidation, suggested that the propene was too strongly bound to the surface of the catalyst. The propene oxidation experiments carried out showed no hydrogenation reaction products, like propane, and the changes in the selectivity confirmed that the effect of different preparation techniques affected the properties of the active sites. Ethanal and acetone were the only other products produced and could have been formed as a result of a series of reactions.

Several active sites were observed in this study which could have accounted for different selectivities and activities towards propene oxidation. One of the active sites suggested was a bimetallic CuAu site which was very active towards propene oxidation but tended to form a variety of products. The activity was markedly improved by co-feeding hydrogen in the reactor feed. The reason for this was unclear but it could have been associated with changes in the reaction mechanism.

Preliminary investigation of the use of CuAu catalysts for other reactions was also discussed. Monometallic Au and $AuCu/SiO_2$ bimetallic catalysts were analysed for hydrogen peroxide synthesis, but only gave a low activity when compared to the conventional Au/Pd catalysts

studied. Au/SiO_2 catalysts prepared by sol immobilisation were tested for glycerol and benzyl alcohol oxidation. This procedure is well known for forming small particles that have a narrow size distribution. A conversion of almost 50% was achieved after 4 hours and its activity appeared to be unaffected by the reaction temperature. At both temperatures (60 ^{o}C and 100 ^{o}C), the main selectivity was towards glyceric acid. Benzyl alcohol oxidation was also investigated and showed minimal activity but this could have been due to the support used and the absence of any thermal treatment.

6.1 Future work

In this section, studies of potential interest for future work are outlined to show what areas could be more extensively explored. In addition, new experiments are discussed that could improve the performance of the catalysts studied in this thesis.

The characterisation techniques - temperature programmed reduction (TPR) and X-ray diffraction (XRD) - should be carried out before and after reduction for the $AuCu/SiO_2$ catalyst, made by sol immobilisation, to get a more in depth understanding of the structure, as this sample showed a promising performance for propene oxidation. Testing the bimetallic $AuCu/SiO_2$ catalysts made by sol immobilisation, with and without hydrogen, would be useful for the propene oxidation study to obtain a complete set of this data. It would also be interesting to investigate the effect on selectivity and conversion of the $AuCu/SiO_2$ bimetallic catalysts for propene oxidation, when the gas space hourly velocity of the reaction is varied. For our catalytic experiments, a gas space hourly velocity of 25,500 h^{-1} was used that was higher than many previous propene oxidation studies, [1,2] which normally used a GSHV between 9000-24000 h^{-1} and resulted in low propene conversions. These studies could help to optimize the reaction conditions for propene epoxidation. The reaction conditions are a key factor that could affect the function of a catalyst, as a potentially good catalyst with

unsuitable reaction conditions could lead to a poor selectivity towards propene oxide or acrolein. Performing experiments at iso-conversion would be beneficial to our investigation to determine the effect of temperature on the selectivity of the catalysts at a constant conversion. Studying the effect of calcination temperature on the activity for propene oxidation could be further explored since, in this thesis, only direct calcination at 400 ^{o}C for 2 h was carried out. Previously, Llorca and co-workers[3] prepared an AuCu/TiO_2 catalyst from thiol-capped nanoparticles and analysed it for propene oxidation. The catalysts were calcined for 2 h and the effect of thermal treatment was studied, by varying the temperatures between 300-600 ^{o}C. They found that high yields of propene oxide could be formed when the catalysts were calcined at 400 ^{o}C. At calcination temperatures above 400 ^{o}C, alloy particles were seen that were covered with oxidised Cu species, which decreased their activity for propene oxidation.

Duplicate experiments were not performed in this study, due to time constraints. Therefore, the accuracy of the data collected in the absence and presence of hydrogen did have limitations. It would be beneficial for future research to carry out more propene oxidation experiments with all the catalysts mentioned in this thesis to obtain more data to help understand the way the catalysts perform more fully.

Hydrogen and oxygen were used for our propene oxidation experiments but it has been shown[1] that N_2O can be an effective oxidant for this reaction. Therefore, it might be useful to try and use N_2O to explore the performance and selectivity of the catalysts with different oxidants. If the use of N_2O showed equivalent activity when using our catalysts (propene conversion of 4.3% at 300 ^{o}C), this would be extremely promising, as N_2O is only converted to N_2 which is environmentally benign.

Preparation of more CuAu/SiO_2 catalysts made by alternative routes would be an idea because the novel Sinfelt method that was used in this study produced propene oxide and

acrolein. It also revealed the need for a reduction step in the catalyst's formation in order to improve its performance. A sol-gel technique has been used by Zhu to prepare CuO-SiO_2 catalysts.[4] Propene oxidation was carried out and showed a selectivity of 78% towards propene oxide in an oxygen rich environment, without the need for pre-reduction. Propene oxidation has been studied by Lambert and co-workers [2] and who prepared a Cu/SiO_2 catalyst by a microemulsion process. This formed a catalyst that had good selectivity and conversion at low temperatures for propene oxidation, without the need for hydrogen in the co-feed (at 225 ^oC 53% selective to propene oxide and conversion of 0.25%). Such a study on different preparation methods could help to establish a general relationship between the catalyst's structure and its performance for propene oxidation. Preparing Cu/SiO_2 and AuCu/SiO_2 catalysts in the above ways could potentially produce an active catalyst.

One of the results from the present investigation for monometallic Cu and Au and bimetallic CuAu/SiO_2 catalysts, was that a reduction stage was vital for an effective catalyst. However, whilst this type of reduction method was not investigated greatly, and this could be important factor in finding the way of reducing a catalyst and revealing its catalytic potential. Drying the catalyst in air at 60 °C for 12 h and a reduction at 200 °C in 5%H_2/He for 1 hour [2] is an example of a different reduction procedure than was used in this study.

Another worthwhile investigation might be to try and establish the factors which are responsible for limiting the selectivity to partial oxidation products, as the conversion increases. Some factors have already been studied in heterogeneous reactions but more studies in this area would be beneficial for progress in the field of selective oxidation. More work on indentifying the active sites for selective oxidation is needed, in order to produce more efficient catalysts with more selective active sites.

Silica was the only support used in our study but the use of other supports, such as TiO_2 or carbon would be interesting as a comparison. Previous investigations for propene oxidation [3]

have mainly used TiO_2, although other studies have also used supports such as Ti-doped high surface area SiO_2 (Ti-SiO_2), and micro- and meso-porous titanosilicates (TS-1 and Ti-MCM). Comparing the catalytic activity of $CuAu/SiO_2$ with copper-gold catalysts, using these other supports, could show the dependence on the choice of support for the selectivity and conversion for propene oxidation. It might also help to look at the support effect and the interface effect between Cu and Au nanoparticles.

An extended X-ray absorption fine structure (EXAFS) study on copper-gold alloys has been by Maurizio *et al.* [5] They investigated the correlation between crystalline structure and interatomic distances for each pair of atomic species (Au–Cu, Au–Au, Cu–Cu), in order to detect a possible deviation from the virtual crystal approximation (VCA). The VCA is a tractable way of studying configurationally disordered systems; traditionally, the potentials which represent atoms of two or more elements are averaged into a composite atomic potential. Semiconductors and ferroelectric materials are two important areas in which small changes in atomic composition dramatically change material properties and the VCA theoretical approach has been formulated to carryout studies in this scientific area. Performing such an EXAFS study on the $AuCu/SiO_2$ catalysts in this study might give more structural and chemical information about the alloys, and why certain catalysts perform better than others.

The catalytic activity for propene oxidation was the main focus of the research reported in this thesis, although preliminary reactions were considered. Most of these reactions, apart from the activity of the sol immobilisation catalyst for glycerol oxidation, didn't show any remarkable performance and were therefore not studied any further. However, supported gold and copper catalysts have previously been studied for CO oxidation.[6,7] In a report by Zhu [6] catalysts were synthesised by deposition precipitation and they proved that the Au-Cu/TiO_2 nanotubes performed better than the Au/TiO_2 nanotubes. Therefore, the possibility of

carrying out experiments for CO oxidation could reveal another potential direction to pursue, especially as this reaction is used in a wide range of applications, e.g the automobile industry. Gold-copper alloys have great capability as redox catalysts and, in this thesis, new ground has been covered to show this potential.

6.2 References

1. R.J. Chimentao, F. Medina, J.L.G. Fierro, J. Llorca, J.E. Sueiras, Y. Cesteros and P. Salagre, *Journal of Molecular Catalysis A: Chemical*, 274 (2007) 159–168.

2. O.P.H. Vaughan, G. Kyriakou, N. Macleod, M. Tikhov and R.M. Lambert, *Journal of Catalysis*, 236 (2005) 401–404.

3. J. Llorca, M. Domínguez, C. Ledesma, R. J. Chimentão, F. Medina, J. Sueiras, I. Angurell, M. Seco and O. Rossell, *Journal of Catalysis*, 258 (2008)187–198.

4. W. Zhu, Q. Zhang, and Y. Wang, *Journal of Physical Chemistry C*, 112 (2008) 7731-7734.

5. C. Maurizio, G. Mattei, P. Mazzoldi, S. Padovani, E. Cattaruzza, F. Gonella, F. D. Acapito and F. Zontone, *Nuclear Instruments and Methods in Physics Research B*, 200 (2003) 178–184.

6. B. Zhu, Q. Guo, X. Huang, S. Wang, S. Zhang, S. Wu and W. Huang, *Journal of Molecular Catalysis A: Chemical*, 249 (2006) 211–217.

7. E. Smolentseva, N. Bogdanchikova, A. Simakov, A. Pestryakov, I. Tusovskaya, M. Avalos, M.H. Farıas, J.A. Dıaz and V. Gurin, *Surface Science*, 600 (2006) 4256–4259.

Appendix

Catalyst Code	Composition	Preparation Method	Calcination Conditions
C97802B	$Cu(Cl)_2/SiO_2$	Impregnation	400 ^oC 2h in air
C97802D	$Cu(NO3)_2/SiO_2$	Impregnation	400 ^oC 2h in air
CF09	Au/SiO_2	Impregnation	400 ^oC 2h in H_2/Ar
C97815B (1)	$Cu(Cl)_2/SiO_2$	Impregnation	400 ^oC in H_2
C97815B (2)	$Cu(Cl)_2/SiO_2$	Impregnation	400 ^oC in N_2
C97815B (3)	$Cu(Cl)_2/SiO_2$	Impregnation	400 ^oC in air
C97819A	Au:Cu/SiO_2 1:1	Co-Impregnation	400 ^oC 2h in air
C97819B	Au:Cu/SiO_2 3:1	Co-impregnation	400^oC 2h in air
C97819C	Au:Cu/SiO_2 1:3	Co-Impregnation	400^oC 2h in air
C97828	$Cu(NO3)_2/SiO_2$	Precipitation	400^oC 2h in air
C97836	$HAuCl_4/SIO_2$	Deposition precipitation	500^oC 2h in air
CF128	Cu/SiO_2	High dispersion	Calcined 400^oC 2hrs in H_2/Ar
C97863 A	1:1 $Cu(Cl)Au/SiO_2$	Co-impregnation	Calcined 400^oC 2h in air
C97863B	1:3 $Cu(Cl)Au/SiO_2$	Co-impregnation	Calcined 400^oC 2h in air
C97863C	3:1 $Cu(Cl)Au/SiO_2$	Co-impregnation	Calcined 400^oC 2h in air
C97865A	1:1 $Cu(Cl)Au/SiO_2$	Co-impregnation	Reduced 315^oC 2h and calcined 676^oC for 15h in air
C97865B	1:3 $Cu(Cl)Au/SiO_2$	Co-impregnation	Reduced 315^oC 2h and calcined 676^oC for 15h in air
C97865C	3:1 $Cu(Cl)Au/SiO_2$	Co-impregnation	Reduced 315^oC 2h and calcined 676^oC for 15h in air
C978/80A	1:1 $Cu(NO_3)_2Au/SiO_2$	Co-impregnation	Reduced in $NaBH_4$
C987/80B	1:3	Co-	Reduced in $NaBH_4$

	$Cu(NO_3)_2Au/SiO2$	impregnation	
C978/80C	3:1 $Cu(NO_3)_2Au/SiO_2$	Co-impregnation	Reduced in $NaBH_4$
C978/80D	Au/SiO_2	Impregnation	Reduced in $NaBH_4$
C978/80E	$Cu(NO_3)_2/SiO_2$	Impregnation	Reduced in $NaBH_4$
C978/87	1:1 $Cu(NO_3)_2Au/SiO_2$	HDC + Au DP prep	400^oC 2h in air
C978/90	1:1 $Cu(NO_3)_2Au/SiO_2$	HDC + Au IW impregnation	400^oC 2h in air
C978/93A	1:1 $Cu(NO_3)_2Au/SiO_2$	Co-impregnation	Reduced in H_2
C978/93B	1:3 $Cu(NO_3)_2Au/SiO_2$	Co-impregnation	Reduced in H_2
C987/93C	3:1 $Cu(NO_3)_2Au/SiO_2$	Co-impregnation	Reduced in H_2
C978/93D	Au/SiO_2	Impregnation	Reduced in H_2
C978/93E	$Cu(NO_3)_2/SiO_2$	Impregnation	Reduced in H_2
C978/99A	1:1 $Cu(Cl)Au/SiO_2$	Co-impregnation	Reduced in H_2
C978/99B	1:3 $Cu(Cl)Au/SiO_2$	Co-impregnation	Reduced in H_2
C978/99C	3:1 $Cu(Cl)Au/SiO_2$	Co-impregnation	Reduced in H_2
C978/99D	$Cu(Cl)/SiO_2$	Impregnation	Reduced in H_2
C978/102	Au/SiO_2	Sol immobilisation	Dried at 110^oC
C978/103	$CuAu/SiO_2$	Sol immobilisation	Dried 110^oC
C978/101A	1:1 $Cu(NO_3)_2Au/SiO_2$	Co-impregnation	Reduced 315^oC 2h and calcined 676^oC for 15h in air
C978/101B	1:3 $Cu(NO_3)_2Au/SiO_2$	Co-impregnation	Reduced 315^oC 2h and calcined 676^oC for 15h in air
C978/101C	3:1 $Cu(NO_3)_2Au/SiO_2$	Co-impregnation	Reduced 315^oC 2h and calcined 676^oC for 15h in air
C978/101D	Au/SiO_2	Impregnation	Reduced 315^oC 2h and calcined 676^oC for 15h in air
C978/101E	$Cu(NO_3)_2/SiO_2$	Impregnation	Reduced 315^oC 2h and calcined 676^oC for 15h in air

Table 1 List of catalyst preparations with catalyst codes.

Catalyst Composition	Uncalcined/ Calcined	Preparation method	BET Surface Area (m^2/g^{-1})
Au/SiO_2	Calcined	Deposition precipitation	440
$CuAu/SiO_2$ (1:1)	Calcined	Impregnation	328
$CuAu/SiO_2$ (1:3)	Calcined	Impregnation	333
$CuAu/SiO_2$ (3:1)	Calcined	Impregnation	311
Au/SiO_2	Calcined	Impregnation	327
Cu/SiO_2	Uncalcined	Impregnation (nitrate)	247
Cu/SiO_2	Calcined	Impregnation (nitrate)	281
Cu/SiO_2	Uncalcined	Impregnation (chloride)	275
Cu/SiO_2	Uncalcined	Precipitation	297
Cu/SiO_2	Calcined in H_2	Impregnation	302
Cu/SiO_2	Calcined in N_2	Impregnation	310
Cu/SiO_2	Calcined in air	Impregnation	294
1:1 $CuAu/SiO_2$	Calcined	Co-impregnation (chloride)	302
1:3 $CuAu/SiO_2$	Calcined	Co-impregnation (chloride)	299
3:1 $CuAu/SiO_2$	Calcined	Co-impregnation (chloride)	283
1:1 $CuAu/SiO_2$	Calcined	Co -impregnation (nitrate)	269
1:3 $CuAu/SiO_2$	Calcined	Co-impregnation (nitrate)	296
3:1 $CuAu/SiO_2$	Calcined	Co-impregnation (nitrate)	294
1:1 $CuAu/SiO_2$	Sinfelt (reduced only)	Co-impregnation (nitrate precursor)	265
1:1 $CuAu/SiO_2$	Sinfelt (reduced and calcined)	Co-impregnation (nitrate precursor)	300
1:3 $CuAu/SiO_2$	Sinfelt (reduced only)	Co-impregnation (nitrate precursor)	268

1:3 $CuAu/SiO_2$	Sinfelt (reduced and calcined)	Co-impregnation (nitrate precursor)	306
3:1 $CuAu/SiO_2$	Sinfelt (reduced only)	Co-impregnation (nitrate precursor)	294
3:1 $CuAu/SiO_2$	Sinfelt (reduced and calcined)	Co-impregnation (nitrate precursor)	283
Cu/SiO_2	uncalcined	High dispersion	173

Table 2 BET surface areas of catalysts

Catalyst	**Au wt%**	**Cu wt%**
C97819A	4.10	1.19
C97819B	4.71	0.46
C97819C	3.45	2.82
C97809	5.42	
C97802D	5.02	
C97836	0.05	
C978 15B(1)		3.96
C97815B(2)		2.47
C97815B(3)		4.56
C97828		3.03
CF02B		4.21
CF128		3.99
C978 63A	3.1	1.3
C97863B	3.5	0.56

C978 63C	1.8	2.3
C978 65A	4.04	1.30
C978 65B	4.33	0.52
C978 65C	2.65	2.53
C978 80A	2.98	0.63
C978 80B	4.16	0.02
C978 80C	2.23	0.49
C978 80D	2.47	
C978 80E		1.69
C978 93A	3.50	1.15
C978 93B	5.15	0.48
C978 93C	2.43	2.20
C978 93D	5.71	
C978 93E		4.78
C978 64A	3.01	1.42
C97864B	5.23	1.59
C978 87	2.36	1.48
C978 90	3.35	1.45
C978 101A	3.39	0.66
C978101B	3.83	0.01
C978 101C	2.12	0.52
C978 101D	4.07	
C978 101E		2.23

Table 3 ICP analysis

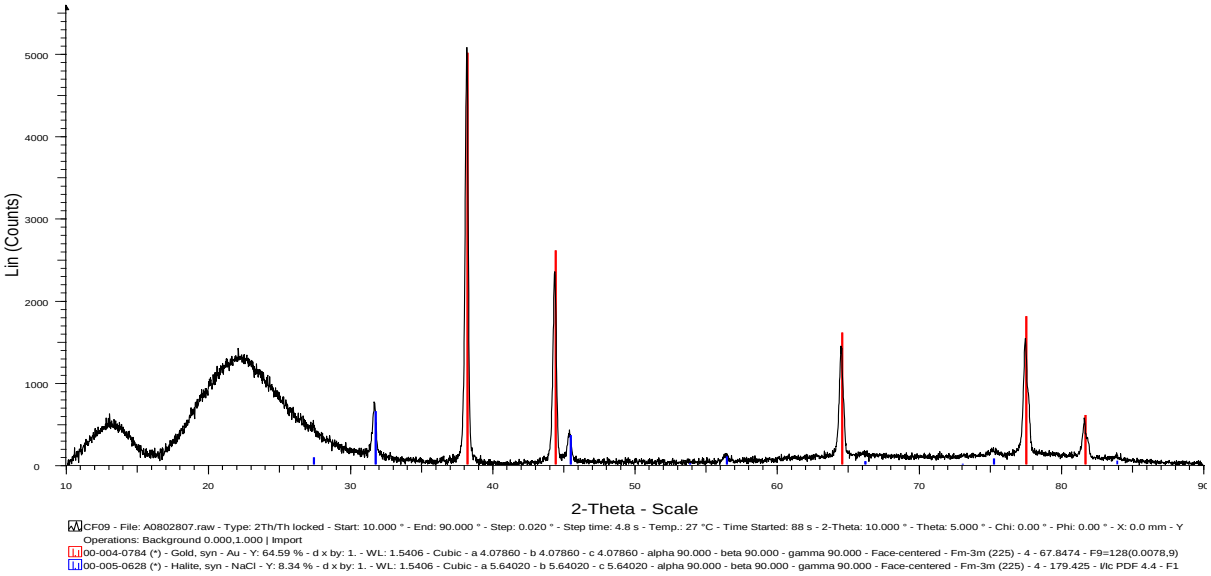

Figure 1 Au/SiO_2 (C97836) XRD

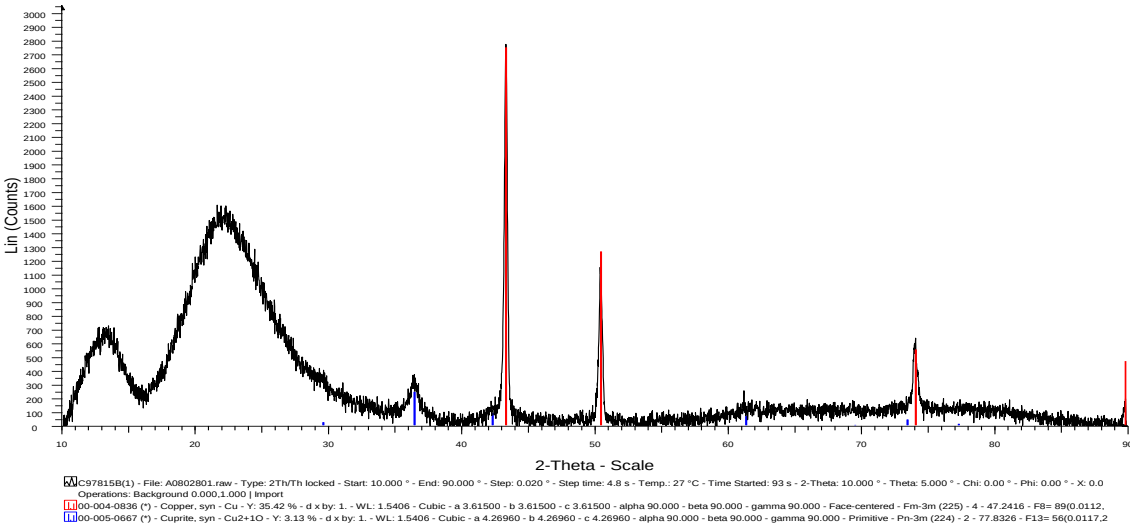

Figure 2 C97815B1 Cu/SiO_2

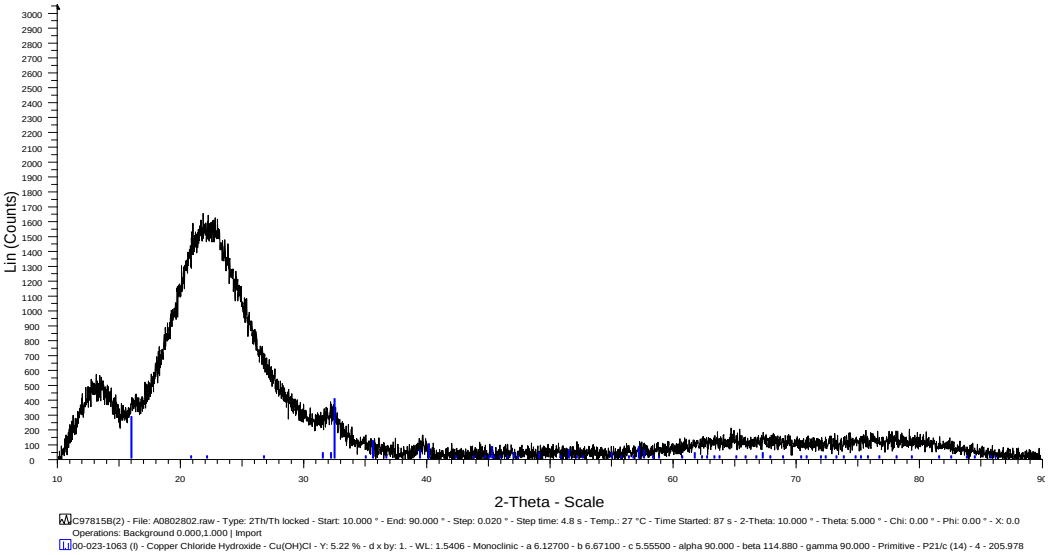

Figure 3 C97815B2 Cu/SiO_2

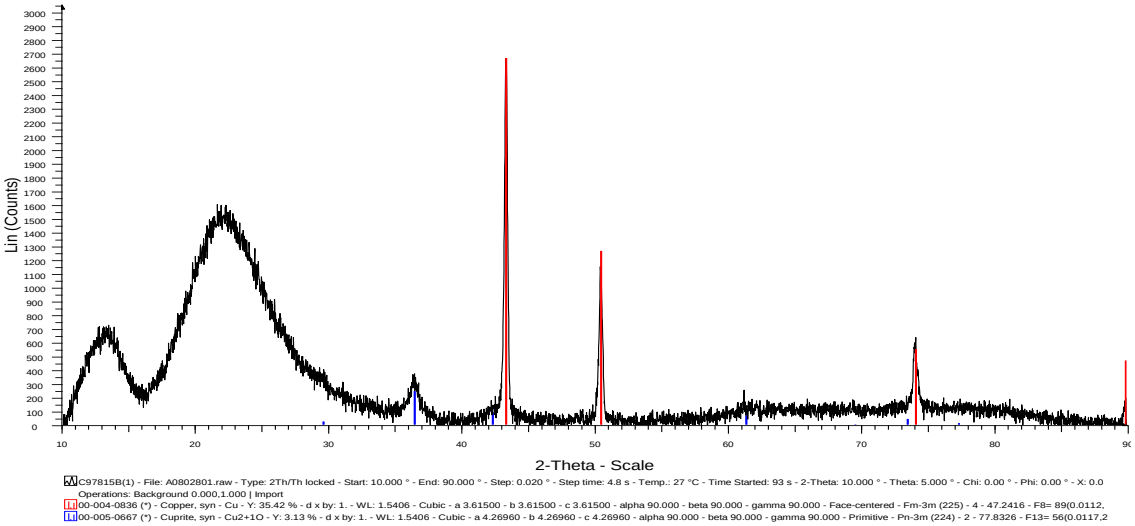

Figure 4 C97815B1 Cu/SiO_2

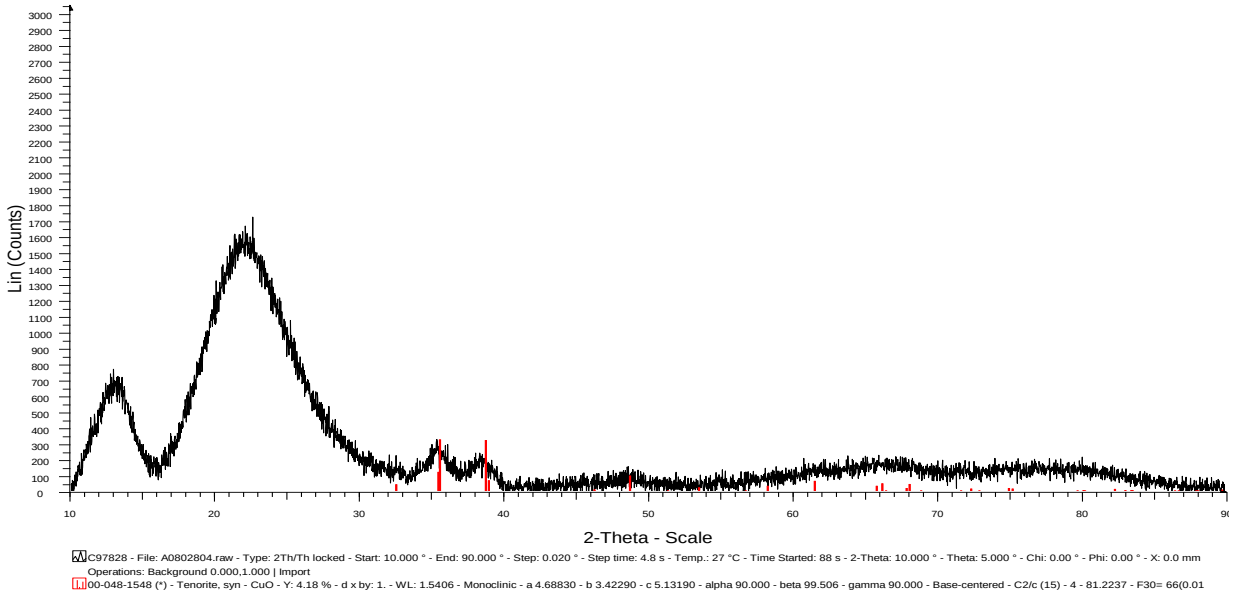

Figure 5 Cu/SiO_2 precipitation

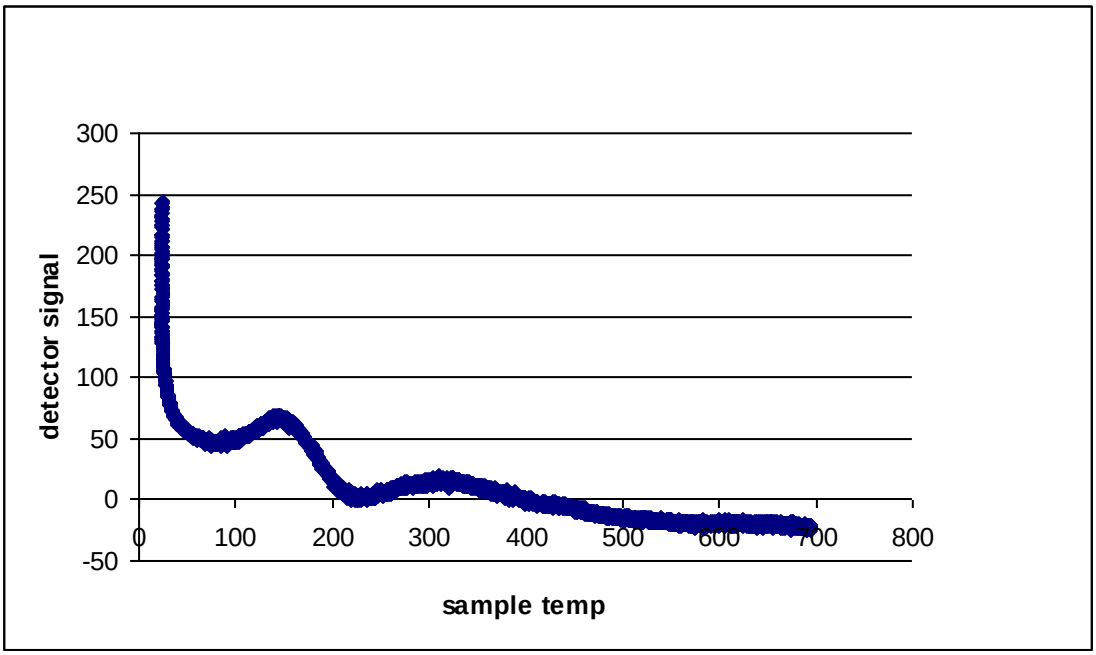

Figure 6 Silica TPR profile

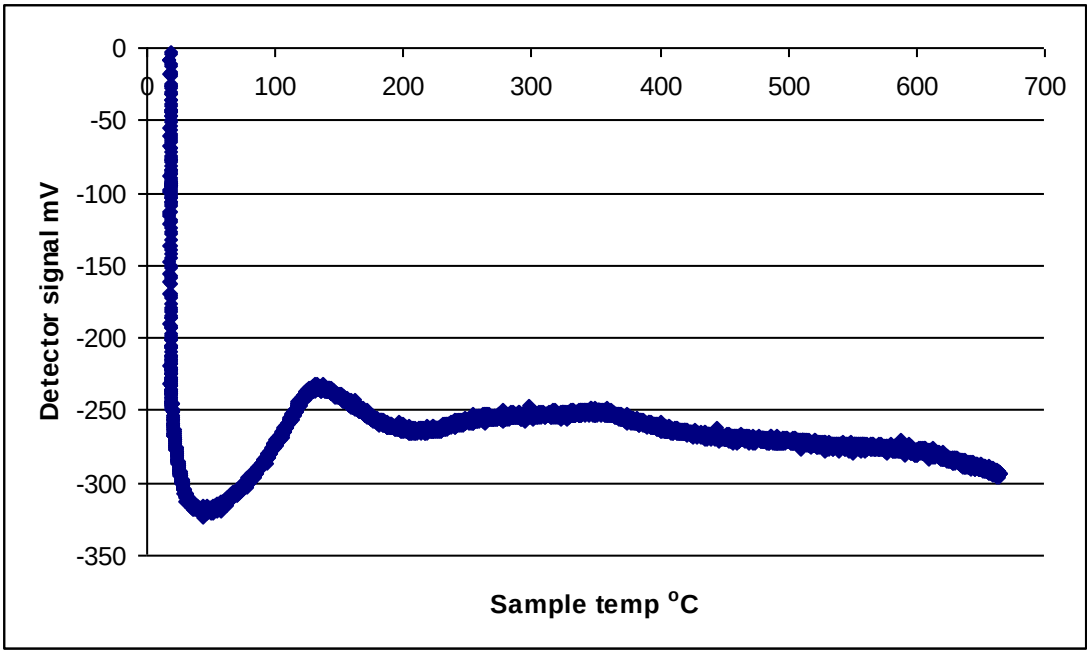

Figure 7 TPR profile of Au/SiO_2 DP (C97836)

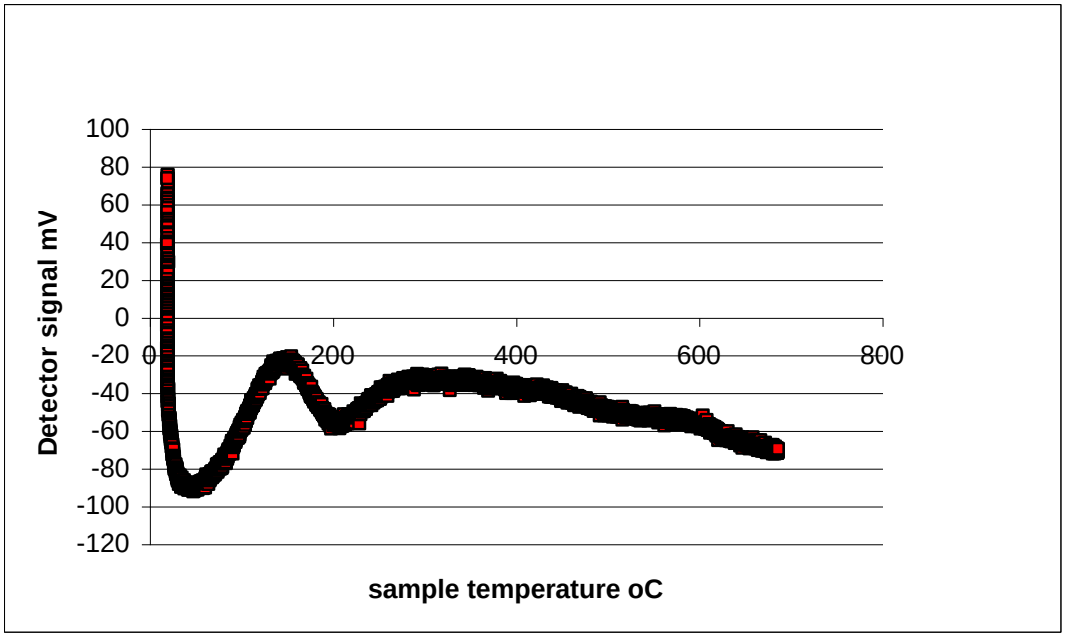

Figure 8 TPR profile of Au/SiO_2 IMP (C978**09)**

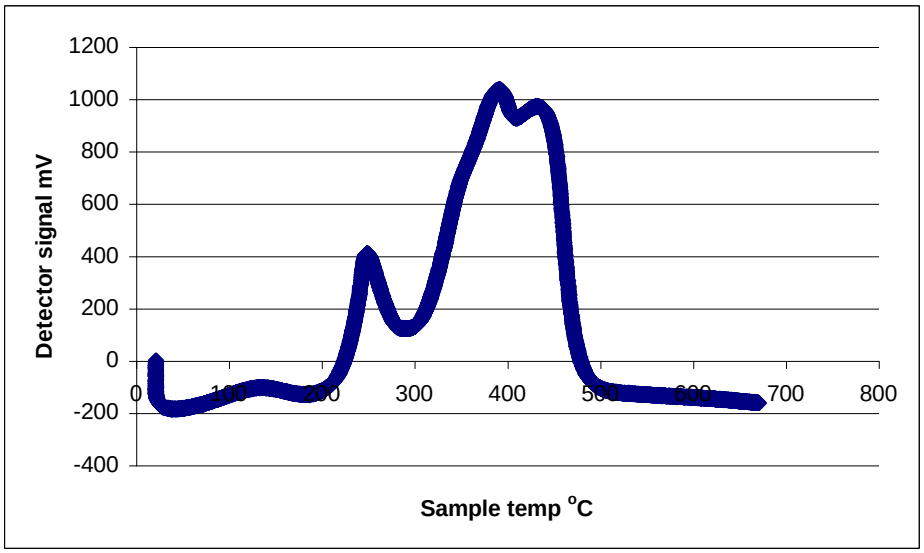

Figure 9 TPR profile of Cu/SiO_2 IMP (C97802D)

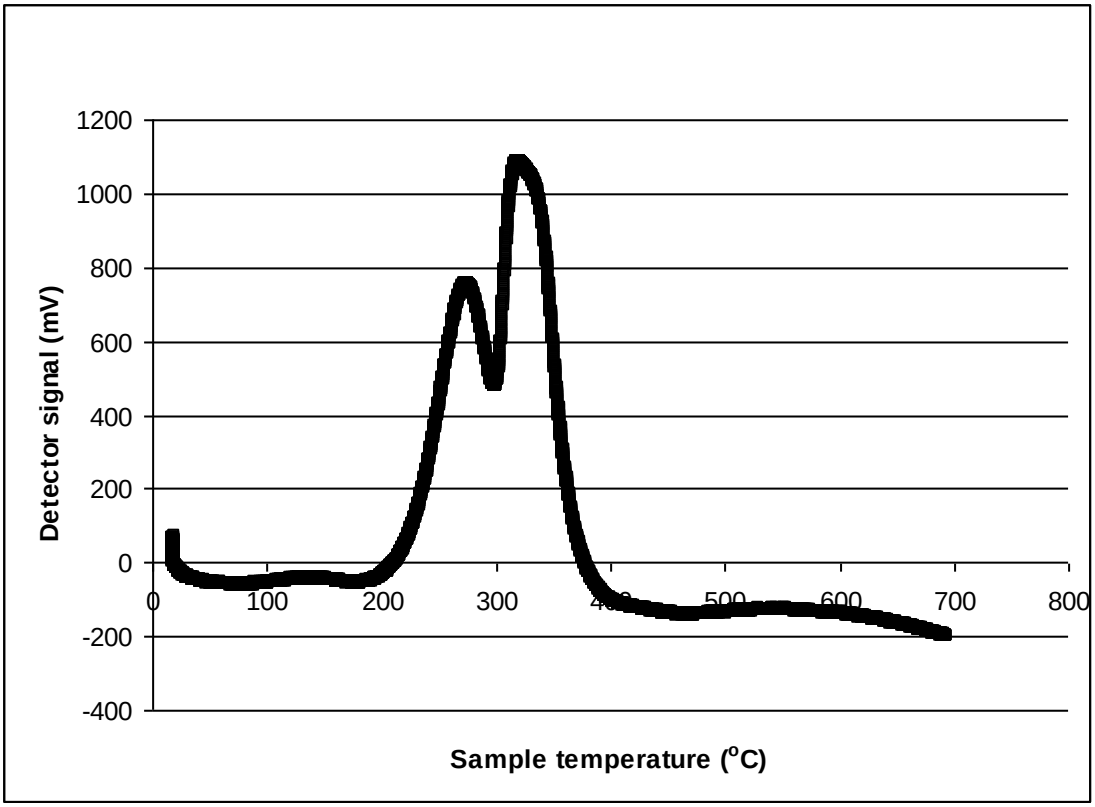

Figure 10 TPR profile of Cu/SiO_2 High dispersion (Cf128)

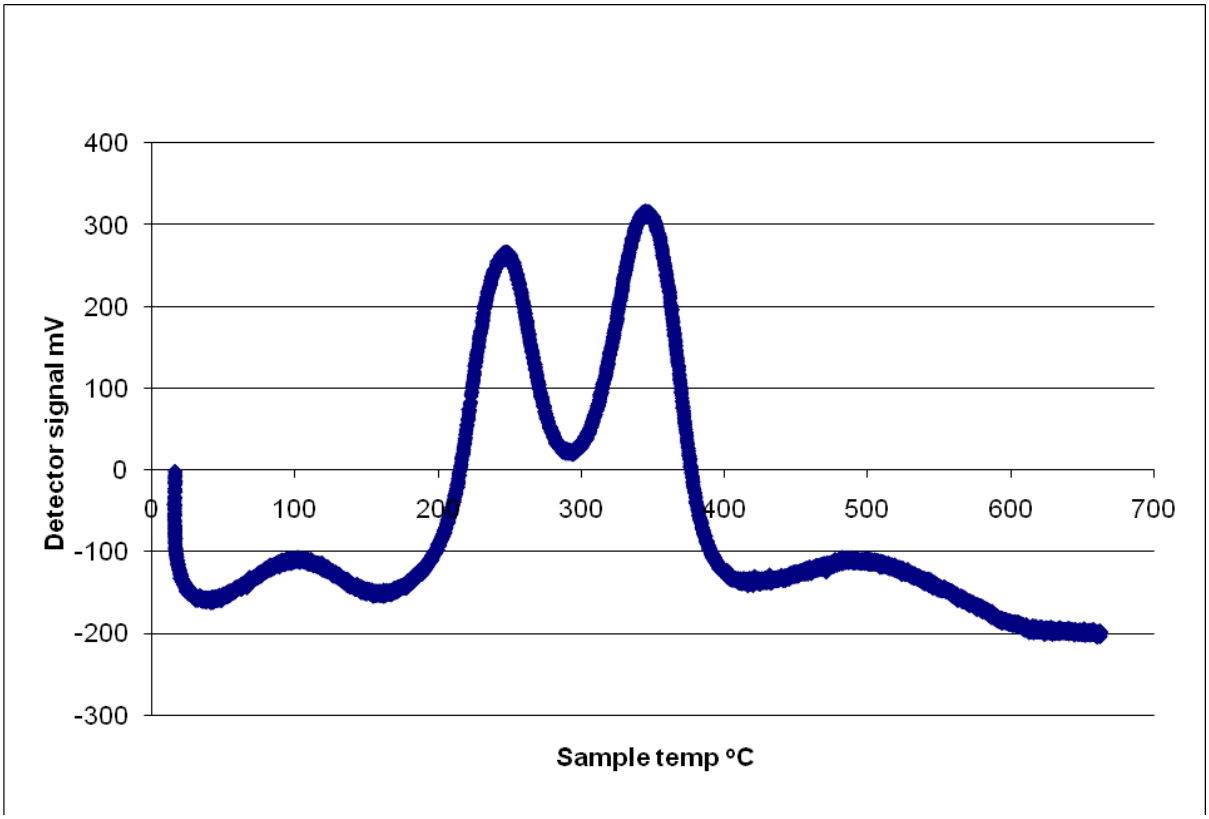

Figure 11 TPR 1 profile of $AuCu/SiO_2$ (C97819C)

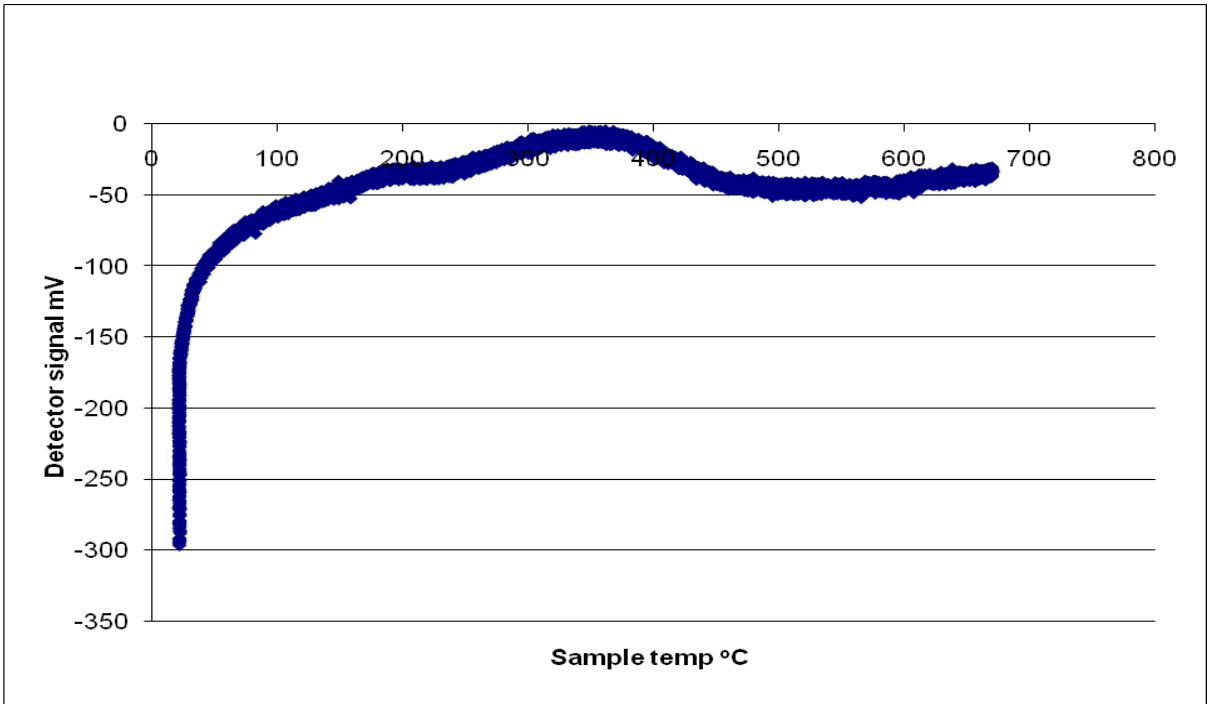

Figure 12 TPO profile $AuCu/SiO_2$ (C97819C)

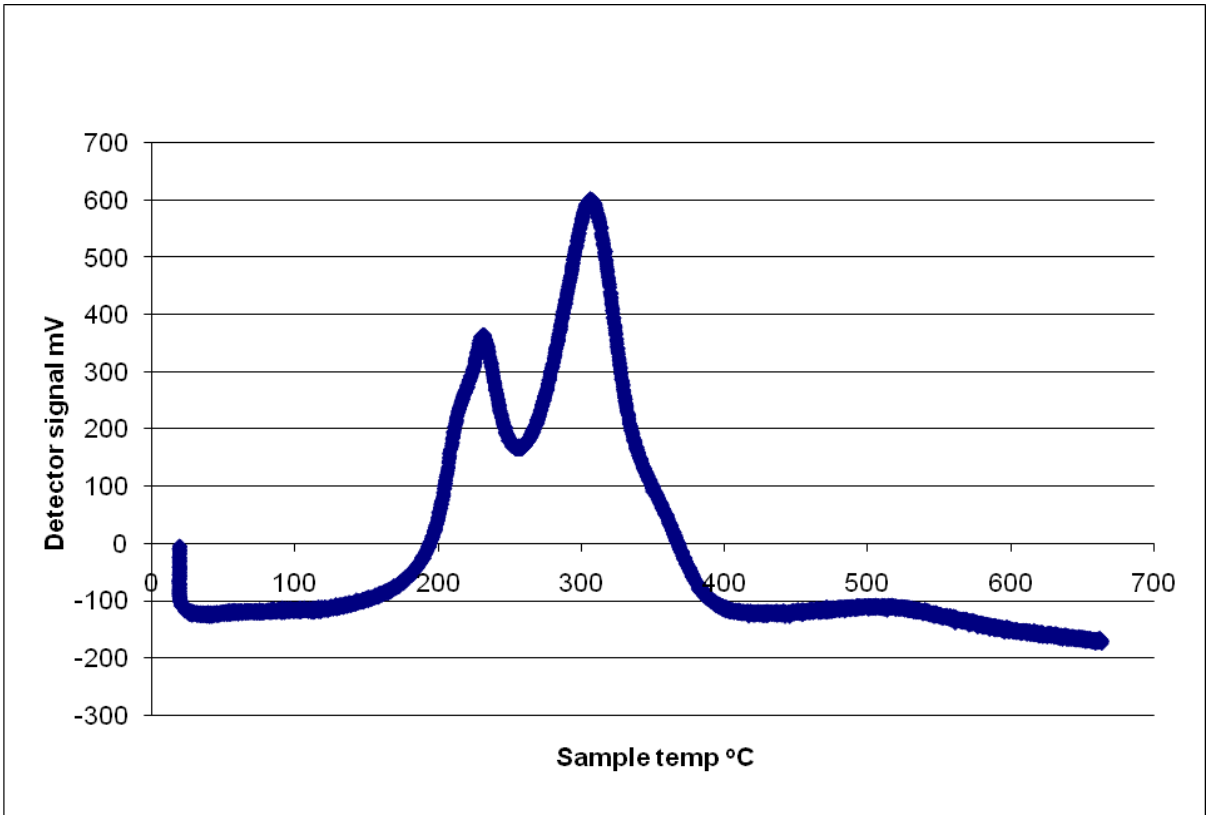

Figure 13 TPR 2 profile $AuCu/SiO_2$ (C97819C)

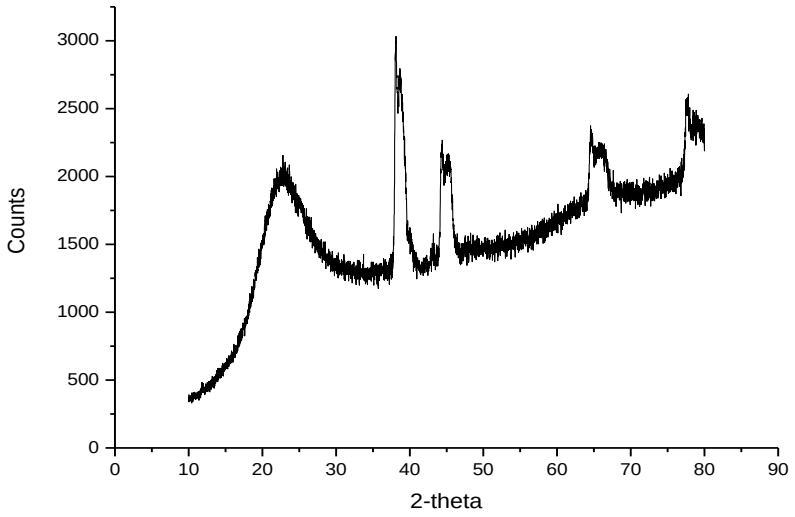

Figure 14 $CuAu/SiO_2$ made by HDC Cu + Au IW (C978 90A)

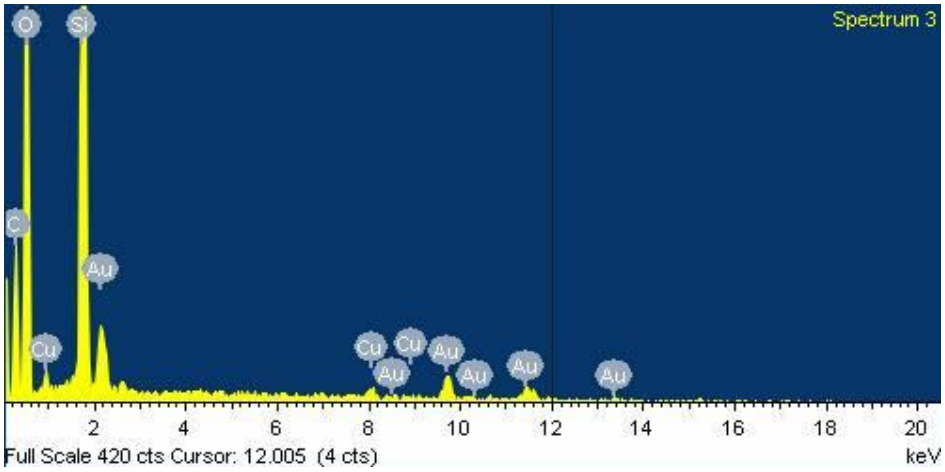

Figure 15 EDX analysis for Cu_3Au/SiO_2 catalyst (C97819C) with direct calcinations in air.

XPS data

Heat Treatment	Cu/Au molar ratio				
	Theory	ICP	XPS		
			Fresh	After use in propene oxidation	
				Without H_2 addition	With H_2 addition
Calcination	0.33	0.34	0.83	2.5	11.4
	1	0.97	3.8	0.66	3.2
	3	2.66	6.4	10.1	12.1
Reduction	0.33	0.36	3.5	0.21	0.45
	1	0.95	3.3	5.69	5.0
	3	2.79	22.4	6.52	27.1
Reduction and Calcination	0.33	0.29	0.37	1.4	2.3
	1	1.02	1.6	4.4	1.1
	3	2.81	7.5	8.0	4.2

Table 4 Analysis of Cu/Au molar ratio by ICP and XPS before and after propene oxidation experiments.

XPS no.	Au:Cu	Calc	Binding energy							
			Cu(2p3/2)	Au(4f7/2)	Cu(2p3/2)/ Si(2p)	Au(4f)/ Si(2p)	Au(4f)/ Cu(2p)	C(1s)/ Si(2p)	O/Si	Au/Cu molar
1	0/1	H_2	932.57		0.036			0.10	2.26	
2	0/1	N_2	933.32		0.106			0.25	2.26	
3	0/1	air	933.19		0.132			0.28	2.21	
4	1/1	air	933.92	83.64	0.047	0.023	0.49	0.16	2.27	0.41
5	3/1	air	weak	83.65	0.025	0.010	0.39	0.28	2.32	0.33
6	1/3	air	933.87	83.95	0.064	0.023	0.36	0.21	2.27	0.30
7	0/1	air	933.37		0.140			0.21	2.27	
8	0/1	air	932.93 935.23		0.585			0.27	2.40	
9	1/0	air		weak		0.003		0.18	2.31	

Table 5 XPS data for figure 3.63 in chapter 3

EDX data

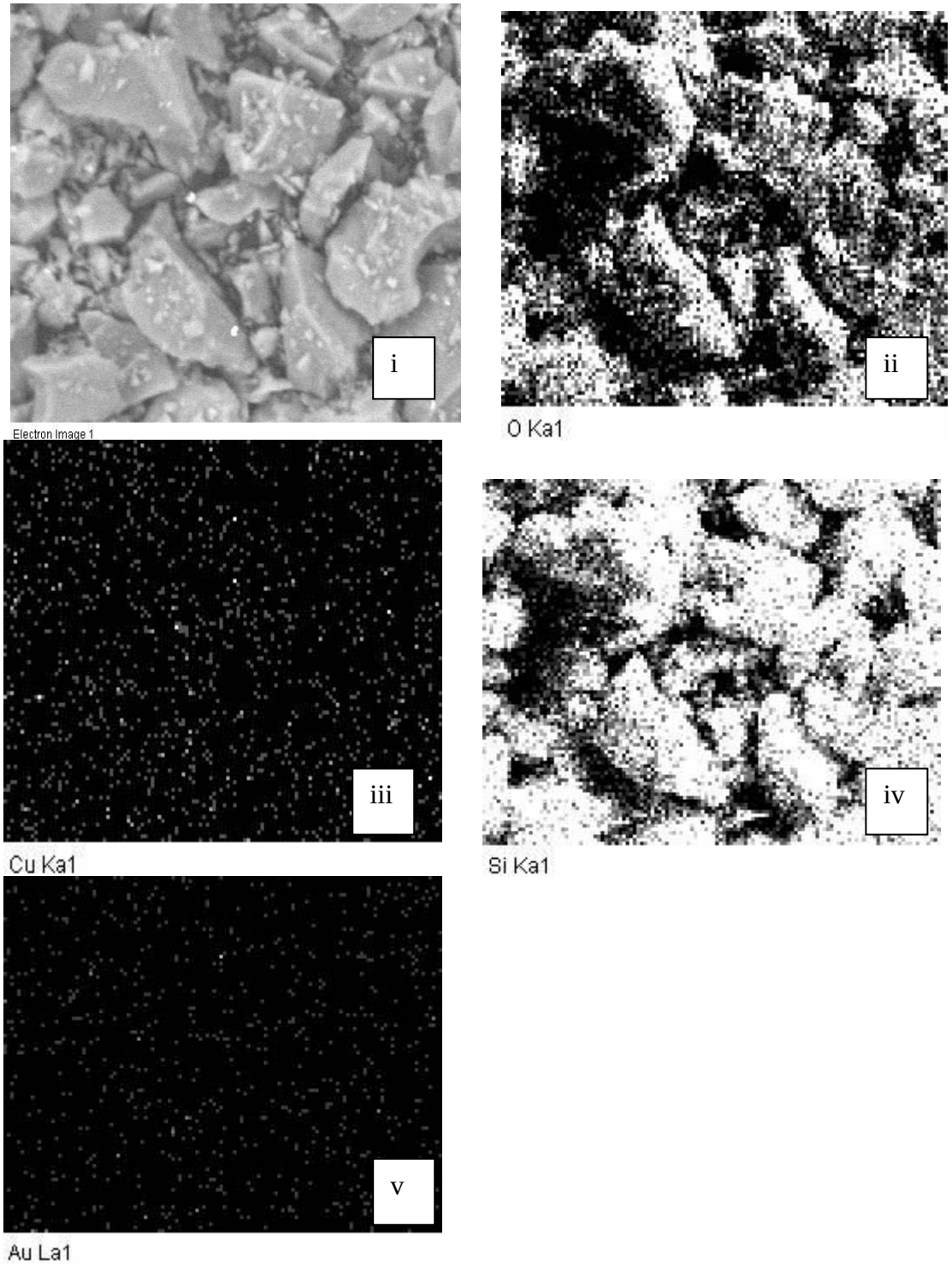

Figure 16 (i) SEM image Cu and Au particles, EDX maps of: (ii) Oxygen (iii) Cu (iv) Si (v) Au

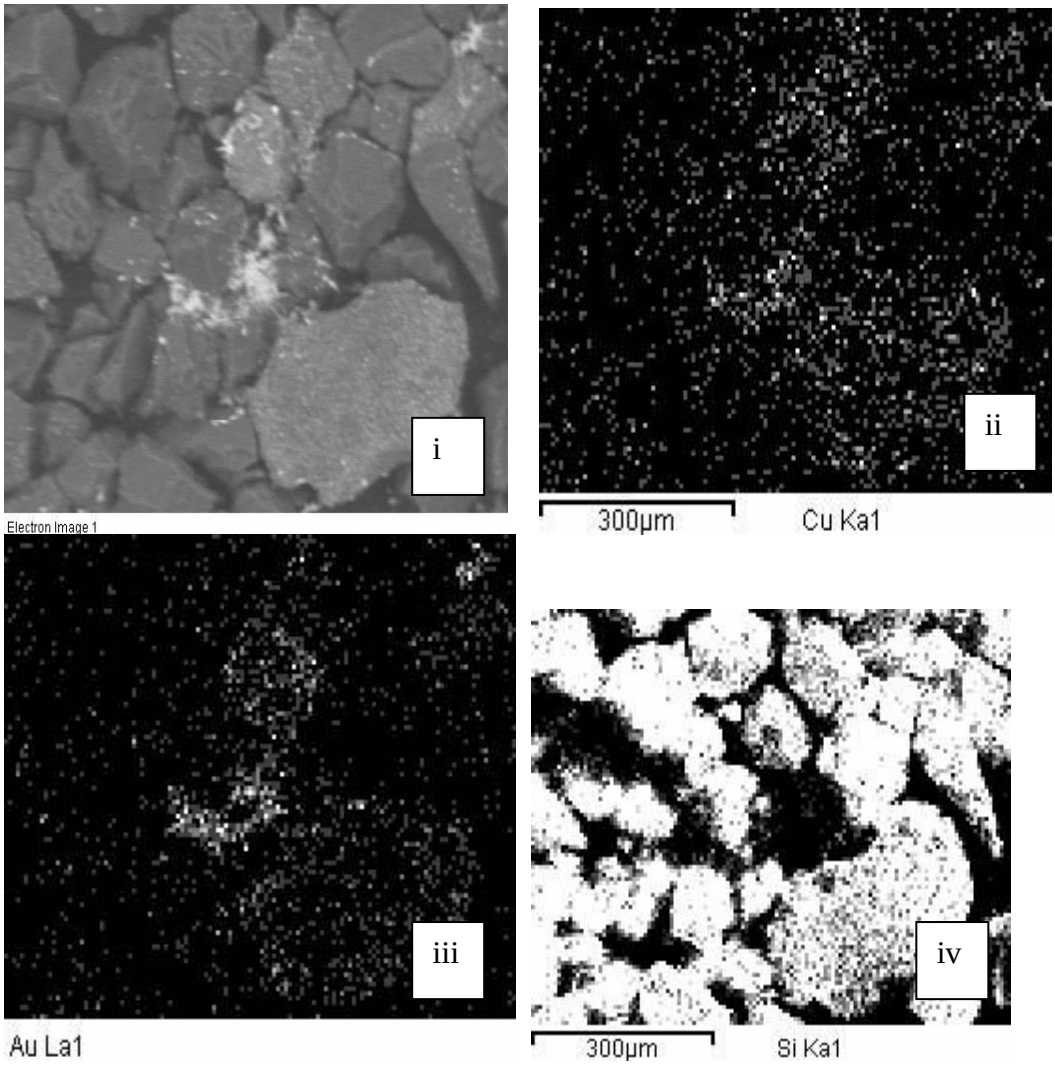

Figure 17 (C978 90) HDC Cu + Au IW (i) SEM image Cu and Au particles, EDX maps of: (ii) Cu (iii) Au (iv) Si

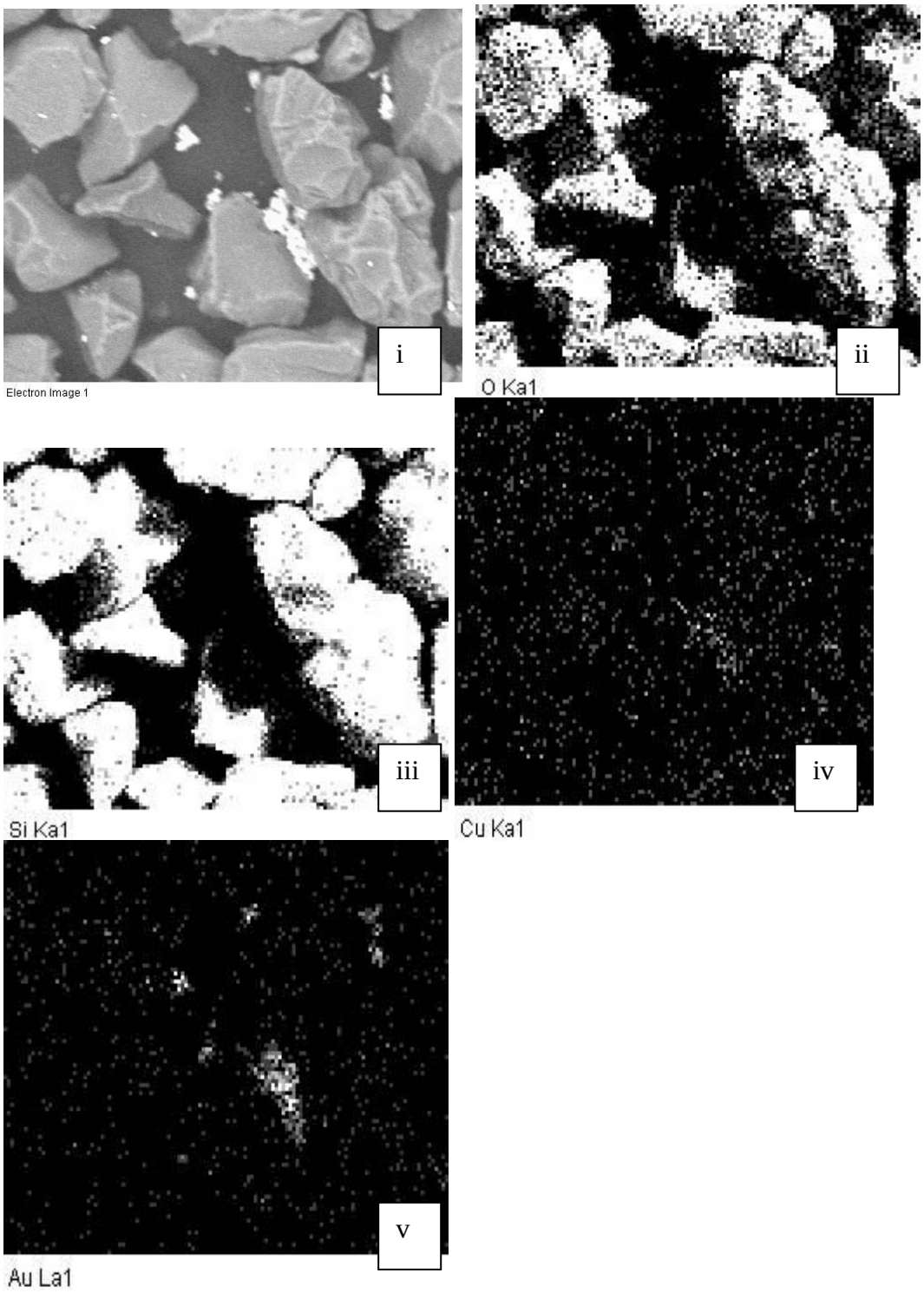

Figure 18 C978 99A 1:1 Cu:Au Cu chloride reduced in H_2 (i) SEM image Cu and Au particles, EDX maps of: (ii) Oxygen (iii) Si (iv) Cu (v) Au

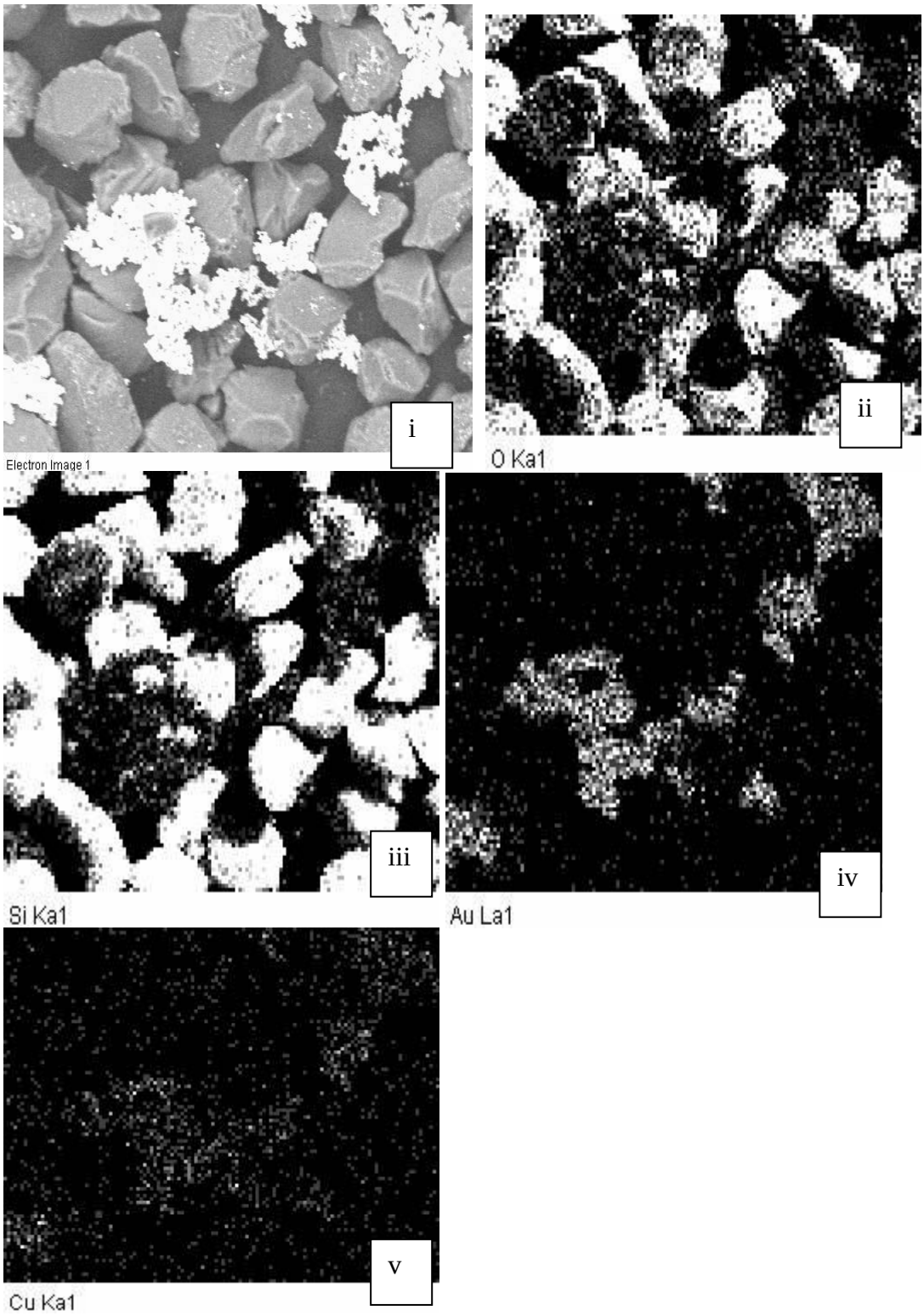

Figure 19 C978 99B 1:3 Cu:Au with Cu chloride reduced in H_2 (i) SEM image Cu and Au particles, EDX maps of: (ii) Oxygen (iii) Si (iv) Au (v) Cu

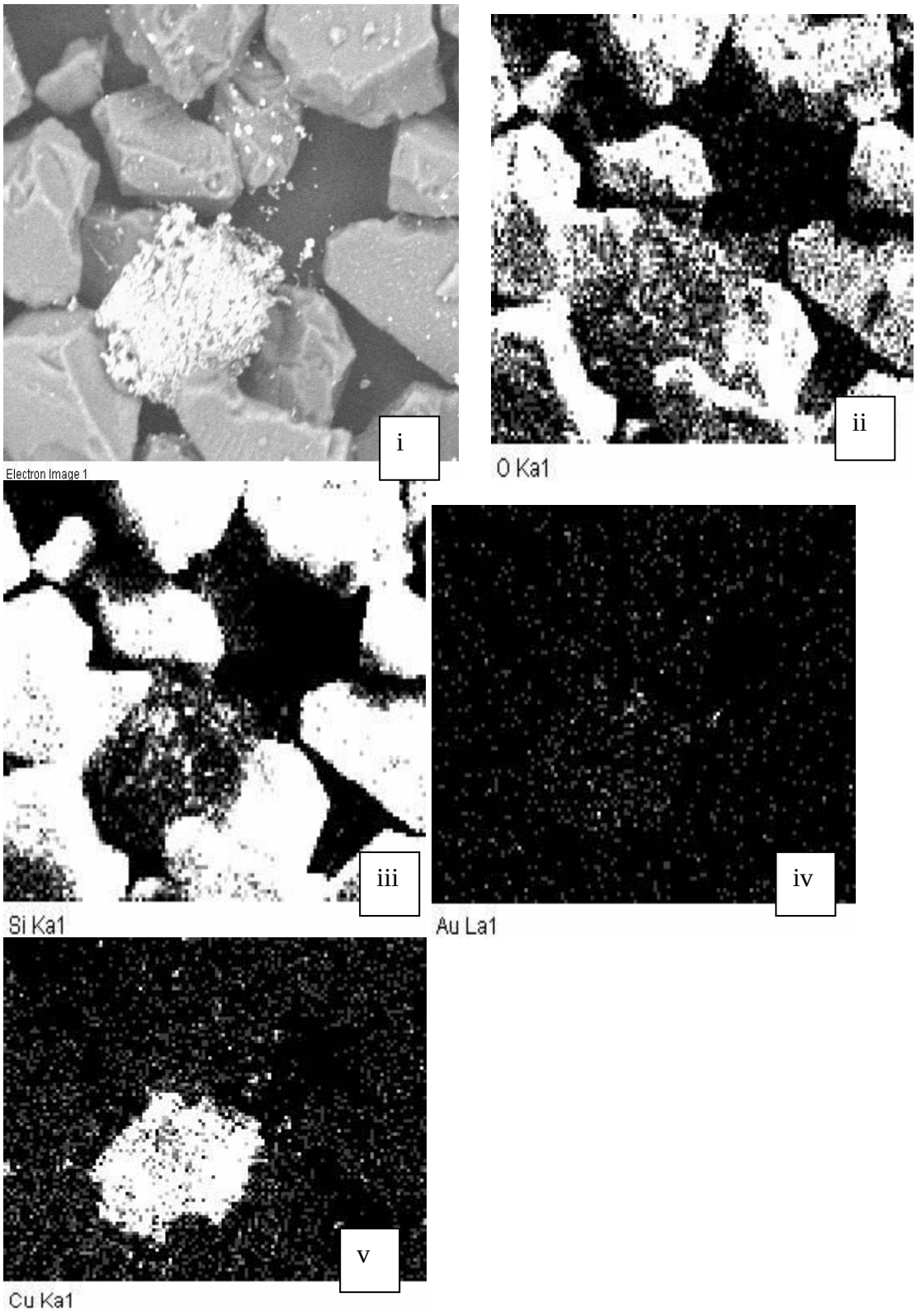

Figure 20 C978 99C 3:1 Cu:Au Cu chloride reduced in H_2 (i) SEM image Cu and Au particles, EDX maps of: (ii) Oxygen (iii) Si (iv) Au (v) Cu

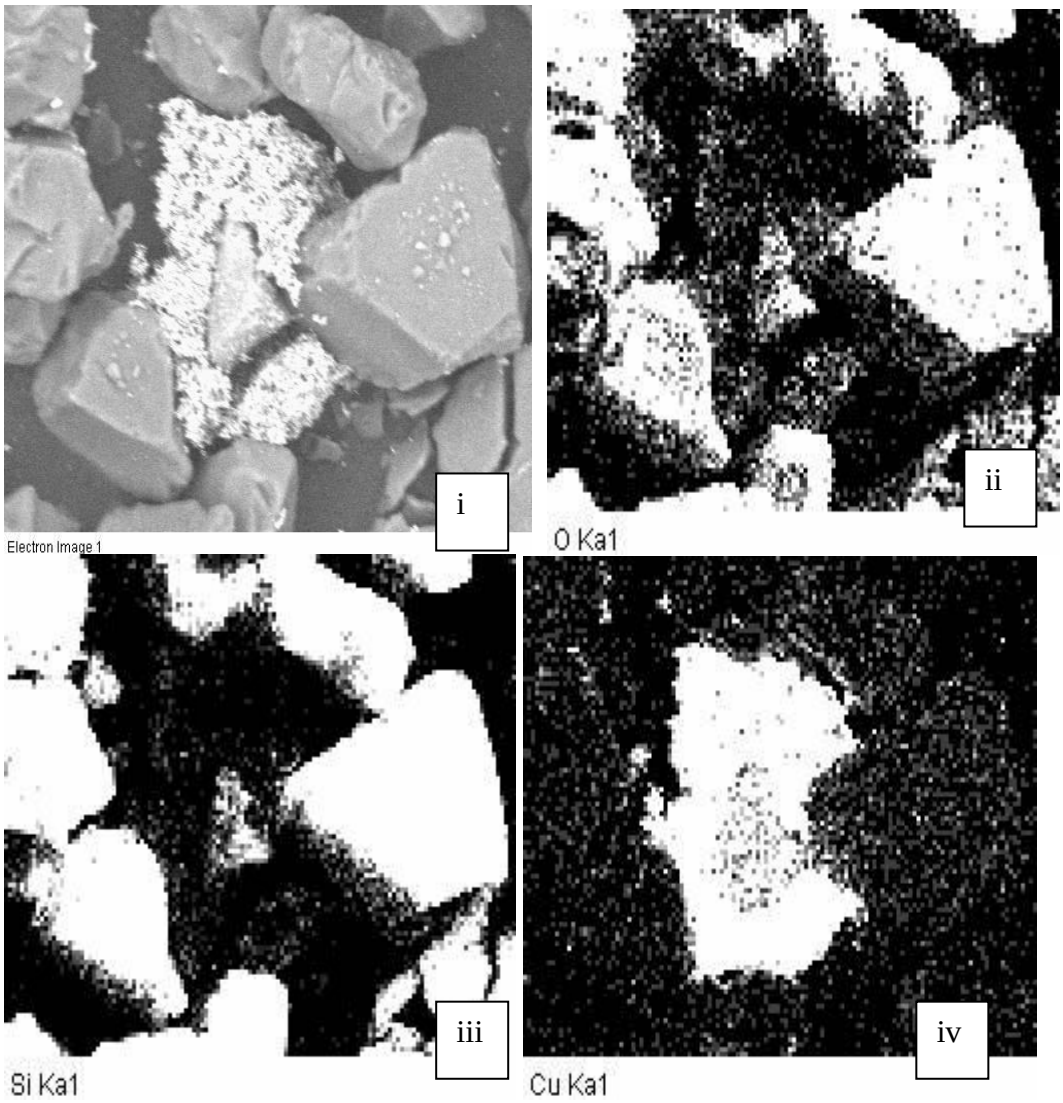

Figure 21 C978 99D Cu/SiO_2 Cu Chloride reduced in H_2.(i) SEM image Cu and Au particles, EDX maps of: (ii) Oxygen (iii) Si (iv) Cu